NTNU – Trondheim
Norwegian University of
Science and Technology

Adaptive speckle tracking algorithms for improved ultrasound blood flow imaging

Linn Siri Drange

Master of Science in Engineering Cybernetics
Submission date: June 2013
Supervisor: Tor Engebret Onshus, ITK
Co-supervisor: Lasse Løvstakken, ISB
Solveig Fadnes, ISB

Norwegian University of Science and Technology
Department of Engineering Cybernetics

Adaptive speckle tracking algorithms for improved ultrasound blood flow imaging

by

Linn Siri Drange

Master of Science in Engineering Cybernetics

Department of Engineering Cybernetics
Norwegian University of Science and Technology

Submission date: June 2013

Supervisor: Tor Engebret Onshus, ITK
Lasse Løvstakken, ISB

Problem description

Two-dimensional speckle tracking algorithms has potential to overcome the main limitations associated with ultrasound Doppler imaging of blood flow. The approach is under evaluation for blood flow imaging both in vascular and pediatric cardiology applications. Current methods are based on a simple algorithm that calculates the most likely displacement of blood scatterers without taking any a priori information about the flow velocity field into account, and measurements are quite noisy. Further, the tracking search and kernel (template) region have previously been fixed. In this work we will investigate the potential gain of using adaptive methods for both temporal regularization as well as more intelligent schemes for iteratively updating the search region in order to improve tracking estimates. Our aim is to improve the overall robustness of the approach so that clinically applicable results can be obtained with minimum spatial smoothing.

Assignment given: January 14th.

Supervisors: Tor Onshus, Lasse Løvstakken

Abstract

This thesis will present several ways to further improve the robustness of the speckle tracking method. The speckle tracking algorithm was made more adaptive to the velocity changes over time, utilizing velocity estimates from the previous flow frame to update the placement and size of the search region. The size of the search region was adjusted to the velocity change from the two previous flow frames, giving a larger search region for a higher acceleration. The tracking grid was also made finer according to the size of the search region, where the distance between the interpolated tracking points was made smaller. Multi-lag tracking was also tested, utilizing previous velocity estimates to adaptively find the best tracking lag over time. A higher tracking lag for small velocities should increase the accuracy of the estimated velocities.

The different methods to improve the robustness of the speckle tracking algorithm was tested with the use of simulated data of a carotid artery from the ultrasound simulation code, Field II. The data collected from the ultrasound simulation code is based on plane wave imaging and parallel receive beam forming to achieve a high frame rate. Results show that the methods tested will improve the tracking estimates, where multi-lag tracking improves the tracking estimates for small velocities.

Sammendrag

I denne oppgaven vil det bli presentert flere metoder for å forbedre robustheten til en speckle tracking metode. Speckle tracking algoritmen ble gjort mer adaptiv, ved å utnytte hastighets estimater fra den forrige flow frame for å oppdatere plasseringen og størrelsen til søkeområdet. Størrelsen til søkeområdet ble justert i forhold til hastighets endring mellom de to forrige flow framene, som gir et større søkeområde for høyere akselerasjon. Avstanden mellom de interpolerte tracking punktene ble gjort mindre i forhold til størrelsen på søkeområdet, som gir et finere grid. Speckle tracking med flere lag ble også testet, hvor hastighetsestimatene fra den forrige flow frame ble utnyttet for å adaptivt finne beste lag over tid. Et høyere tracking lag for mindre hastigheter burde øke nøyaktigheten til hastighetsestimatene. Disse metodene ble testet på et simulert data sett av en carotis åre fra ultralyd simulerings koden, Filed II. Dataene fra ultralyd simulerings koden er basert på plan bølge avbildning og parallell recieve beam forming for å oppnå en høy frame rate. Resultatene viser at metodene som ble teste vil forbedre tracking estimatene, hvor tracking med flere lag forbedre estimatene for de små hastighetene.

Acknowledgements

This thesis, and the work it presents, it the culmination of my masters degree at the Department of Engineering Cybernetics at the Norwegian University of Science and Technology (NTNU). I would like to thank my main supervisor at the Department of Engineering Cybernetics, Professor Tor Onshus for his support. I would also like to thank my supervisors at the Department of Circulation and Medical Imaging, Lasse Løvstakken and Solveig Fadnes for all their guidance and support during this work.

Contents

1 Introduction **26**

2 Theory **29**
2.1 Doppler ultrasound 29
2.1.1 Continuous Wave Doppler (CW-Doppler) 30
2.1.2 Pulsed Wave Doppler (PW-Doppler) 30
2.1.3 Color flow imaging 32
2.2 2D-velocity estimation 33
2.2.1 Vector Doppler 33
2.2.2 Speckle tracking 35
2.3 Conventional versus plane wave imaging 39
2.4 Blood flow over one heart cycle 39
2.5 Carotid artery 41

3 Methods **44**
3.1 Simulation data 44
3.2 The Speckle tracking algorithm 44
3.3 The adaptive speckle tracking algorithm 46
3.4 Adaptive speckle tracking over one flow frame 47
3.5 Multi-lag 48
3.5.1 Multi-lag -same interpolation factor for different lags . 48
3.5.2 Multi-lag variance 50
3.6 Adaptive tracking -adjusted to acceleration over flow frames . 50
3.7 Multi-lag tracking 51

4 Results **53**
4.1 Adaptive speckle tracking over one flow frame 53
4.1.1 Results from area 1 54
4.1.2 Results from area 2 57
4.1.3 Results from area 3 60

4.2 Multi-lag 62
4.2.1 Multi-lag -same interpolation-factor for different lags . 62
4.2.2 Multi-lag variance 97
4.3 Adaptive speckle tracking algorithm -adjusted to the acceleration over flow frames/ Multi-lag tracking 145

5 Discussion **174**
5.1 Adaptive speckle tracking over one flow frame 174
5.2 Multi-lag 177
5.2.1 Multi-lag -same interpolation-factor for different lags . 177
5.2.2 Multi-lag variance 178
5.3 Adaptive speckle tracking algorithm -adjusted to the acceleration over flow frames/ Multi-lag tracking 180

6 Conclusion **182**

List of Figures

2.1 Pulsed wave Doppler spectrum. 31
2.2 Color Flow image of carotid artery. 33
2.3 The vector Doppler approach introduced by Peronneau et al. (1974,1977) [6]. A two transducer vector Doppler system, with the transducers oriented with an angle, δ, between them. . . . 34
2.4 Geometry for speckle tracking. A small kernel region is identified from the blood vessel and the best match for the kernel region is found in a later acquisition within the search region. The location of the best match relative to the kernel defines the displacement vector for that particular kernel. 36
2.5 Diagram [15] showing various events during systole and diastole 40
2.6 Illustration of the heart [14] during diastole and systole . . . 41
2.7 B-mode image of the carotid artery with area one outlined . . 42
2.8 B-mode image of the carotid artery with area two outlined . . 42
2.9 B-mode image of the carotid artery with area three outlined . 43

3.1 Search and kernel region of the original speckle tracking algorithm. 46

4.1 Velocity estimate from the adaptive speckle tracking algorithm in x-direction with SNR=30 at area 1 flow frame 4 54
4.2 Velocity estimate from the adaptive speckle tracking algorithm in z-direction with SNR=30 at area 1 Flow frame 4 54
4.3 Velocity estimate from the adaptive speckle tracking algorithm in x-direction with SNR=20 at area 1 Flow frame 4 55
4.4 Velocity estimate from the adaptive speckle tracking algorithm in z-direction with SNR=20 at area 1 Flow frame 4 56
4.5 Velocity estimate from the adaptive speckle tracking algorithm in x-direction with SNR=30 at area 2 Flow frame 4 57

4.6 Velocity estimate from the adaptive speckle tracking algorithm in z-direction with SNR=30 at area 2 Flow frame 4 57
4.7 Velocity estimate from the adaptive speckle tracking algorithm in x-direction with SNR=20 at area 2 Flow frame 4 58
4.8 Velocity estimate from the adaptive speckle tracking algorithm in z-direction with SNR=20 at area 2 Flow frame 4 59
4.9 Velocity estimate from the adaptive speckle tracking algorithm in x-direction with SNR=30 at area 3 Flow frame 4 60
4.10 Velocity estimate from the adaptive speckle tracking algorithm in z-direction with SNR=30 at area 3 Flow frame 4 60
4.11 Velocity estimate from the adaptive speckle tracking algorithm in x-direction with SNR=20 at area 3 Flow frame 4 61
4.12 Velocity estimate from the adaptive speckle tracking algorithm in z-direction with SNR=20 at area 3 Flow frame 4 62
4.13 velocity estimation in the x-direction for different lags from area 1 with same interpolation factor flow frame 2 63
4.14 velocity estimation in the x-direction for different lags with from area 1 same interpolation factor flow frame 4 64
4.15 velocity estimation in the x-direction for different lags from area 1 with same interpolation factor flow frame 6 64
4.16 velocity estimation in the x-direction for different lags from area 1 with same interpolation factor flow frame 7 65
4.17 velocity estimation in the x-direction for different lags from area 1 with same interpolation factor flow frame 11 65
4.18 velocity estimation in the x-direction for different lags from area 1 with same interpolation factor flow frame 16 66
4.19 velocity estimation in the x-direction for different lags from area 1 with same interpolation factor flow frame 24 66
4.20 velocity estimation in the x-direction for different lags from area 1 with same interpolation factor flow frame 27 67
4.21 velocity estimation in the x-direction for different lags from area 1 with same interpolation factor flow frame 36 67
4.22 velocity estimation in the z-direction for different lags from area 1 with same interpolation factor flow frame 2 68
4.23 velocity estimation in the z-direction for different lags from area 1 with same interpolation factor flow frame 4 68
4.24 velocity estimation in the z-direction for different lags from area 1 with same interpolation factor flow frame 6 69
4.25 velocity estimation in the z-direction for different lags from area 1 with same interpolation factor flow frame 7 69

4.26 velocity estimation in the z-direction for different lags from area 1 with same interpolation factor flow frame 11 70
4.27 velocity estimation in the z-direction for different lags from area 1 with same interpolation factor flow frame 16 70
4.28 velocity estimation in the z-direction for different lags from area 1 with same interpolation factor flow frame 24 71
4.29 velocity estimation in the z-direction for different lags from area 1 with same interpolation factor flow frame 27 71
4.30 velocity estimation in the z-direction for different lags from area 1 with same interpolation factor flow frame 36 72
4.31 Standard deviation for the velocity estimates in the z-direction for different lags from area 1 with the same interpolation-factor 72
4.32 Standard deviation for the velocity estimates in the x-direction for different lags from area 1 with the same interpolation-factor 73
4.33 Mean cross-correlation for all lags over all frames for area 1 . . 73
4.34 Bias for the velocity estimates in the x-direction for different lags from area 1 with the same interpolation-factor 74
4.35 Bias for the velocity estimates in the z-direction for different lags from area 1 with the same interpolation-factor 74
4.36 Velocity estimates in the x-direction for different lags from area 1 with the same interpolation-factor in the middle of the tube for all flow frames 75
4.37 Velocity estimates in the z-direction for different lags from area 1 with the same interpolation-factor in the middle of the tube for all flow frames 75
4.38 velocity estimation in the x-direction for different lags from area 2 with same interpolation-factor flow frame 2 76
4.39 velocity estimation in the x-direction for different lags from area 2 with same interpolation-factor flow frame 4 76
4.40 velocity estimation in the x-direction for different lags from area 2 with same interpolation-factor flow frame 6 77
4.41 velocity estimation in the x-direction for different lags from area 2 with same interpolation-factor flow frame 7 77
4.42 velocity estimation in the x-direction for different lags from area 2 with same interpolation-factor flow frame 11 78
4.43 velocity estimation in the x-direction for different lags from area 2 with same interpolation-factor flow frame 16 78
4.44 velocity estimation in the x-direction for different lags from area 2 with same interpolation-factor flow frame 24 79
4.45 velocity estimation in the x-direction for different lags from area 2 with same interpolation-factor flow frame 27 79

4.46 velocity estimation in the x-direction for different lags from area 2 with same interpolation-factor flow frame 36 80
4.47 velocity estimation in the z-direction for different lags from area 2 with same interpolation-factor flow frame 2 80
4.48 velocity estimation in the z-direction for different lags from area 2 with same interpolation-factor flow frame 4 81
4.49 velocity estimation in the z-direction for different lags from area 2 with same interpolation-factor flow frame 6 81
4.50 velocity estimation in the z-direction for different lags from area 2 with same interpolation-factor flow frame 7 82
4.51 velocity estimation in the z-direction for different lags from area 2 with same interpolation-factor flow frame 11 82
4.52 velocity estimation in the z-direction for different lags from area 2 with same interpolation-factor flow frame 16 83
4.53 velocity estimation in the z-direction for different lags from area 2 with same interpolation-factor flow frame 24 83
4.54 velocity estimation in the z-direction for different lags from area 2 with same interpolation-factor flow frame 27 84
4.55 velocity estimation in the z-direction for different lags from area 2 with same interpolation-factor flow frame 36 84
4.56 Standard deviation for the velocity estimates in the z-direction for different lags from area 2 with the same interpolation-factor 85
4.57 Standard deviation for the velocity estimates in the x-direction for different lags from area 2 with the same interpolation-factor 85
4.58 Mean cross-correlation for all lags over all frames for area 2 . . 86
4.59 Bias for the velocity estimates in the x-direction for different lags from area 2 with the same interpolation-factor 86
4.60 Bias for the velocity estimates in the z-direction for different lags from area 2 with the same interpolation-factor 87
4.61 Velocity estimates in the x-direction for different lags from area 2 with the same interpolation-factor in the middle of the tube for all flow frames 87
4.62 Velocity estimates in the z-direction for different lags from area 2 with the same interpolation-factor in the middle of the tube for all flow frames 88
4.63 velocity estimation in the x-direction for different lags from area 3 with same interpolation-factor flow frame 2 88
4.64 velocity estimation in the x-direction for different lags from area 3 with same interpolation-factor flow frame 4 89
4.65 velocity estimation in the x-direction for different lags from area 3 with same interpolation-factor flow frame 6 89

4.66 velocity estimation in the x-direction for different lags from area 2 with same interpolation-factor flow frame 11 90
4.67 velocity estimation in the x-direction for different lags from area 3 with same interpolation-factor flow frame 16 90
4.68 velocity estimation in the x-direction for different lags from area 3 with same interpolation-factor flow frame 27 91
4.69 velocity estimation in the z-direction for different lags from area 3 with same interpolation-factor flow frame 2 91
4.70 velocity estimation in the z-direction for different lags from area 3 with same interpolation-factor flow frame 4 92
4.71 velocity estimation in the z-direction for different lags from area 3 with same interpolation-factor flow frame 6 92
4.72 velocity estimation in the z-direction for different lags from area 3 with same interpolation-factor flow frame 11 93
4.73 velocity estimation in the z-direction for different lags from area 3 with same interpolation-factor flow frame 16 93
4.74 velocity estimation in the z-direction for different lags from area 3 with same interpolation-factor flow frame 27 94
4.75 Standard deviation for the velocity estimates in the x-direction for different lags from area 3 with the same interpolation-factor 94
4.76 Standard deviation for the velocity estimates in the z-direction for different lags from area 3 with the same interpolation-factor 95
4.77 Mean cross-correlation for all lags over all frames for area 3 . . 95
4.78 Bias for the velocity estimates in the x-direction for different lags from area 3 with the same interpolation-factor 96
4.79 Bias for the velocity estimates in the z-direction for different lags from area 3 with the same interpolation-factor 96
4.80 Velocity estimates in the x-direction for different lags from area 3 with the same interpolation-factor in the middle of the tube for all flow frames 97
4.81 Velocity estimates in the z-direction for different lags from area 3 with the same interpolation-factor in the middle of the tube for all flow frames 97
4.82 Velocity estimation in the x-direction for lag=1, lag=2, lag=3, lag=4 and the median of all the lags for flow frame 2 from area 1 98
4.83 Velocity estimation in the z-direction for lag=1, lag=2, lag=3, lag=4 and the median of all the lags for flow frame 2 from area 1 99
4.84 Cross correlation for lag=1, lag=2,lag=3 and lag=4 for flow frame 2 from area 1 99
4.85 Velocity estimation in the x-direction for lag=1, lag=2, lag=3, lag=4 and the median of all the lags for flow frame 4 from area 1100

4.86 Velocity estimation in the z-direction for lag=1, lag=2, lag=3, lag=4 and the median of all the lags for flow frame 4 from area 1 100
4.87 Cross correlation for lag=1, lag=2,lag=3 and lag=4 for flow frame 4 from area 1 101
4.88 Velocity estimation in the x-direction for lag=1, lag=2, lag=3, lag=4 and the median of all the lags for flow frame 6 from area 1 101
4.89 Velocity estimation in the z-direction for lag=1, lag=2, lag=3, lag=4 and the median of all the lags for flow frame 6 from area 1 102
4.90 Cross correlation for lag=1, lag=2,lag=3 and lag=4 for flow frame 6 from area 1 102
4.91 Velocity estimation in the x-direction for lag=1, lag=2, lag=3, lag=4 and the median of all the lags for flow frame 7 from area 1 103
4.92 Velocity estimation in the z-direction for lag=1, lag=2, lag=3, lag=4 and the median of all the lags for flow frame 7 from area 1 103
4.93 Cross correlation for lag=1, lag=2,lag=3 and lag=4 for flow frame 7 from area 1 104
4.94 Velocity estimation in the x-direction for lag=1, lag=2, lag=3, lag=4 and the median of all the lags for flow frame 11 from area 1 104
4.95 Velocity estimation in the z-direction for lag=1, lag=2, lag=3, lag=4 and the median of all the lags for flow frame 11 from area 1 105
4.96 Cross correlation for lag=1, lag=2,lag=3 and lag=4 for flow frame 11 from area 1 105
4.97 Velocity estimation in the x-direction for lag=1, lag=2, lag=3, lag=4 and the median of all the lags for flow frame 16 from area 1 106
4.98 Velocity estimation in the z-direction for lag=1, lag=2, lag=3, lag=4 and the median of all the lags for flow frame 16 from area 1 106
4.99 Cross correlation for lag=1, lag=2,lag=3 and lag=4 for flow frame 16 from area 1 107
4.100 Velocity estimation in the x-direction for lag=1, lag=2, lag=3, lag=4 and the median of all the lags for flow frame 24 from area 1 107
4.101 Velocity estimation in the z-direction for lag=1, lag=2, lag=3, lag=4 and the median of all the lags for flow frame 24 from area 1 108
4.102 Cross correlation for lag=1, lag=2,lag=3 and lag=4 for flow frame 24 from area 1 108

4.103Velocity estimation in the x-direction for lag=1, lag=2, lag=3, lag=4 and the median of all the lags for flow frame 27 from area 1 109
4.104Velocity estimation in the z-direction for lag=1, lag=2, lag=3, lag=4 and the median of all the lags for flow frame 27 from area 1 109
4.105Cross correlation for lag=1, lag=2,lag=3 and lag=4 for flow frame 27 from area 1 110
4.106Velocity estimation in the x-direction for lag=1, lag=2, lag=3, lag=4 and the median of all the lags for flow frame 36 from area 1 110
4.107Velocity estimation in the z-direction for lag=1, lag=2, lag=3, lag=4 and the median of all the lags for flow frame 36 from area 1 111
4.108Cross correlation for lag=1, lag=2,lag=3 and lag=4 for flow frame 36 from area 1 111
4.109Standard deviation for the velocity estimates in the x-direction for lag= 1, lag=2, lag=3, lag=4 and median of all lags from area 1 112
4.110Standard deviation for the velocity estimates in the z-direction for lag= 1, lag=2, lag=3, lag=4 and median of all lags from area 1 112
4.111Bias between the velocity estimates in the x-direction for lag= 1, lag=2, lag=3 and lag=4 and ground truth from area 1 . . . 113
4.112Bias between the velocity estimates in the z-direction for lag= 1, lag=2, lag=3 and lag=4 and ground truth from area 1 . . . 113
4.113Velocity estimates in the x-direction for lag= 1, lag=2, lag=3, lag=4 and the median of all the lags in the middle of the tube for all flow frames from area 1 114
4.114Velocity estimates in the z-direction for lag= 1, lag=2, lag=3, lag=4 and the median of all the lags in the middle of the tube for all flow frames from area 1 114
4.115Velocity estimation in the x-direction for lag=1, lag=2, lag=3, lag=4 and the median of all the lags for flow frame 2 from area 2115
4.116Velocity estimation in the z-direction for lag=1, lag=2, lag=3, lag=4 and the median of all the lags for flow frame 2 from area 2115
4.117Cross correlation for lag=1, lag=2,lag=3 and lag=4 for flow frame 2 from area 2 116
4.118Velocity estimation in the x-direction for lag=1, lag=2, lag=3, lag=4 and the median of all the lags for flow frame 4 from area 2116

4.119Velocity estimation in the z-direction for lag=1, lag=2, lag=3, lag=4 and the median of all the lags for flow frame 4 from area 2 117
4.120Cross correlation for lag=1, lag=2,lag=3 and lag=4 for flow frame 4 from area 2 117
4.121Velocity estimation in the x-direction for lag=1, lag=2, lag=3, lag=4 and the median of all the lags for flow frame 6 from area 2 118
4.122Velocity estimation in the z-direction for lag=1, lag=2, lag=3, lag=4 and the median of all the lags for flow frame 6 from area 2 118
4.123Cross correlation for lag=1, lag=2,lag=3 and lag=4 for flow frame 6 from area 2 119
4.124Velocity estimation in the x-direction for lag=1, lag=2, lag=3, lag=4 and the median of all the lags for flow frame 7 from area 2 119
4.125Velocity estimation in the z-direction for lag=1, lag=2, lag=3, lag=4 and the median of all the lags for flow frame 7 from area 2 120
4.126Cross correlation for lag=1, lag=2,lag=3 and lag=4 for flow frame 7 from area 2 120
4.127Velocity estimation in the x-direction for lag=1, lag=2, lag=3, lag=4 and the median of all the lags for flow frame 11 from area 2 121
4.128Velocity estimation in the z-direction for lag=1, lag=2, lag=3, lag=4 and the median of all the lags for flow frame 11 from area 2 121
4.129Cross correlation for lag=1, lag=2,lag=3 and lag=4 for flow frame 11 from area 2 122
4.130Velocity estimation in the x-direction for lag=1, lag=2, lag=3, lag=4 and the median of all the lags for flow frame 16 from area 2 122
4.131Velocity estimation in the z-direction for lag=1, lag=2, lag=3, lag=4 and the median of all the lags for flow frame 16 from area 2 123
4.132Cross correlation for lag=1, lag=2,lag=3 and lag=4 for flow frame 16 from area 2 123
4.133Velocity estimation in the x-direction for lag=1, lag=2, lag=3, lag=4 and the median of all the lags for flow frame 24 from area 2 124
4.134Velocity estimation in the z-direction for lag=1, lag=2, lag=3, lag=4 and the median of all the lags for flow frame 24 from area 2 124
4.135Cross correlation for lag=1, lag=2,lag=3 and lag=4 for flow frame 24 from area 2 125

4.136Velocity estimation in the x-direction for lag=1, lag=2, lag=3, lag=4 and the median of all the lags for flow frame 27 from area 2 125
4.137Velocity estimation in the z-direction for lag=1, lag=2, lag=3, lag=4 and the median of all the lags for flow frame 27 from area 2 126
4.138Cross correlation for lag=1, lag=2,lag=3 and lag=4 for flow frame 2 from area 27 126
4.139Velocity estimation in the x-direction for lag=1, lag=2, lag=3, lag=4 and the median of all the lags for flow frame 36 from area 2 127
4.140Velocity estimation in the z-direction for lag=1, lag=2, lag=3, lag=4 and the median of all the lags for flow frame 36 from area 2 127
4.141Cross correlation for lag=1, lag=2,lag=3 and lag=4 for flow frame 36 from area 2 128
4.142Standard deviation for the velocity estimates in the x-direction for lag= 1, lag=2, lag=3, lag=4 and median of all lags from area 2 128
4.143Standard deviation for the velocity estimates in the z-direction for lag= 1, lag=2, lag=3, lag=4 and median of all lags from area 2 129
4.144Bias between the velocity estimates in the x-direction for lag= 1, lag=2, lag=3 and lag=4 and ground truth from area 2 . . . 129
4.145Bias between the velocity estimates in the z-direction for lag= 1, lag=2, lag=3 and lag=4 and ground truth from area 2 . . . 130
4.146Velocity estimates in the x-direction for lag= 1, lag=2, lag=3, lag=4 and the median of all the lags in the middle of the tube for all flow frames from area 2 130
4.147Velocity estimates in the z-direction for lag= 1, lag=2, lag=3, lag=4 and the median of all the lags in the middle of the tube for all flow frames from area 2 131
4.148Velocity estimation in the x-direction for lag=1, lag=2, lag=3, lag=4 and the median of all the lags for flow frame 2 from area 3131
4.149Velocity estimation in the z-direction for lag=1, lag=2, lag=3, lag=4 and the median of all the lags for flow frame 2 from area 3132
4.150Cross correlation for lag=1, lag=2,lag=3 and lag=4 for flow frame 2 from area 3 132
4.151Velocity estimation in the x-direction for lag=1, lag=2, lag=3, lag=4 and the median of all the lags for flow frame 4 from area 3133

4.152Velocity estimation in the z-direction for lag=1, lag=2, lag=3, lag=4 and the median of all the lags for flow frame 4 from area 3 133
4.153Cross correlation for lag=1, lag=2,lag=3 and lag=4 for flow frame 4 from area 3 134
4.154Velocity estimation in the x-direction for lag=1, lag=2, lag=3, lag=4 and the median of all the lags for flow frame 6 from area 3 134
4.155Velocity estimation in the z-direction for lag=1, lag=2, lag=3, lag=4 and the median of all the lags for flow frame 6 from area 3 135
4.156Cross correlation for lag=1, lag=2,lag=3 and lag=4 for flow frame 6 from area 3 135
4.157Velocity estimation in the x-direction for lag=1, lag=2, lag=3, lag=4 and the median of all the lags for flow frame 11 from area 3 136
4.158Velocity estimation in the z-direction for lag=1, lag=2, lag=3, lag=4 and the median of all the lags for flow frame 11 from area 3 136
4.159Cross correlation for lag=1, lag=2,lag=3 and lag=4 for flow frame 11 from area 3 137
4.160Velocity estimation in the x-direction for lag=1, lag=2, lag=3, lag=4 and the median of all the lags for flow frame 16 from area 3 137
4.161Velocity estimation in the z-direction for lag=1, lag=2, lag=3, lag=4 and the median of all the lags for flow frame 16 from area 3 138
4.162Cross correlation for lag=1, lag=2,lag=3 and lag=4 for flow frame 16 from area 3 138
4.163Velocity estimation in the x-direction for lag=1, lag=2, lag=3, lag=4 and the median of all the lags for flow frame 27 from area 3 139
4.164Velocity estimation in the z-direction for lag=1, lag=2, lag=3, lag=4 and the median of all the lags for flow frame 27 from area 3 139
4.165Cross correlation for lag=1, lag=2,lag=3 and lag=4 for flow frame 27 from area 3 140
4.166Velocity estimation in the x-direction for lag=1, lag=2, lag=3, lag=4 and the median of all the lags for flow frame 36 from area 3 140
4.167Velocity estimation in the z-direction for lag=1, lag=2, lag=3, lag=4 and the median of all the lags for flow frame 36 from area 3 141

4.168Cross correlation for lag=1, lag=2,lag=3 and lag=4 for flow frame 36 from area 3 141
4.169Standard deviation for the velocity estimates in the x-direction for lag= 1, lag=2, lag=3, lag=4 and median of all lags from area 3 142
4.170Standard deviation for the velocity estimates in the z-direction for lag= 1, lag=2, lag=3, lag=4 and median of all lags from area 3 142
4.171Bias between the velocity estimates in the x-direction for lag= 1, lag=2, lag=3 and lag=4 and ground truth from area 3 . . . 143
4.172Bias between the velocity estimates in the z-direction for lag= 1, lag=2, lag=3 and lag=4 and ground truth from area 3 . . . 143
4.173Velocity estimates in the x-direction for lag= 1, lag=2, lag=3, lag=4 and the median of all the lags in the middle of the tube for all flow frames from area 3 144
4.174Velocity estimates in the z-direction for lag= 1, lag=2, lag=3, lag=4 and the median of all the lags in the middle of the tube for all flow frames from area 3 144
4.175Velocity estimations in the x-direction with the original speckle tracking algorithm, the adaptive speckle tracking algorithm with finer grid and multi-lag tracking for flow frame 2 from area 1 145
4.176Velocity estimations in the z-direction with the original speckle tracking algorithm, the adaptive speckle tracking algorithm with finer grid and multi-lag tracking for flow frame 2 from area 1 146
4.177Velocity estimations in the x-direction with the original speckle tracking algorithm, the adaptive speckle tracking algorithm with finer grid and multi-lag tracking for flow frame 5 from area 1 146
4.178Velocity estimations in the z-direction with the original speckle tracking algorithm, the adaptive speckle tracking algorithm with finer grid and multi-lag tracking for flow frame 5 from area 1 147
4.179Velocity estimations in the x-direction with the original speckle tracking algorithm, the adaptive speckle tracking algorithm with finer grid and multi-lag tracking for flow frame 6 from area 1 147

4.180 Velocity estimations in the z-direction with the original speckle tracking algorithm, the adaptive speckle tracking algorithm with finer grid and multi-lag tracking for flow frame 6 from area 1 . . . 148
4.181 Velocity estimations in the x-direction with the original speckle tracking algorithm, the adaptive speckle tracking algorithm with finer grid and multi-lag tracking for flow frame 16 from area 1 . . . 148
4.182 Velocity estimations in the z-direction with the original speckle tracking algorithm, the adaptive speckle tracking algorithm with finer grid and multi-lag tracking for flow frame 16 from area 1 . . . 149
4.183 Velocity estimations in the x-direction with the original speckle tracking algorithm, the adaptive speckle tracking algorithm with finer grid and multi-lag tracking for flow frame 24 from area 1 . . . 149
4.184 Velocity estimations in the z-direction with the original speckle tracking algorithm, the adaptive speckle tracking algorithm with finer grid and multi-lag tracking for flow frame 24 from area 1 . . . 150
4.185 Velocity estimations in the x-direction with the original speckle tracking algorithm, the adaptive speckle tracking algorithm with finer grid and multi-lag tracking for flow frame 27 from area 1 . . . 150
4.186 Velocity estimations in the z-direction with the original speckle tracking algorithm, the adaptive speckle tracking algorithm with finer grid and multi-lag tracking for flow frame 27 from area 1 . . . 151
4.187 Mean cross correlation between the kernel and best match for the original speckle tracking algorithm, the adaptive speckle tracking algorithm with finer grid and multi-lag tracking for all frames from area 1 . . . 151
4.188 Standard deviation in velocity estimations in the x-direction with the original speckle tracking algorithm, the adaptive speckle tracking algorithm with finer grid and multi-lag tracking from area 2 . . . 152
4.189 Standard deviation in velocity estimations in the z-direction with the original speckle tracking algorithm, the adaptive speckle tracking algorithm with finer grid and multi-lag tracking from area 1 . . . 152

4.190Bias between the velocity estimates in the x-direction with the original speckle tracking algorithm, the adaptive speckle tracking algorithm with finer grid and multi-lag tracking from area 1 153
4.191Bias between the velocity estimates in the z-direction with the original speckle tracking algorithm, the adaptive speckle tracking algorithm with finer grid and multi-lag tracking from area 2 153
4.192Velocity estimates in the middle of the artery in the x-direction with the original speckle tracking algorithm, the adaptive speckle tracking algorithm with finer grid and multi-lag tracking from area 1 154
4.193Velocity estimates in the middle in the z-direction with the original speckle tracking algorithm, the adaptive speckle tracking algorithm with finer grid and multi-lag tracking from area 1 154
4.194Velocity estimations in the x-direction with the original speckle tracking algorithm, the adaptive speckle tracking algorithm with finer grid and multi-lag tracking for flow frame 2 from area 2 155
4.195Velocity estimations in the z-direction with the original speckle tracking algorithm, the adaptive speckle tracking algorithm with finer grid and multi-lag tracking for flow frame 2 from area 2 155
4.196Velocity estimations in the x-direction with the original speckle tracking algorithm, the adaptive speckle tracking algorithm with finer grid and multi-lag tracking for flow frame 5 from area 2 156
4.197Velocity estimations in the z-direction with the original speckle tracking algorithm, the adaptive speckle tracking algorithm with finer grid and multi-lag tracking for flow frame 5 from area 2 156
4.198Velocity estimations in the x-direction with the original speckle tracking algorithm, the adaptive speckle tracking algorithm with finer grid and multi-lag tracking for flow frame 6 from area 2 157
4.199Velocity estimations in the z-direction with the original speckle tracking algorithm, the adaptive speckle tracking algorithm with finer grid and multi-lag tracking for flow frame 6 from area 2 157

4.200 Velocity estimations in the x-direction with the original speckle tracking algorithm, the adaptive speckle tracking algorithm with finer grid and multi-lag tracking for flow frame 16 from area 2 . . . 158
4.201 Velocity estimations in the z-direction with the original speckle tracking algorithm, the adaptive speckle tracking algorithm with finer grid and multi-lag tracking for flow frame 16 from area 2 . . . 158
4.202 Velocity estimations in the x-direction with the original speckle tracking algorithm, the adaptive speckle tracking algorithm with finer grid and multi-lag tracking for flow frame 24 from area 2 . . . 159
4.203 Velocity estimations in the z-direction with the original speckle tracking algorithm, the adaptive speckle tracking algorithm with finer grid and multi-lag tracking for flow frame 24 from area 2 . . . 159
4.204 Velocity estimations in the x-direction with the original speckle tracking algorithm, the adaptive speckle tracking algorithm with finer grid and multi-lag tracking for flow frame 27 from area 2 . . . 160
4.205 Velocity estimations in the z-direction with the original speckle tracking algorithm, the adaptive speckle tracking algorithm with finer grid and multi-lag tracking for flow frame 27 from area 2 . . . 160
4.206 Mean cross correlation between the kernel and best match for the original speckle tracking algorithm, the adaptive speckle tracking algorithm with finer grid and multi-lag tracking for all frames from area 2 . . . 161
4.207 Standard deviation in velocity estimations in the x-direction with the original speckle tracking algorithm, the adaptive speckle tracking algorithm with finer grid and multi-lag tracking from area 2 . . . 161
4.208 Standard deviation in velocity estimations in the z-direction with the original speckle tracking algorithm, the adaptive speckle tracking algorithm with finer grid and multi-lag tracking from area 2 . . . 162
4.209 Bias between the velocity estimates in the x-direction with the original speckle tracking algorithm, the adaptive speckle tracking algorithm with finer grid and multi-lag tracking from area 2 . . . 162

4.210Bias between the velocity estimates in the z-direction with the original speckle tracking algorithm, the adaptive speckle tracking algorithm with finer grid and multi-lag tracking from area 2 163
4.211Velocity estimates in the middle of the artery in the x-direction with the original speckle tracking algorithm, the adaptive speckle tracking algorithm with finer grid and multi-lag tracking from area 2 163
4.212Velocity estimates in the middle in the z-direction with the original speckle tracking algorithm, the adaptive speckle tracking algorithm with finer grid and multi-lag tracking from area 2 164
4.213Velocity estimations in the x-direction with the original speckle tracking algorithm, the adaptive speckle tracking algorithm with finer grid and multi-lag tracking for flow frame 2 from area 3 164
4.214Velocity estimations in the z-direction with the original speckle tracking algorithm, the adaptive speckle tracking algorithm with finer grid and multi-lag tracking for flow frame 2 from area 3 165
4.215Velocity estimations in the x-direction with the original speckle tracking algorithm, the adaptive speckle tracking algorithm with finer grid and multi-lag tracking for flow frame 5 from area 3 165
4.216Velocity estimations in the z-direction with the original speckle tracking algorithm, the adaptive speckle tracking algorithm with finer grid and multi-lag tracking for flow frame 5 from area 3 166
4.217Velocity estimations in the x-direction with the original speckle tracking algorithm, the adaptive speckle tracking algorithm with finer grid and multi-lag tracking for flow frame 6 from area 3 166
4.218Velocity estimations in the z-direction with the original speckle tracking algorithm, the adaptive speckle tracking algorithm with finer grid and multi-lag tracking for flow frame 6 from area 3 167
4.219Velocity estimations in the x-direction with the original speckle tracking algorithm, the adaptive speckle tracking algorithm with finer grid and multi-lag tracking for flow frame 16 from area 3 167

4.220 Velocity estimations in the z-direction with the original speckle tracking algorithm, the adaptive speckle tracking algorithm with finer grid and multi-lag tracking for flow frame 16 from area 3 . . . 168
4.221 Velocity estimations in the x-direction with the original speckle tracking algorithm, the adaptive speckle tracking algorithm with finer grid and multi-lag tracking for flow frame 24 from area 3 . . . 168
4.222 Velocity estimations in the z-direction with the original speckle tracking algorithm, the adaptive speckle tracking algorithm with finer grid and multi-lag tracking for flow frame 24 from area 3 . . . 169
4.223 Velocity estimations in the x-direction with the original speckle tracking algorithm, the adaptive speckle tracking algorithm with finer grid and multi-lag tracking for flow frame 27 from area 3 . . . 169
4.224 Velocity estimations in the z-direction with the original speckle tracking algorithm, the adaptive speckle tracking algorithm with finer grid and multi-lag tracking for flow frame 27 from area 3 . . . 170
4.225 Mean cross correlation between the kernel and best match for the original speckle tracking algorithm, the adaptive speckle tracking algorithm with finer grid and multi-lag tracking for all frames from area 3 . . . 170
4.226 Standard deviation in velocity estimations in the x-direction with the original speckle tracking algorithm, the adaptive speckle tracking algorithm with finer grid and multi-lag tracking from area 3 . . . 171
4.227 Standard deviation in velocity estimations in the z-direction with the original speckle tracking algorithm, the adaptive speckle tracking algorithm with finer grid and multi-lag tracking from area 3 . . . 171
4.228 Bias between the velocity estimates in the x-direction with the original speckle tracking algorithm, the adaptive speckle tracking algorithm with finer grid and multi-lag tracking from area 3 . . . 172
4.229 Bias between the velocity estimates in the z-direction with the original speckle tracking algorithm, the adaptive speckle tracking algorithm with finer grid and multi-lag tracking from area 3 . . . 172

4.230Velocity estimates in the middle of the artery in the x-direction with the original speckle tracking algorithm, the adaptive speckle tracking algorithm with finer grid and multi-lag tracking from area 3 173
4.231Velocity estimates in the middle of the artery in the z-direction with the original speckle tracking algorithm, the adaptive speckle tracking algorithm with finer grid and multi-lag tracking from area 3 173

5.1 Mean velocity in the x-direction from round 4 in the adaptive speckle tracking algorithm with the region of interest indicated by the blue dots area 3 Flow frame 4 176
5.2 Velocity from Ground Truth in the x-direction with the region of interest indicated by the white lines area 3 Flow frame 4 . 176

List of Tables

4.1 Standard deviation of the velocity estimates in area 1 flow frame 4 with SNR=30 55
4.2 Standard deviation of the velocity estimates in area 1 flow frame 4 with SNR=20 56
4.3 Standard deviation of the velocity estimates in area 2 flow frame 4 with SNR=30 58
4.4 Standard deviation of the velocity estimates in area 2 flow frame 4 with SNR=20 59
4.5 Standard deviation of the velocity estimates in area 3 flow frame 4 with SNR=30 61
4.6 Standard deviation of the velocity estimates in area 3 flow frame 4 with SNR=20 62

Chapter 1

Introduction

Cardiac flow patterns may reveal several kinds of cardiovascular diseases. Well known examples include the detection and quantification of leaky heart valves and poor systolic and diastolic function. Doppler ultrasound has become widespread for imaging of flow and quantifying blood and tissue velocities. However, the use of conventional blood flow imaging techniques is limited because they can only measure the velocity component along the beam, i.e they are angel dependant. In addition conventional imaging techniques are limited by aliasing [1]. Speckle tracking methods have the potential to overcome these limitations. The speckle tracking method make use of the correlation between the movement of the speckle patterns in the ultrasound image and the movement of the ultrasound scatters. The blood speckle patterns are tracked to find the velocity estimates of blood flow in the axial and lateral direction [2]. Blood speckle tracking has not yet been established for clinical use, mostly due to lack of robustness of the estimates. Current speckle tracking methods are based on an algorithm that calculates the most likely displacement of the speckle patterns. This is done without taking into account any a priori knowledge of the blood flow velocity. Thus, the aim of this master thesis was to overall improve the robustness of the current speckle tracking algorithm. This thesis is a continuation of my project work. Several methods for improving the robustness of the speckle tracking algorithm was tested. The speckle tracking algorithm was made more adaptive, by utilizing speckle tracking estimates from the previous flow frame to adaptively place and update the size of the search region to the velocity changes over the heart cycle. While minimizing the search region, the tracking grid was made finer, by increasing the points in the beam and range tracking vectors. A multi-lag tracking method was also proposed and tested, by adaptively finding the best

tracking lag at the specific location over time. The proposed methods was tested on simulated data of a Carotid artery.

Chapter 2

Theory

In this chapter the required background material is presented. First conventional Doppler methods are introduced, where Pulsed Wave Doppler, Continuous Wave Doppler and Color Flow imaging are discussed. Then methods for two-dimensional velocity estimation are presented. After that different pattern matching algorithms are presented, including Sum of Squared Differences, Sum of Absolute Differences and the Normalized correlation algorithm.

2.1 Doppler ultrasound

Doppler ultrasound techniques are used to measure and display blood flow in the body. The Doppler Effect is the perceived change in frequency as a sound source is moving away or towards an observer. Sound is mechanical disturbance and the frequency perceived is the effective periodicity of the wave fronts. If the source is moving towards the observer the peaks appear closer together and this gives the illusion of higher frequency. The Doppler imaging technique use the fact that if the scatterers are moving, the frequency of the back scattered signal will be different from the transmitted frequency. This change in frequency is called the Doppler effect [3]. The equation for the Doppler shift, the difference in frequency between the transmitted and received frequency is given by,

$$f_d = 2f_0 \frac{v \cos\theta}{c}, \tag{2.1}$$

where f_0 is the transmit frequency, c is the speed of sound in the medium,

v is the velocity of the scatterer and θ is the angle between the ultrasound beam and the direction of the velocity of the scatterer.

The Doppler shift is used to estimate the blood velocity, the movement of the red blood cells. The Doppler shift given in eq 2.1 is angle dependent, so θ must be estimated to get the blood velocity. Angle correction is not always easy and can lead to under- or over-estimation of the blood flow. This characteristic of the Doppler shift is one of the main limitations of the Doppler imaging techniques. When the ultrasound beam is perpendicular to the direction of the blood the radial component of the velocity is zero, and no Doppler shift is registered.

2.1.1 Continuous Wave Doppler (CW-Doppler)

With the Continuous Wave Doppler method an ultrasound beam is continuously transmitted from one transducer into the tissue and continuously received at another transducer [3]. The ultrasound probe is usually divided into two equal parts, one for transmitting the ultrasound beam and one for receiving it. The received frequency is compared to the transmitted frequency. Since the returned signal is continuous the CW Doppler have no range resolution, therefore it is not possible to find the location in depth of the scatterers. One advantage of imaging with the CW Doppler is that there is no frequency aliasing, meaning there is no limit on the maximum velocity that can be measured.

2.1.2 Pulsed Wave Doppler (PW-Doppler)

Pulsed Wave Doppler [3] transmits and receives one ultrasound pulse at the time. Ultrasound pulses of a certain length are send to a target at a certain range. In PW Doppler the received echo is compared to an echo transmission. The phase or time shift between the echoes is used to estimate the blood velocity. It is this feature about the PW-Doppler that makes it possible to find the location of depth of the scatters [3] [4]. With PW-Doppler the sampling frequency of the transmitted beam sets a limit to the maximum possible velocity that can be imaged. The maximum possible velocity that can be imaged without frequency aliasing is determined by the Nyquist limit on the frequency,

$$f_d < \frac{f_s}{2}, \tag{2.2}$$

where f_d is the Doppler shift and f_s is the sampling frequency. With PW-Doppler the signal is sampled for every pulse transmitted, e.i the sampling frequency is the pulse repetition frequency (PRF). The Nyquist limit is the requirement of the Shannon sampling theorem for reconstruction of a signal without errors. If the Doppler shift is above the Nyquist limit frequency aliasing occurs. Frequency aliasing is frequency downfolding; if the Doppler shift is above the Nyquist limit the top of the frequency spectrum is cut off and moved to negative frequencies.

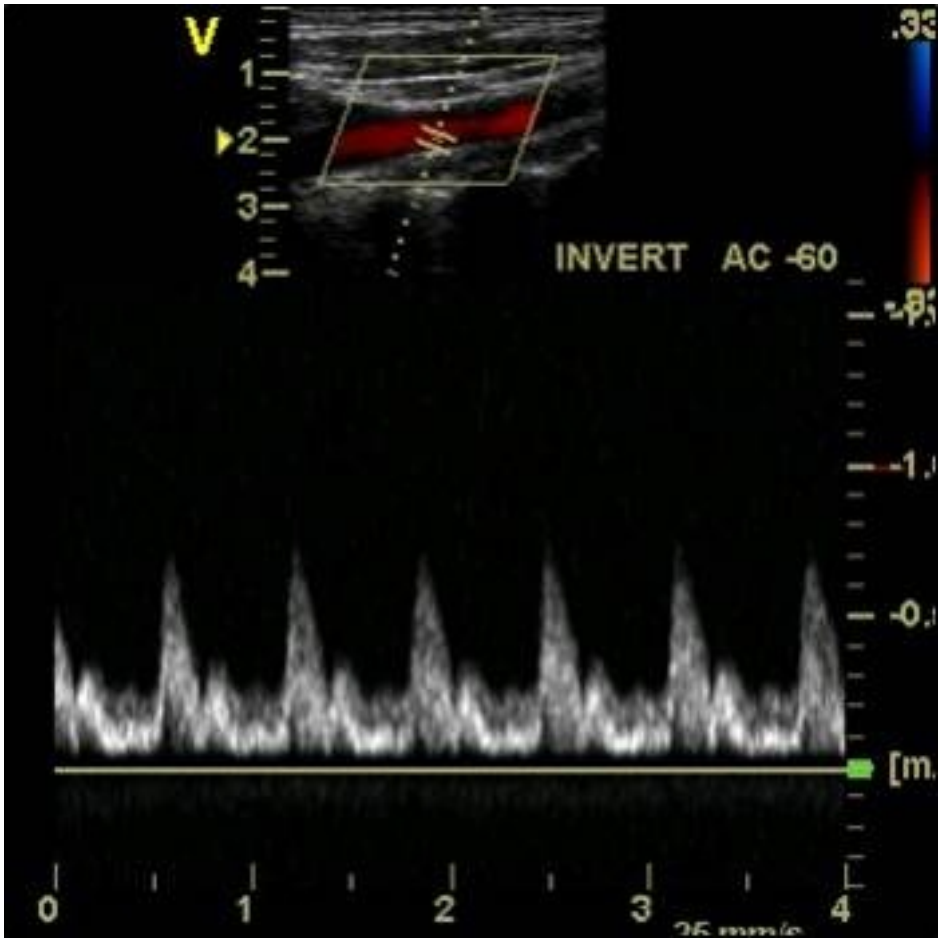

Figure 2.1: Pulsed wave Doppler spectrum.

To increase the Nyquist limit from the Shannon sampling theorem it is possible to increase the pulse repetition frequency. Increasing the pulse repeti-

tion frequency means reducing the time between the transmitted pulses, this might lead to several pulses in the blood pool at the same time. This can cause range ambiguity, concerning which range the sampled signal is coming from.

To avoid having more than one pulse propagating in the blood pool at the same time, a low pulse repetition frequency must be used. This produces a low Nyquist limit according to equation 2.2. The velocities in the various jet flows found in heart defects (valve stenoses and regurgitations, ventricular septal defects, and patent ductus arterious) often produces Doppler shifts that exceeds the Nyquist limit [3]. The Pulsed Wave Doppler cannot be used to image these Doppler shifts without aliasing.

2.1.3 Color flow imaging

In color flow imaging, the image region is scanned line by line and series of ultrasound pulses are transmitted in each beam direction at a certain pulse repetition frequency [4] [5]. A 2D color map of the estimated ultrasound velocities are displayed on top of a B-mode image. B-mode imaging displays the amplitude of the sampled signal with brightness. The B-mode image is acquired by sweeping the transmitted sound wave across the plane to produce a 2D image, where depth is on the z-axis and azimuth is along the x-axis. The position of the echo is determined by its acoustic transmit time and beam direction in the plane. The color image depicts an estimate of the blood flow mean velocity, where a color code is used to indicate the direction and the magnitude of the blood flow. A red color is used for positive frequencies, denoting flow towards the transducer, and blue is used for negative frequencies, denoting blood flow away from the transducer. Turbulence is denoted by a green color. The magnitude of the blood flow is represented by the color strength, where a larger magnitude is displayed with a stronger color and a smaller magnitude is denoted by a lighter color.

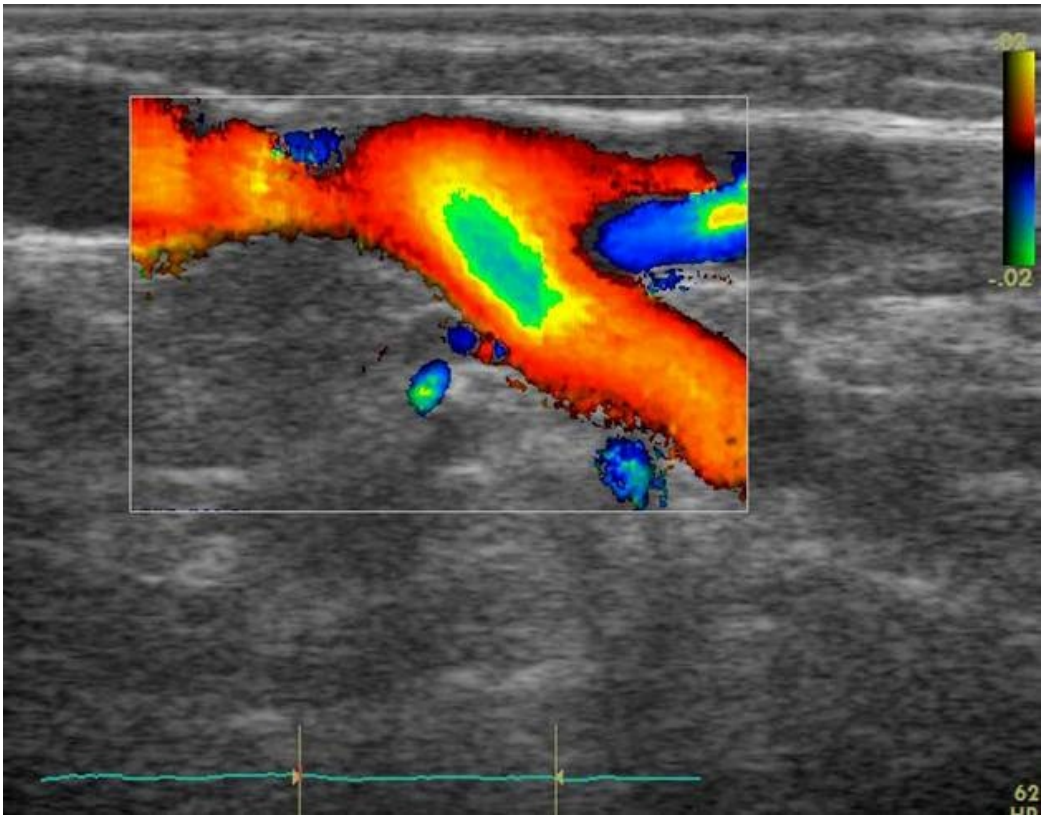

Figure 2.2: Color Flow image of carotid artery.

2.2 2D-velocity estimation

Conventional Doppler methods can only find velocity estimates in one-dimension. In this section two ways of doing 2D-velocity estimation is presented, vector Doppler and Speckle tracking.

2.2.1 Vector Doppler

In section 2.1 conventional Doppler imaging techniques was discussed. One limitation of Doppler imaging is angle dependency. With Doppler imaging it is only possible to find velocity along the ultrasound beam. It is only possible to use Doppler imaging to find velocity estimates along the ultrasound beam. However, in many clinical areas complex flow patterns are present, making the assumption of the beam-to-vessel angle insufficient [6]. The vec-

tor Doppler method is one way to overcome the angle dependency limitation of Doppler imaging and doing two-dimensional velocity estimation. With vector Doppler the flow vector is obtained by combining Doppler measurements taken at a region from multiple independent directions. The Doppler measurements can be found either by the use of one single transducer moved through multiple positions, or by arrangement of multiple transducers at different positions. Several solutions for how the vector Doppler method is to be done in practice have been proposed, but in this work this will not be discussed, only one of these solutions will be discussed to explain the principal of the vector Doppler method. For further reading on vector Doppler see [6]. A general approach with the use of two transducers are depicted in figure 2.3.

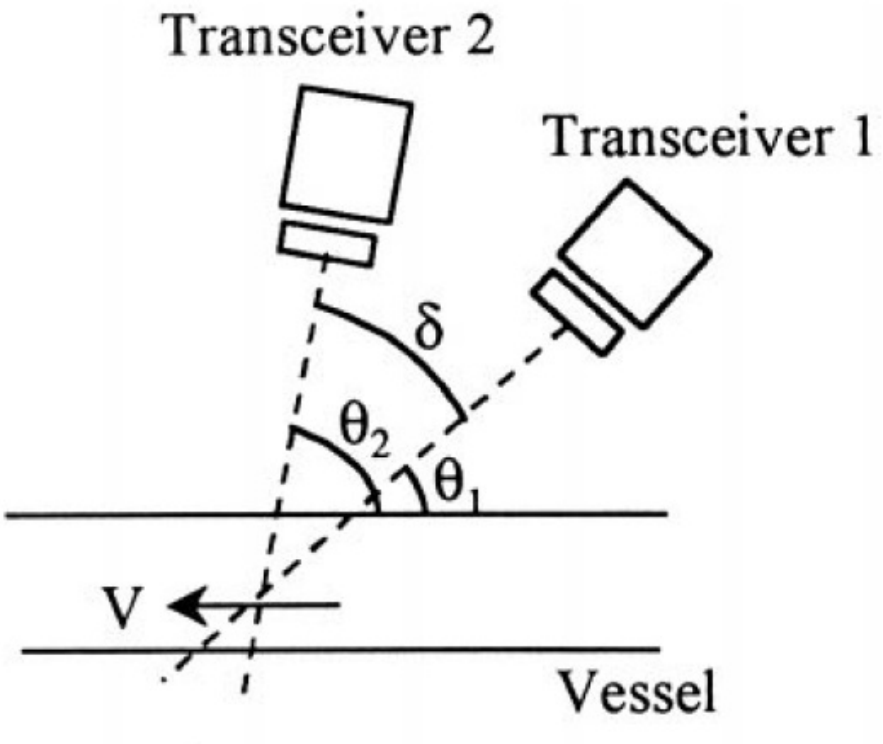

Figure 2.3: The vector Doppler approach introduced by Peronneau et al. (1974,1977) [6]. A two transducer vector Doppler system, with the transducers oriented with an angle, δ, between them.

This approach was introduced by Peronneau et al.(1974,1977). The two transducers are oriented with a known angle δ to each other. The equations for the direction θ_1 and the magnitude of the velocity $|V|$ are:

$$|V| = \frac{c}{2f_0}\frac{1}{\sin\delta}\sqrt{f_1^2 + f_2^2 - 2f_1 f_2 \cos\delta} \tag{2.3}$$

$$\theta_1 = \arctan\left(\frac{\cos\delta - \frac{f_2}{f_1}}{\sin\delta}\right) \tag{2.4}$$

The angle between the transducers are given by δ, and f_1 and f_2 are the Doppler shifts from transceiver 1 and transceiver 2 , respectively.

2.2.2 Speckle tracking

For imaging of flow and quantifying of blood and tissue velocities, Doppler ultrasound has become widespread. The use of Doppler ultrasound for imaging of blood flow have limitations, because it is an one-dimensional and angle dependent measurement method [4]. Speckle tracking overcomes these limitations and provides angle-independent two-dimensional velocity estimates [1].

The basic principle of speckle tracking is based on the interference of the reflected ultrasound giving rise to an irregular, random speckle pattern. The speckle patterns in blood flow is caused by destructive and constructive interference between the red blood cells in blood [7]. The speckle pattern depends on the frequency and shape of the transmitted pulse and the beam width. With increasing frequency the speckles get finer grained, because the spatial variation is determined by the wavelength. Speckles are not a completely random process in the sense that when imaging under the same conditions the same object will create the exact same speckles [5]. This is why it is possible to track the speckles. As the red blood cells move with the blood flow, so does the speckle pattern. The random distribution of the speckle pattern ensures that each region has a unique pattern. There are two features about the speckle pattern that makes it possible to use speckle patterns to track blood flow. First, the speckle pattern is random, meaning one speckle pattern can be differentiated from another. Second, the speckle patterns remain reasonably stable, and the speckle patterns follow the blood flow. Speckle tracking measures multidimensional blood flow by tracking the displacement of these speckle patterns generated by scatterers in blood. The tracking is completed by searching for the most similar part by applying a pattern matching algorithm across a search region in the next acquisition.

In speckle tracking [2] a kernel region is first identified in the blood flow, this kernel region is then tracked within a defined search region to find the best match in a later acquisition. In figure 2.4 the speckle tracking geometry is given. The search region is defined to be sufficiently large to allow for tracking of a given maximum velocity. It is used a pattern matching algorithm, discussed in section 2.2.2, to find the best match to the kernel within the search region. The size of the search region relative to the kernel defines the velocity range, while the size of the kernel region defines the spatial velocity resolution. The location of the best match relative to the kernel is defined by displacement in both the lateral and axial direction. This displacement vector together with the time between acquisitions is used to calculate the velocity vector. After calculating the velocity vector for the kernels throughout the region of interest a velocity map is found for this region. Both the axial and the lateral components of the motion vector are defined. Typically the kernel and the search region is small relative to the region of interest, this is to achieve fine spatial velocity resolution.

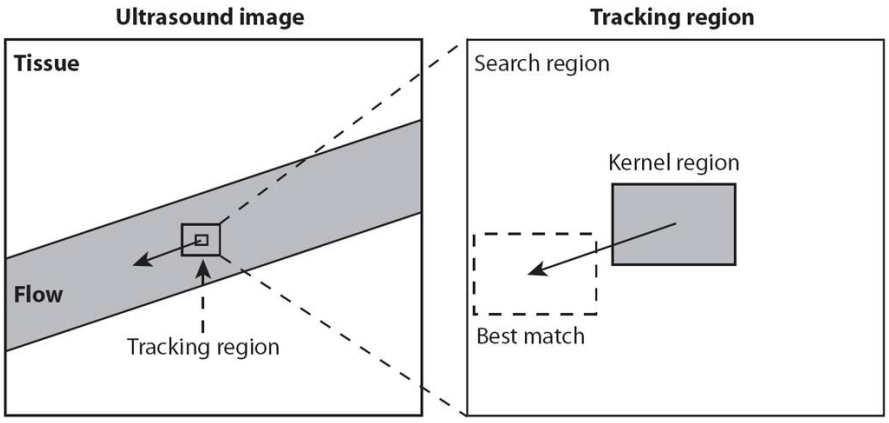

Figure 2.4: Geometry for speckle tracking. A small kernel region is identified from the blood vessel and the best match for the kernel region is found in a later acquisition within the search region. The location of the best match relative to the kernel defines the displacement vector for that particular kernel.

Pattern matching algorithms

Pattern matching algorithms in speckle tracking is used to find the best match to the kernel in the next acquisition. The pattern matching algorithm

searches for the best match among possible matching locations within the defined search region. There are a few pattern matching algorithms that can be used in speckle tracking. Three of those are Sum of Squared Difference (SSD), Sum of Absolute Difference (SAD) and Normalized correlation algorithm. In this work SSD is the pattern matching algorithm used.

Sum of Squared Difference

The equation for the Sum of Squared Difference (SSD) algorithm [8] is given by,

$$d(u,v) = \sum_{x,y}(F(x+u, y+v) - T(x,y))^2 \tag{2.5}$$

In equation (2.5) the quantity d is the SSD coefficient, F is the image and T is the template. Where the image $F(x,y)$ displaced (u,v) is compared to the template, the kernel region. The coordinates (u,v) relative to the center of the search region that produces the smallest value of the SSD coefficient are the ones used to compute the time between the acquisition of the kernel and search regions, and thereby the velocity estimates.

Sum of Absolute Difference

The equation for the Sum of Absolute Difference (SAD) algorithm [2] is given by,

$$\epsilon(\alpha,\beta) = \sum_{i=1}^{l}\sum_{j=1}^{k} |\ X_0(i,j) - \ X_1(i+\alpha, j+\beta)| \tag{2.6}$$

The quantity ϵ is the SAD coefficient. The SAD coefficient represent the error in matching a kernel region in acquisition X_0 with a trail matching region in a search region in acquisition X_1. (α,β) are the lateral and axial coordinates of the trial matching region relative to the center of the search region. $l \times k$ are the kernel dimensions in the lateral and axial direction in pixels. The lateral and axial coordinates, (α,β), that produces the minimum value of the SAD coefficient are the ones used to compute the velocity magnitude and angle, given the time between the acquisition of the kernel and search regions.

Normalized correlation algorithm

The equation for the normalized correlation algorithm [2] is given by,

$$\rho(\alpha,\beta) = \frac{\sum_{i=1}^{l}\sum_{j=1}^{k}[\ X_0(i,j) - \overline{X_0}][\ X_1(i+\alpha, j+\beta) - \overline{X_1}]}{\sqrt{\sum_{i=1}^{l}\sum_{j=1}^{k}[\ X_0(i,j) - \overline{X_0}]^2 \sum_{i=1}^{l}\sum_{j=1}^{k}[\ X_1(i+\alpha, j+\beta) - \overline{X_1}]^2}} \tag{2.7}$$

In equation 2.7, X_0 and X_1, contain the kernel and the search regions, respectively. (α, β) are the coordinates of the matching region in X_1. lxk is the lateral and axial dimensions of the kernel region and $\overline{X_0}$ and $\overline{X_1}$ are the spatial mean pixel values of the corresponding image regions. The SAD and the SSD algorithms are more computationally efficient than the normalized correlation algorithm and are therefore to prefer.

Subsample interpolation

Subsample interpolation is utilized to improve the velocity accuracy. The subsample interpolation method used in this speckle tracking algorithm is parabolic. The parabolic interpolation method fits a parabola through three consecutively points and finds the extreme (i.e its maximum or minimum). If $f_1 = \frac{1}{d(u,v)}$ where $d(u,v)$ is the minimum value found from the Sum of Squared Difference pattern matching algorithm and the two nearest neighbouring points are f_0 and f_2. Then the subsample correction offset for the displacement is given by,

$$\hat{\delta} = \frac{f_0 - f_2}{2\left(f_0 - 2f_1 + f_2\right)} \tag{2.8}$$

The subsample interpolation was done on the axial and the lateral direction separately. Where in the lateral direction

$$f_0 = \frac{1}{d(u, v-1)} \tag{2.9}$$

,

$$f_2 = \frac{1}{d(u, v+1)} \tag{2.10}$$

and in the axial direction

$$f_0 = \frac{1}{d(u-1,v)} \tag{2.11}$$

,

$$f_2 = \frac{1}{d(u+1,v)} \tag{2.12}$$

2.3 Conventional versus plane wave imaging

In conventional ultrasound imaging a image is formed from several focused ultrasound transmission. The image is formed line by line so that each scan line is obtained from one transmitted pulse with a pulse repetition frequency. The image of the whole region of interest is formed by sliding the aperture along the scan plane. Another approach to form an image is the use of plane wave imaging. With plane wave imaging one single unfocused pulse that covers the whole region of interest is transmitted, and several parallel beams is received. This is accomplished with parallel beamforming [9]. Plane wave imaging and parallel beamforming have a high acquisition rate which makes it possible to have a high frame rate. A high frame rate is crucial when imaging the heart. With plane wave imaging the unfocused transmitted beam will give a loss in penetration and decrease in lateral resolution and image contrast compared to a imaging technique with a focusing. Despite this plane wave imaging of blood flow is preferable because of the high frame rate that can be achieved with plane wave imaging.

2.4 Blood flow over one heart cycle

The data set of the carotid artery consists of flow frames, where each flow frame represents the carotid artery at a certain time of the heart cycle. All the frames together illustrates the blood flow in the carotid artery over one whole heart cycle. The velocity in the carotid artery varies over one heart cycle in systole/diastole [13]. Systole is the period of time when the heart contracts to push blood out of the heart. In systole the velocity increases as the pressure in the heart increases to push the blood out. Diastole is the resting period after systole. The pressure drops from the peak it reaches in systole. In diastole the heart fills up with blood again. In diastole the velocity in the carotid artery decreases.

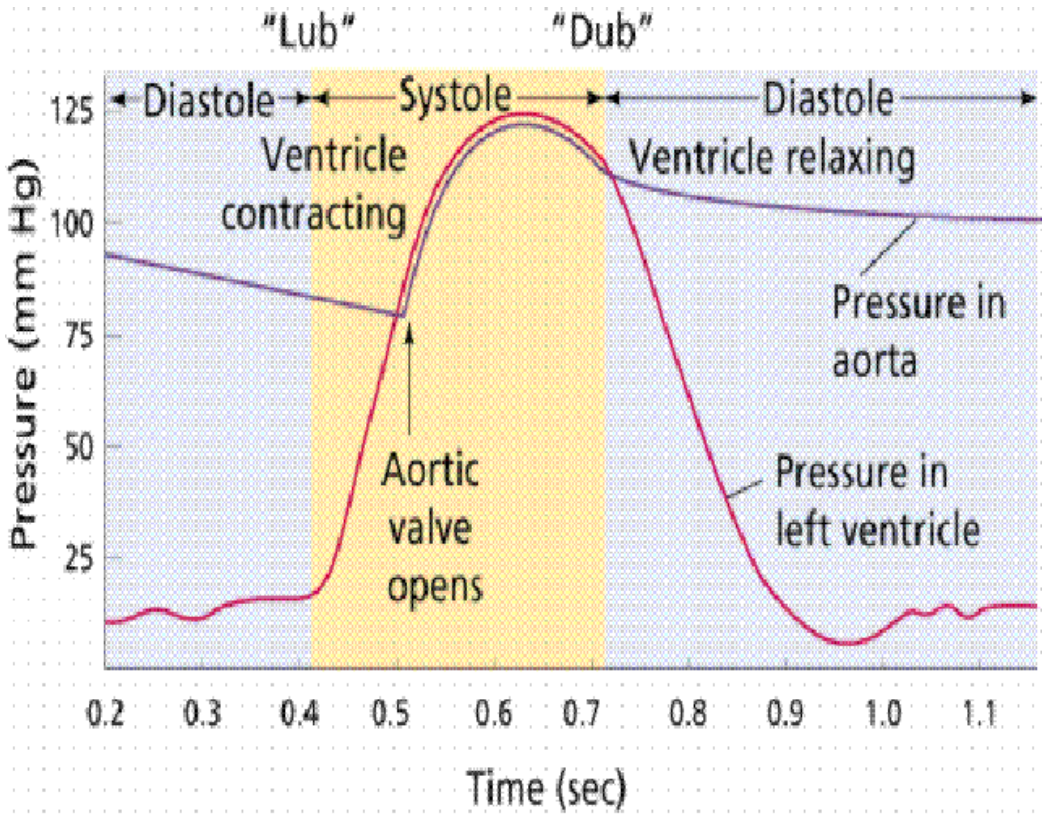

Figure 2.5: Diagram [15] showing various events during systole and diastole

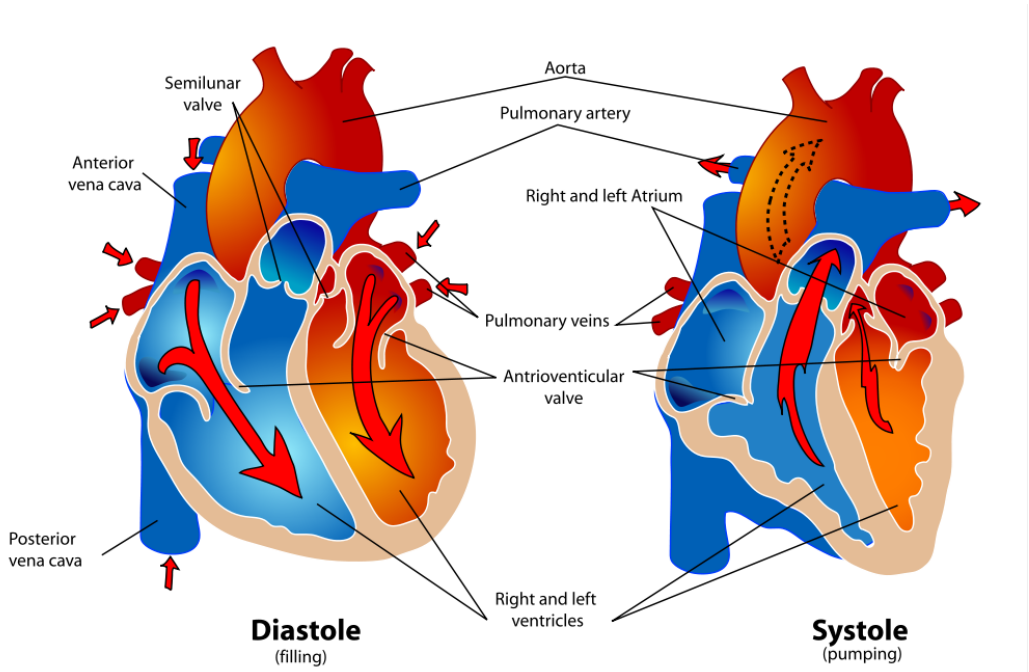

Figure 2.6: Illustration of the heart [14] during diastole and systole

2.5 Carotid artery

The left and right carotid arteries [12] supplies the head and the neck with oxygenated blood from the heart. Each of the common carotid arteries divides into the external and the internal carotid artery. The common carotid arteries are paired, meaning they each supply oxygenated blood to their part of the head, where the left common carotid artery supply blood to the left part of the brain and the right common carotid artery supply blood to the right part of the brain. As mentioned the common carotid arteries divide into to parts, the external and the internal carotid artery. The internal carotid artery supplies oxygenated blood to the brain and the external carotid artery supply blood other parts of the head, such as the face, meninges, skull and scalp. The speckle tracking algorithm was utilized to find the velocity estimates in the Carotid artery. Three areas of the Carotid artery was chosen to look at the blood flow in the carotid artery, one area in the common Carotid artery, before the Carotid artery divides into the internal and the external. Figure 2.7 show B-mode image of the Carotid artery that was simulated with the region of interest outlined. The second area that the speckle tracking al-

gorithm was run over was chosen after the split of the Carotid artery, 2.8 shows a B-mode image of the Carotid artery where this region of interest is outlined.

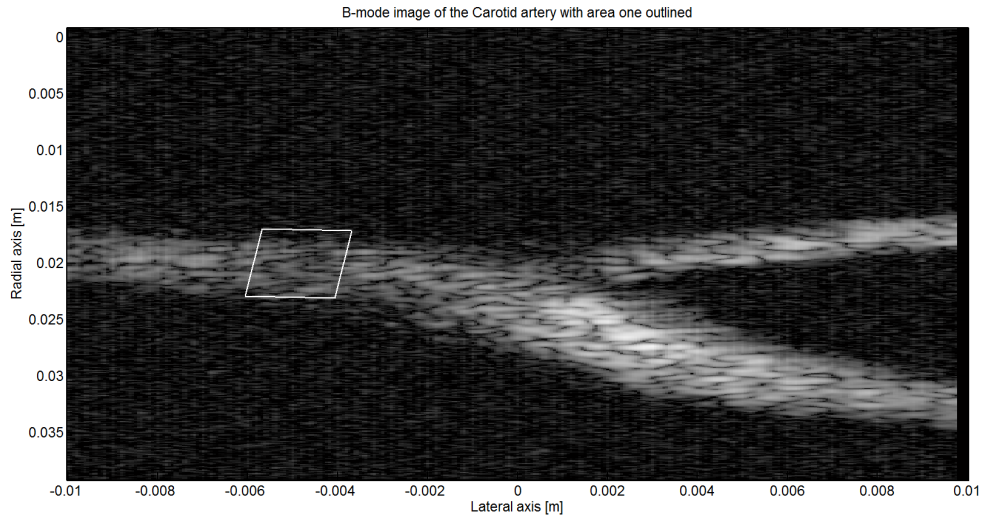

Figure 2.7: B-mode image of the carotid artery with area one outlined

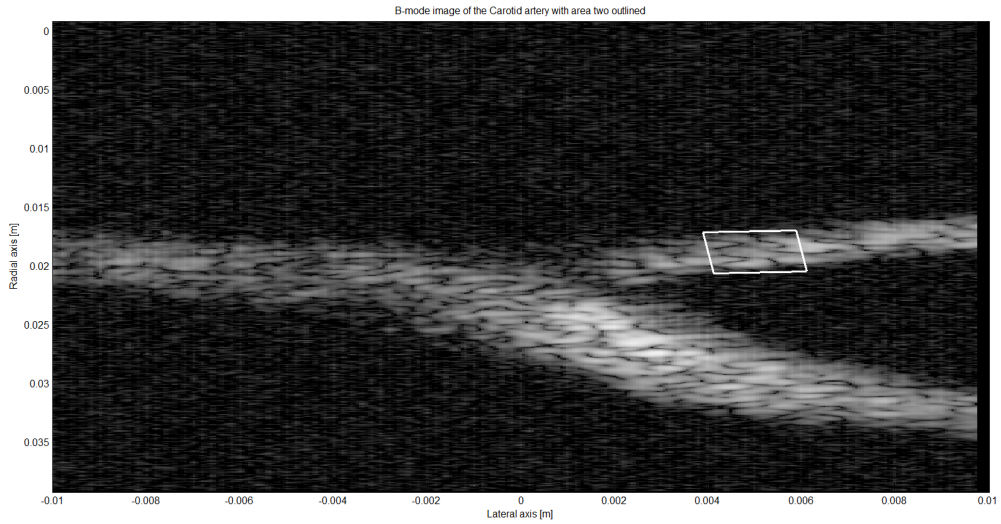

Figure 2.8: B-mode image of the carotid artery with area two outlined

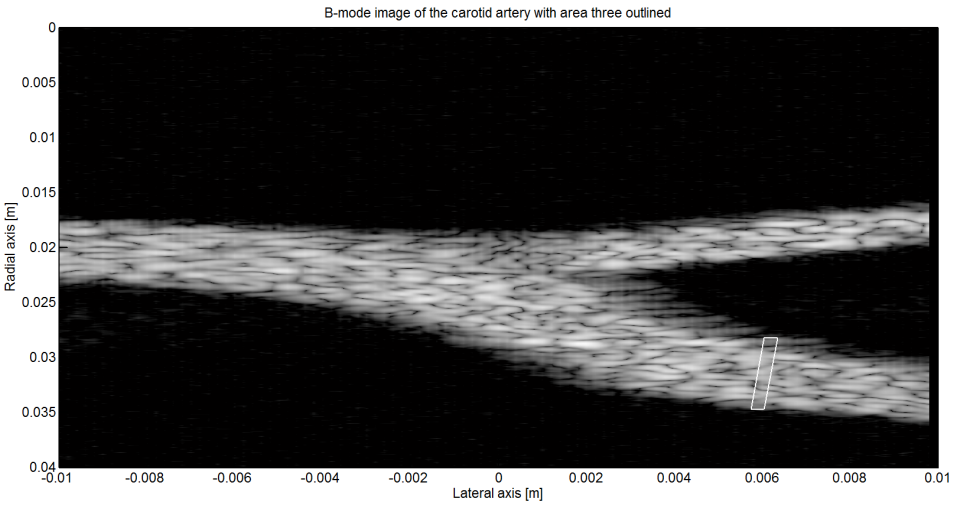

Figure 2.9: B-mode image of the carotid artery with area three outlined

Chapter 3

Methods

3.1 Simulation data

The simulated data in this work is from a carotid artery. The data of the carotid artery is simulated by an ultrasound simulation code, called Field II [11]. The Field II program calculates the pulse-echo response according to the velocity and placement of the scatters inside the phantom. Then the echo-signal is IQ-demodulated.

Plane wave imaging was used to collect the data, in plane wave imaging the probe sends out a wave over the whole region that is to be imaged. A plane wave is transmitted from the probe and 100 beams are received. A specifies number of frames were collected with a high frame rate equal to the pulse repetition frequency, PRF=4 kHz. The frame rate is number of images collected per second. The data set consist of a matrix [Np, Nr, Nb, flow frames]. Np is the number of frames, Nr is how many lines in depth the image consists of, Nb is number of beams and flow frames are collected at specified times over one hearts cycle. The data set consist of 41 flow frames, where each flow frame consist of a number of frames, Nr and a number of beams.

3.2 The Speckle tracking algorithm

In this section the speckle tracking algorithm used in this work is explained. First, a search and a kernel region is defined. Where the best match in

the next acquisition to the kernel region is found by the use of the Sum of Squared Differences pattern matching algorithm discussed in section 2.2.2.

The region of interest, in this case the straight tube, is divided into points specified by the beam and range tracking vectors. Where the points in the x-direction are the beam tracking positions and the points in the z-direction are the range tracking positions. The center of the search region is a point (z, x), where x is the points in the beam tracking vector, and z is the points in the range tracking vector. The speckle tracking algorithm uses a pattern matching algorithm, here Sum of Squared Differences is used, to find the best match for the kernel in the next acquisition. The location of the best match relative to the kernel defines the vector of movement for that kernel. After the displacement in the x-and z-direction of the best match relative to the kernel is found subsample interpolation, explained in section 2.2.2 is applied. This is done for all of the frames in time within the search region with center at that point. The best match is found within the search region for all the frames, with a lag =1, which specifies that frame number 2 is compared to frame number 1, corresponding to the next acquisition, in the next acquisition frame number 3 is compared to frame number 2 and so on for all the frames.

After the displacement of the best match relative to the kernel is found for all the frames and the velocity is calculated, the center of the search region and kernel region is moved one step in the z-direction, to the next point in the range tracking vector. Then the best match to the kernel is found for all the frames, and the velocity estimates are found for all the frames in that position. After this is done for all the frames the center is moved one more step on the range tracking vector, etc. until the end of the range tracking vector. After the velocity estimates for all the frames of the point at the end of the range tracking vector is found the center is moved one step in the x-direction on the beam tracking vector. Then the tracking algorithm begins at the start on the range tracking vector again. This is done for all points in the range tracking vector and the beam tracking vector. Giving a velocity map of the whole region of interest.

In the original speckle tracking algorithm the kernel is set to be at the center of the search region, meaning that the algorithm searches for the best match within the surrounding search region. See figure 3.1. The location of the best match relative to the kernel defines the motion vector for that particular kernel region. When this is done successively for a region of interest, it creates a velocity map for the region.

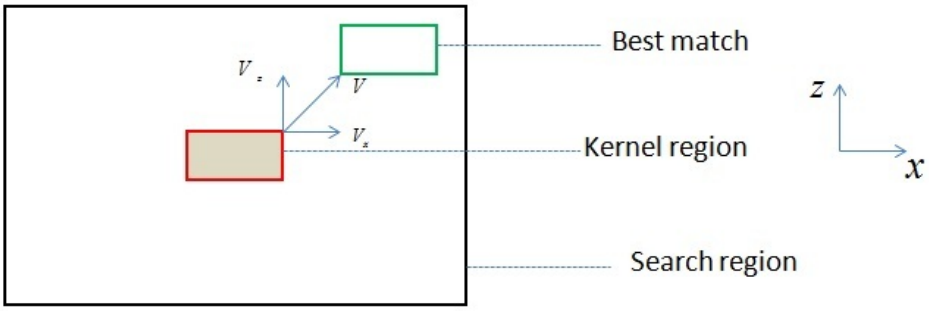

Figure 3.1: Search and kernel region of the original speckle tracking algorithm.

3.3 The adaptive speckle tracking algorithm

In the original speckle tracking algorithm the search region is based on a pre-set value of the velocity to determine the size of the search region. In real life the velocity is not known, so a speckle tracking algorithm where the search region is based on previous estimates will be a more robust speckle tracking algorithm.

The tracking algorithm was changed to implement an adaptive search region based on previous velocity estimates. The velocity estimates found by the original tracking algorithm is used to find new estimates of the velocity. This was done by using velocity estimates from the speckle tracking with pre-set values for the search region. Where the search region is set to be as in figure 3.1 and with the size of the search region being defined by the maximum velocity set. The velocity estimates found was then used to adapt the search region in size and placement.

The velocity estimates was used to set an offset to the center of the search region, where in the original speckle tracking algorithm the center of the search region is specified by the range and beam tracking vectors. In the adaptive speckle tracking algorithm the new center of the search region is the range and beam tracking vector point with an offset value added. This offset is a value equal to the displacement the tracking algorithm found in that specific point. The displacement is calculated from the velocity estimates found from the previous tracking.

Let the center of the search region specified by the range and beam tracking

vector be (z, x), an the offset be $offset_z, offset_x$. Where the offset is given by,

$$offset_z(z) = \frac{v_z(z)}{vResZ} \tag{3.1}$$

$$offset_x(x) = \frac{v_x(x)}{vResX} \tag{3.2}$$

$vResZ$ and $vResX$ are the velocity resolution in the axial and lateral direction, respectively. There is an offset for the x-direction and one for the z-direction, corresponding to the velocity estimate found in the x- and z-direction. Then the new center of the search region is the center given by the range and beam tracking vectors with the offset given by the velocity estimates added. Meaning the adaptive search region has a center at the position where the original tracking algorithm found the best match for the kernel.

In addition the search region was made smaller for each round of the adaptive speckle tracking algorithm. The number of points the search region is to contain, e.i the size of the search region is set by,

$$NSxI = \frac{A \times p.vMax}{\frac{vResXI}{p.trackLags(1)}} + \frac{p.kernelX}{latIncI} \tag{3.3}$$

$$NSzI = \frac{A \times p.vMax}{\frac{vResZI}{p.trackLags(1)}} + \frac{p.kernelZ}{depthIncI} \tag{3.4}$$

where NSxI is the number of points in the x-direction and NSzI is the number of points in the z-direction. The last terms of equation 3.3 and 3.4 is to make sure that the search region is always larger than the kernel region. A is a constant, in the original speckle tracking algorithm the constant is set to be 2. Then the velocity estimates were calculated from the displacement of the best match found in the next acquisition with the added offset values.

3.4 Adaptive speckle tracking over one flow frame

The adaptive speckle tracking algorithm from section 3.3 was tested on the simulated carotid data set, where previous velocity estimates were utilized to

find a new estimate of the velocity. The adaptive speckle tracking algorithm was run several times, where in each round the velocity estimates from the previous round was utilized to set the new center of the search region. In round 1 of the adaptive speckle tracking algorithm the velocity estimates from the original speckle tracking algorithm were used to set the offsets to the center of the search region. In the next round the velocity estimates from round 1 were used to set the offset, and in round 3 the velocity estimates from round 2 were used to set the offsets, etc. for round 4. In the original speckle tracking the constant A in 3.3 and 3.4 is set to 2, and in the different rounds of the adaptive speckle tracking algorithm the size is made smaller by setting the constant to 1.333, 0.8889, 0.5926 and 0.3951 for round 1, 2, 3 and 4, respectively.

The speckle tracking algorithm was tested on the simulated data set for flow frame 4, to see if one could lower the spurious outliers, the large errors.

3.5 Multi-lag

3.5.1 Multi-lag -same interpolation factor for different lags

The speckle tracking algorithm was run with the same interpolation-factor for lag 1, 2 and 3. The interpolation factor is specified by the parameters, vMin and lag, where vMin is the smallest velocity that can be tracked. In the speckle tracking algorithm it is possible to choose which lag one wants to do the speckle tracking with, it is also possible to do the speckle tracking with multiple lags at the same time. When tracking with multiple lags at the same time the range and beam tracking density as well as the size of the search region is set by the first tracking lag in the array of tracking lags. For a higher lag, the displacement of the speckle pattern is higher between each frame and that is why a larger search region is needed for tracking of the same velocities for a higher lag. The parameter lag specifies at which interval the frames is to be compared to each other. Lag =1 specifies that all the frames are to be compared sequentially to the next frame. Frame number 2 is compared to frame number 1, corresponding to the next acquisition, in the next acquisition frame number 3 is compared to frame number 2, and so on for all the frames. This gives the best correlation between the best match in the search region and the kernel region. By increasing the parameter lag, to for example lag =2 the correlation decreases since the blood flows further

between each time the kernel is compared to the best match. With lag =2 frame number 3 is compared to frame number 1, corresponding to the next acquisition, in the next acquisition frame number 4 is compared to frame number 2 and so on for all frames.

The interpolation factor (given in equation 3.13)is specified by the parameter lag and vMin. The interpolation factor specifies how much the lateral and depth increment is to be interpolated, how fine the tracking grid is in the lateral and axial direction. Where lag decreases the interpolation factor and makes the tracking grid coarser and the parameter vMin increases the interpolation factor, which leads to a finer grid. The density of the tracking grid decides how many points it is in the range and beam tracking vectors.

The interpolation-factor in the lateral and axial detection is given by:

$$Interpolation factor = \frac{latInc}{latIncI} \tag{3.5}$$

$$Interpolation factor = \frac{depthInc}{depthIncI} \tag{3.6}$$

where

$$latInc = \frac{width}{Nb} \tag{3.7}$$

$$depthInc = \frac{depth}{Nr} \tag{3.8}$$

where $width$ is the width of the tracking region, Nb is the number of beams, $depth$ is the depth of the tracking region and Nr specifies range.

$$latIncI = \frac{latInc \times vMin}{\frac{vResXOrg}{trackingLags}} \tag{3.9}$$

$$depthIncI = \frac{depthInc \times vMin}{\frac{vResZOrg}{trackingLags}} \tag{3.10}$$

where $trackingLags$ is the specified lag, and $vResXOrg$ and $vResZOrg$ is the velocity resolution in the original sampled data given by,

$$vResXOrg = \frac{latInc}{PRF} \tag{3.11}$$

$$vResZOrg = \frac{depthInc}{PRF} \tag{3.12}$$

PRF is the pulse repetition frequency.

$$Interpolation factor = \frac{latInc}{latIncI} = \frac{latInc}{\frac{latInc \times vMin}{\frac{vResXOrg}{trackingLags}}} = \frac{trackingLags}{vMin \times vResXOrg} \tag{3.13}$$

$$Interpolation factor = \frac{depthInc}{depthIncI} = \frac{depthInc}{\frac{depthInc \times vMin}{\frac{vResZOrg}{trackingLags}}} = \frac{trackingLags}{vMin \times vResZOrg} \tag{3.14}$$

The speckle tracking algorithm was run with the same interpolation factor, where for lag=1 vMin was set to 0.05 and for lag=2 vMin was set to 0.025 and for lag=3 vMin is equal to 0.0125 to achieve the same interpolation factor for all lags.

3.5.2 Multi-lag variance

The speckle tracking algorithm was run for tracking lag equal to 1, 2, 3 and 4 separately over all the flow frames from the simulated data set for the carotid artery, and then compared to the ground truth. The median of the velocity estimates for the different lags was calculated. The median of the tracking estimates for the different lags was calculated to see if the variance in the estimates would get lower.

3.6 Adaptive tracking -adjusted to acceleration over flow frames

In the original speckle tracking algorithm the size of the search region is based on a pre-set value of the velocity. In the carotid artery the maximum velocity

changes with time during the diastole/systole periods of the heart cycle. By adaptively tracking the velocity change over time, one might achieve better velocity estimates. The speckle tracking algorithm was made adaptive by adjusting the size and placement of the search region to the velocity changes over the heart cycle. Since the velocity ranges from 0.1 m/s to approximate 0.6 m/s at the maximum the search region needs to be adjusted to the velocity changes to makes sure it is large enough for the high velocities. The velocity estimates found by the speckle tracking algorithm in the previous flow frame was used to adjust the placement of the search region as in the adaptive speckle tracking algorithm as explained in section 3.3. In addition the size of the search region was adjusted to the change in velocity from flow frame to flow frame, where the acceleration of the velocity between the two previous flow frames was used to set the size of the search region in the current flow frame. The maximum of the mean velocity estimates from the two previous flow frames was used to find the acceleration of between the two previous flow frames, and the search region size was updated from flow frame to flow frame according to the acceleration between the two previous flow frames. In addition to using previous velocity estimates to find the new placement and size of the search region, the parameter vMin was also adjusted to the size of the search region, achieving a finer grid for small velocities.

3.7 Multi-lag tracking

The speckle tracking algorithm was made adaptive, utilizing velocity estimates from the previous flow frame to adjust the search region size and placement. In addition utilizing the previous velocity estimates to adaptively find the best lag at the specific location in the image over time. The velocity at the edges of the carotid artery can be very small. For lag =1 the displacement of the speckles between each frame can be very small for small velocities, often only a fraction of the interpolated tracking points. So the velocity estimates in very dependant on the subsample-interpolator, that can have a bias. By using a higher lag, for example lag=2 the displacement between the frames increases to the double of the displacement with lag=1, and thereby decreasing the dependency on the subsample-interpolator.

The purpose of using multiple lags is to adaptively adjust lag to the velocity at the specific point, thereby hopefully increasing the accuracy of the velocity estimates for small velocities, and reducing the computing time. The interpolation factor as explained earlier is dependant on lag, where increasing lag

decreases the interpolation factor. So by increasing lag to 2 the interpolation-factor is half of the interpolation factor with lag=1, while achieving the same data resolution as with lag=1. From the results from section 3.5.2, where multiple lags was utilized to find the median of lag=1, lag=2, lag=3 and lag=4, which lag that was used for which veloity was chosen. The results from section 3.5.2 show that the variance and bias for lag=4 is quit large, that is why lag=4 was not chosen to be used. The decorrelation increases when the displacement of the speckle pattern increases for every sample point. From the results from 3.5.2 lag=1 was chosen for velocities from 0.4 m/s and above, since any lag higher than lag=1 underestimates such high velcoities. For velocities between 0.15 m/s and 0.4 m/s lag=2 was used for tracking, and for velcoities below 0.15 m/s lag=3 was used. The results from section 3.5.1 also supports this chose of limits.

Chapter 4

Results

4.1 Adaptive speckle tracking over one flow frame

The adaptive speckle tracking algorithm was tested on a simulated data set of the blood flow in a Carotid artery, where previous velocity estimates was utilized to find new estimates. The adaptive speckle tracking algorithm was run several times over flow frame 4, where in each round the velocity estimates from the previous round was used to in new velocity estimates. The search region was also reduced for each round.

In the preceding figures the velocity estimates in the lateral, x-direction, and the radial, z-direction, are plotted for the mean velocity of the selected areas of the carotid artery. The velocity estimates are the results of running the original speckle tracking algorithm and several rounds of the adaptive speckle tracking algorithm. These values are compared to the true value of the velocity in the same area. The velocity estimates are found for signal-to-noise ratio (SNR) equal to 30 and 20.

Tables 4.1, 4.2, 4.3, 4.4, 4.5 and 4.6 contains the standard deviation of the velocity estimates in the lateral and the radial direction for area 1, 2 and 3 respectively, for the different rounds of the adaptive speckle tracking algorithm.

4.1.1 Results from area 1

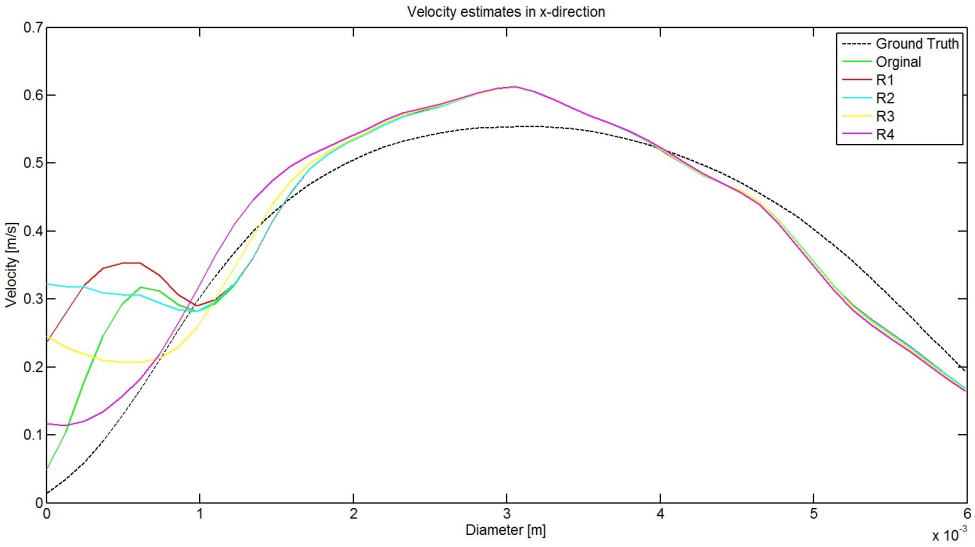

Figure 4.1: Velocity estimate from the adaptive speckle tracking algorithm in x-direction with SNR=30 at area 1 flow frame 4

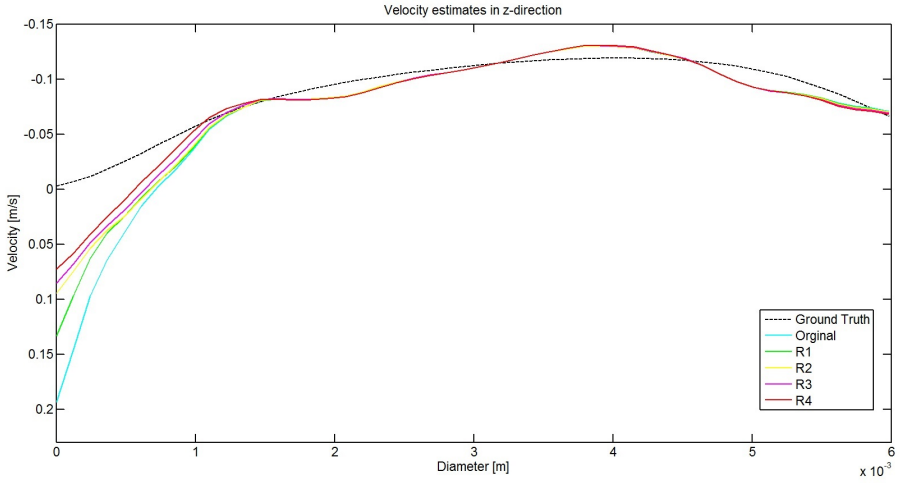

Figure 4.2: Velocity estimate from the adaptive speckle tracking algorithm in z-direction with SNR=30 at area 1 Flow frame 4

Table 4.1: Standard deviation of the velocity estimates in area 1 flow frame 4 with SNR=30

	Standard deviation of Vx	*Standard deviation of Vz*
Original	0.1540	0.0700
Round 1	0.1337	0.0590
Round 2	0.1337	0.0545
Round 3	0.1345	0.0525
Round 4	0.1655	0.0492

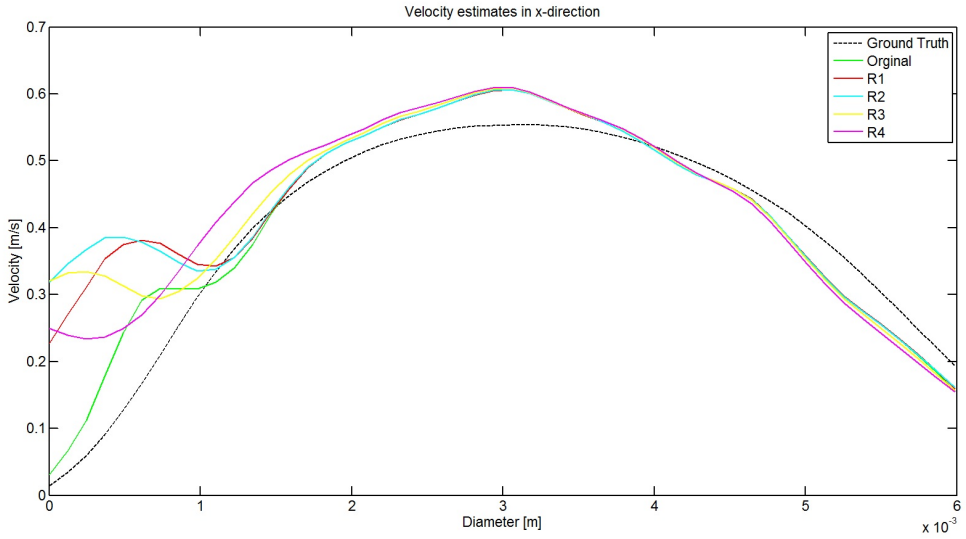

Figure 4.3: Velocity estimate from the adaptive speckle tracking algorithm in x-direction with SNR=20 at area 1 Flow frame 4

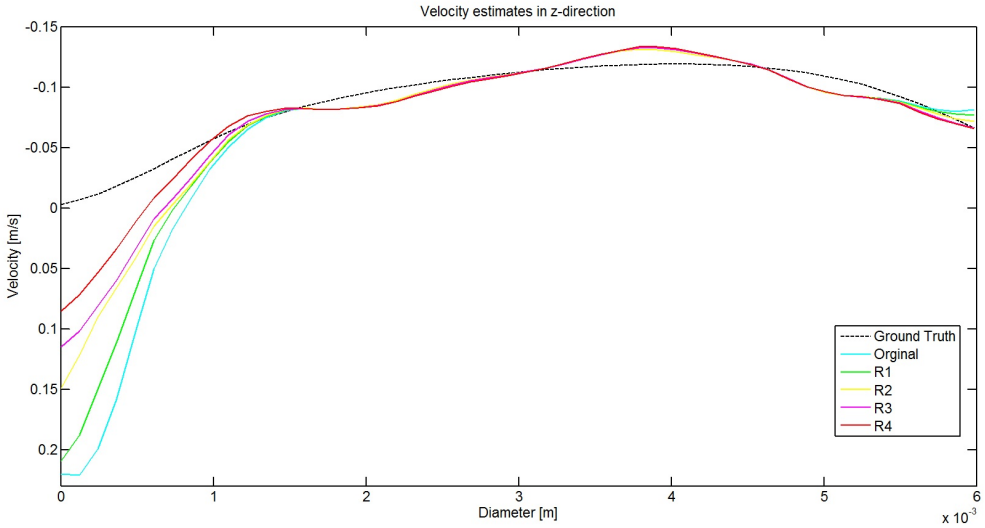

Figure 4.4: Velocity estimate from the adaptive speckle tracking algorithm in z-direction with SNR=20 at area 1 Flow frame 4

Table 4.2: Standard deviation of the velocity estimates in area 1 flow frame 4 with SNR=20

	Standard deviation of Vx	*Standard deviation of Vz*
Original	0.1589	0.0906
Round 1	0.1289	0.0803
Round 2	0.1234	0.0654
Round 3	0.1310	0.0606
Round 4	0.1423	0.0522

4.1.2 Results from area 2

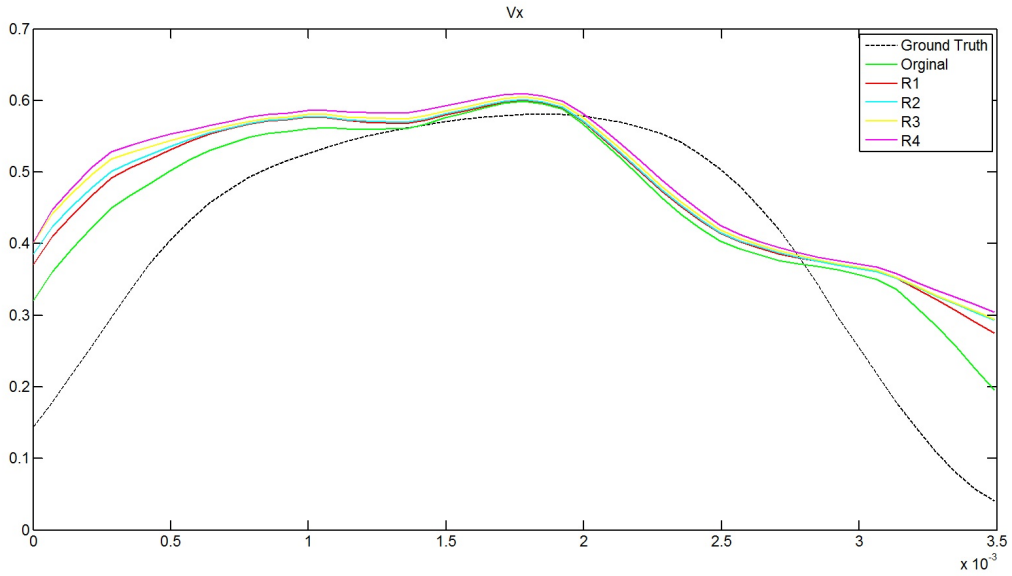

Figure 4.5: Velocity estimate from the adaptive speckle tracking algorithm in x-direction with SNR=30 at area 2 Flow frame 4

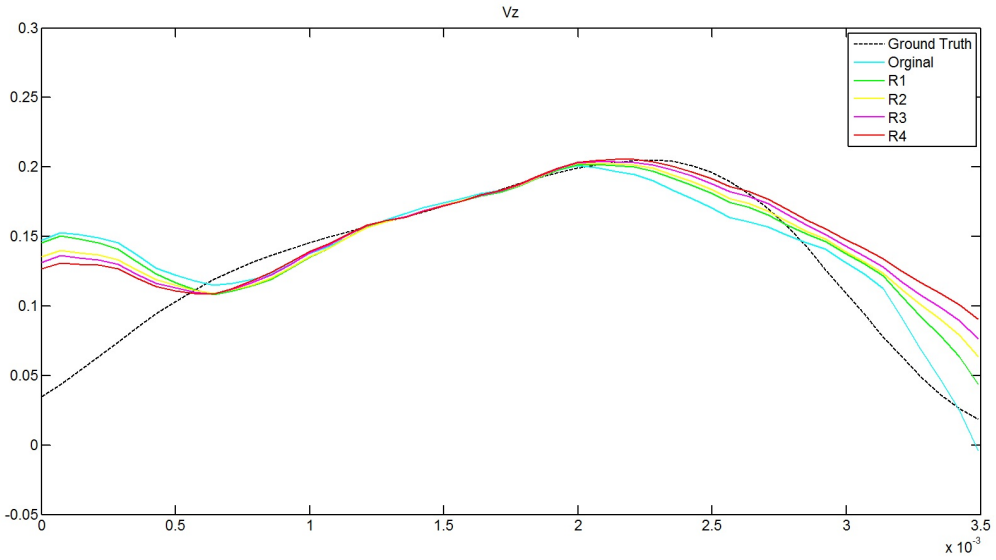

Figure 4.6: Velocity estimate from the adaptive speckle tracking algorithm in z-direction with SNR=30 at area 2 Flow frame 4

Table 4.3: Standard deviation of the velocity estimates in area 2 flow frame 4 with SNR=30

	Standard deviation of Vx	*Standard deviation of Vz*
Original	0.1102	0.0433
Round 1	0.0995	0.0372
Round 2	0.0975	0.0355
Round 3	0.0982	0.0347
Round 4	0.0984	0.0340

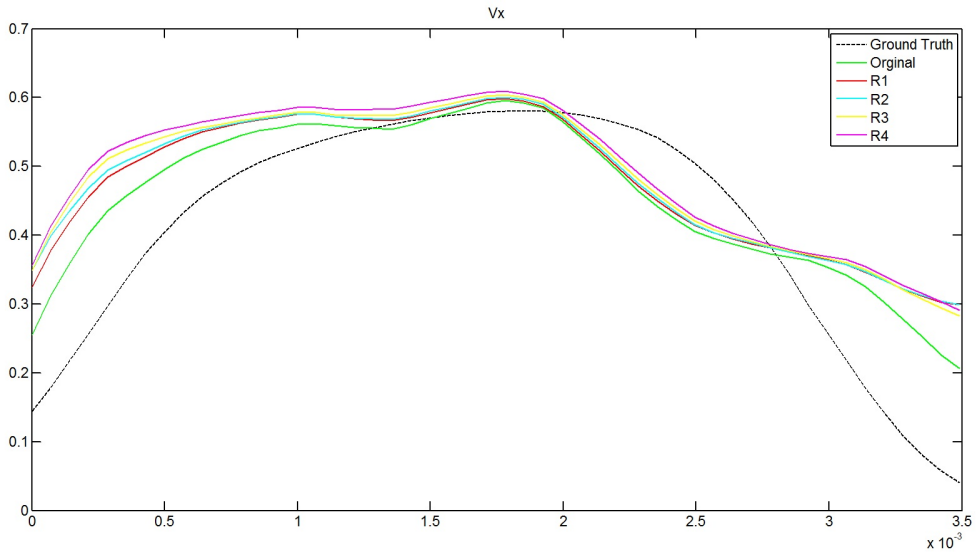

Figure 4.7: Velocity estimate from the adaptive speckle tracking algorithm in x-direction with SNR=20 at area 2 Flow frame 4

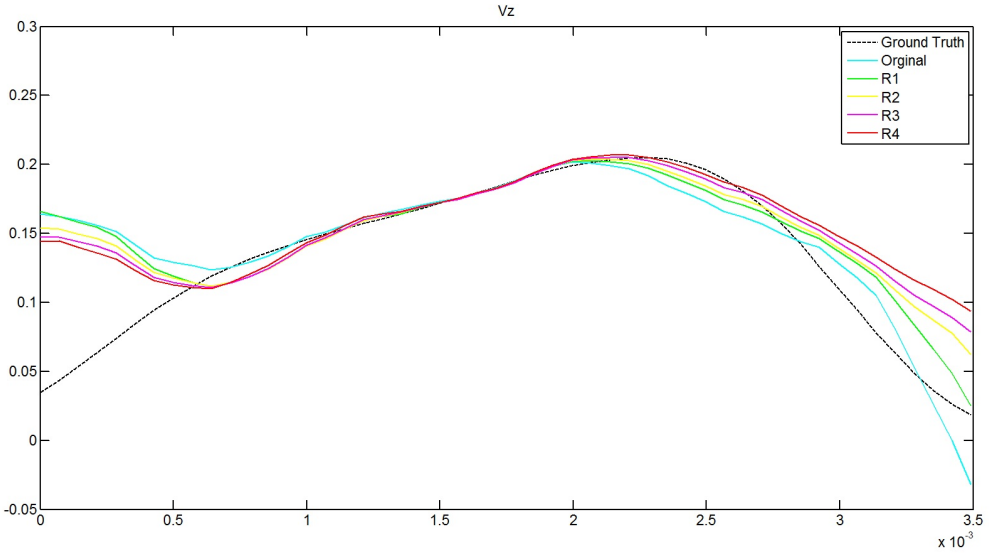

Figure 4.8: Velocity estimate from the adaptive speckle tracking algorithm in z-direction with SNR=20 at area 2 Flow frame 4

Table 4.4: Standard deviation of the velocity estimates in area 2 flow frame 4 with SNR=20

	Standard deviation of Vx	*Standard deviation of Vz*
Original	0.1129	0.0488
Round 1	0.0994	0.0398
Round 2	0.0989	0.0353
Round 3	0.1011	0.0342
Round 4	0.1019	0.0331

4.1.3 Results from area 3

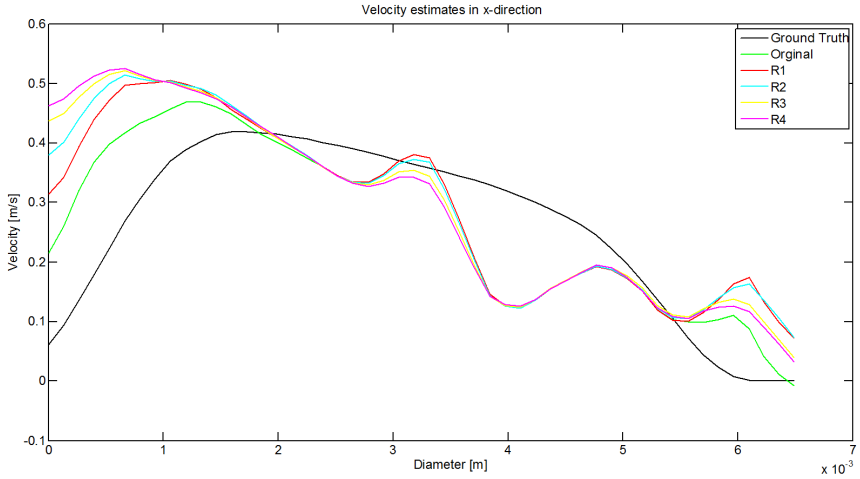

Figure 4.9: Velocity estimate from the adaptive speckle tracking algorithm in x-direction with SNR=30 at area 3 Flow frame 4

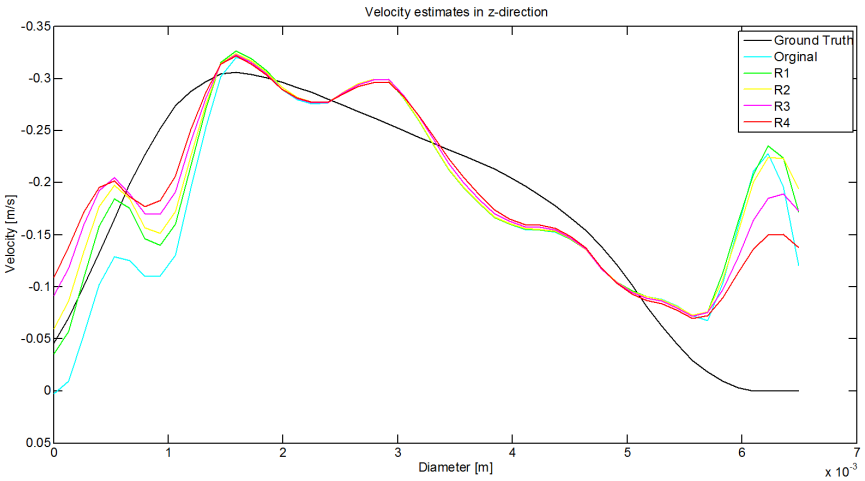

Figure 4.10: Velocity estimate from the adaptive speckle tracking algorithm in z-direction with SNR=30 at area 3 Flow frame 4

Table 4.5: Standard deviation of the velocity estimates in area 3 flow frame 4 with SNR=30

	Standard deviation of Vx	*Standard deviation of Vz*
Original	0.1418	0.0877
Round 1	0.1429	0.0810
Round 2	0.1471	0.0783
Round 3	0.1538	0.0767
Round 4	0.1577	0.0777

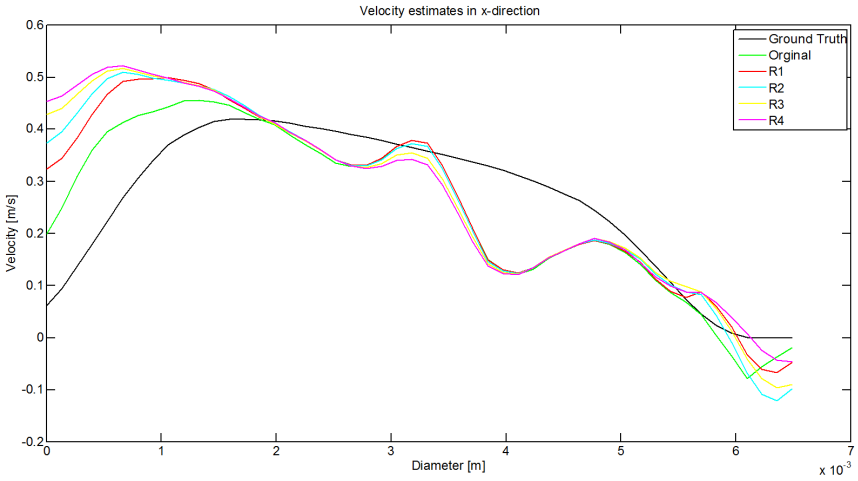

Figure 4.11: Velocity estimate from the adaptive speckle tracking algorithm in x-direction with SNR=20 at area 3 Flow frame 4

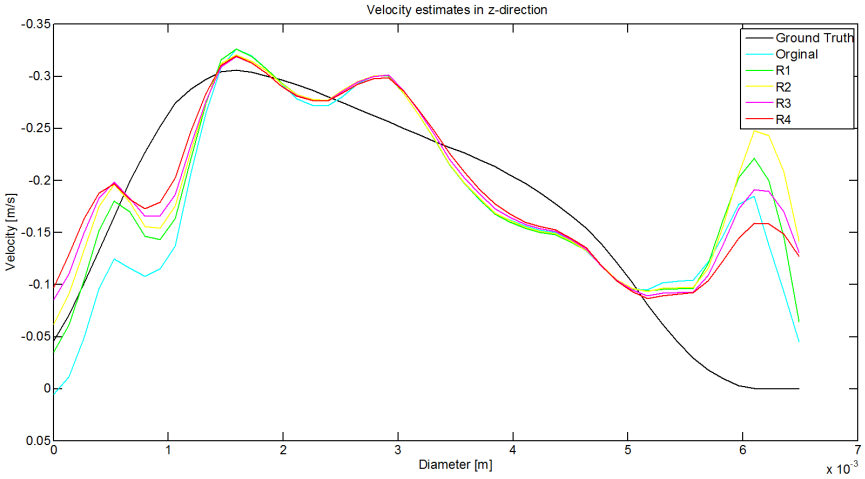

Figure 4.12: Velocity estimate from the adaptive speckle tracking algorithm in z-direction with SNR=20 at area 3 Flow frame 4

Table 4.6: Standard deviation of the velocity estimates in area 3 flow frame 4 with SNR=20

	Standard deviation of Vx	*Standard deviation of Vz*
Original	0.1611	0.0881
Round 1	0.1706	0.0805
Round 2	0.1829	0.0755
Round 3	0.1805	0.0739
Round 4	0.1750	0.0746

4.2 Multi-lag

4.2.1 Multi-lag -same interpolation-factor for different lags

In the preceding figures the velocity estimates in the lateral and axial direction are plotted for the mean velocity in the different regions of interest. In the figures the velocity profiles of the estimated velocities in the lateral and axial direction is given for a chosen sub-sample of the flow frames. The velocity was estimated for a given interpolation factor with different lags.

Figure 4.36, 4.37 , 4.61, 4.62, 4.80 and 4.81 show the estimated velocity in the middle of the carotid artery for all the flow frames in one heart cycle for the velocity estimated by the original speckle tracking algorithm with lag 1, lag 2 and lag 3 for the same interpolation factor compared to the ground truth. From these figure one can see as mentioned earlier that the velocity changes over the flow frames during the heart cycle. Figures 4.32 ,4.31 ,4.57 ,4.56 ,4.75 and 4.76 shows the standard deviation he velocity estimates over each flow frame in the lateral and radial direction. Figure 4.34 and 4.35, 4.59 and 4.60, 4.78 and 4.79 shows the bias between the velocity estimated and the ground truth for all the flow frames. Where a negative bias represents a under estimated velocity and a positive bias represents a overestimated bias.

Results area 1

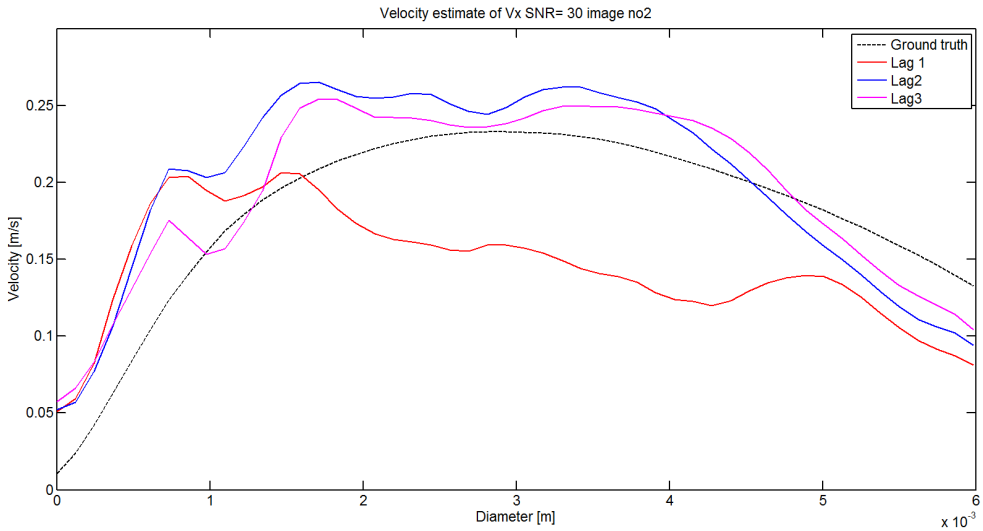

Figure 4.13: velocity estimation in the x-direction for different lags from area 1 with same interpolation factor flow frame 2

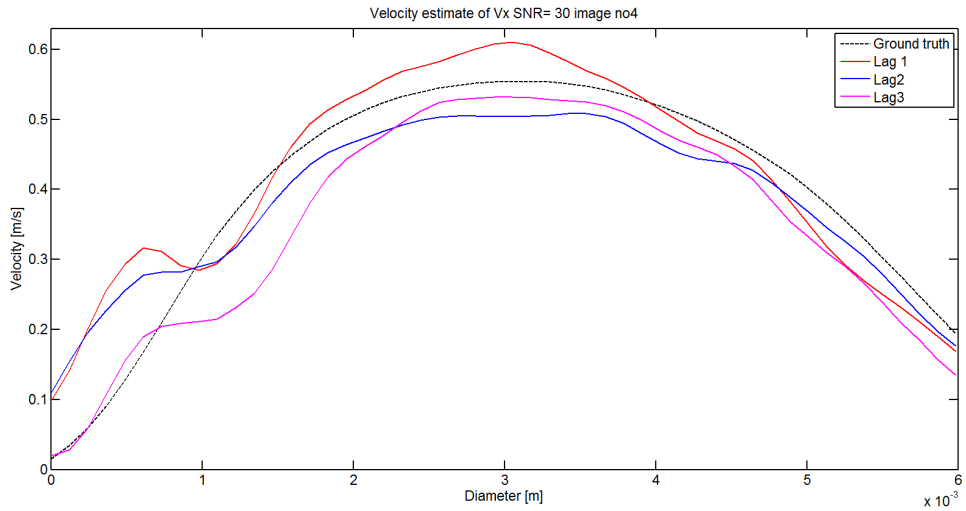

Figure 4.14: velocity estimation in the x-direction for different lags with from area 1 same interpolation factor flow frame 4

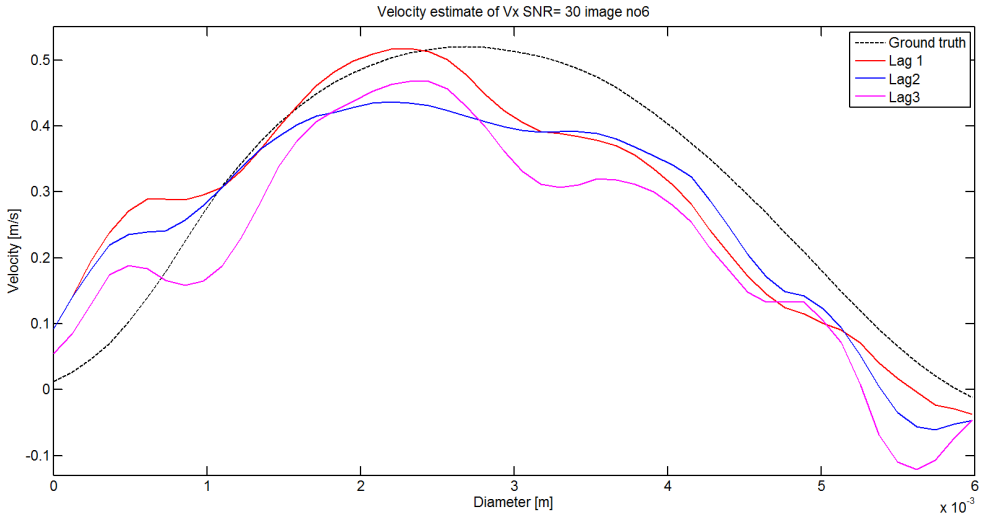

Figure 4.15: velocity estimation in the x-direction for different lags from area 1 with same interpolation factor flow frame 6

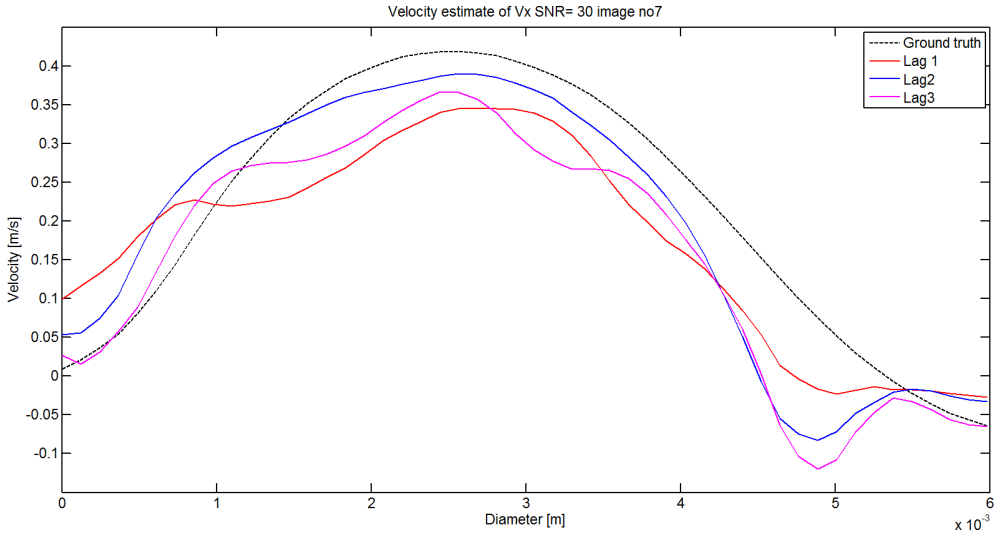

Figure 4.16: velocity estimation in the x-direction for different lags from area 1 with same interpolation factor flow frame 7

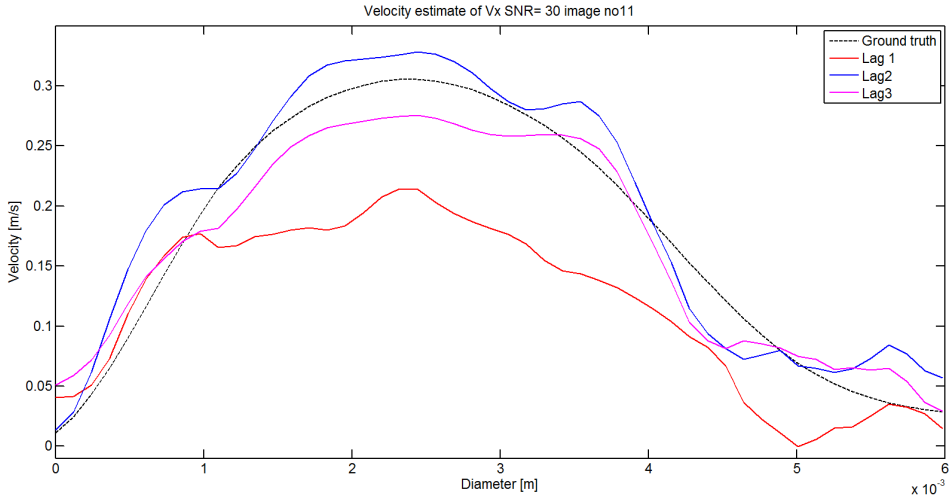

Figure 4.17: velocity estimation in the x-direction for different lags from area 1 with same interpolation factor flow frame 11

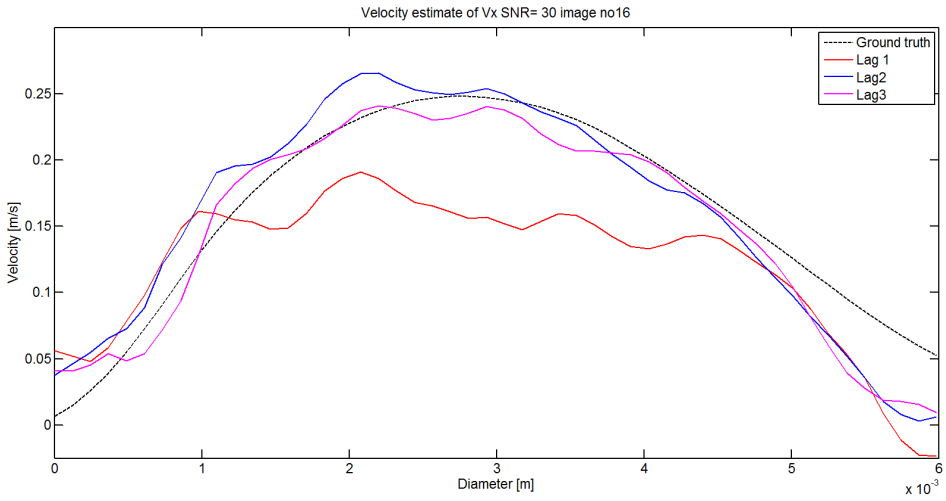

Figure 4.18: velocity estimation in the x-direction for different lags from area 1 with same interpolation factor flow frame 16

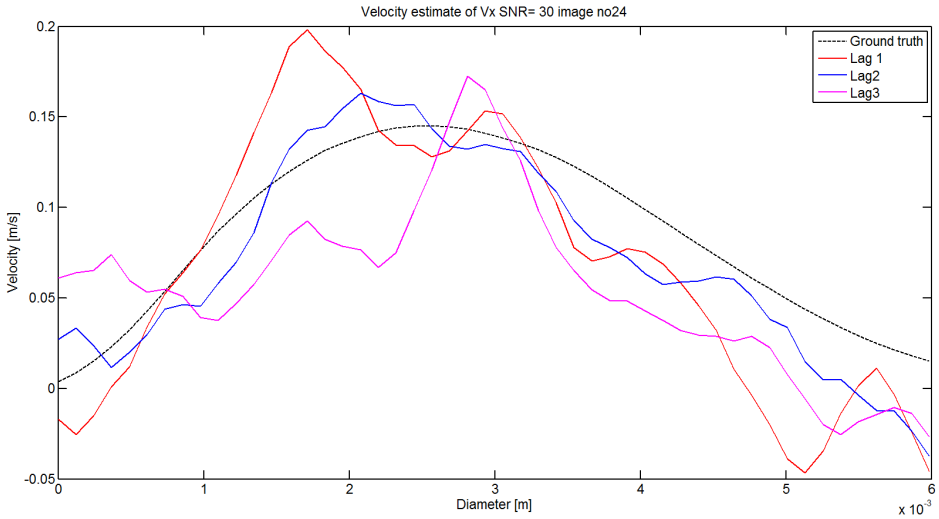

Figure 4.19: velocity estimation in the x-direction for different lags from area 1 with same interpolation factor flow frame 24

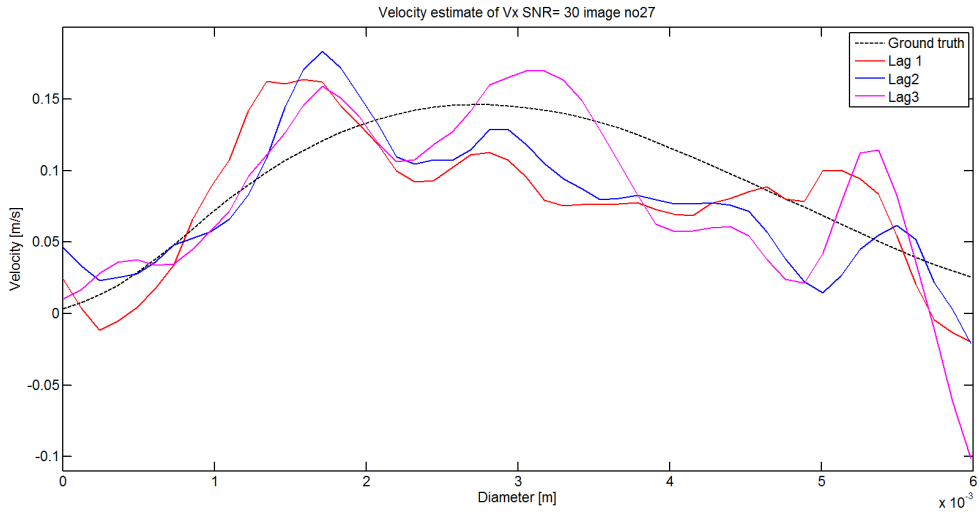

Figure 4.20: velocity estimation in the x-direction for different lags from area 1 with same interpolation factor flow frame 27

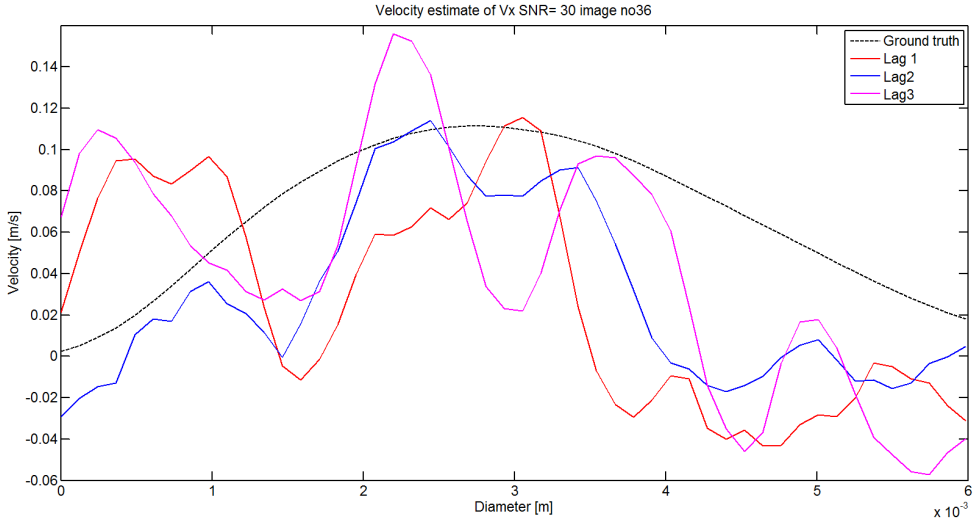

Figure 4.21: velocity estimation in the x-direction for different lags from area 1 with same interpolation factor flow frame 36

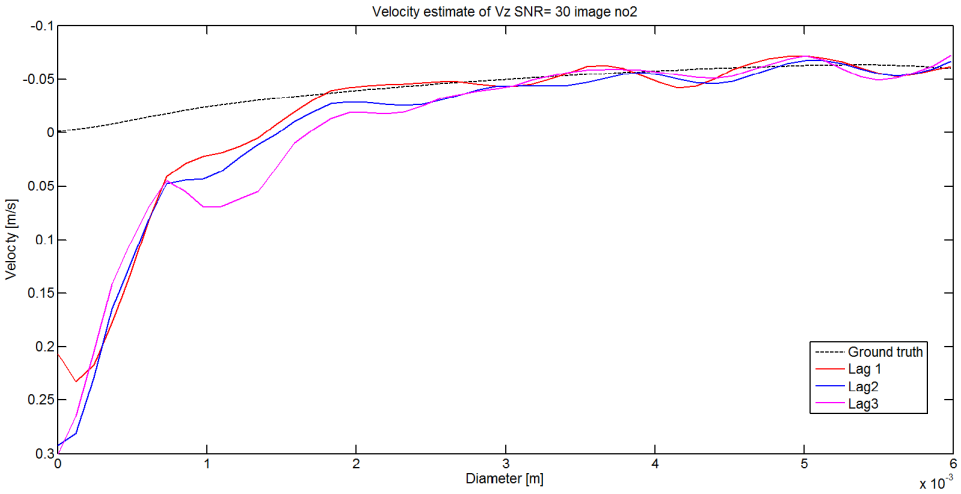

Figure 4.22: velocity estimation in the z-direction for different lags from area 1 with same interpolation factor flow frame 2

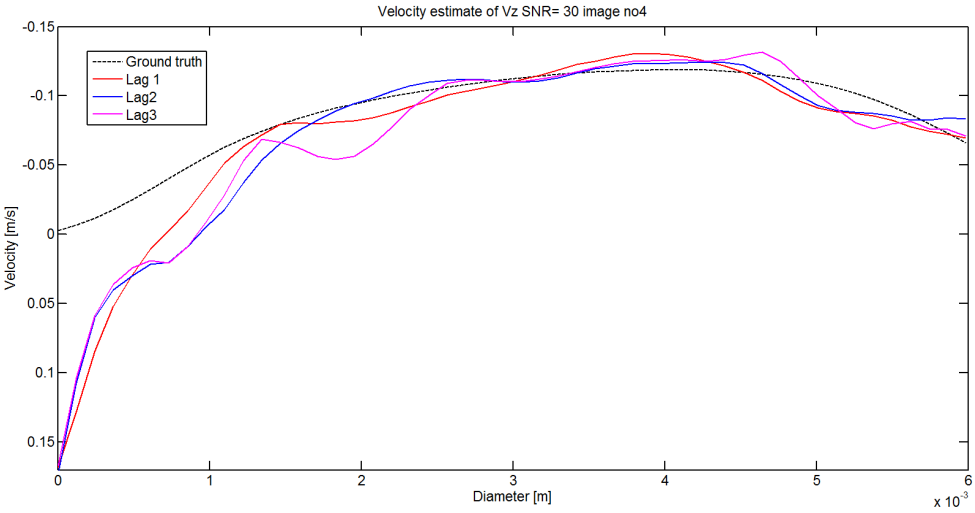

Figure 4.23: velocity estimation in the z-direction for different lags from area 1 with same interpolation factor flow frame 4

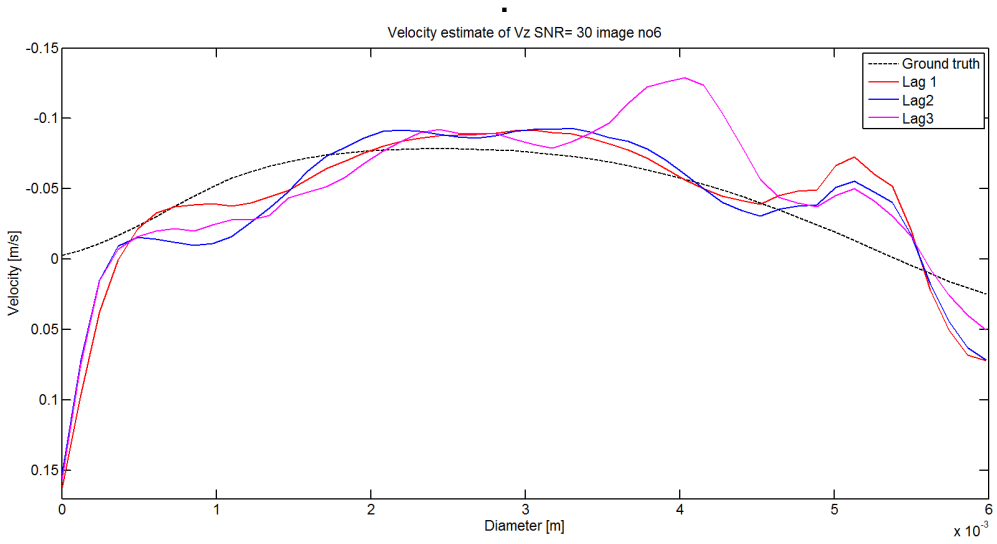

Figure 4.24: velocity estimation in the z-direction for different lags from area 1 with same interpolation factor flow frame 6

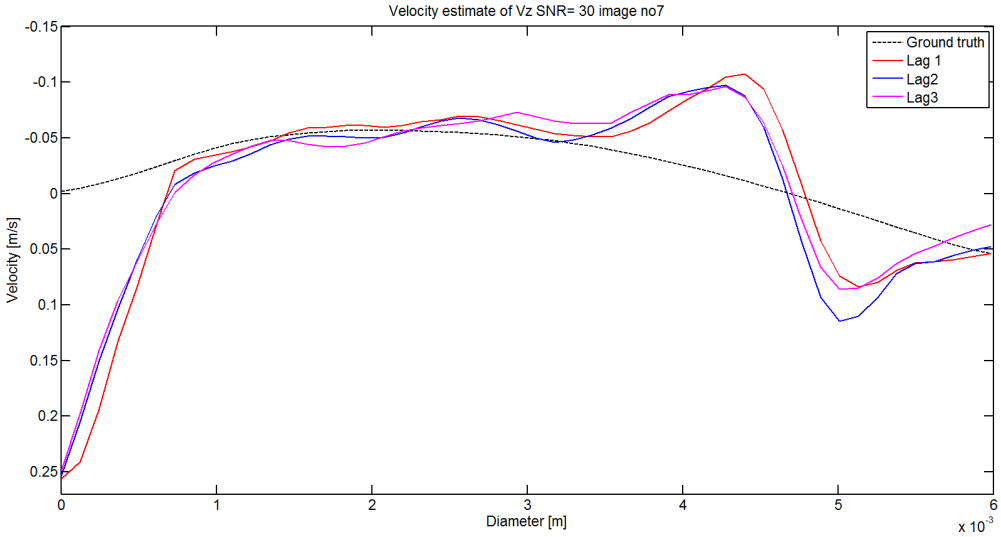

Figure 4.25: velocity estimation in the z-direction for different lags from area 1 with same interpolation factor flow frame 7

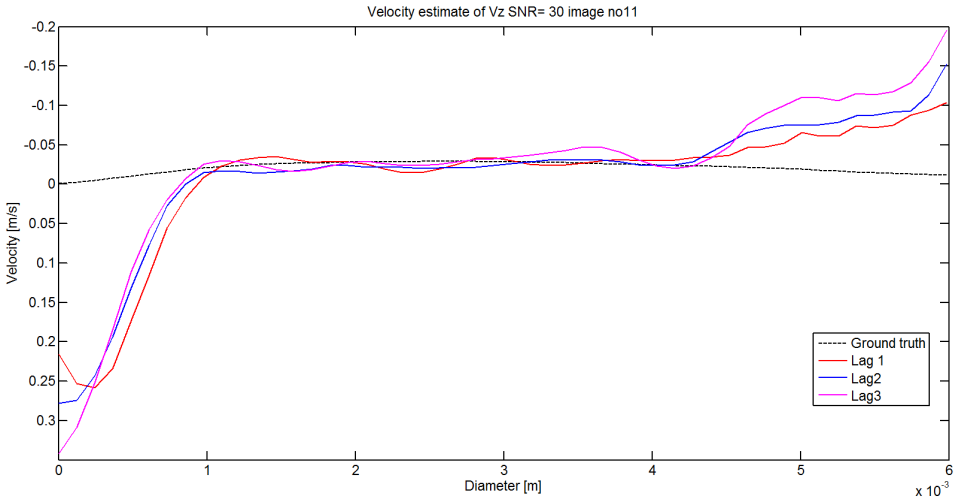

Figure 4.26: velocity estimation in the z-direction for different lags from area 1 with same interpolation factor flow frame 11

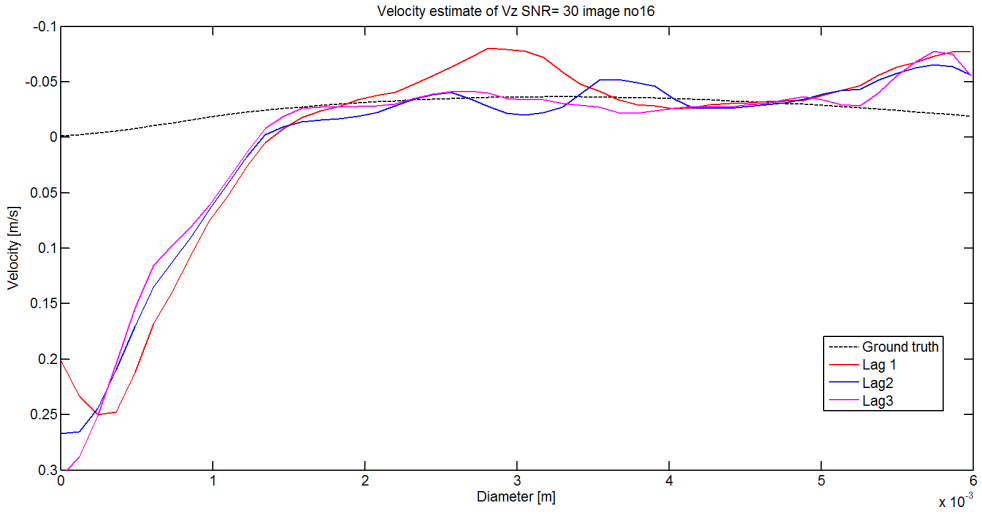

Figure 4.27: velocity estimation in the z-direction for different lags from area 1 with same interpolation factor flow frame 16

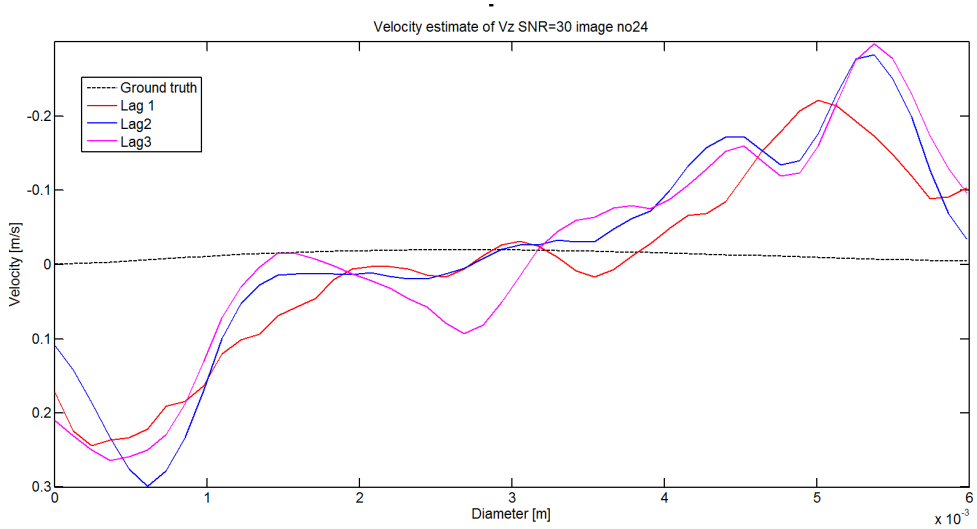

Figure 4.28: velocity estimation in the z-direction for different lags from area 1 with same interpolation factor flow frame 24

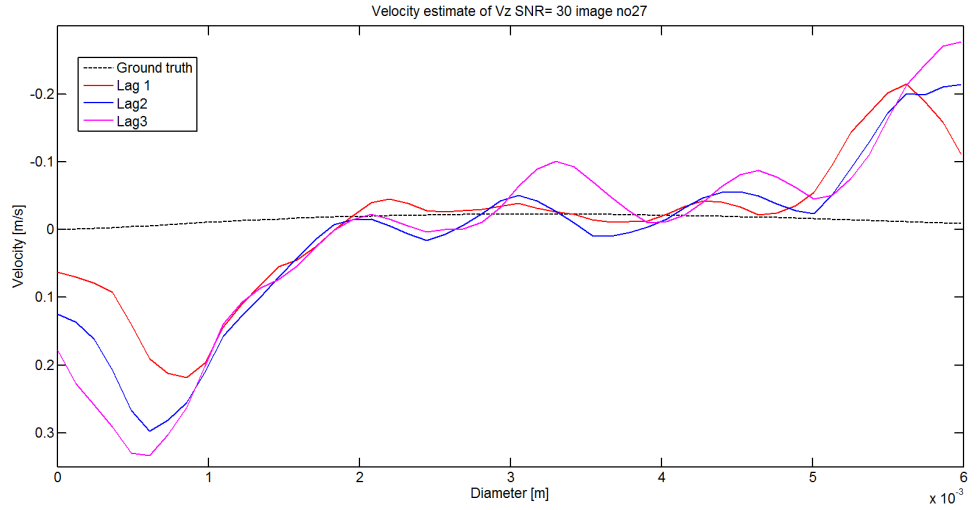

Figure 4.29: velocity estimation in the z-direction for different lags from area 1 with same interpolation factor flow frame 27

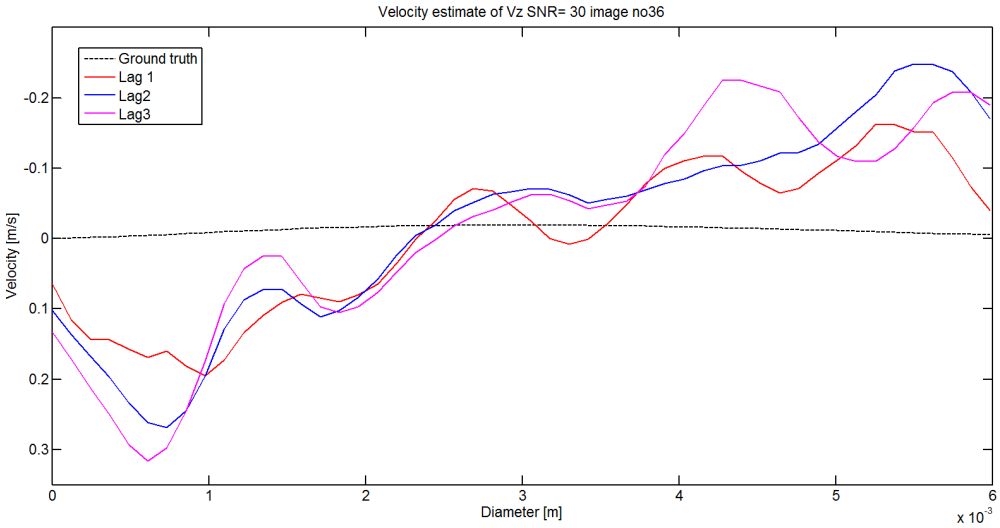

Figure 4.30: velocity estimation in the z-direction for different lags from area 1 with same interpolation factor flow frame 36

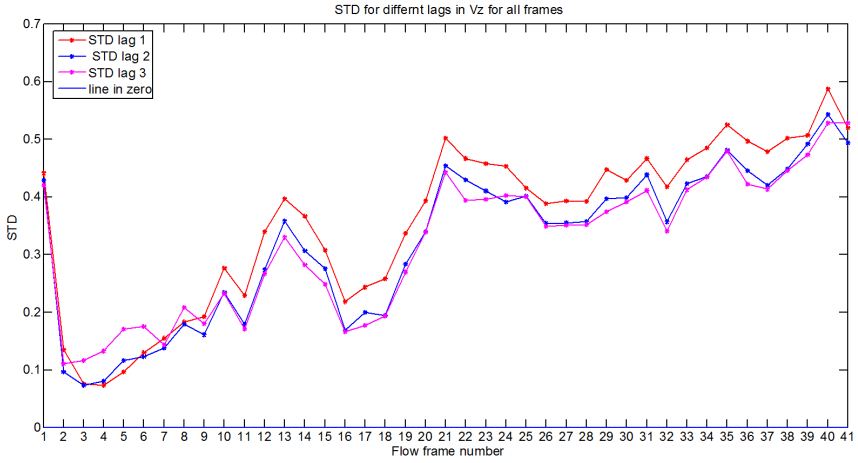

Figure 4.31: Standard deviation for the velocity estimates in the z-direction for different lags from area 1 with the same interpolation-factor

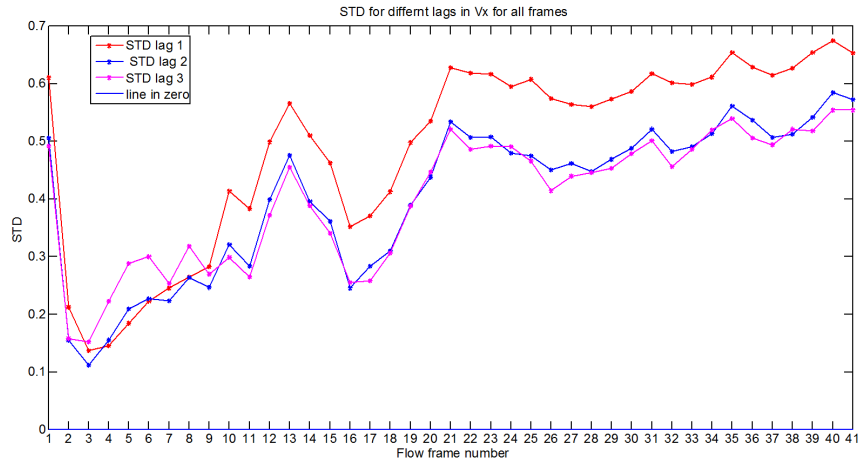

Figure 4.32: Standard deviation for the velocity estimates in the x-direction for different lags from area 1 with the same interpolation-factor

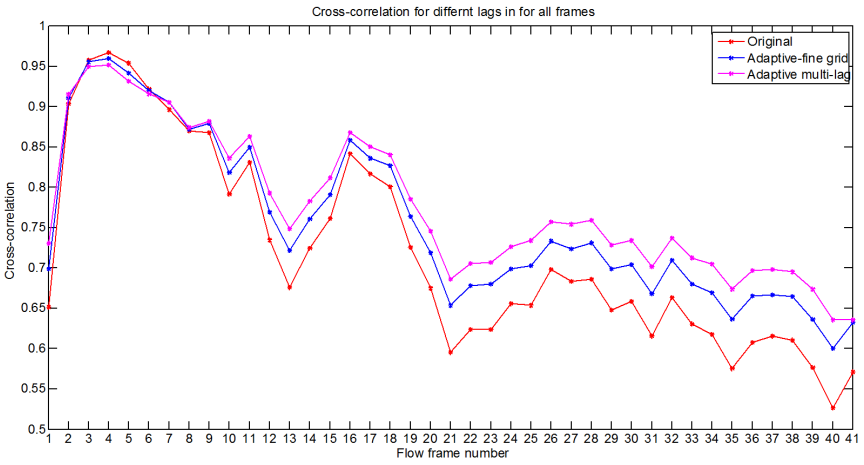

Figure 4.33: Mean cross-correlation for all lags over all frames for area 1

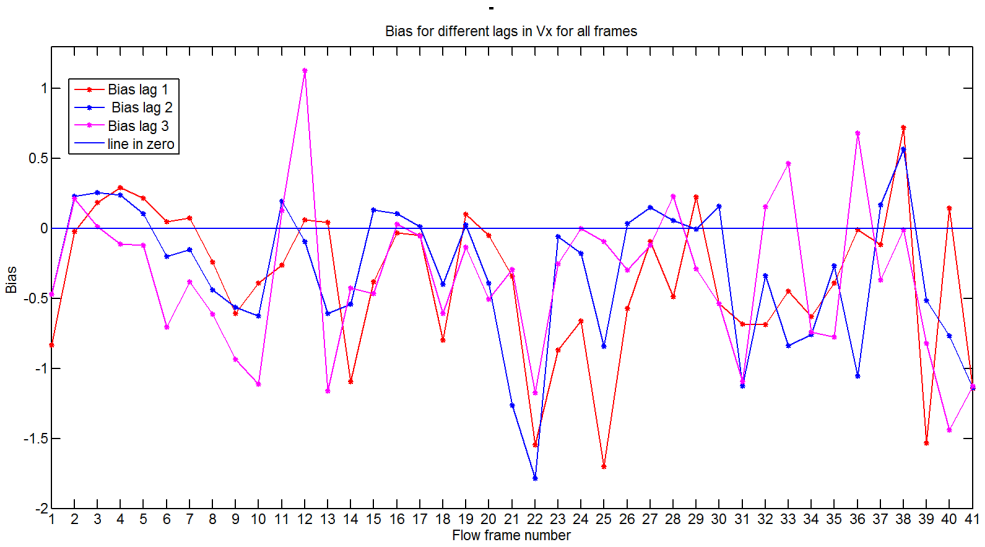

Figure 4.34: Bias for the velocity estimates in the x-direction for different lags from area 1 with the same interpolation-factor

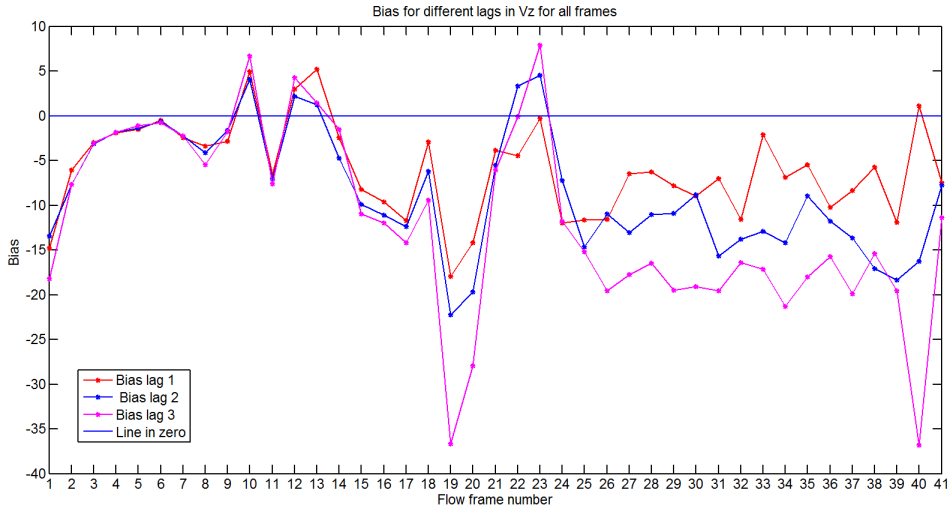

Figure 4.35: Bias for the velocity estimates in the z-direction for different lags from area 1 with the same interpolation-factor

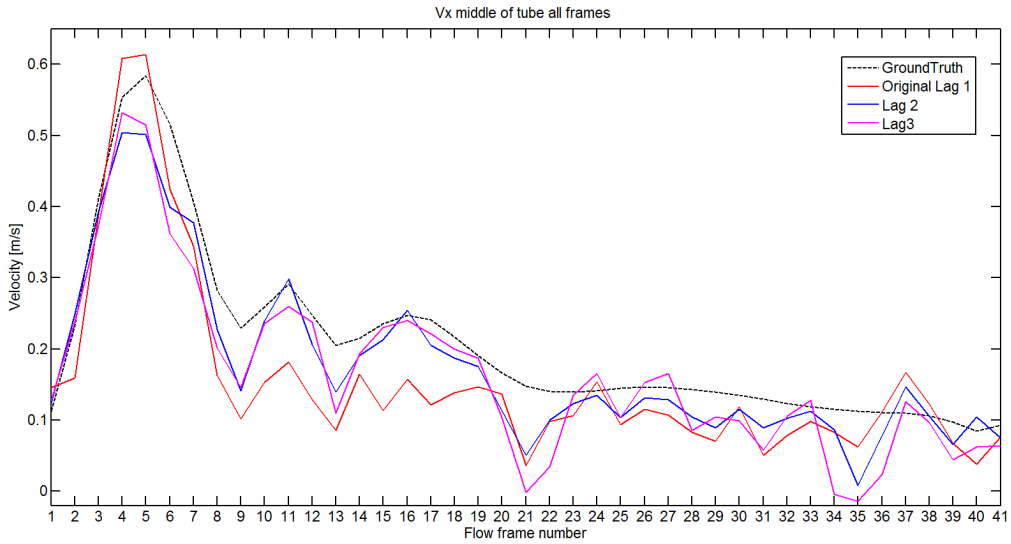

Figure 4.36: Velocity estimates in the x-direction for different lags from area 1 with the same interpolation-factor in the middle of the tube for all flow frames

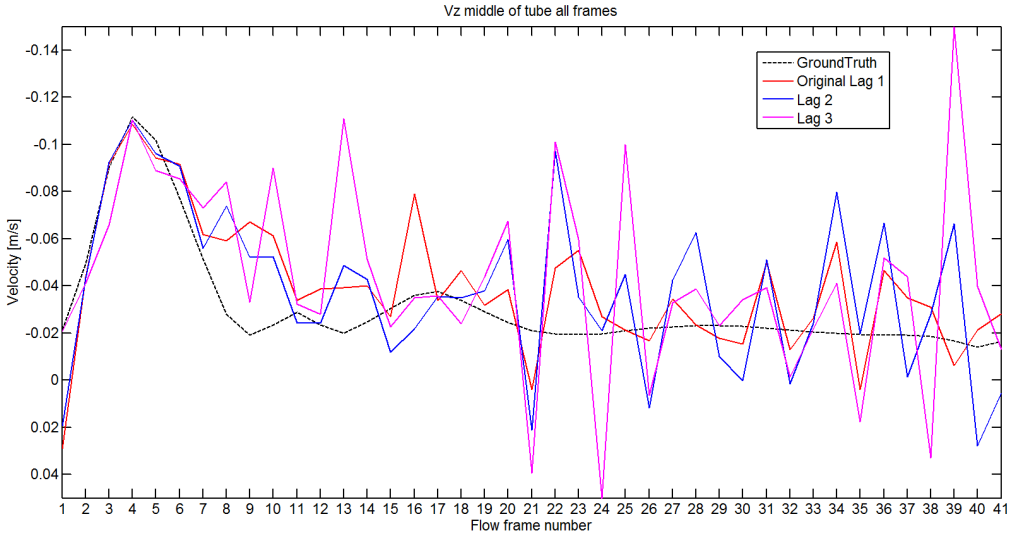

Figure 4.37: Velocity estimates in the z-direction for different lags from area 1 with the same interpolation-factor in the middle of the tube for all flow frames

Results area 2

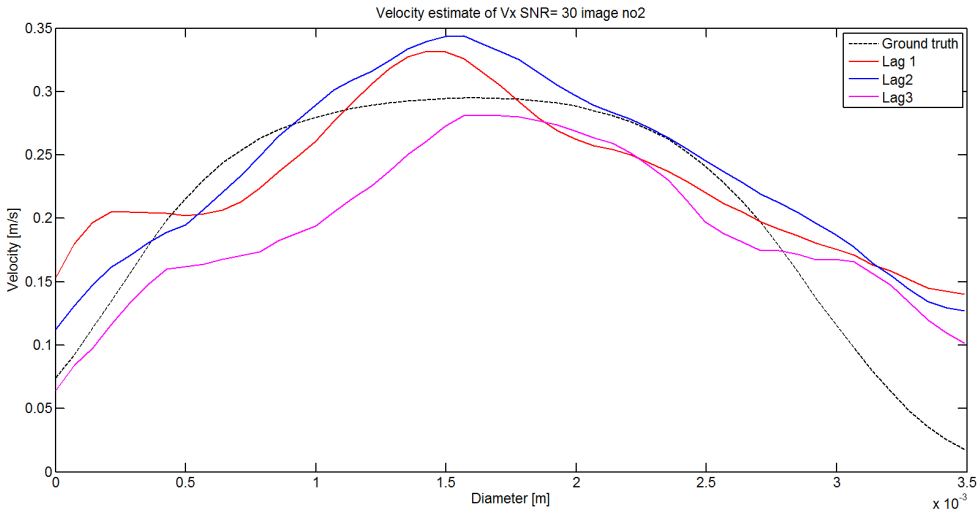

Figure 4.38: velocity estimation in the x-direction for different lags from area 2 with same interpolation-factor flow frame 2

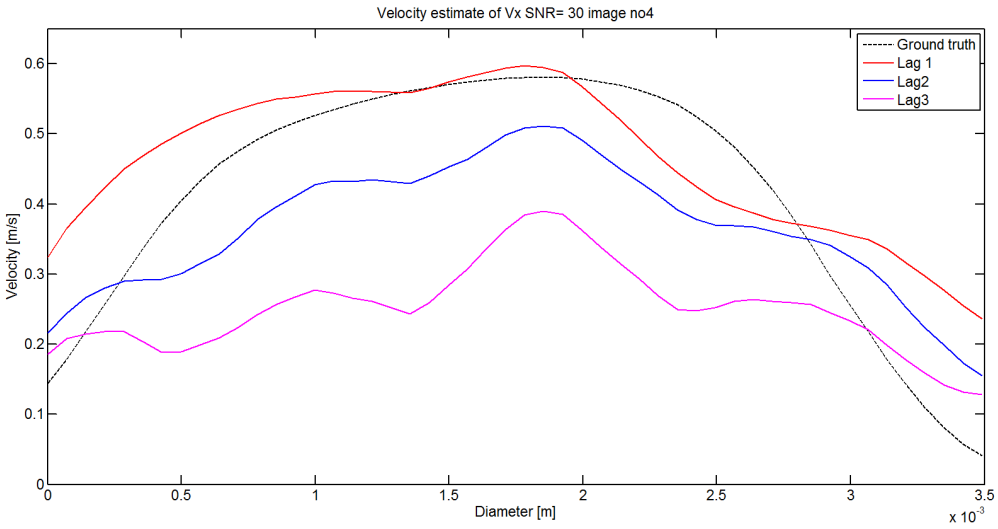

Figure 4.39: velocity estimation in the x-direction for different lags from area 2 with same interpolation-factor flow frame 4

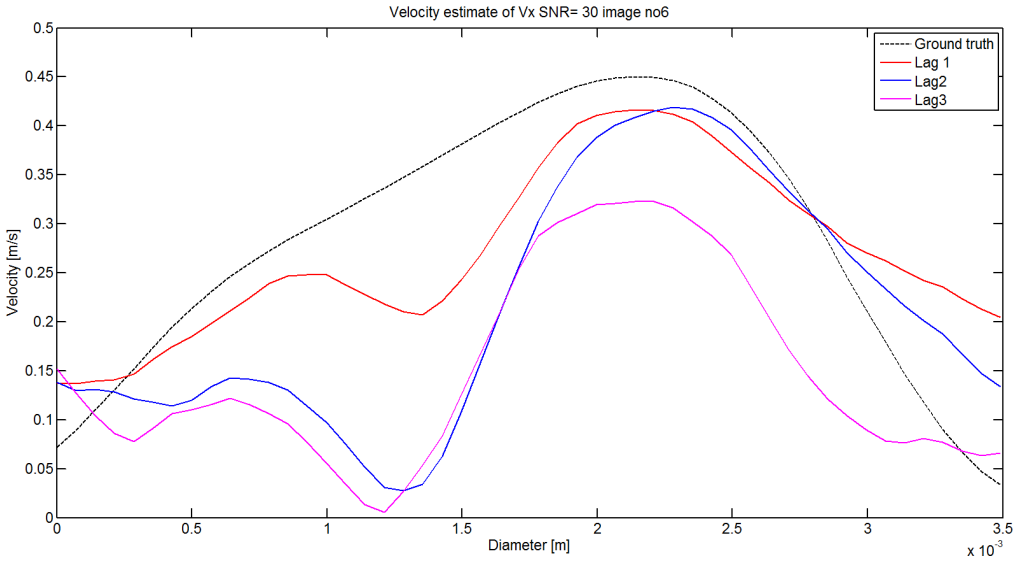

Figure 4.40: velocity estimation in the x-direction for different lags from area 2 with same interpolation-factor flow frame 6

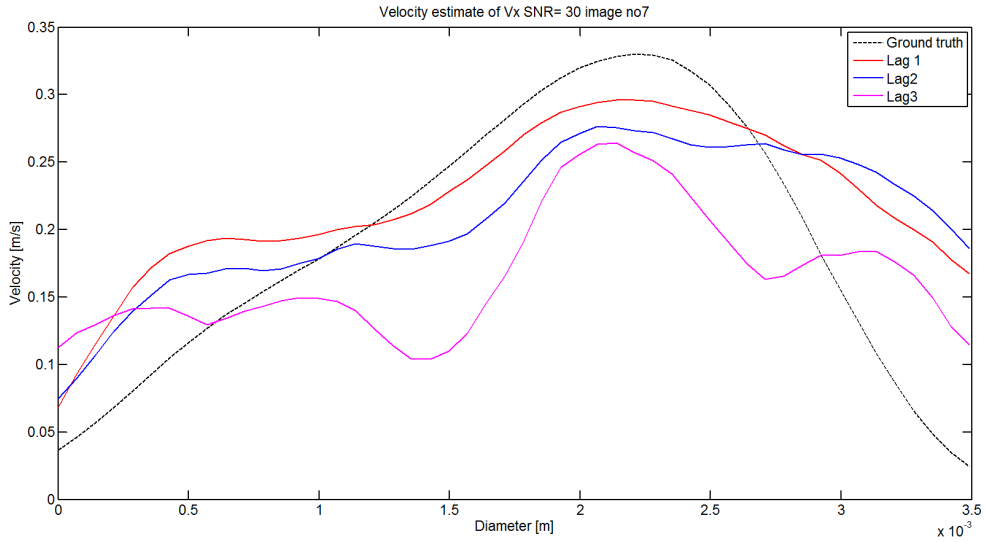

Figure 4.41: velocity estimation in the x-direction for different lags from area 2 with same interpolation-factor flow frame 7

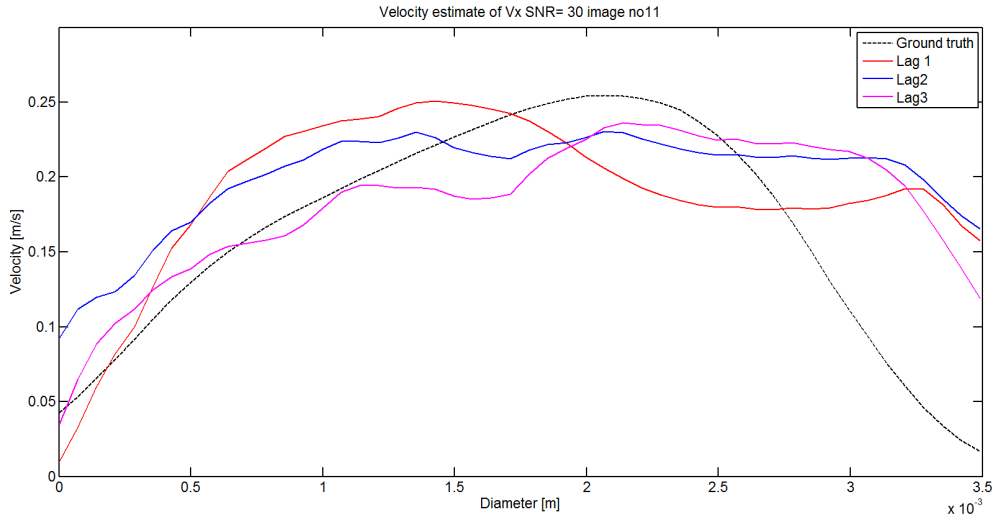

Figure 4.42: velocity estimation in the x-direction for different lags from area 2 with same interpolation-factor flow frame 11

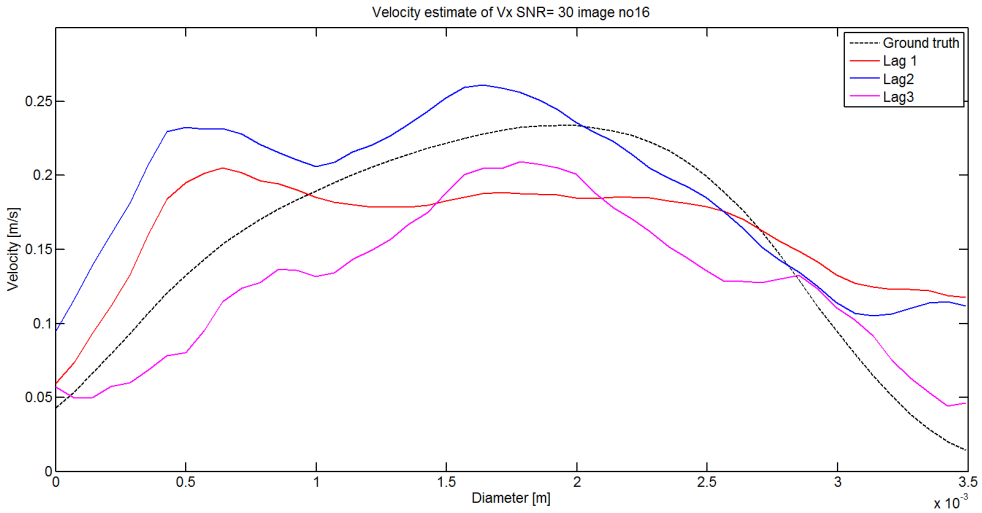

Figure 4.43: velocity estimation in the x-direction for different lags from area 2 with same interpolation-factor flow frame 16

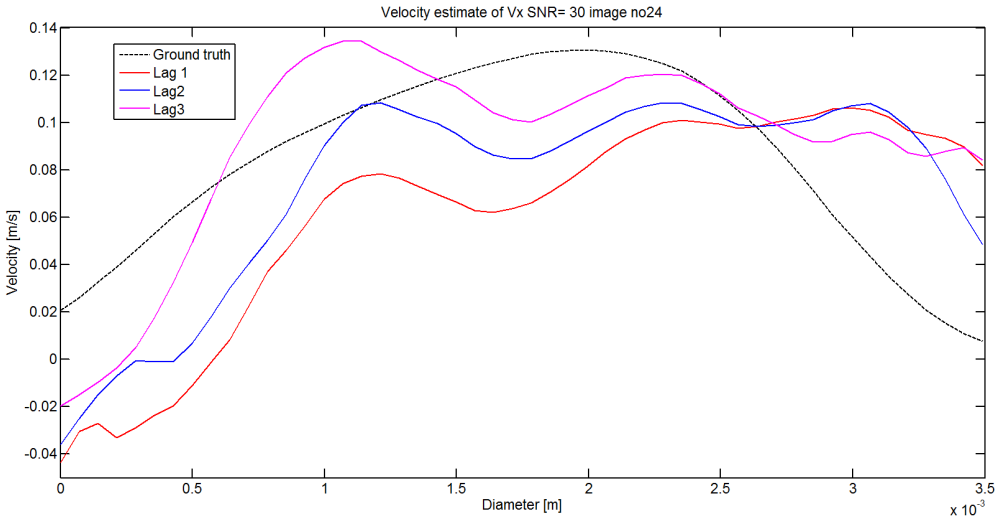

Figure 4.44: velocity estimation in the x-direction for different lags from area 2 with same interpolation-factor flow frame 24

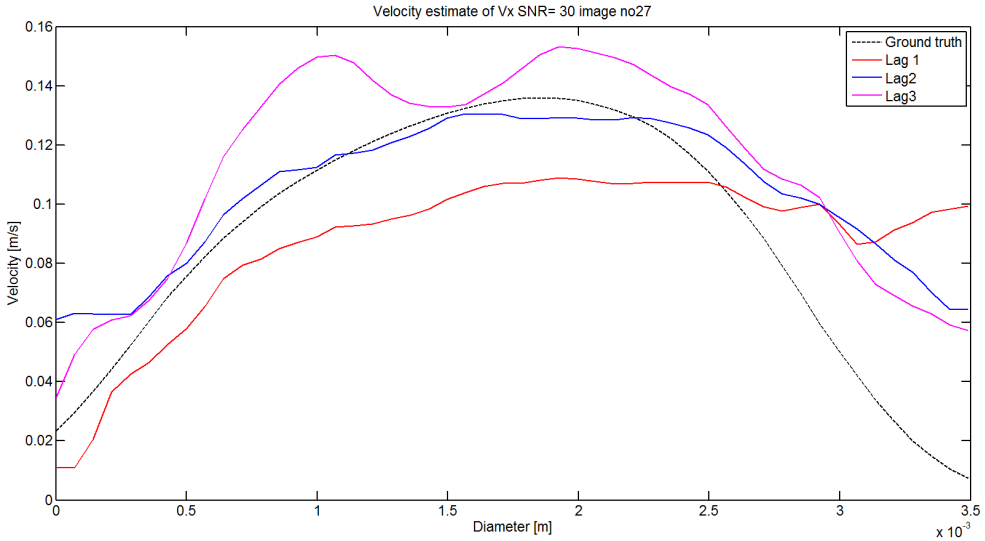

Figure 4.45: velocity estimation in the x-direction for different lags from area 2 with same interpolation-factor flow frame 27

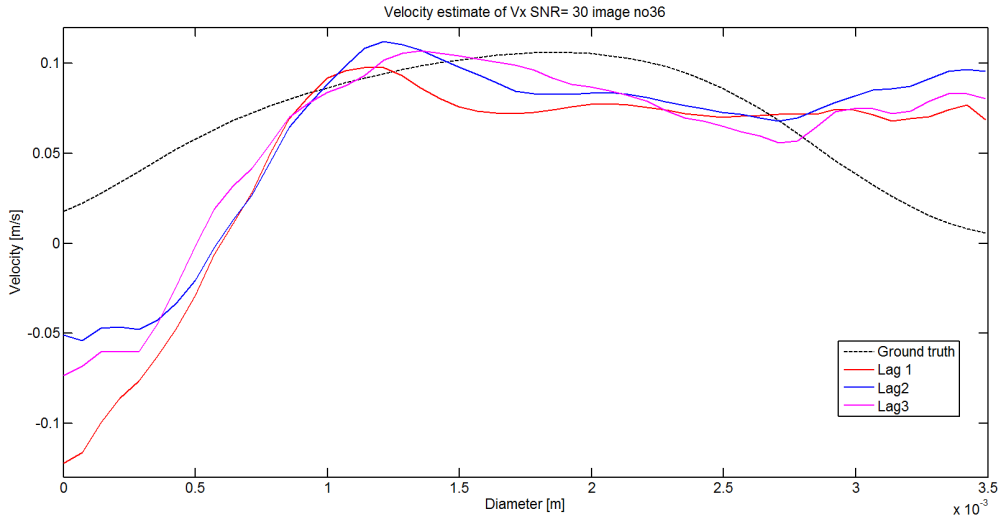

Figure 4.46: velocity estimation in the x-direction for different lags from area 2 with same interpolation-factor flow frame 36

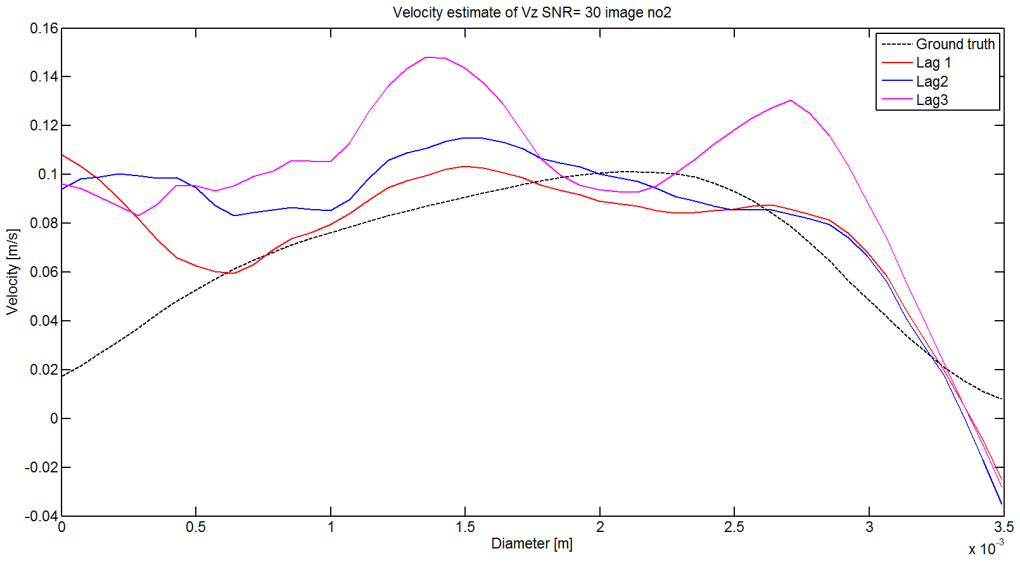

Figure 4.47: velocity estimation in the z-direction for different lags from area 2 with same interpolation-factor flow frame 2

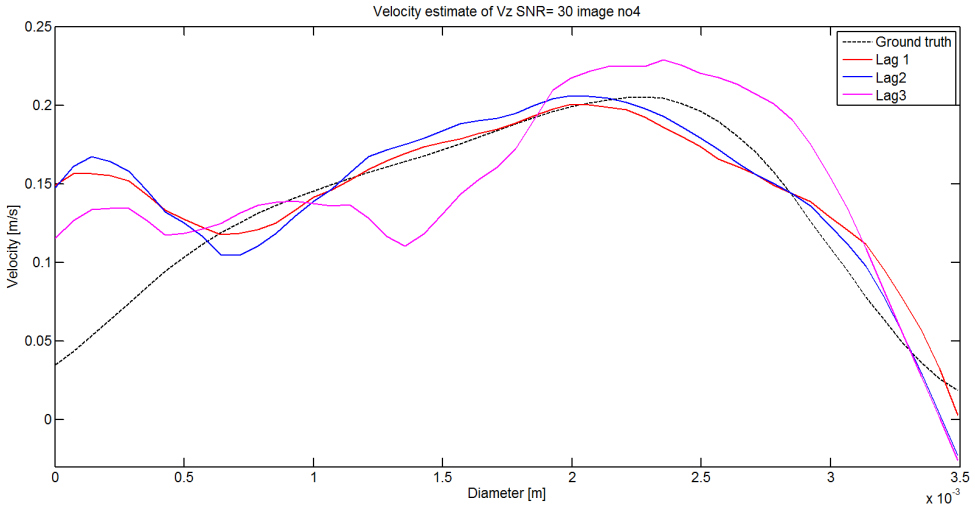

Figure 4.48: velocity estimation in the z-direction for different lags from area 2 with same interpolation-factor flow frame 4

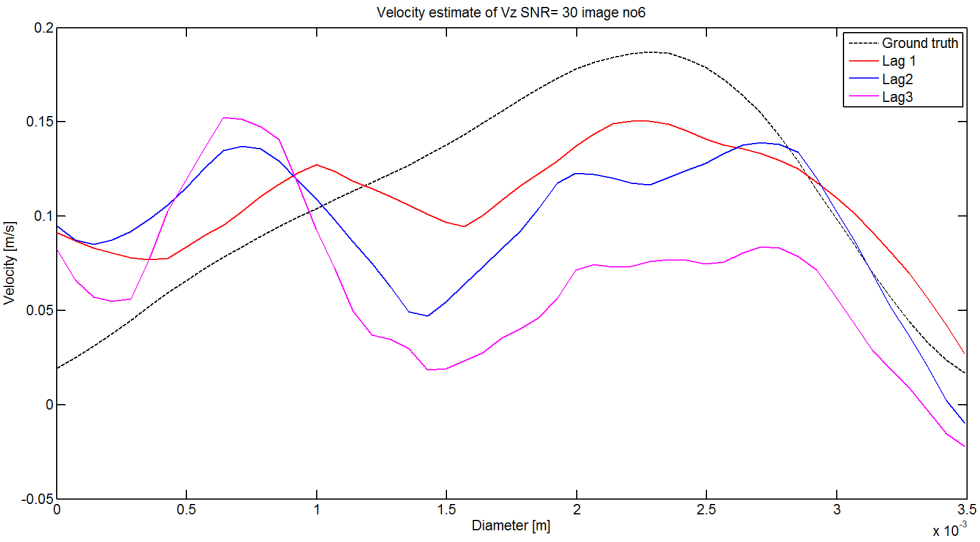

Figure 4.49: velocity estimation in the z-direction for different lags from area 2 with same interpolation-factor flow frame 6

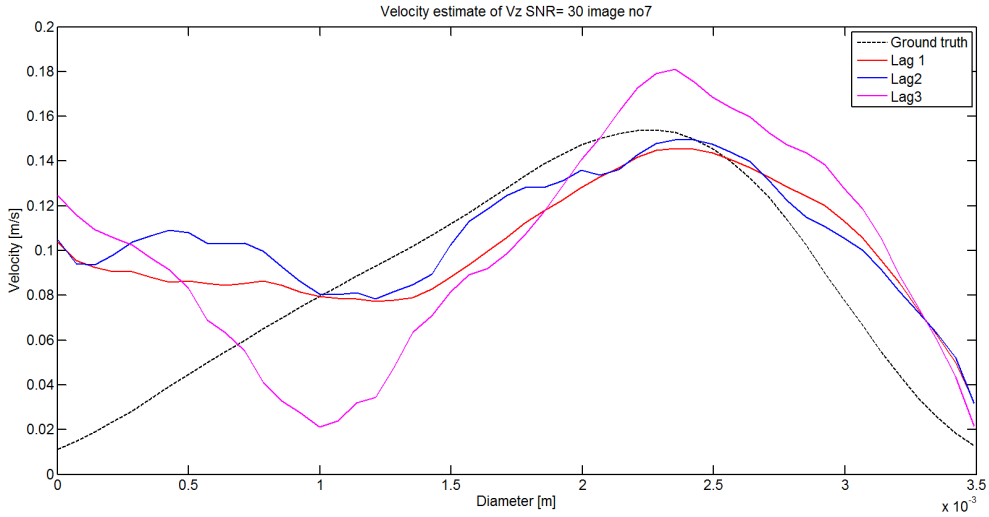

Figure 4.50: velocity estimation in the z-direction for different lags from area 2 with same interpolation-factor flow frame 7

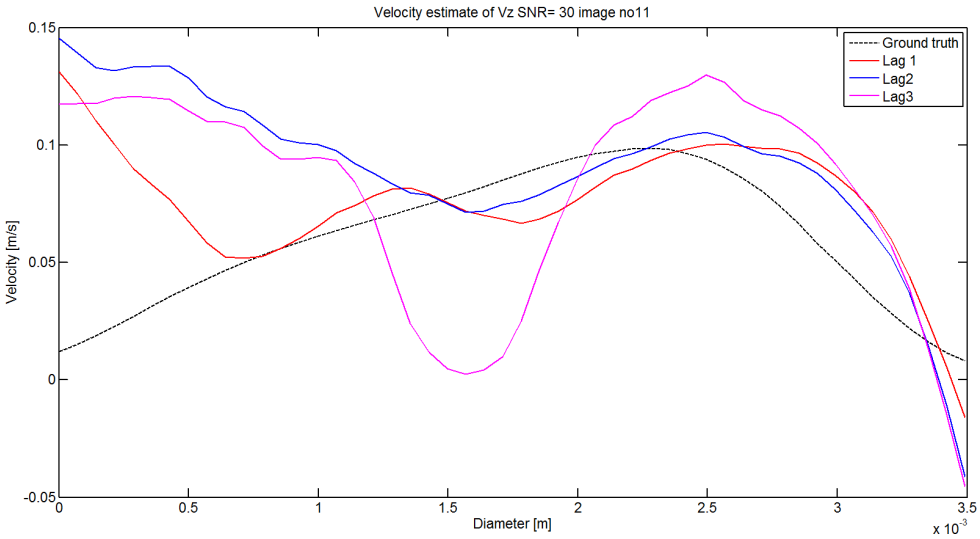

Figure 4.51: velocity estimation in the z-direction for different lags from area 2 with same interpolation-factor flow frame 11

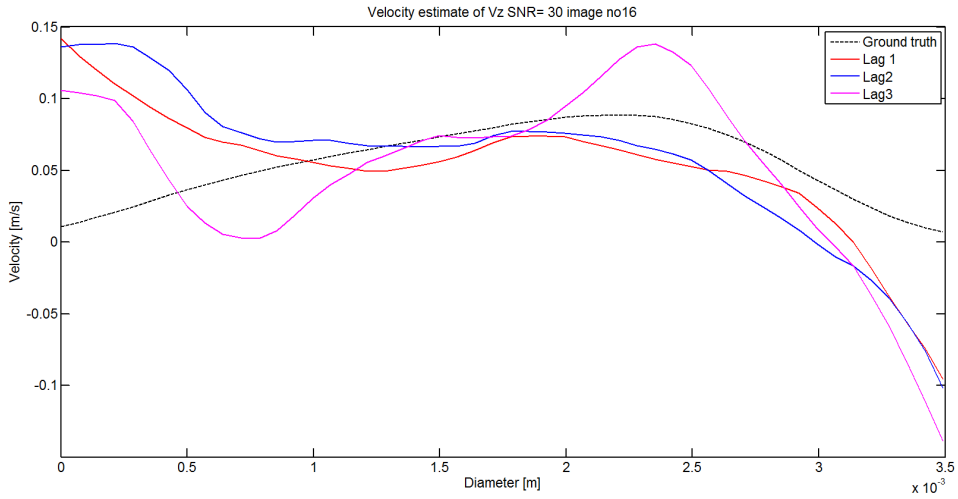

Figure 4.52: velocity estimation in the z-direction for different lags from area 2 with same interpolation-factor flow frame 16

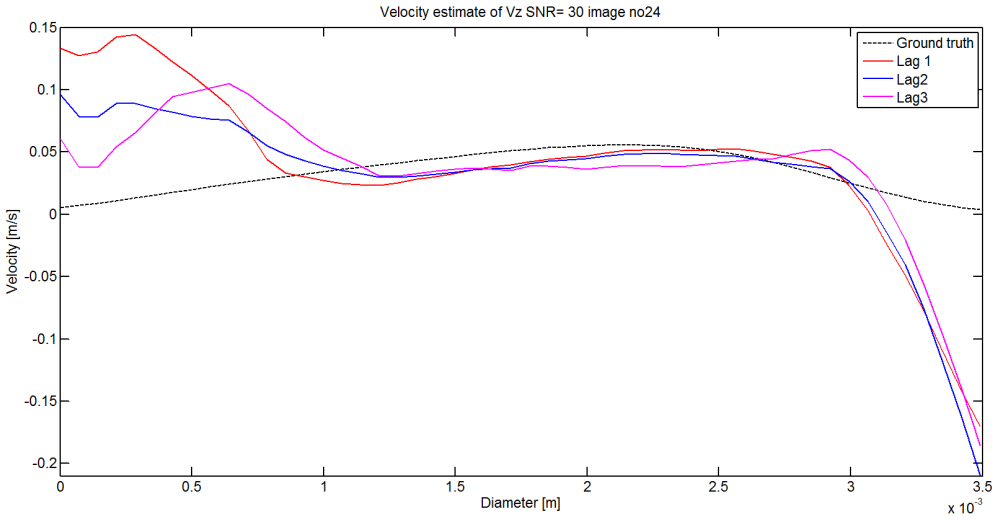

Figure 4.53: velocity estimation in the z-direction for different lags from area 2 with same interpolation-factor flow frame 24

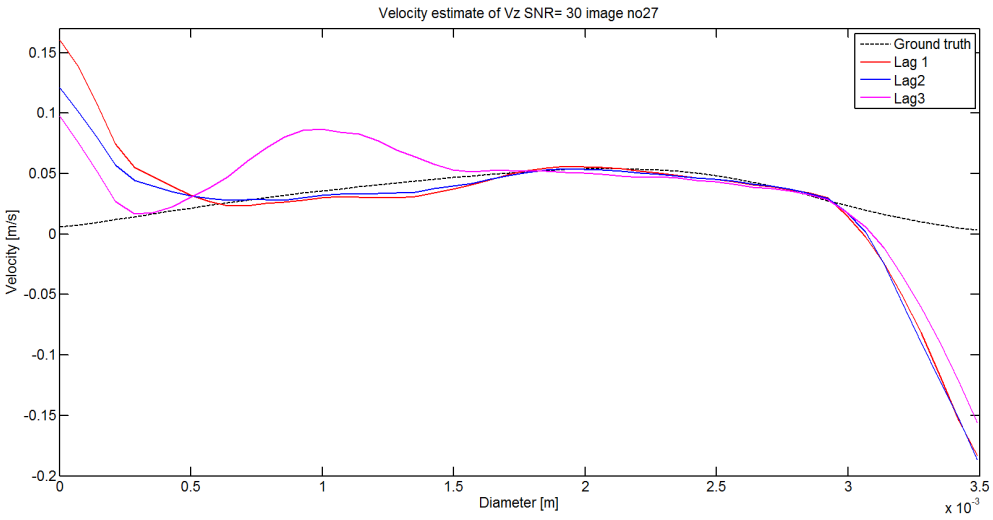

Figure 4.54: velocity estimation in the z-direction for different lags from area 2 with same interpolation-factor flow frame 27

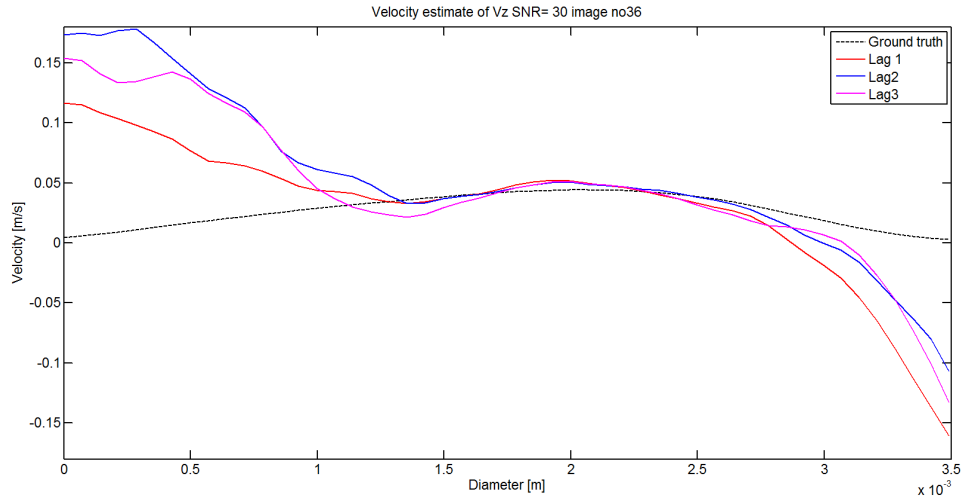

Figure 4.55: velocity estimation in the z-direction for different lags from area 2 with same interpolation-factor flow frame 36

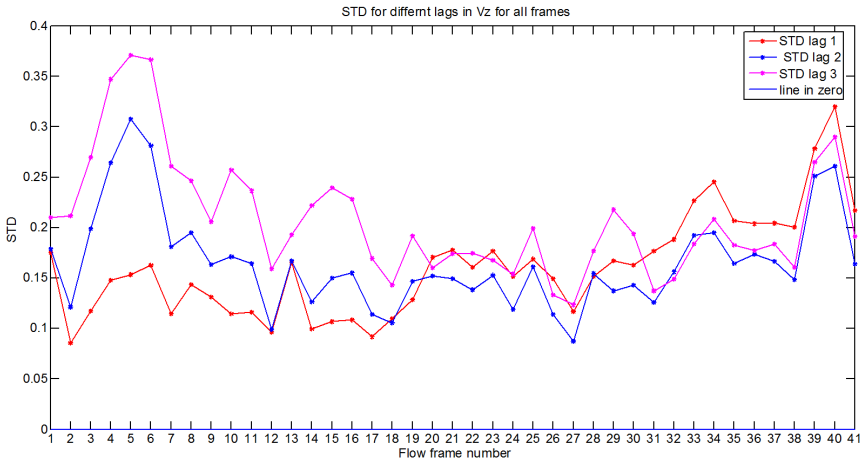

Figure 4.56: Standard deviation for the velocity estimates in the z-direction for different lags from area 2 with the same interpolation-factor

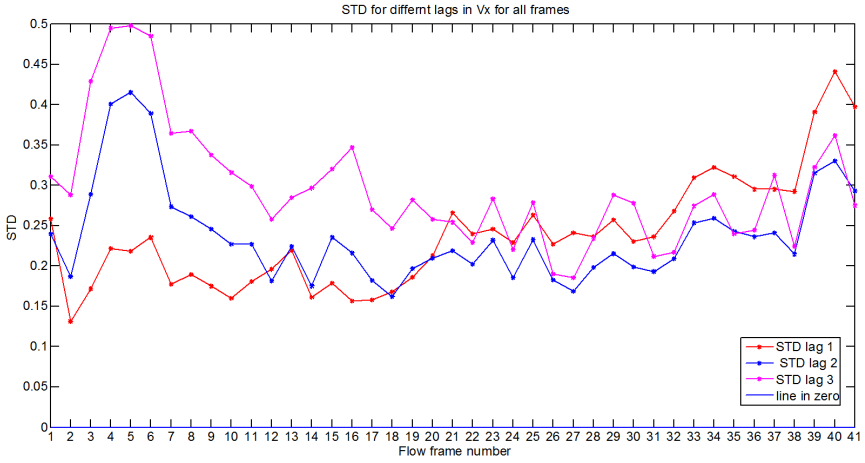

Figure 4.57: Standard deviation for the velocity estimates in the x-direction for different lags from area 2 with the same interpolation-factor

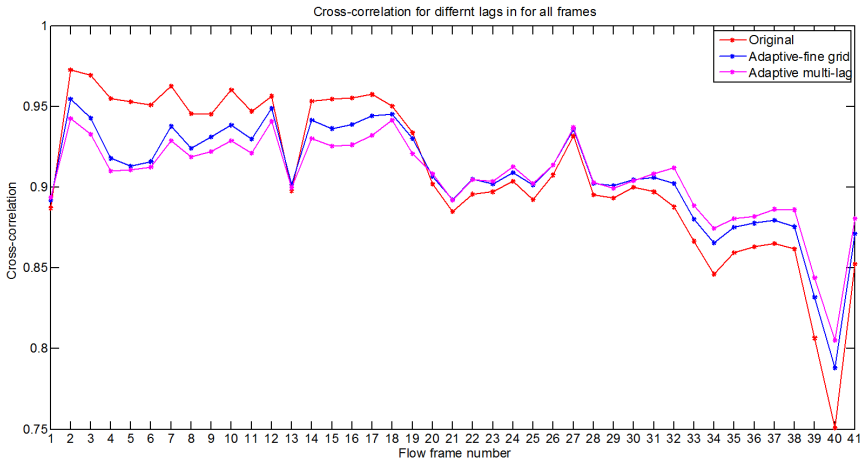

Figure 4.58: Mean cross-correlation for all lags over all frames for area 2

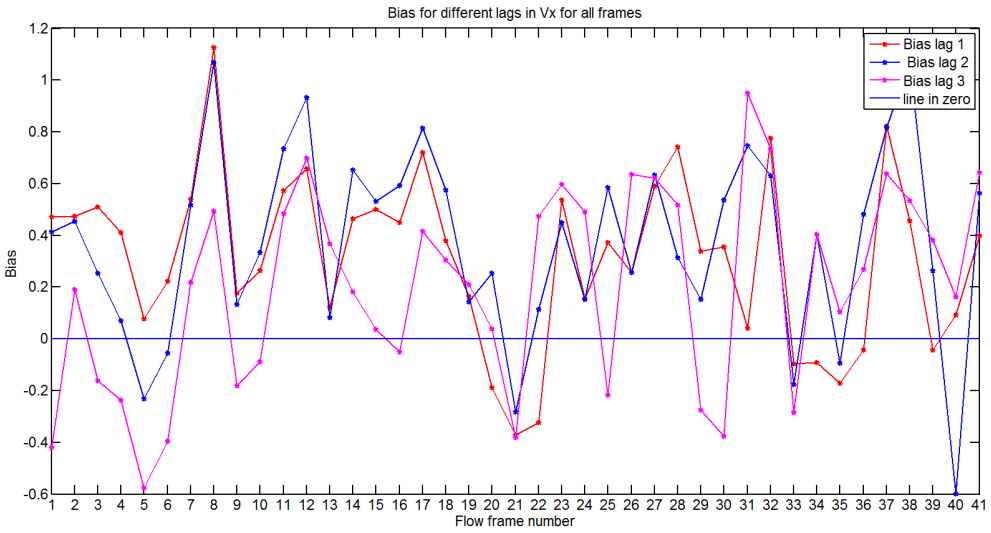

Figure 4.59: Bias for the velocity estimates in the x-direction for different lags from area 2 with the same interpolation-factor

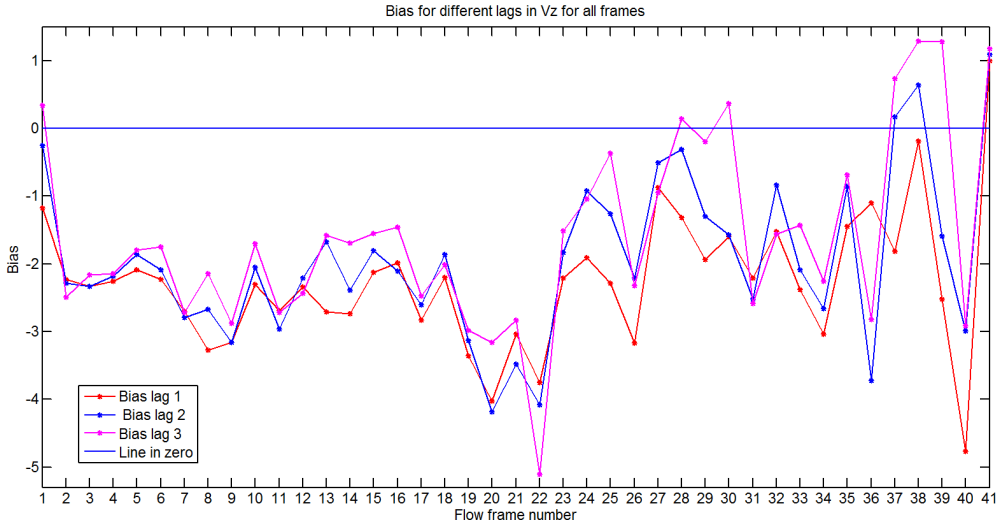

Figure 4.60: Bias for the velocity estimates in the z-direction for different lags from area 2 with the same interpolation-factor

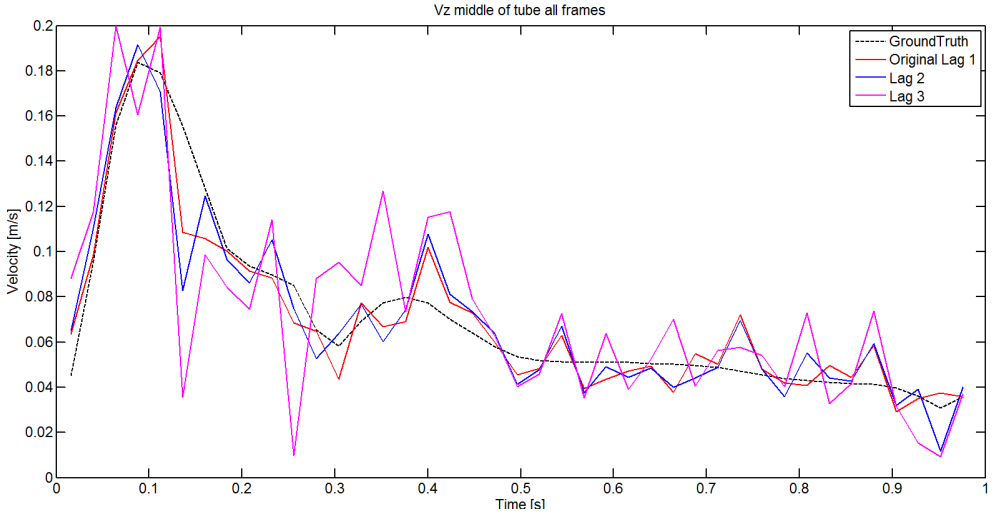

Figure 4.61: Velocity estimates in the x-direction for different lags from area 2 with the same interpolation-factor in the middle of the tube for all flow frames

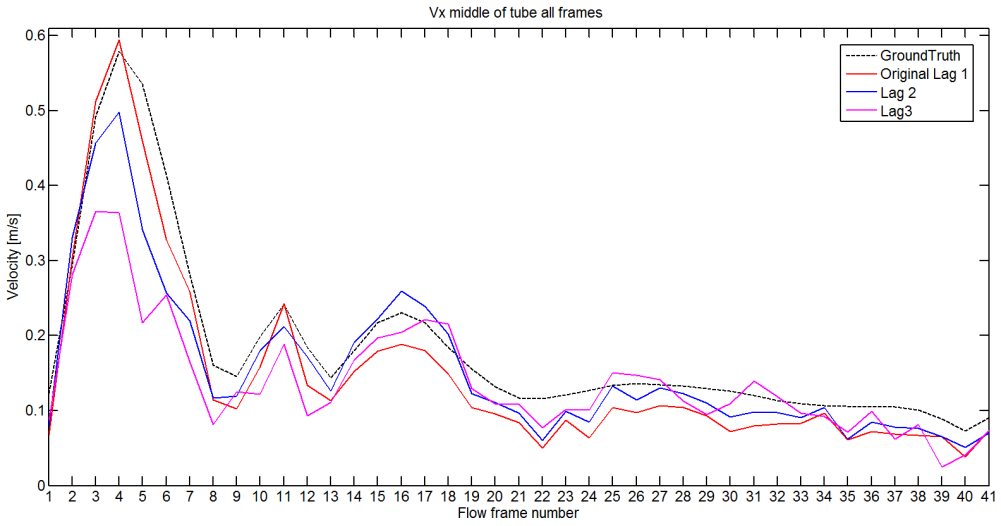

Figure 4.62: Velocity estimates in the z-direction for different lags from area 2 with the same interpolation-factor in the middle of the tube for all flow frames

Results area 3

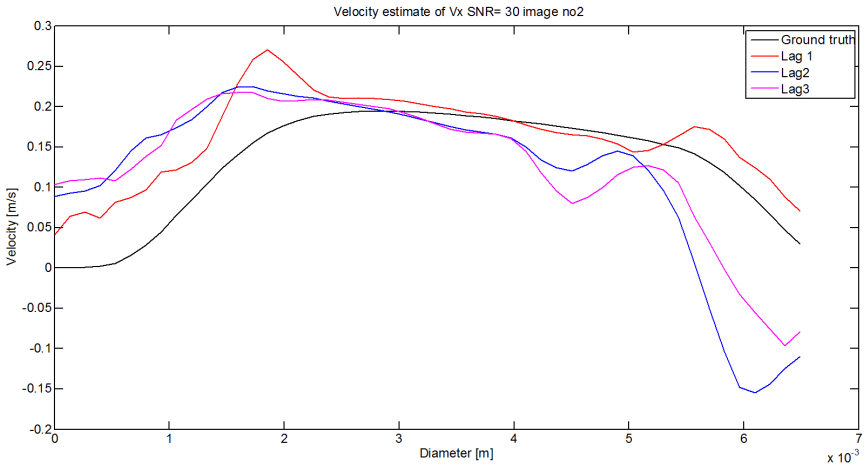

Figure 4.63: velocity estimation in the x-direction for different lags from area 3 with same interpolation-factor flow frame 2

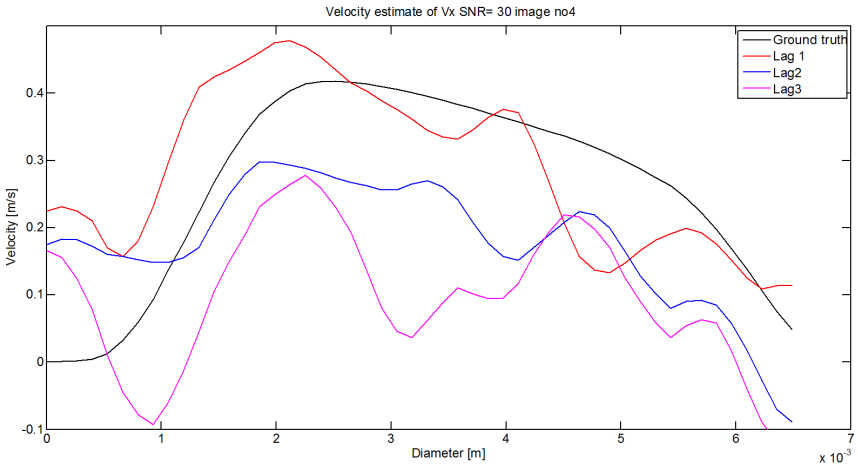

Figure 4.64: velocity estimation in the x-direction for different lags from area 3 with same interpolation-factor flow frame 4

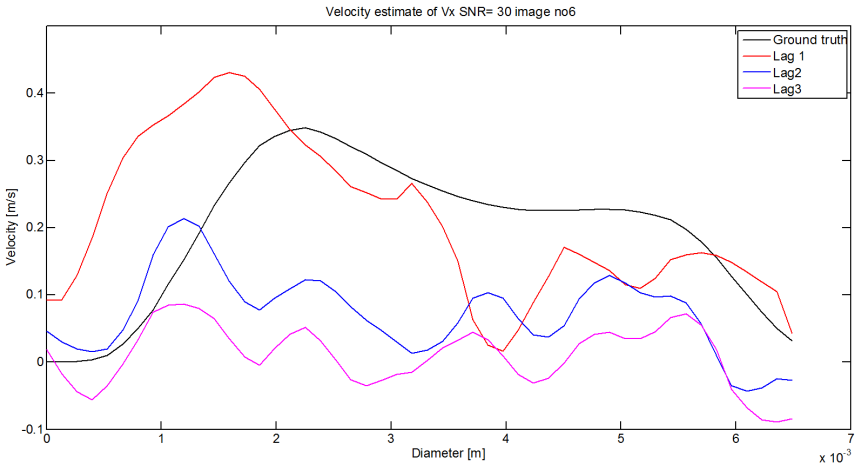

Figure 4.65: velocity estimation in the x-direction for different lags from area 3 with same interpolation-factor flow frame 6

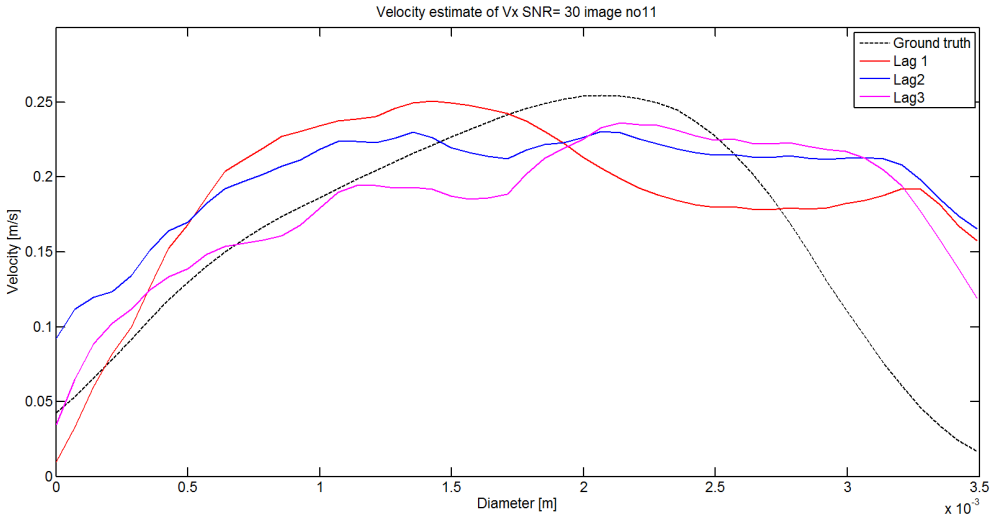

Figure 4.66: velocity estimation in the x-direction for different lags from area 2 with same interpolation-factor flow frame 11

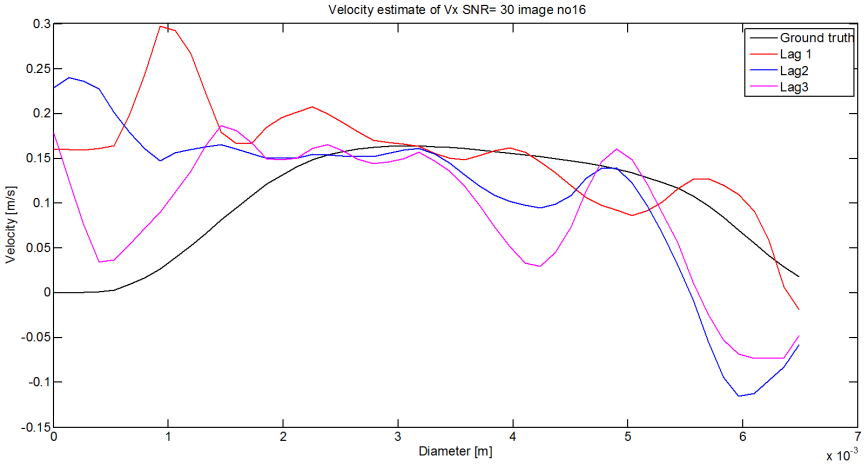

Figure 4.67: velocity estimation in the x-direction for different lags from area 3 with same interpolation-factor flow frame 16

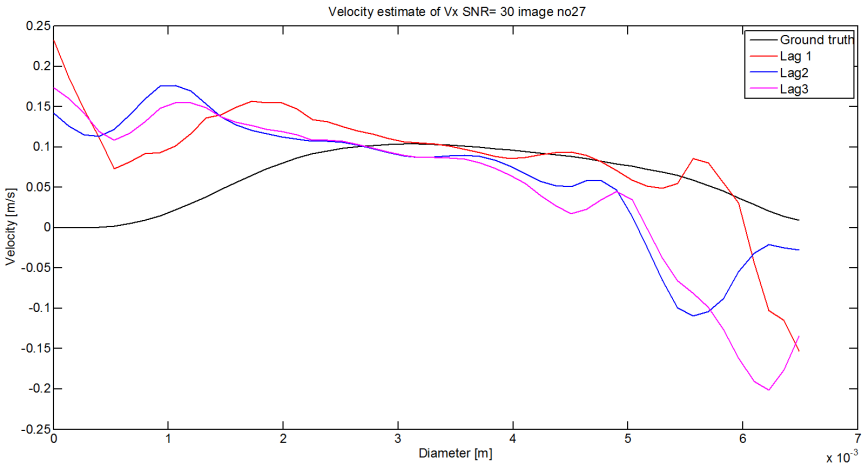

Figure 4.68: velocity estimation in the x-direction for different lags from area 3 with same interpolation-factor flow frame 27

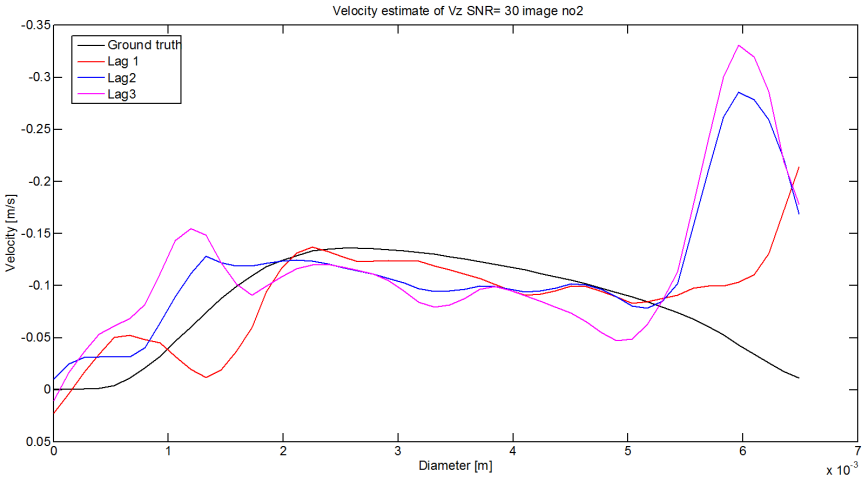

Figure 4.69: velocity estimation in the z-direction for different lags from area 3 with same interpolation-factor flow frame 2

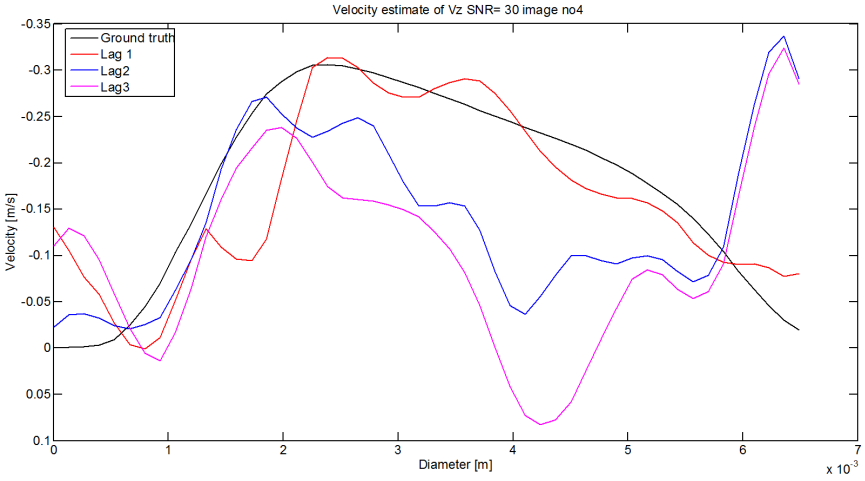

Figure 4.70: velocity estimation in the z-direction for different lags from area 3 with same interpolation-factor flow frame 4

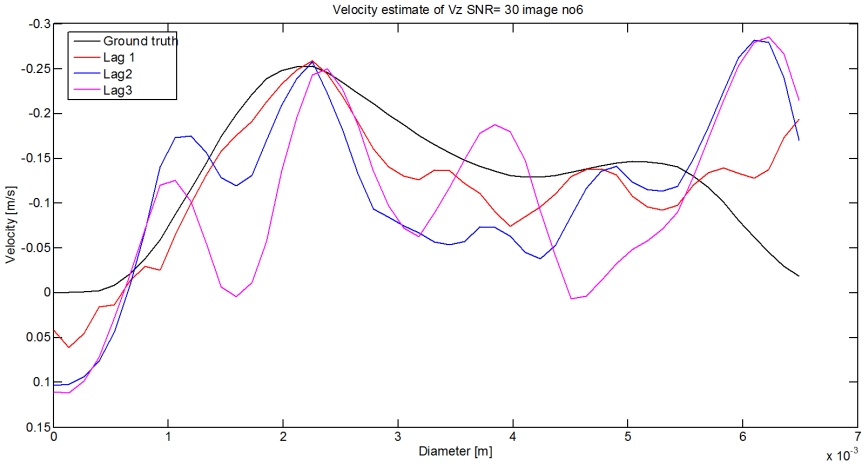

Figure 4.71: velocity estimation in the z-direction for different lags from area 3 with same interpolation-factor flow frame 6

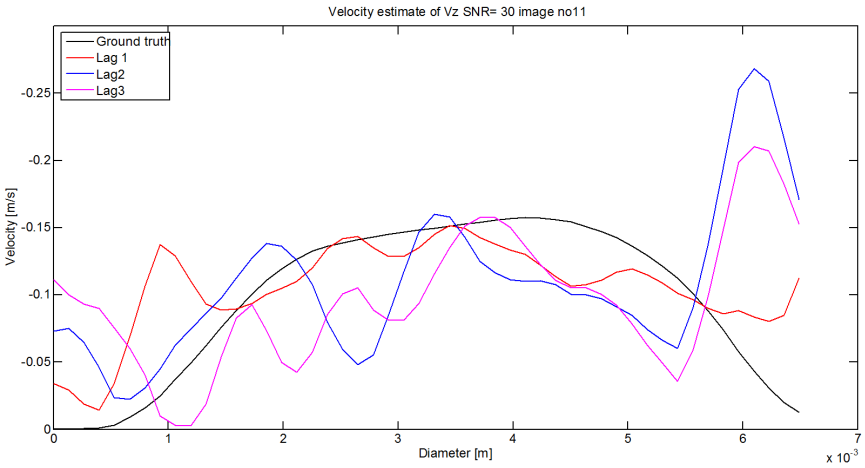

Figure 4.72: velocity estimation in the z-direction for different lags from area 3 with same interpolation-factor flow frame 11

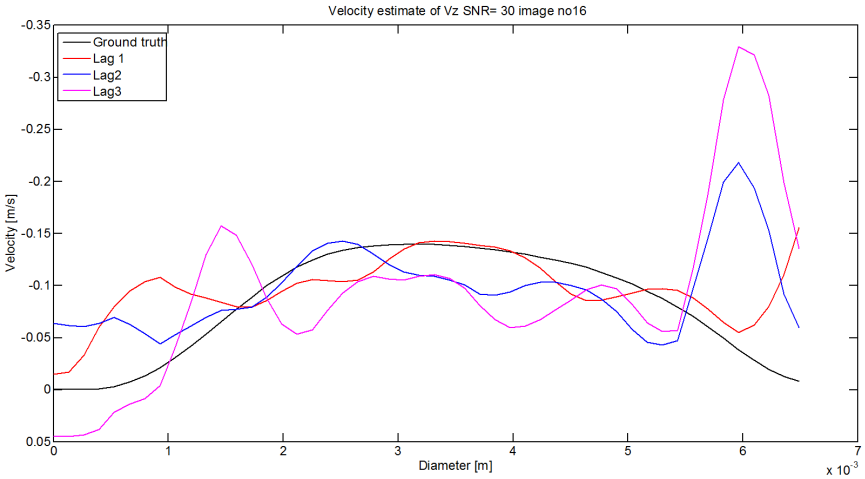

Figure 4.73: velocity estimation in the z-direction for different lags from area 3 with same interpolation-factor flow frame 16

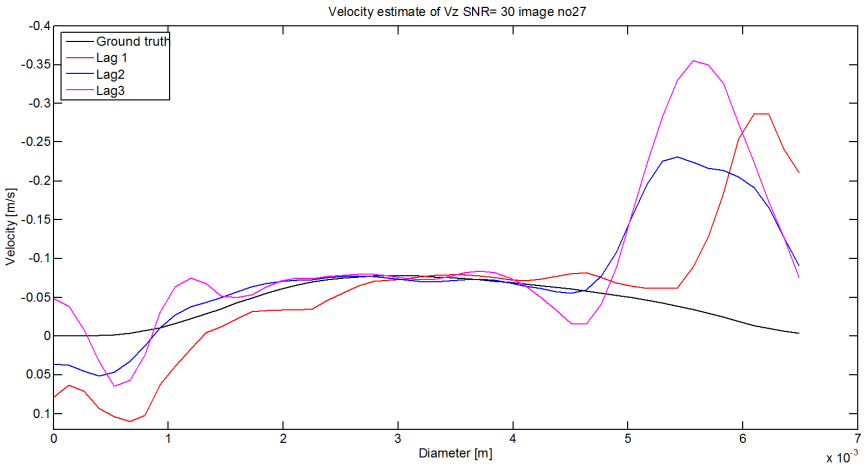

Figure 4.74: velocity estimation in the z-direction for different lags from area 3 with same interpolation-factor flow frame 27

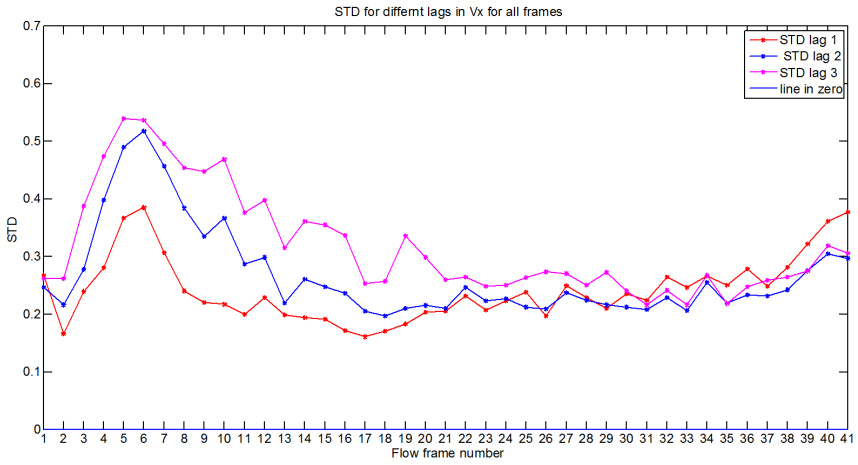

Figure 4.75: Standard deviation for the velocity estimates in the x-direction for different lags from area 3 with the same interpolation-factor

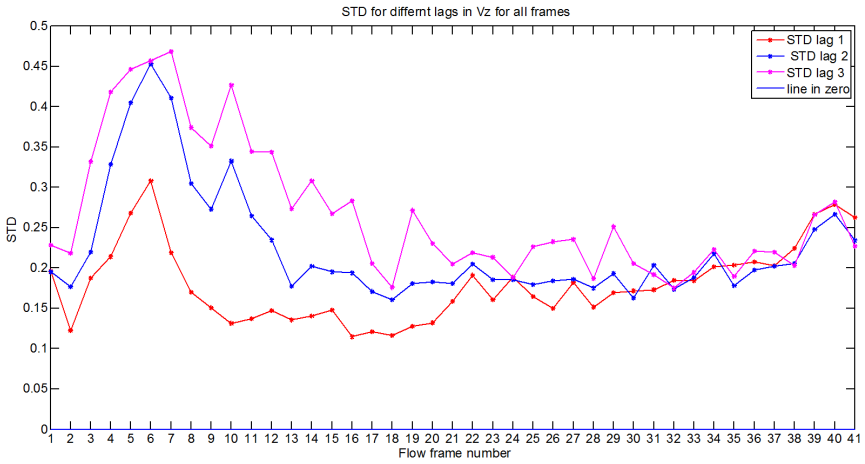

Figure 4.76: Standard deviation for the velocity estimates in the z-direction for different lags from area 3 with the same interpolation-factor

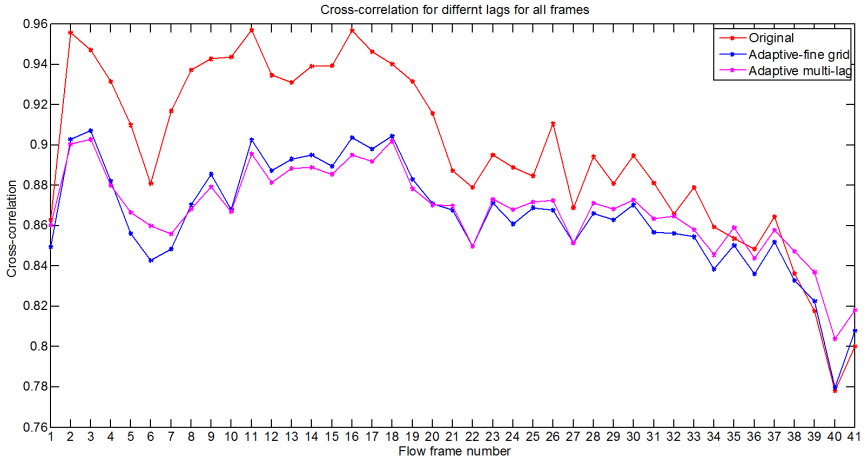

Figure 4.77: Mean cross-correlation for all lags over all frames for area 3

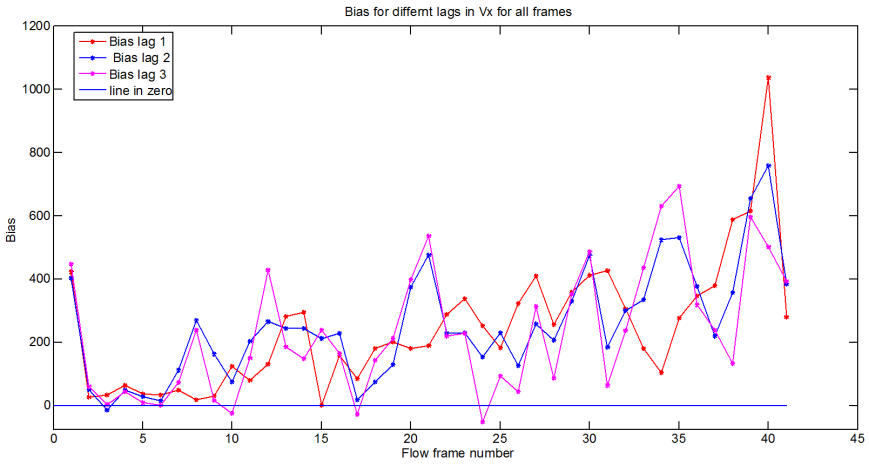

Figure 4.78: Bias for the velocity estimates in the x-direction for different lags from area 3 with the same interpolation-factor

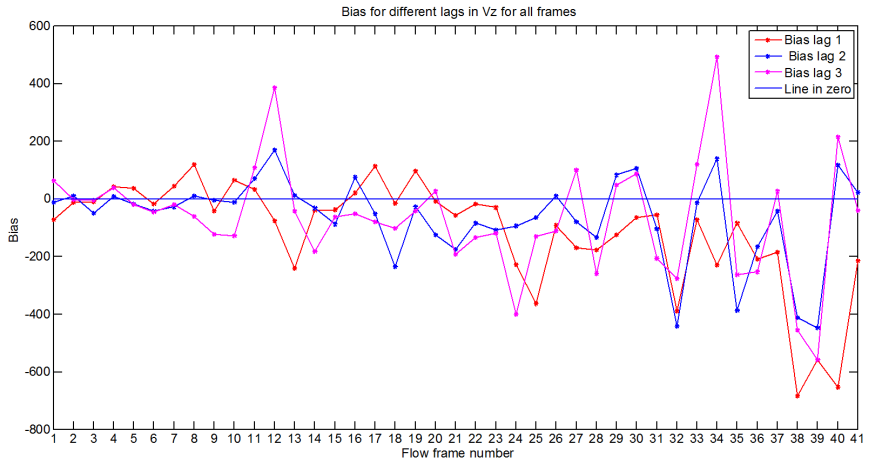

Figure 4.79: Bias for the velocity estimates in the z-direction for different lags from area 3 with the same interpolation-factor

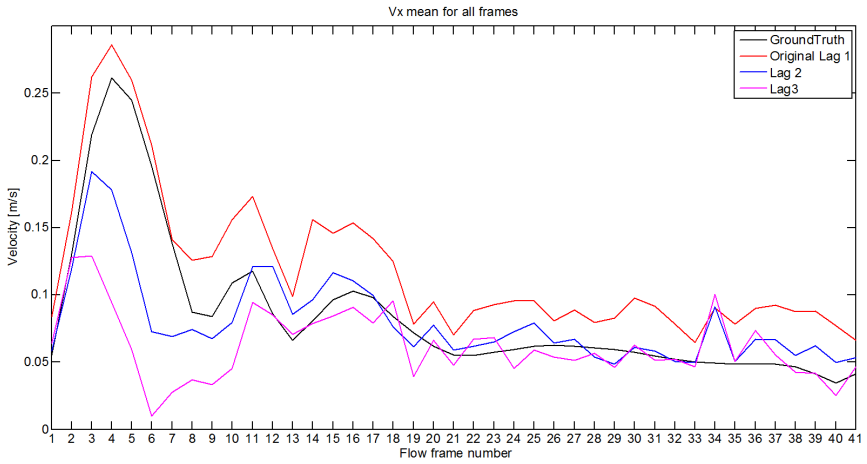

Figure 4.80: Velocity estimates in the x-direction for different lags from area 3 with the same interpolation-factor in the middle of the tube for all flow frames

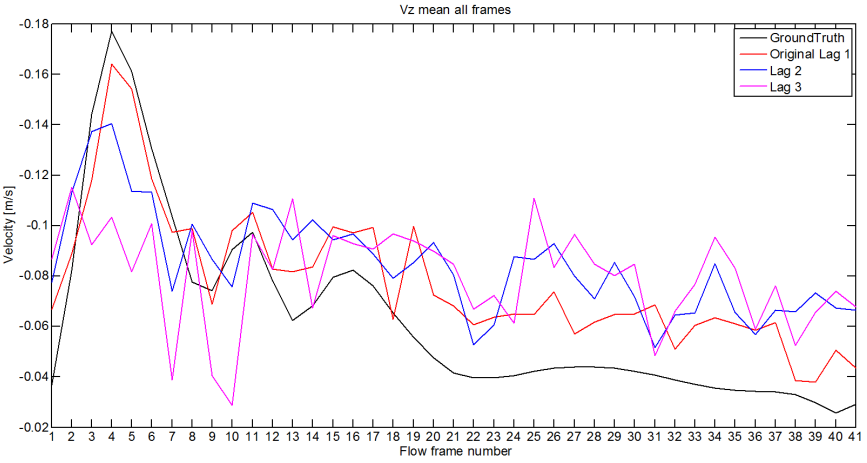

Figure 4.81: Velocity estimates in the z-direction for different lags from area 3 with the same interpolation-factor in the middle of the tube for all flow frames

4.2.2 Multi-lag variance

The preceding figures shows the velocity profiles of the mean velocity of the estimated velocities in the lateral and axial direction for a sub-sample of flow

frames for area 1, 2 and 3. The figures displays the velocity profiles for 4 different lags, lag=1, lag=2, lag=3 and lag=4 and the median of all these lags were calculated and compared to the true value, the ground truth.

The bias between the mean velocity of the estimations in the lateral and radial direction respectively, and the ground truth was found and plotted in the figures for all flow frames. In figure 4.109, 4.110, 4.142, 4.143 ,4.169 and 4.170 the standard deviation in the velocity estimates in the lateral and axial direction for all the lags in all flow frames are plotted. Figure 4.113, 4.114, 4.146, 4.147, 4.173 and 4.174 represents the velocity in the middle of the tube in the lateral and axial direction, respectively, for all lags in all flow frames for area 1, 2 and 3. The normalized cross-correlation over all frames between the best match and the kernel for the specific point was also computed and displayed in figures as a function of the diameter of the artery.

Results from area 1

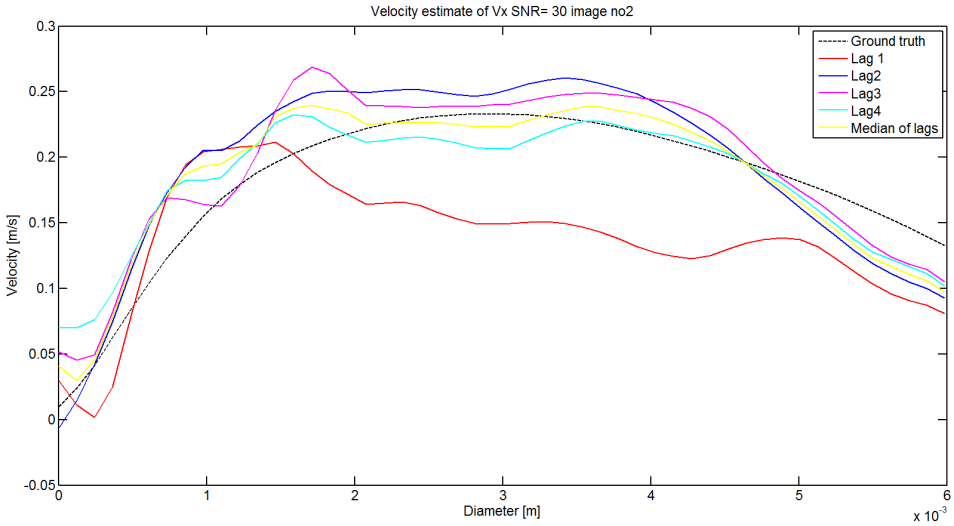

Figure 4.82: Velocity estimation in the x-direction for lag=1, lag=2, lag=3, lag=4 and the median of all the lags for flow frame 2 from area 1

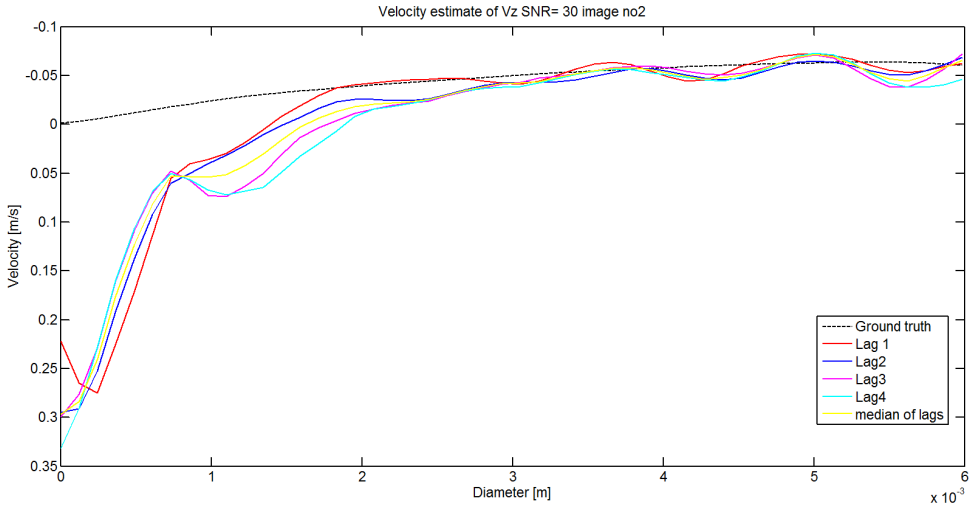

Figure 4.83: Velocity estimation in the z-direction for lag=1, lag=2, lag=3, lag=4 and the median of all the lags for flow frame 2 from area 1

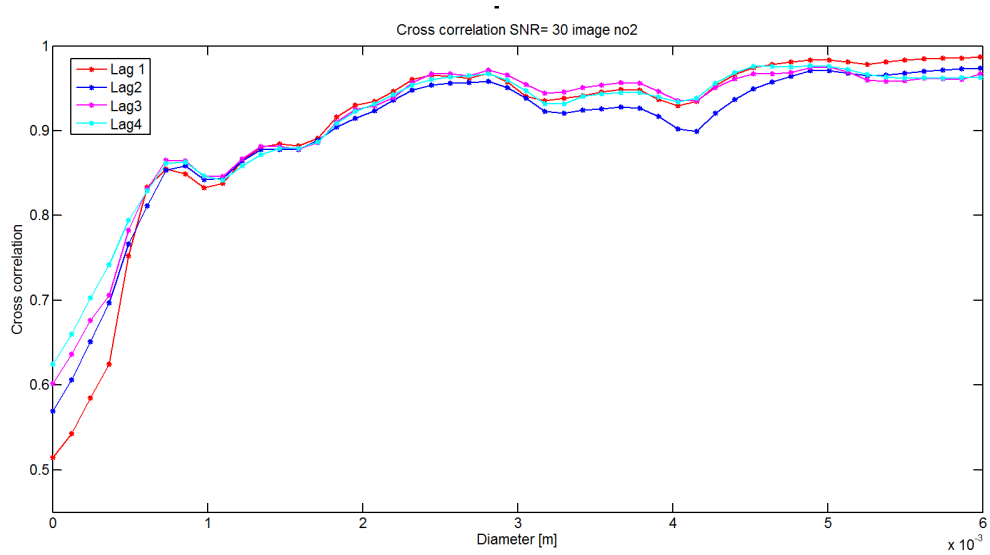

Figure 4.84: Cross correlation for lag=1, lag=2,lag=3 and lag=4 for flow frame 2 from area 1

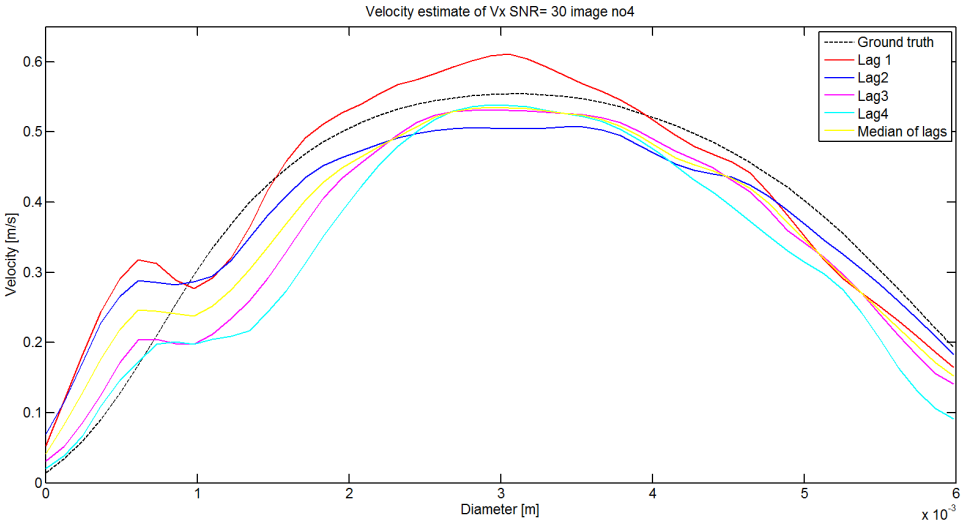

Figure 4.85: Velocity estimation in the x-direction for lag=1, lag=2, lag=3, lag=4 and the median of all the lags for flow frame 4 from area 1

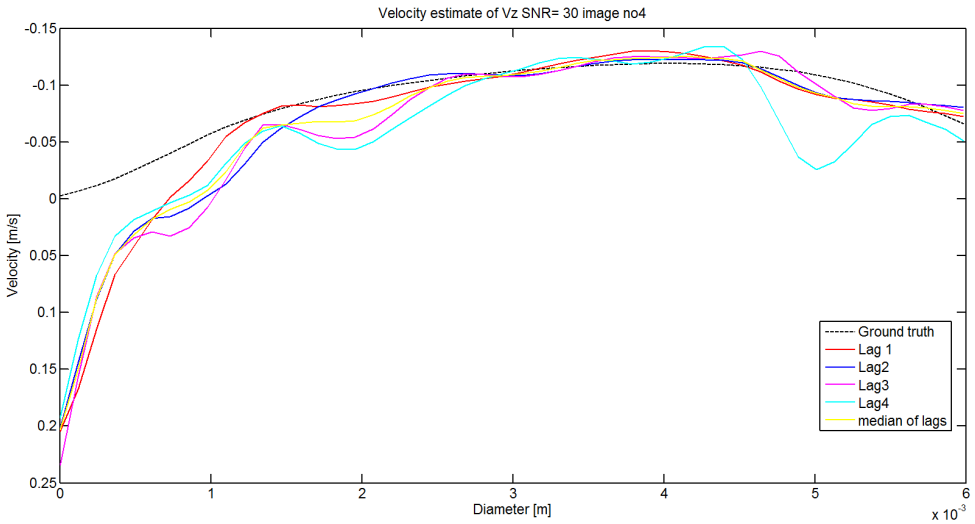

Figure 4.86: Velocity estimation in the z-direction for lag=1, lag=2, lag=3, lag=4 and the median of all the lags for flow frame 4 from area 1

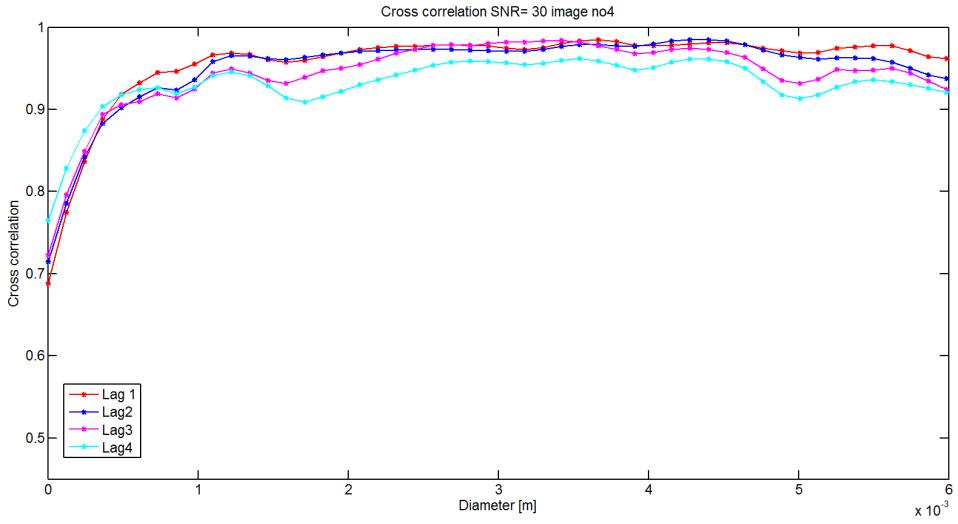

Figure 4.87: Cross correlation for lag=1, lag=2,lag=3 and lag=4 for flow frame 4 from area 1

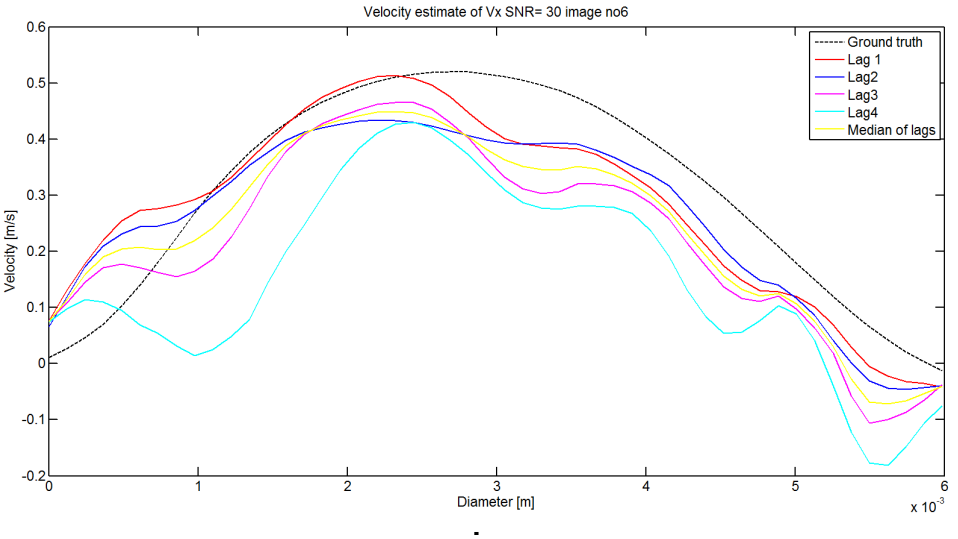

Figure 4.88: Velocity estimation in the x-direction for lag=1, lag=2, lag=3, lag=4 and the median of all the lags for flow frame 6 from area 1

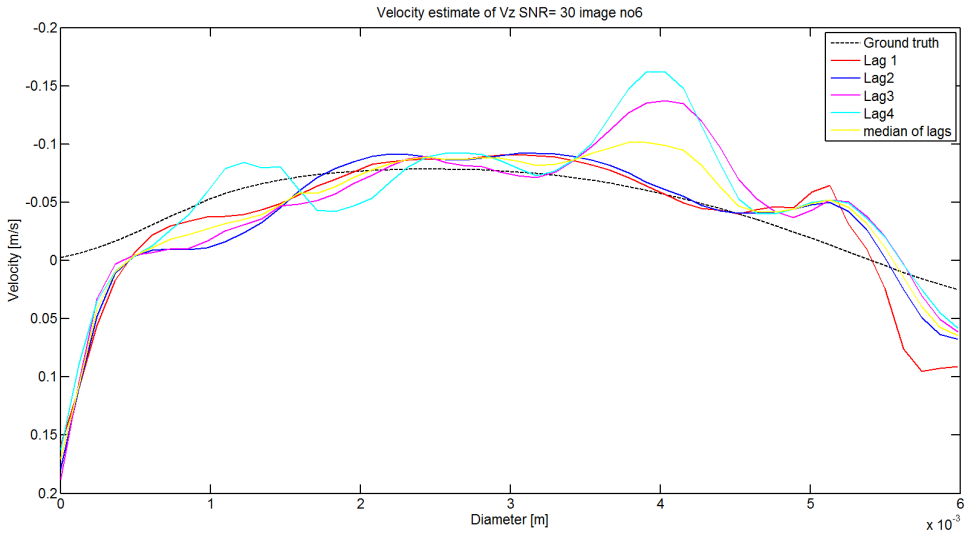

Figure 4.89: Velocity estimation in the z-direction for lag=1, lag=2, lag=3, lag=4 and the median of all the lags for flow frame 6 from area 1

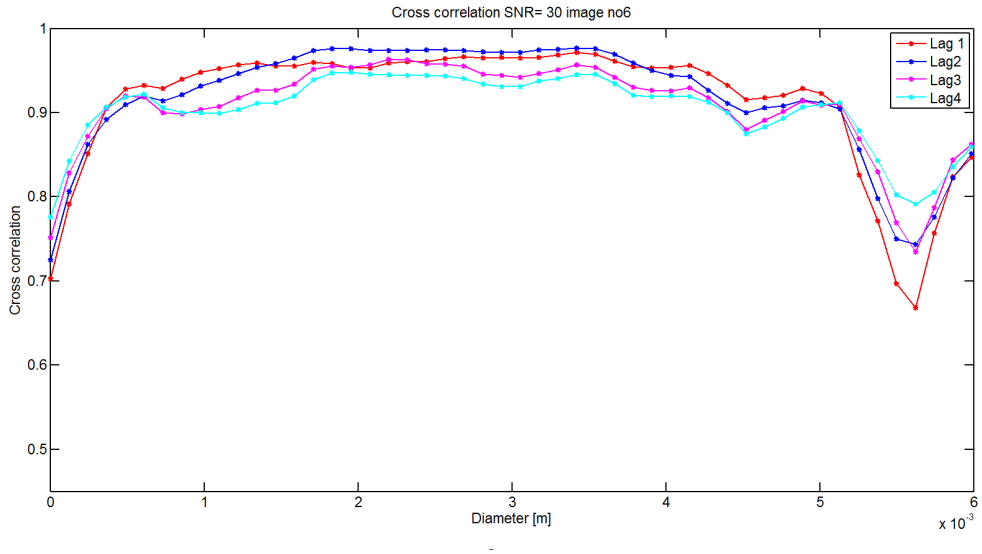

Figure 4.90: Cross correlation for lag=1, lag=2,lag=3 and lag=4 for flow frame 6 from area 1

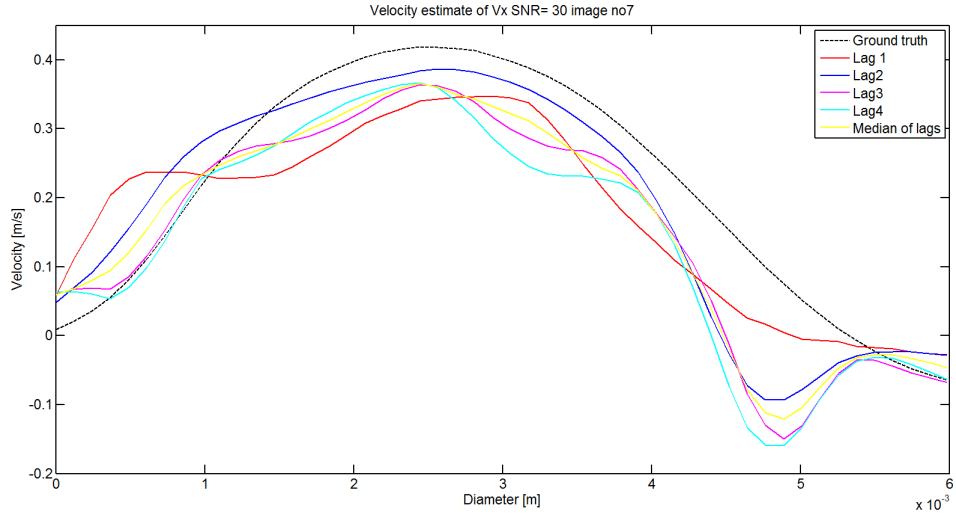

Figure 4.91: Velocity estimation in the x-direction for lag=1, lag=2, lag=3, lag=4 and the median of all the lags for flow frame 7 from area 1

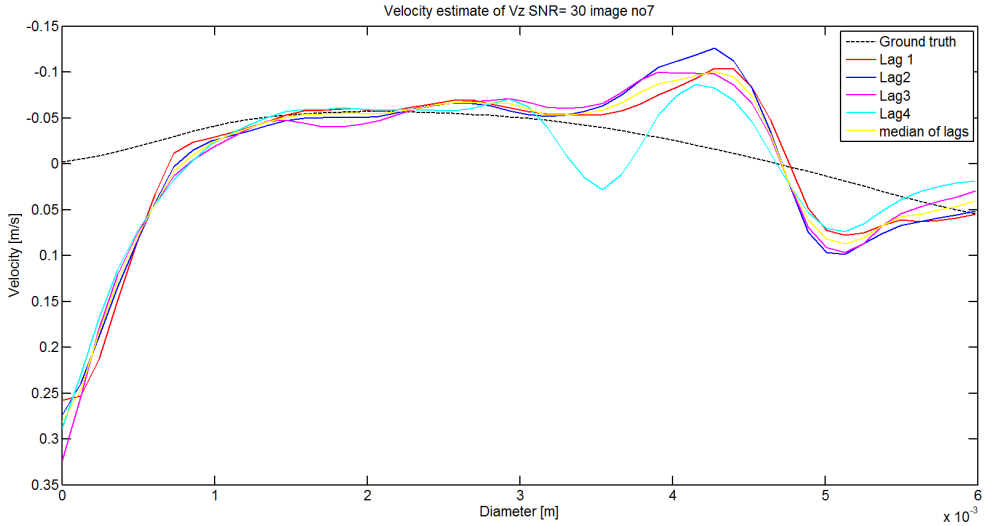

Figure 4.92: Velocity estimation in the z-direction for lag=1, lag=2, lag=3, lag=4 and the median of all the lags for flow frame 7 from area 1

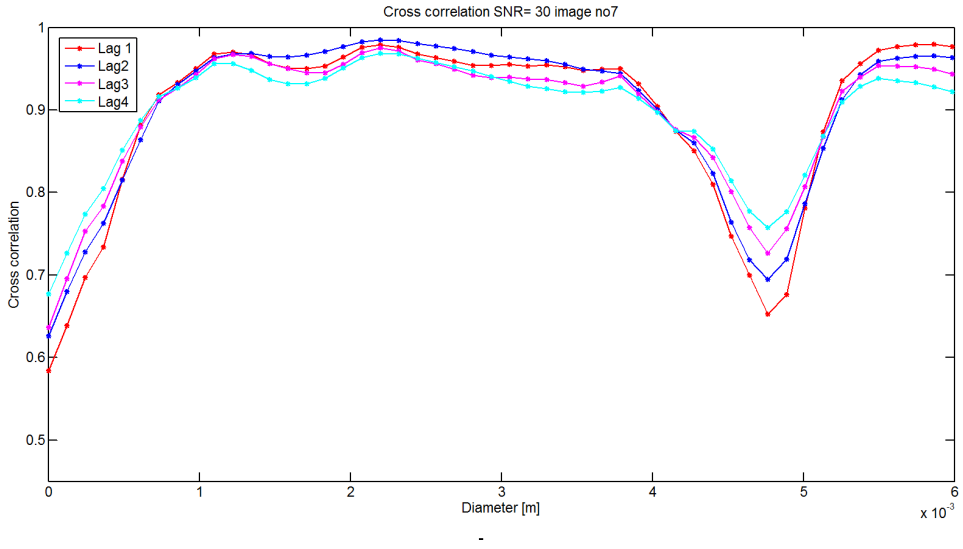

Figure 4.93: Cross correlation for lag=1, lag=2,lag=3 and lag=4 for flow frame 7 from area 1

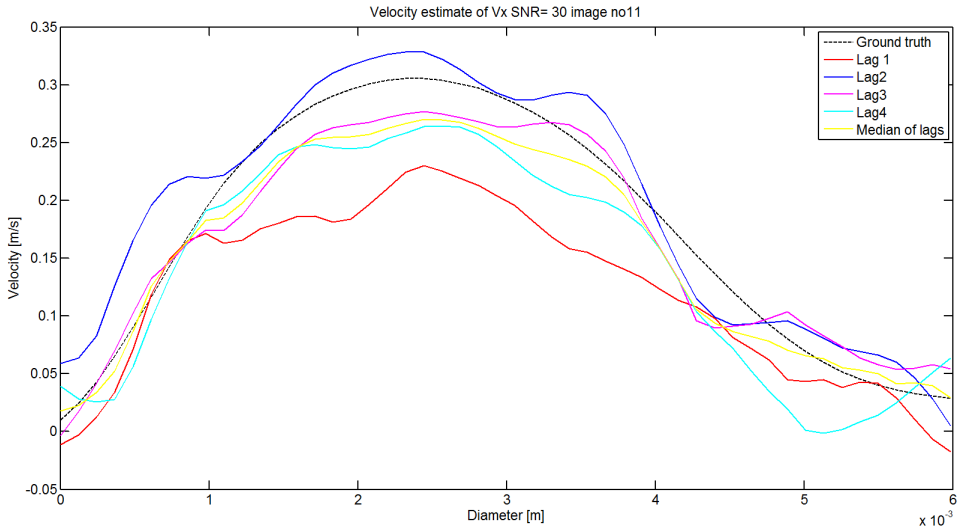

Figure 4.94: Velocity estimation in the x-direction for lag=1, lag=2, lag=3, lag=4 and the median of all the lags for flow frame 11 from area 1

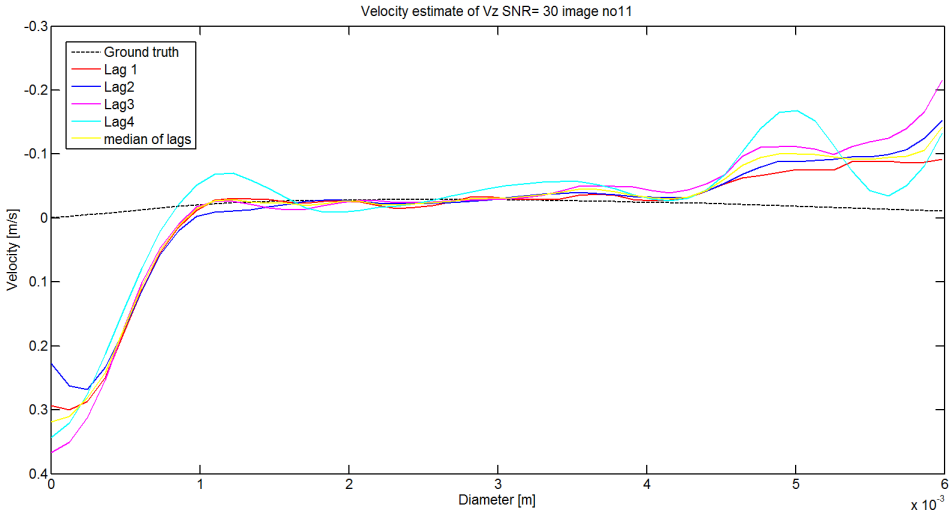

Figure 4.95: Velocity estimation in the z-direction for lag=1, lag=2, lag=3, lag=4 and the median of all the lags for flow frame 11 from area 1

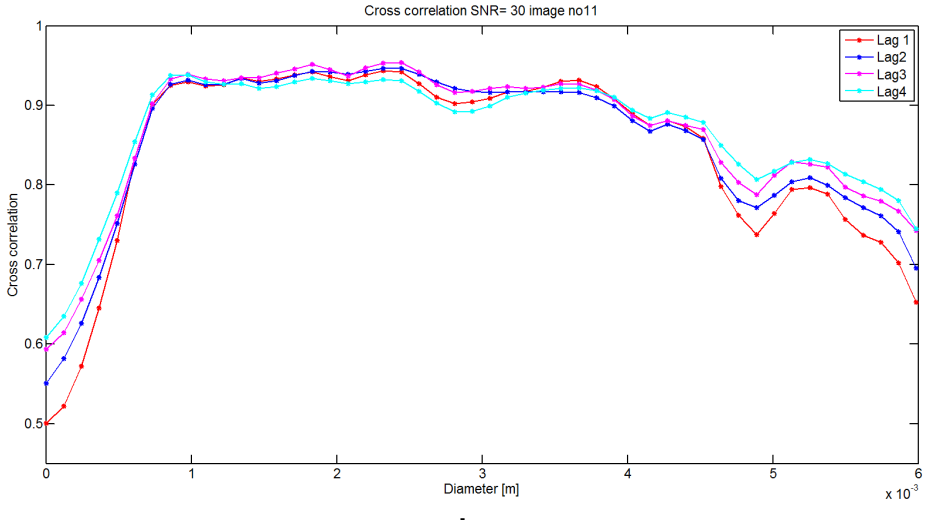

Figure 4.96: Cross correlation for lag=1, lag=2,lag=3 and lag=4 for flow frame 11 from area 1

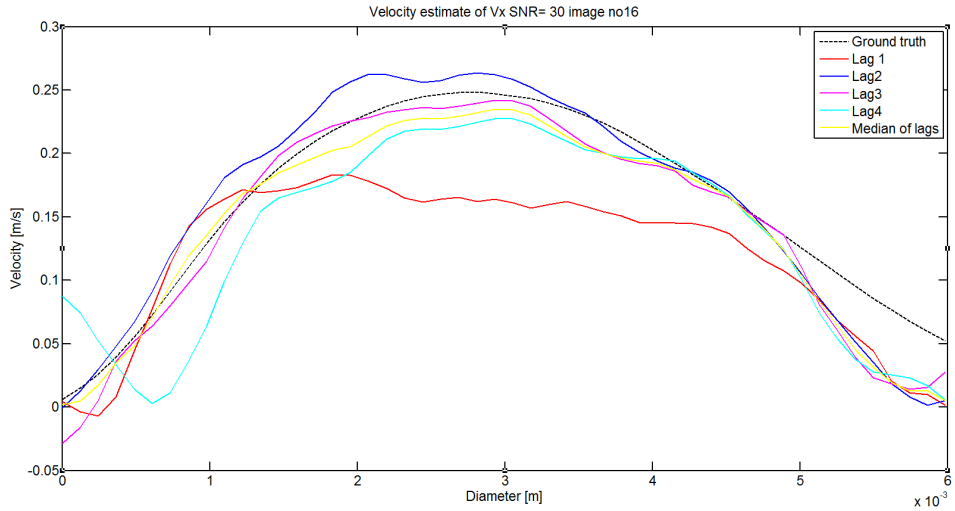

Figure 4.97: Velocity estimation in the x-direction for lag=1, lag=2, lag=3, lag=4 and the median of all the lags for flow frame 16 from area 1

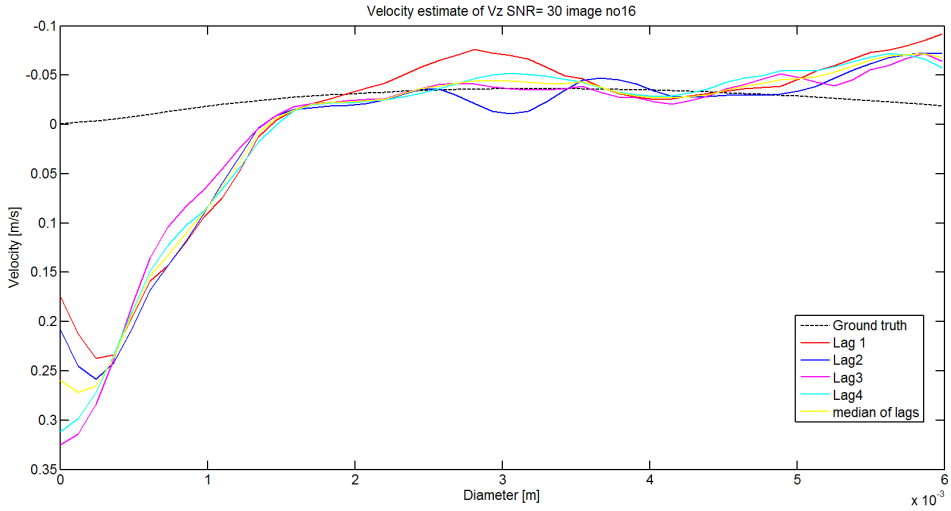

Figure 4.98: Velocity estimation in the z-direction for lag=1, lag=2, lag=3, lag=4 and the median of all the lags for flow frame 16 from area 1

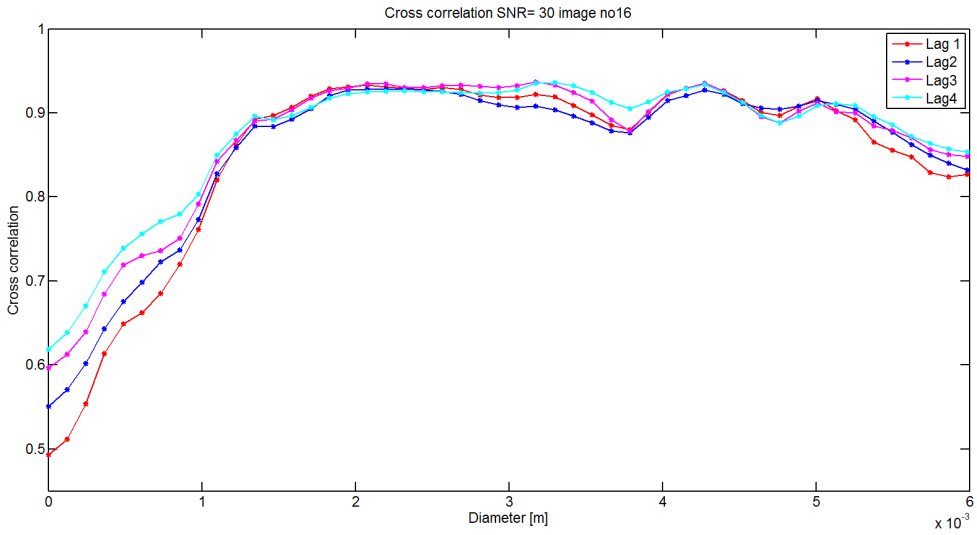

Figure 4.99: Cross correlation for lag=1, lag=2,lag=3 and lag=4 for flow frame 16 from area 1

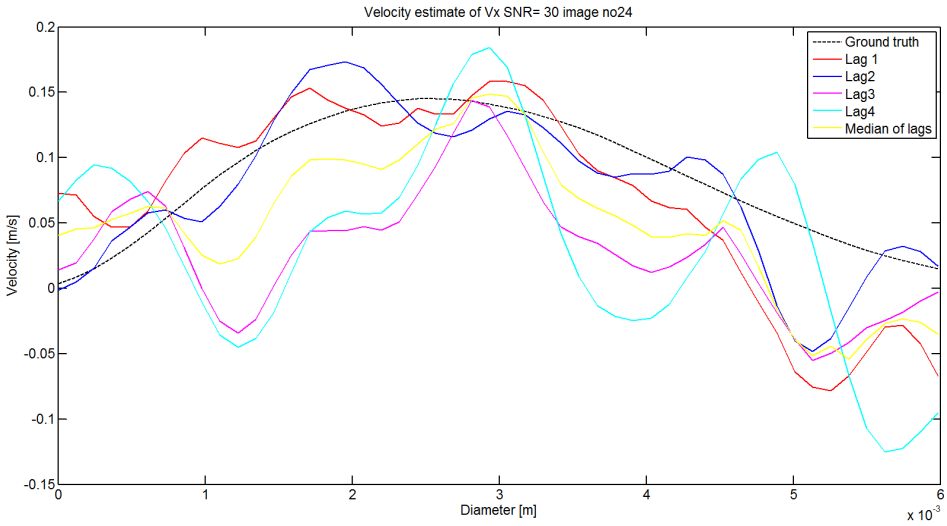

Figure 4.100: Velocity estimation in the x-direction for lag=1, lag=2, lag=3, lag=4 and the median of all the lags for flow frame 24 from area 1

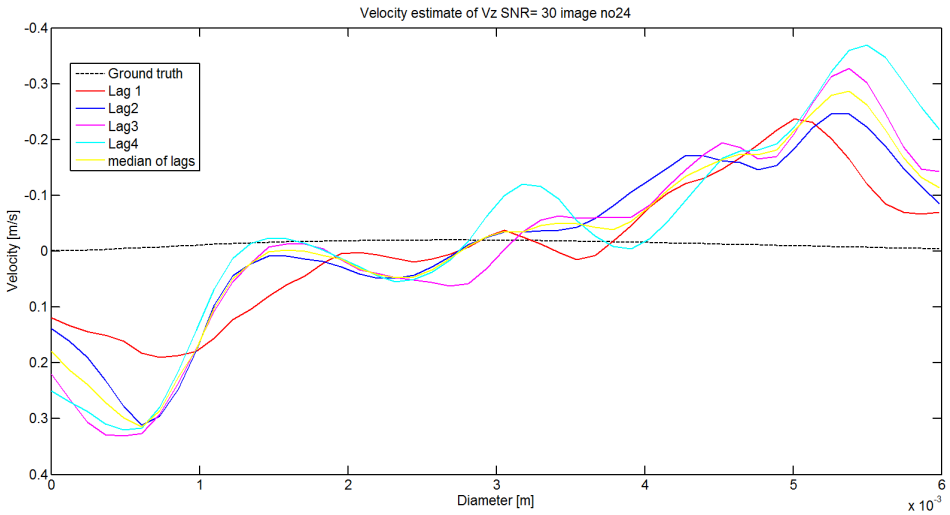

Figure 4.101: Velocity estimation in the z-direction for lag=1, lag=2, lag=3, lag=4 and the median of all the lags for flow frame 24 from area 1

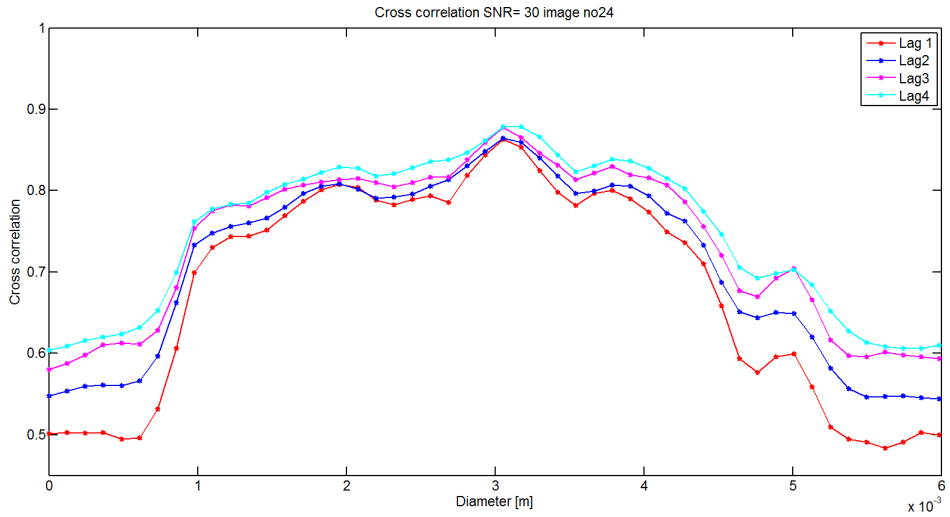

Figure 4.102: Cross correlation for lag=1, lag=2,lag=3 and lag=4 for flow frame 24 from area 1

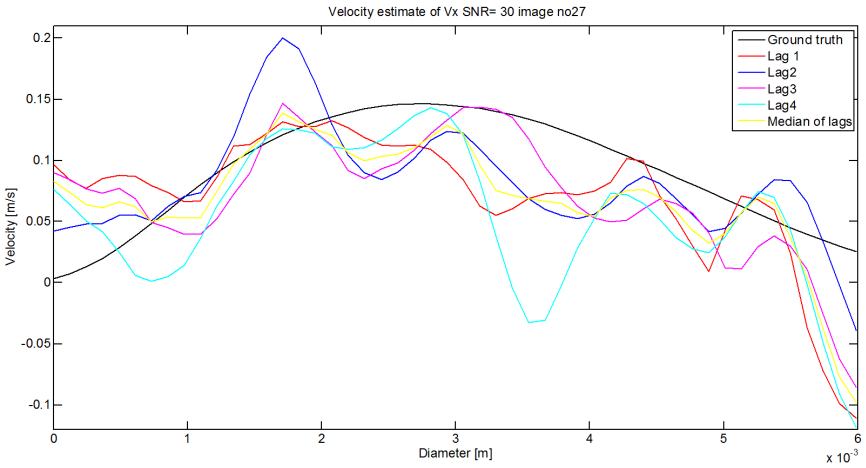

Figure 4.103: Velocity estimation in the x-direction for lag=1, lag=2, lag=3, lag=4 and the median of all the lags for flow frame 27 from area 1

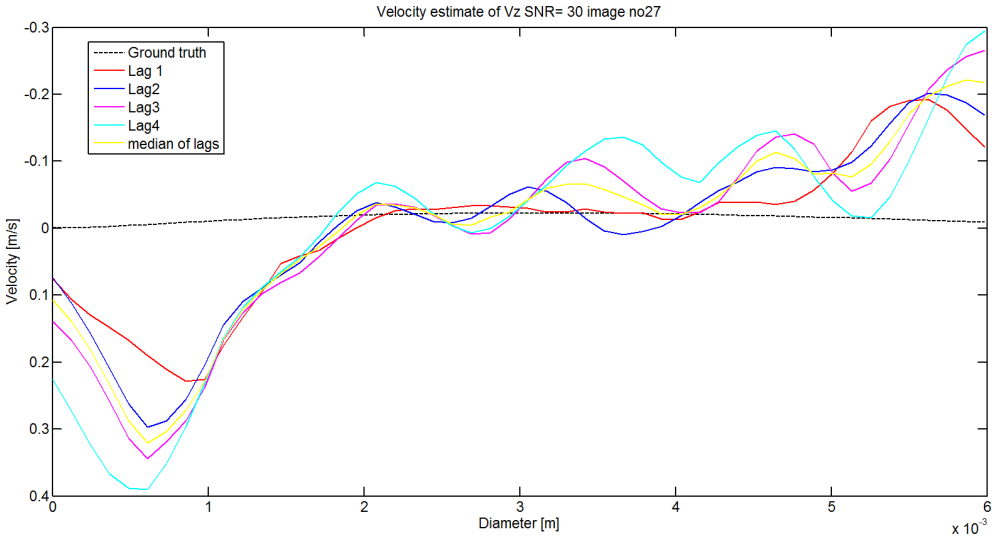

Figure 4.104: Velocity estimation in the z-direction for lag=1, lag=2, lag=3, lag=4 and the median of all the lags for flow frame 27 from area 1

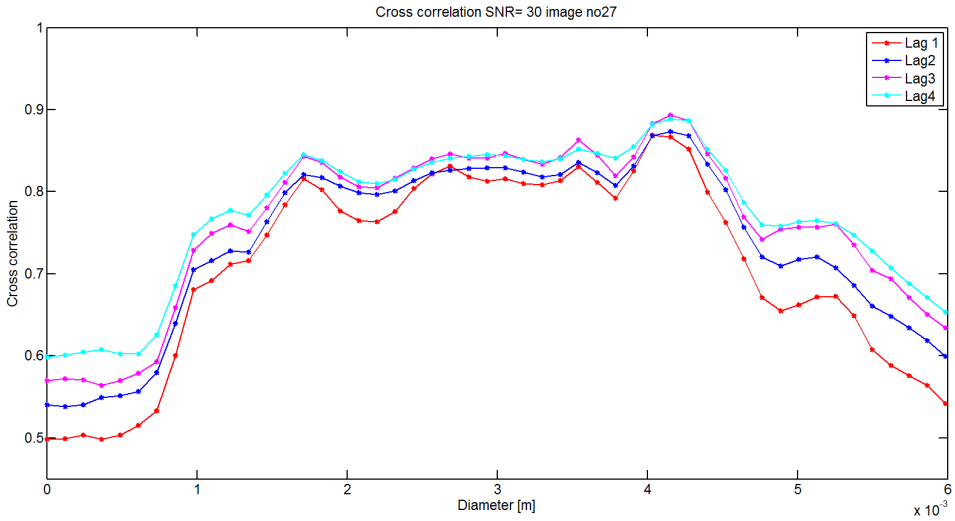

Figure 4.105: Cross correlation for lag=1, lag=2,lag=3 and lag=4 for flow frame 27 from area 1

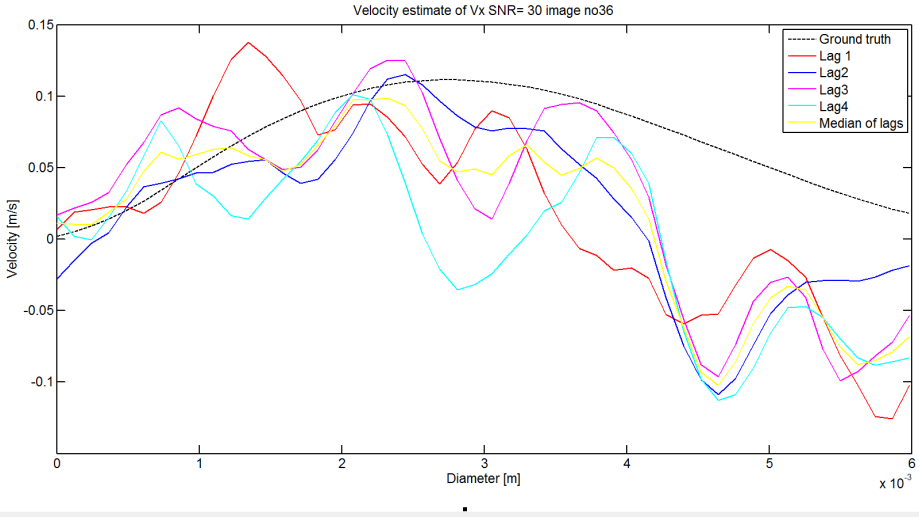

Figure 4.106: Velocity estimation in the x-direction for lag=1, lag=2, lag=3, lag=4 and the median of all the lags for flow frame 36 from area 1

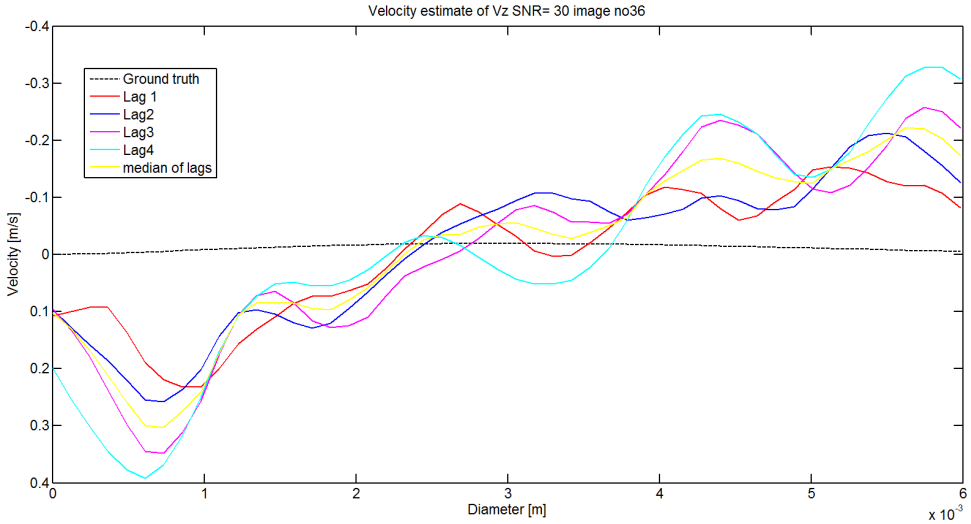

Figure 4.107: Velocity estimation in the z-direction for lag=1, lag=2, lag=3, lag=4 and the median of all the lags for flow frame 36 from area 1

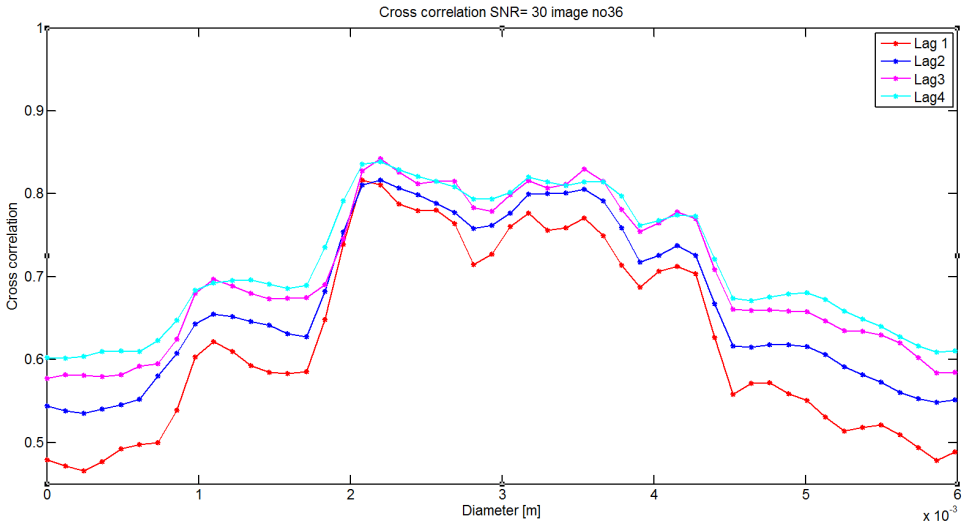

Figure 4.108: Cross correlation for lag=1, lag=2,lag=3 and lag=4 for flow frame 36 from area 1

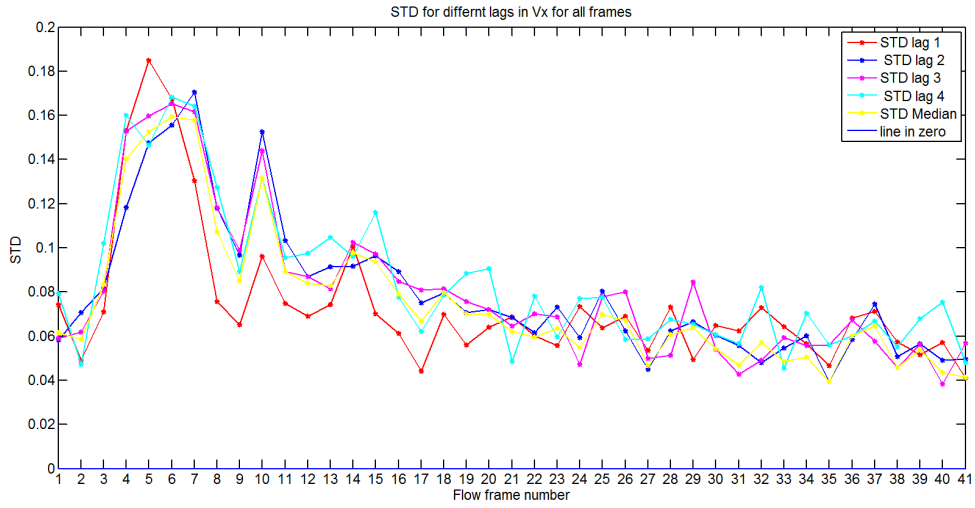

Figure 4.109: Standard deviation for the velocity estimates in the x-direction for lag= 1, lag=2, lag=3, lag=4 and median of all lags from area 1

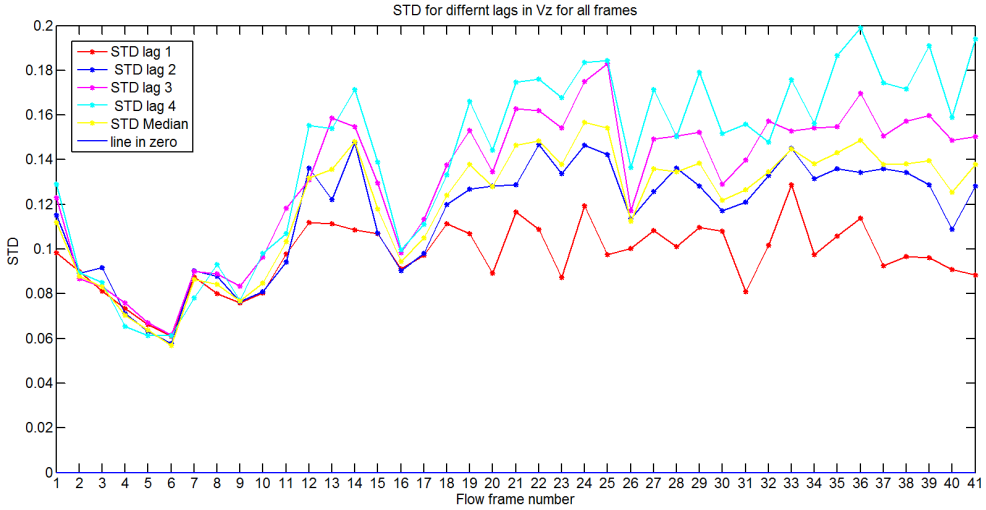

Figure 4.110: Standard deviation for the velocity estimates in the z-direction for lag= 1, lag=2, lag=3, lag=4 and median of all lags from area 1

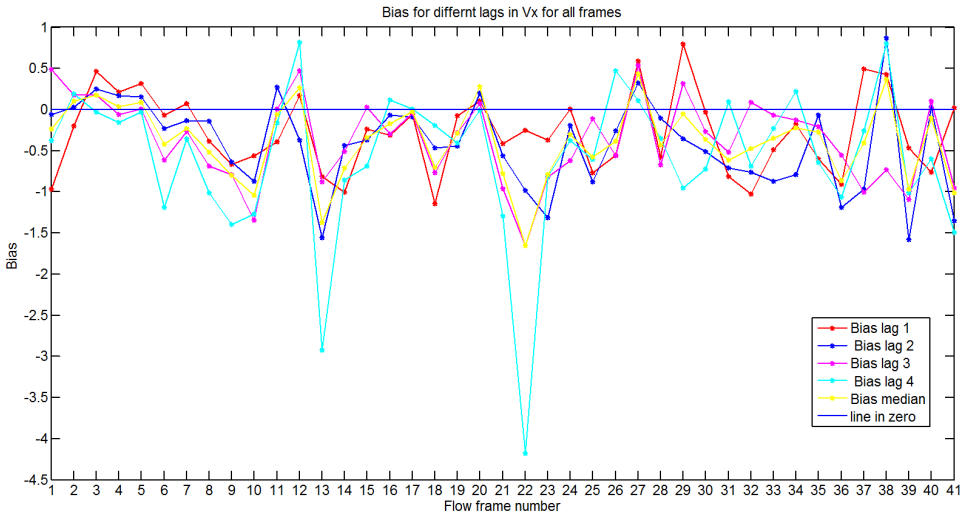

Figure 4.111: Bias between the velocity estimates in the x-direction for lag= 1, lag=2, lag=3 and lag=4 and ground truth from area 1

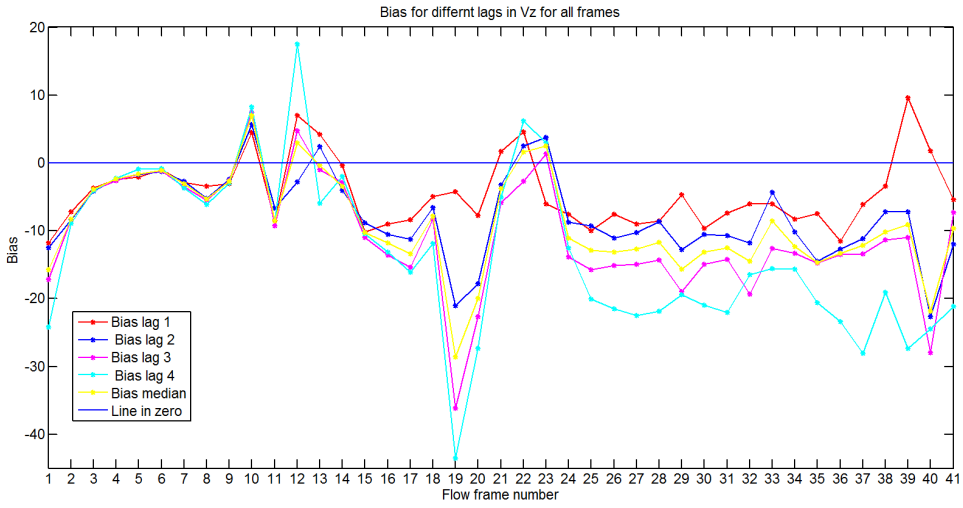

Figure 4.112: Bias between the velocity estimates in the z-direction for lag= 1, lag=2, lag=3 and lag=4 and ground truth from area 1

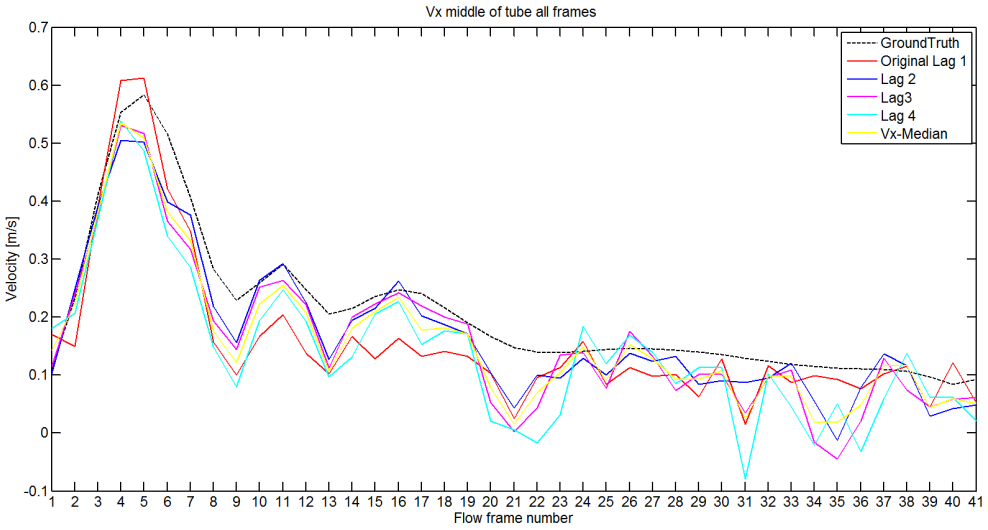

Figure 4.113: Velocity estimates in the x-direction for lag= 1, lag=2, lag=3, lag=4 and the median of all the lags in the middle of the tube for all flow frames from area 1

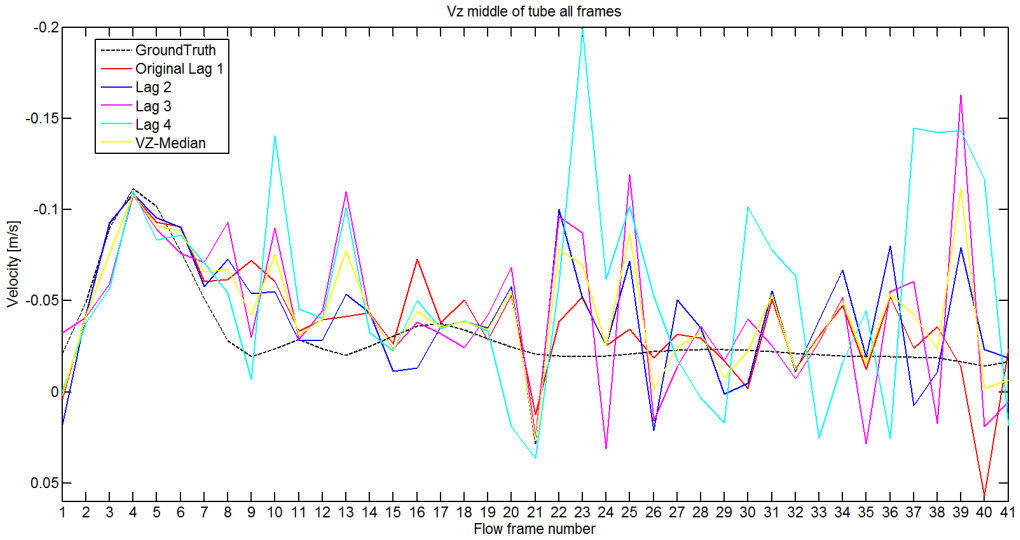

Figure 4.114: Velocity estimates in the z-direction for lag= 1, lag=2, lag=3, lag=4 and the median of all the lags in the middle of the tube for all flow frames from area 1

Results from area 2

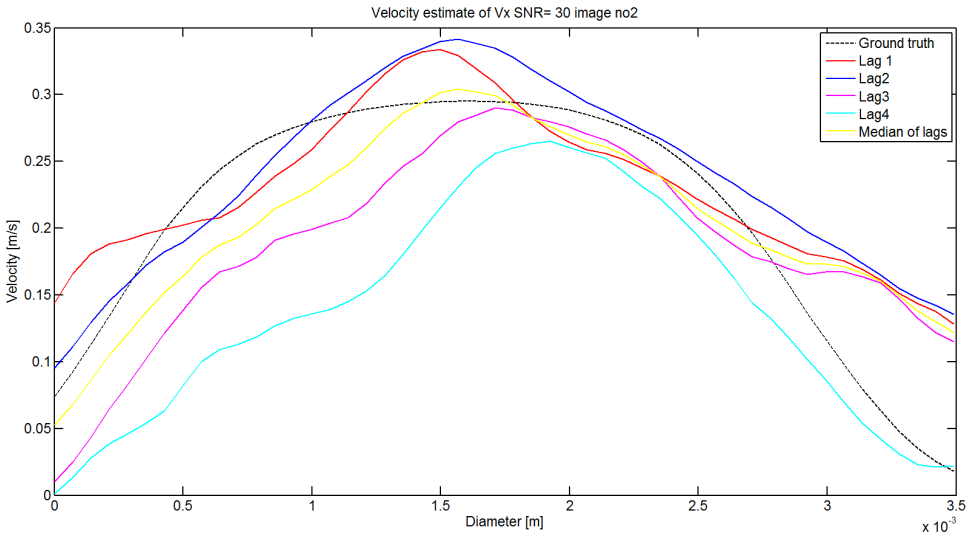

Figure 4.115: Velocity estimation in the x-direction for lag=1, lag=2, lag=3, lag=4 and the median of all the lags for flow frame 2 from area 2

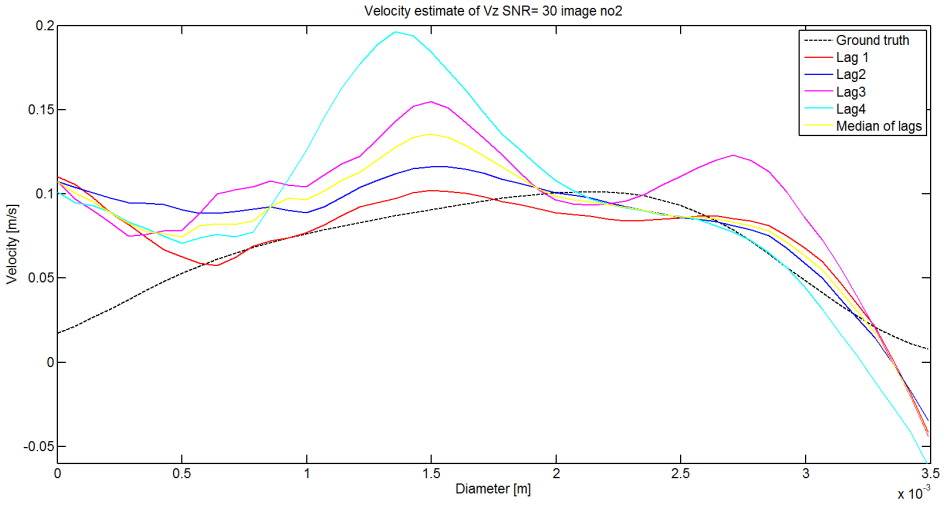

Figure 4.116: Velocity estimation in the z-direction for lag=1, lag=2, lag=3, lag=4 and the median of all the lags for flow frame 2 from area 2

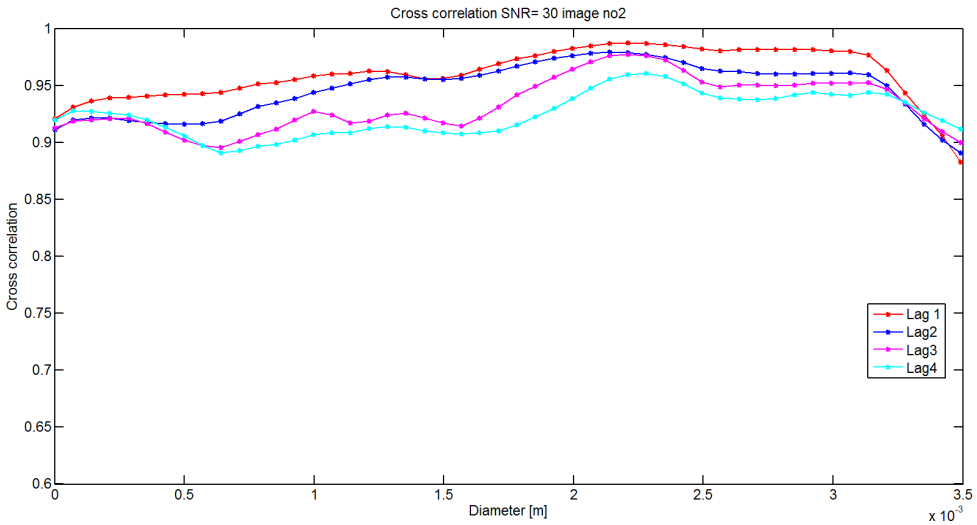

Figure 4.117: Cross correlation for lag=1, lag=2,lag=3 and lag=4 for flow frame 2 from area 2

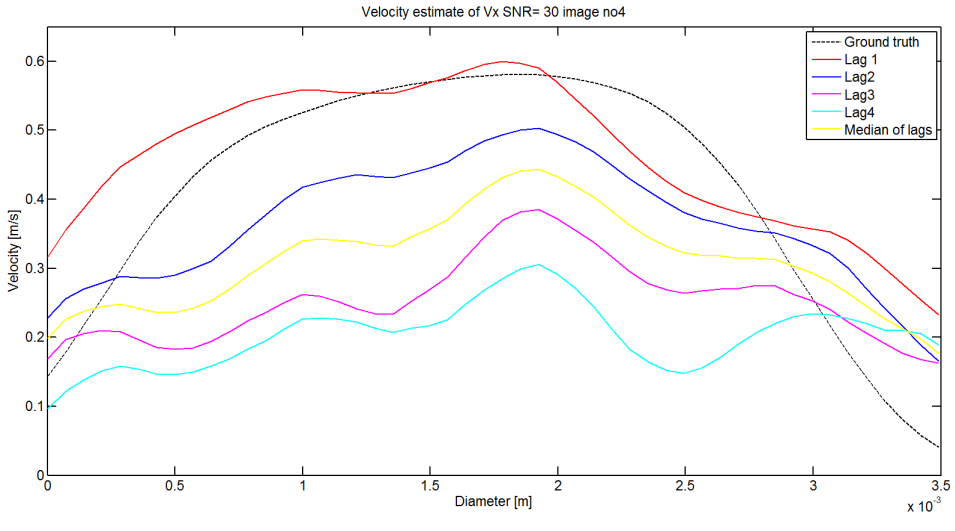

Figure 4.118: Velocity estimation in the x-direction for lag=1, lag=2, lag=3, lag=4 and the median of all the lags for flow frame 4 from area 2

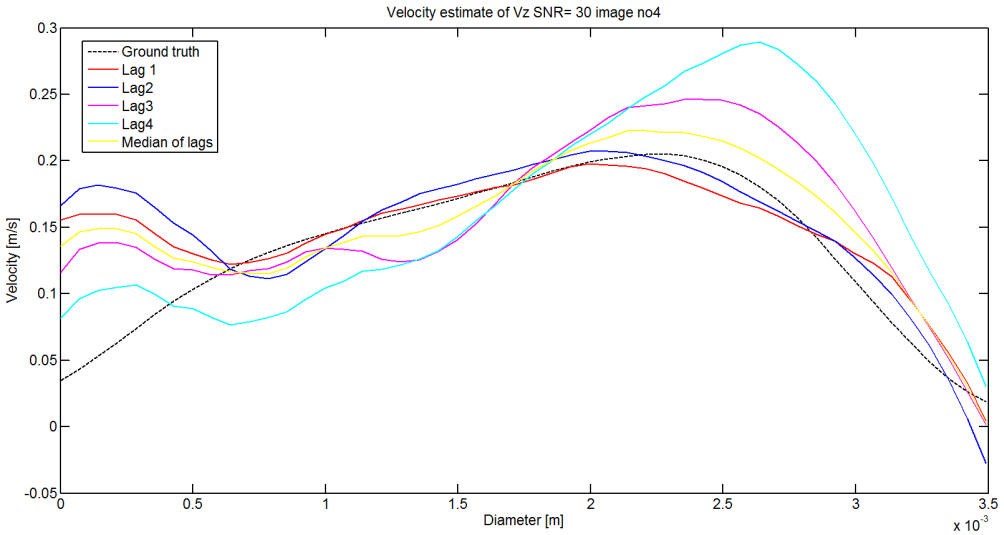

Figure 4.119: Velocity estimation in the z-direction for lag=1, lag=2, lag=3, lag=4 and the median of all the lags for flow frame 4 from area 2

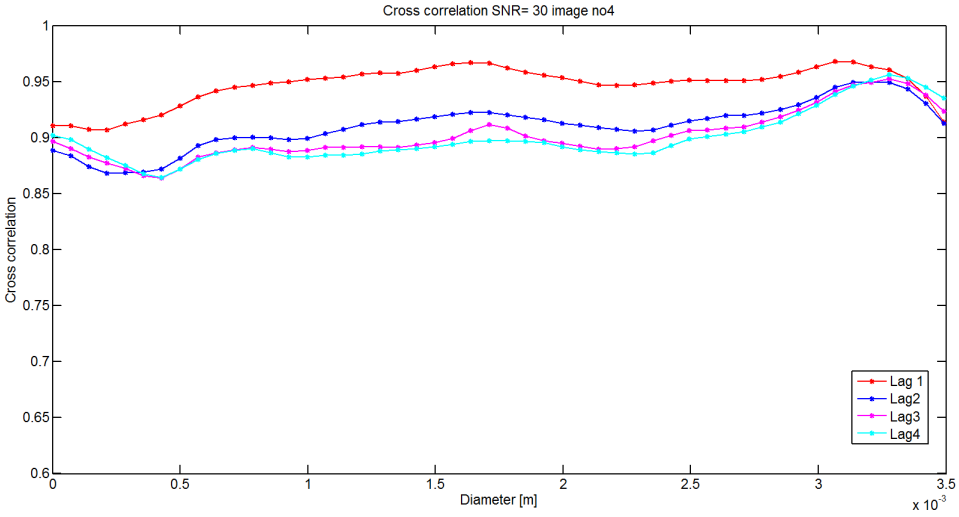

Figure 4.120: Cross correlation for lag=1, lag=2,lag=3 and lag=4 for flow frame 4 from area 2

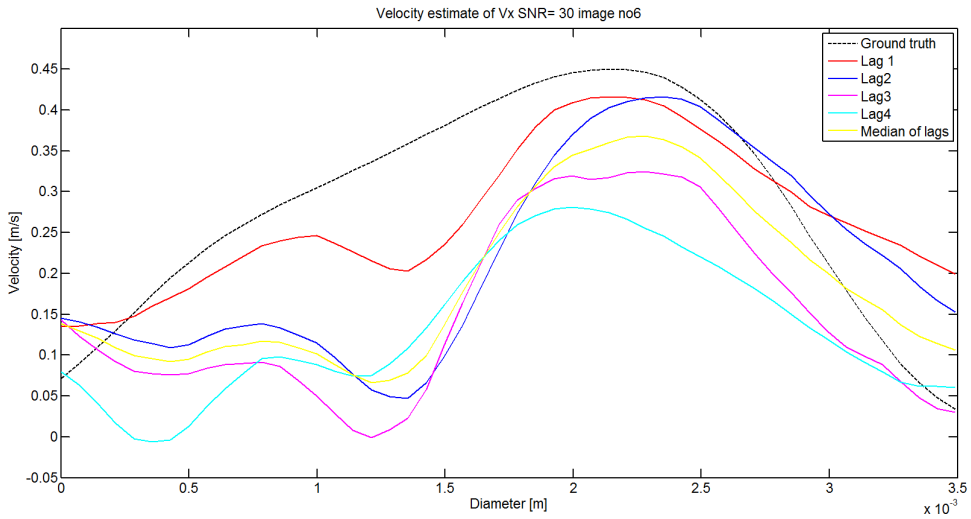

Figure 4.121: Velocity estimation in the x-direction for lag=1, lag=2, lag=3, lag=4 and the median of all the lags for flow frame 6 from area 2

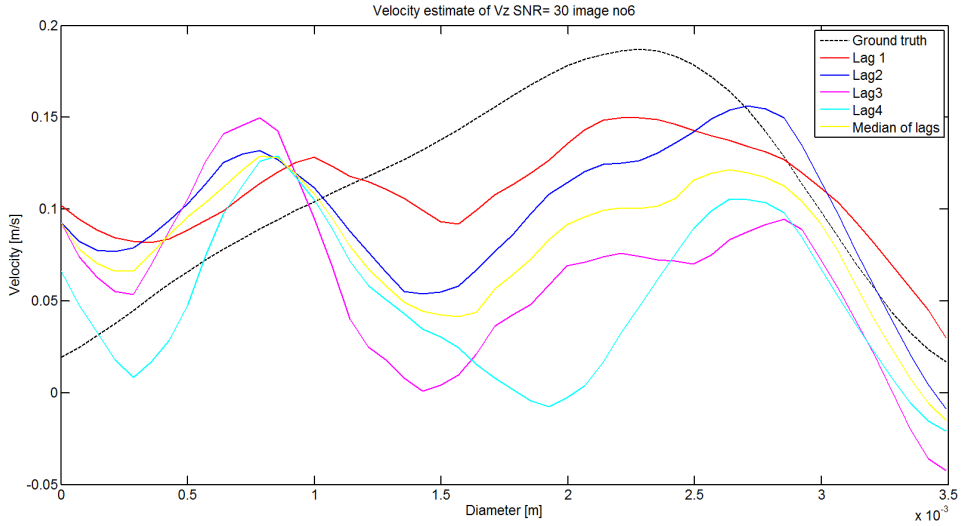

Figure 4.122: Velocity estimation in the z-direction for lag=1, lag=2, lag=3, lag=4 and the median of all the lags for flow frame 6 from area 2

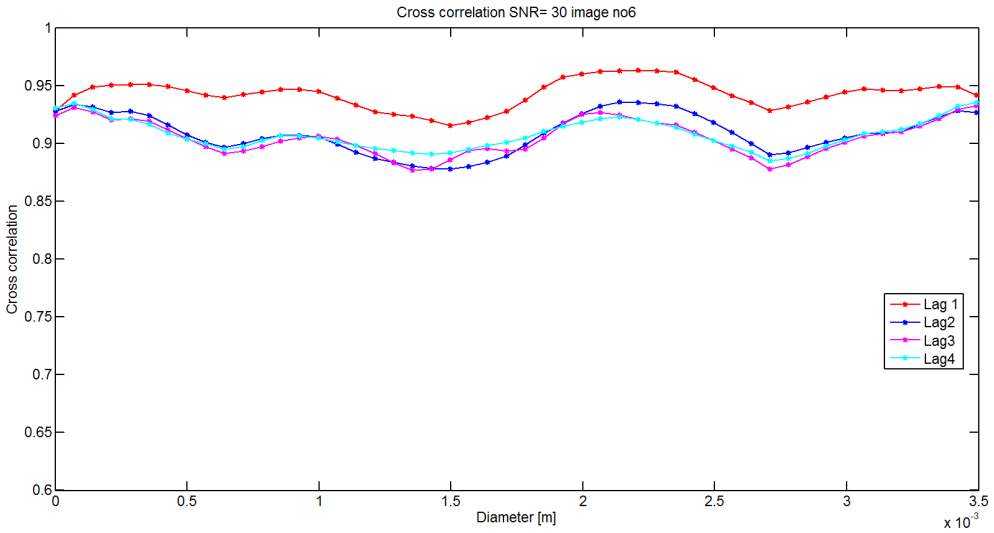

Figure 4.123: Cross correlation for lag=1, lag=2,lag=3 and lag=4 for flow frame 6 from area 2

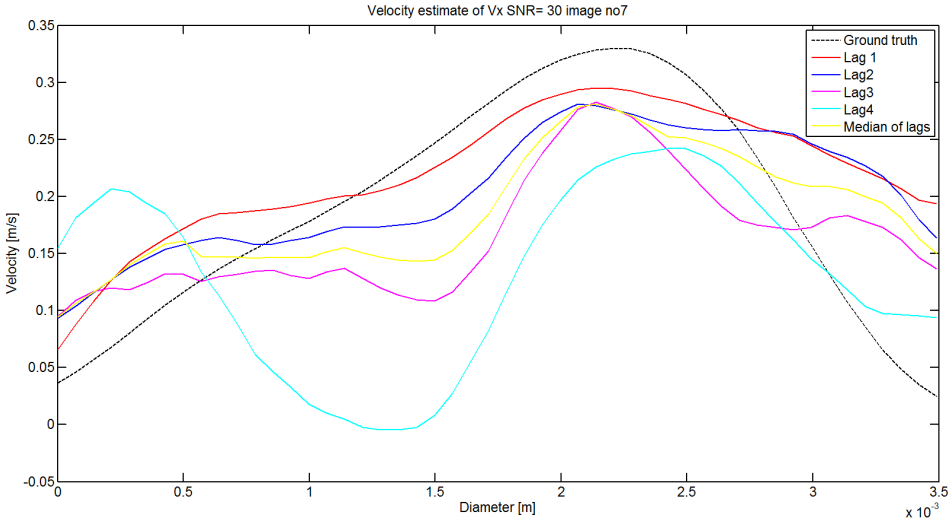

Figure 4.124: Velocity estimation in the x-direction for lag=1, lag=2, lag=3, lag=4 and the median of all the lags for flow frame 7 from area 2

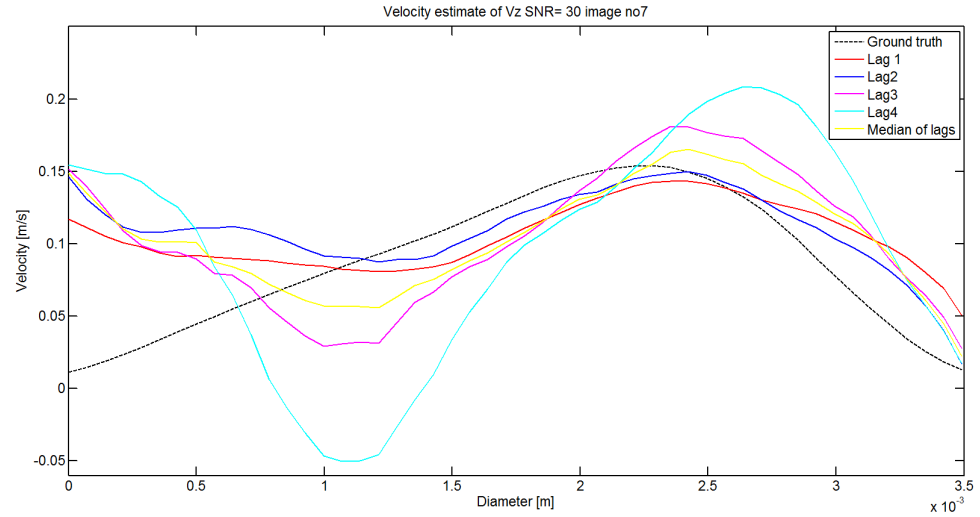

Figure 4.125: Velocity estimation in the z-direction for lag=1, lag=2, lag=3, lag=4 and the median of all the lags for flow frame 7 from area 2

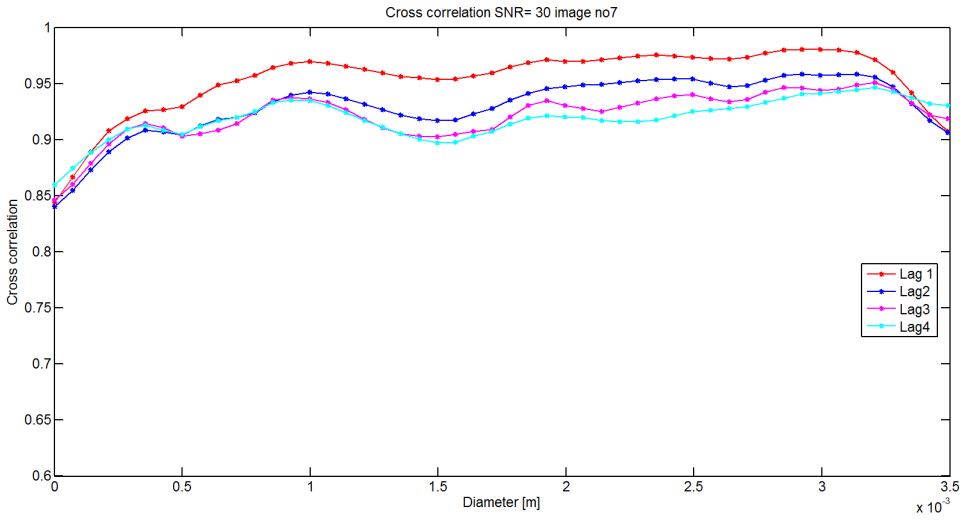

Figure 4.126: Cross correlation for lag=1, lag=2,lag=3 and lag=4 for flow frame 7 from area 2

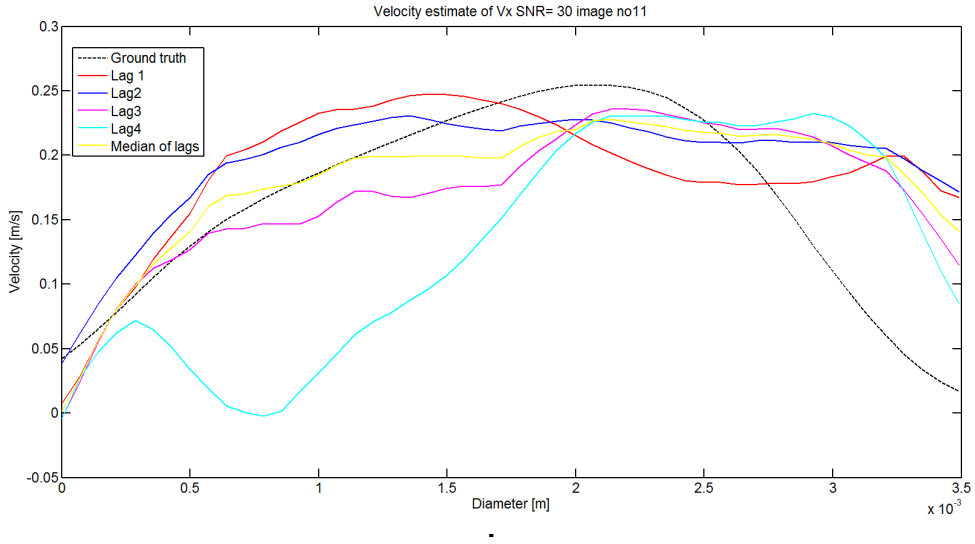

Figure 4.127: Velocity estimation in the x-direction for lag=1, lag=2, lag=3, lag=4 and the median of all the lags for flow frame 11 from area 2

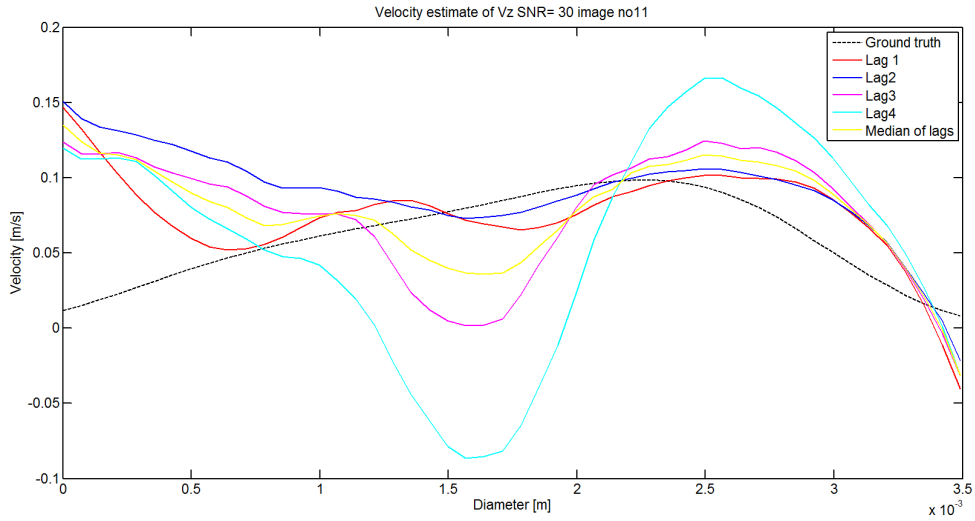

Figure 4.128: Velocity estimation in the z-direction for lag=1, lag=2, lag=3, lag=4 and the median of all the lags for flow frame 11 from area 2

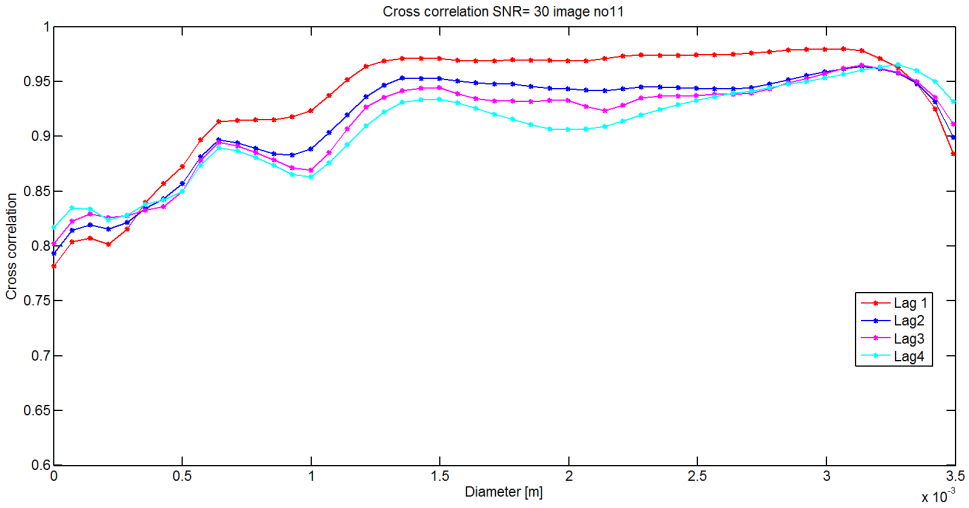

Figure 4.129: Cross correlation for lag=1, lag=2,lag=3 and lag=4 for flow frame 11 from area 2

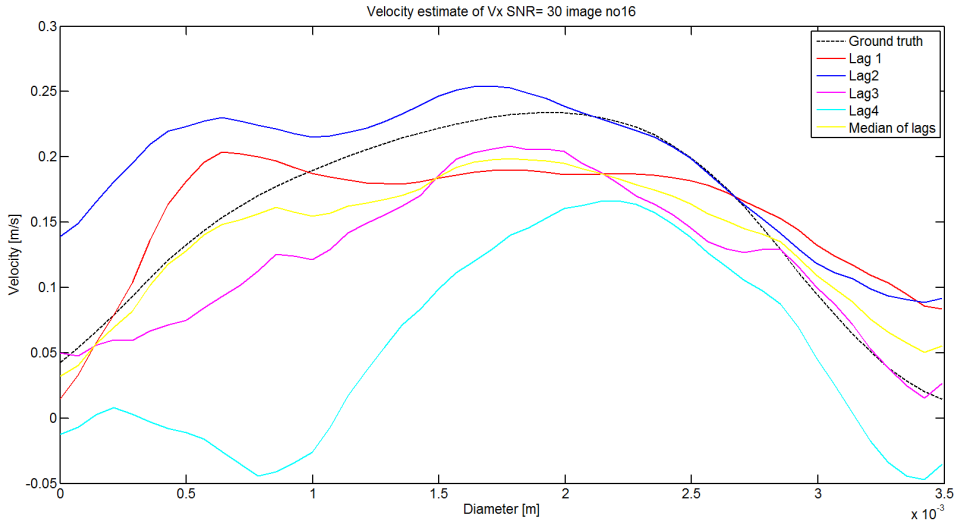

Figure 4.130: Velocity estimation in the x-direction for lag=1, lag=2, lag=3, lag=4 and the median of all the lags for flow frame 16 from area 2

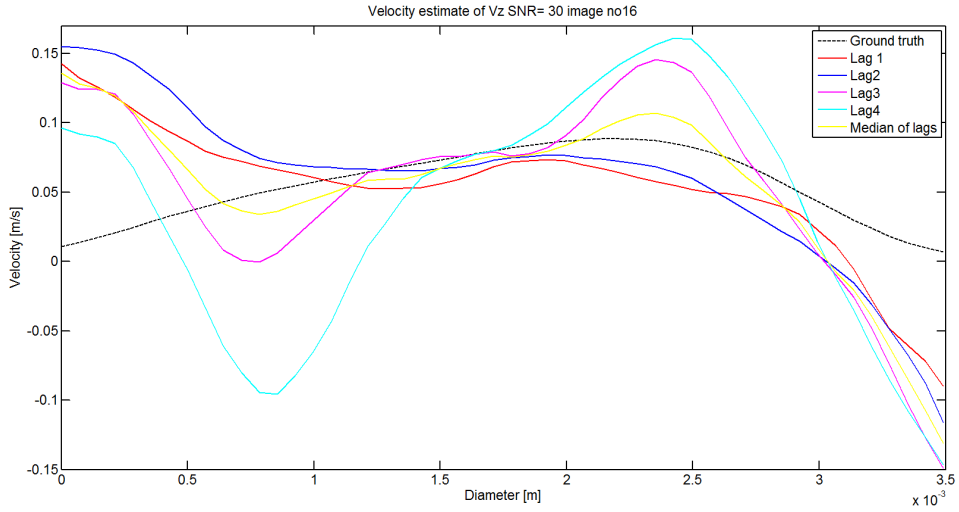

Figure 4.131: Velocity estimation in the z-direction for lag=1, lag=2, lag=3, lag=4 and the median of all the lags for flow frame 16 from area 2

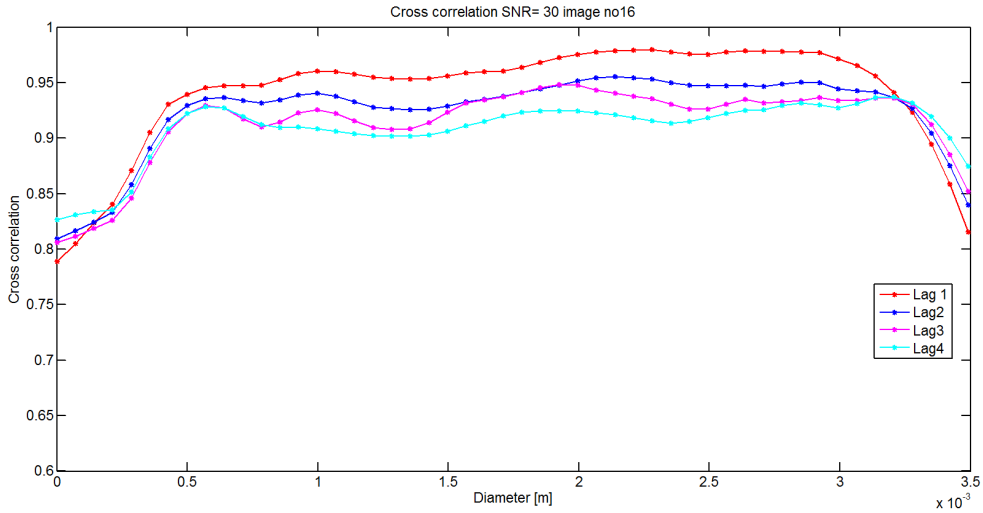

Figure 4.132: Cross correlation for lag=1, lag=2,lag=3 and lag=4 for flow frame 16 from area 2

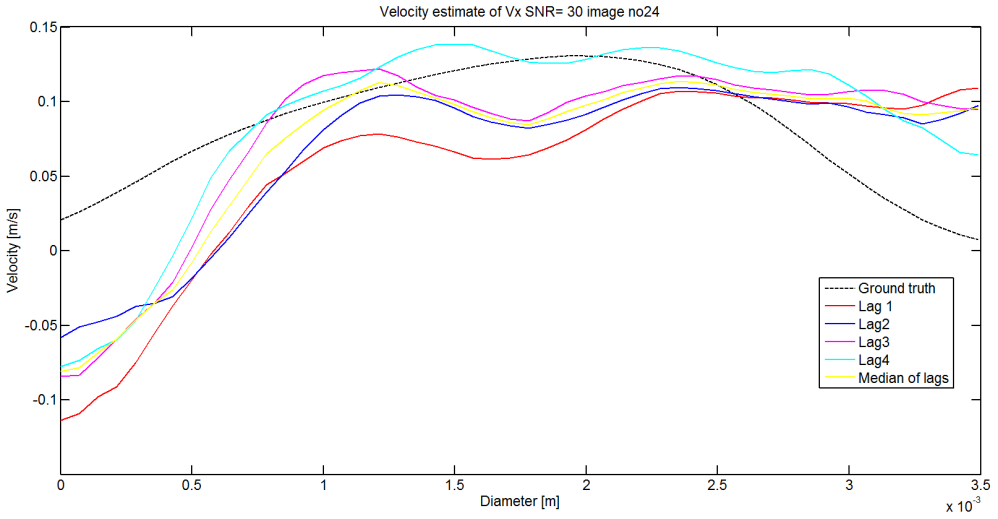

Figure 4.133: Velocity estimation in the x-direction for lag=1, lag=2, lag=3, lag=4 and the median of all the lags for flow frame 24 from area 2

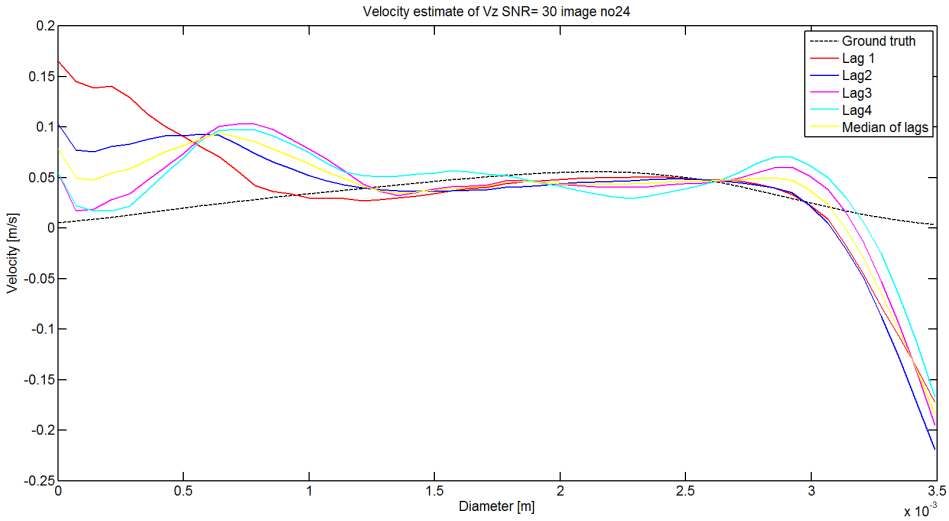

Figure 4.134: Velocity estimation in the z-direction for lag=1, lag=2, lag=3, lag=4 and the median of all the lags for flow frame 24 from area 2

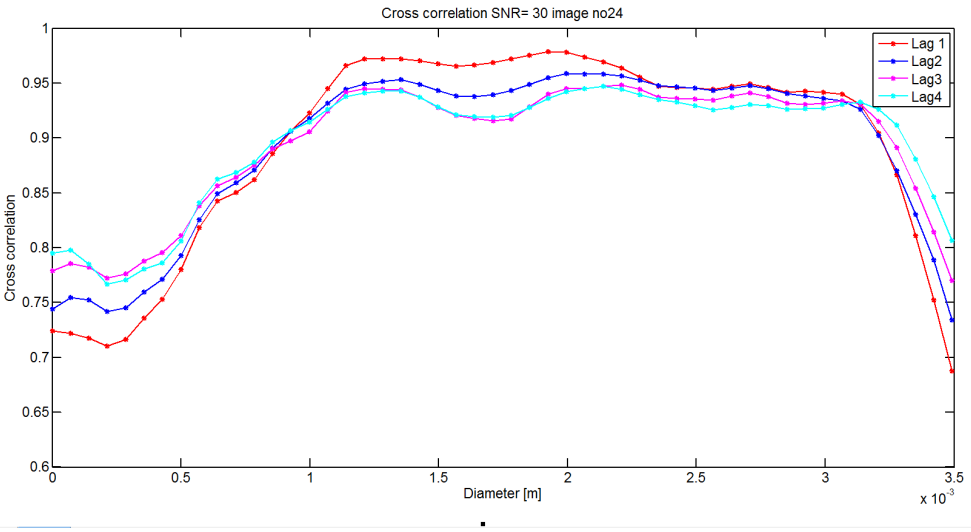

Figure 4.135: Cross correlation for lag=1, lag=2,lag=3 and lag=4 for flow frame 24 from area 2

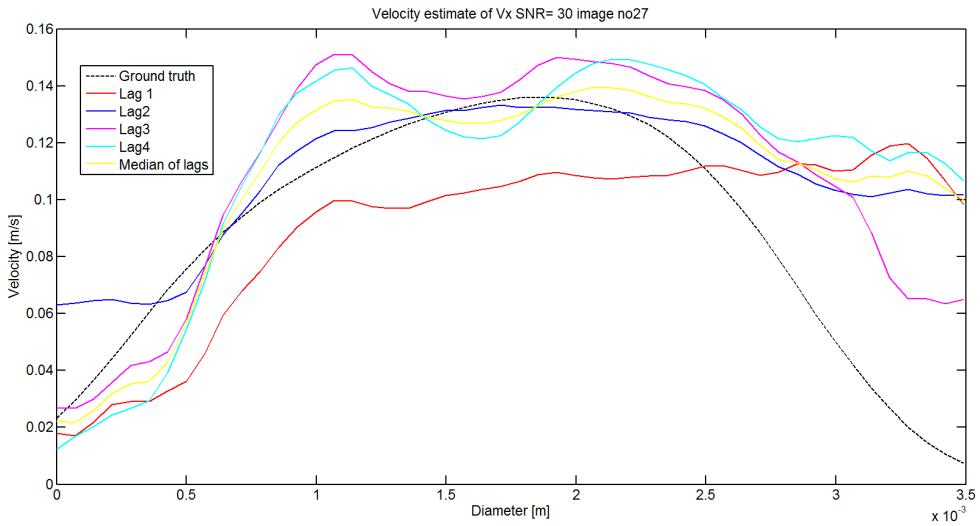

Figure 4.136: Velocity estimation in the x-direction for lag=1, lag=2, lag=3, lag=4 and the median of all the lags for flow frame 27 from area 2

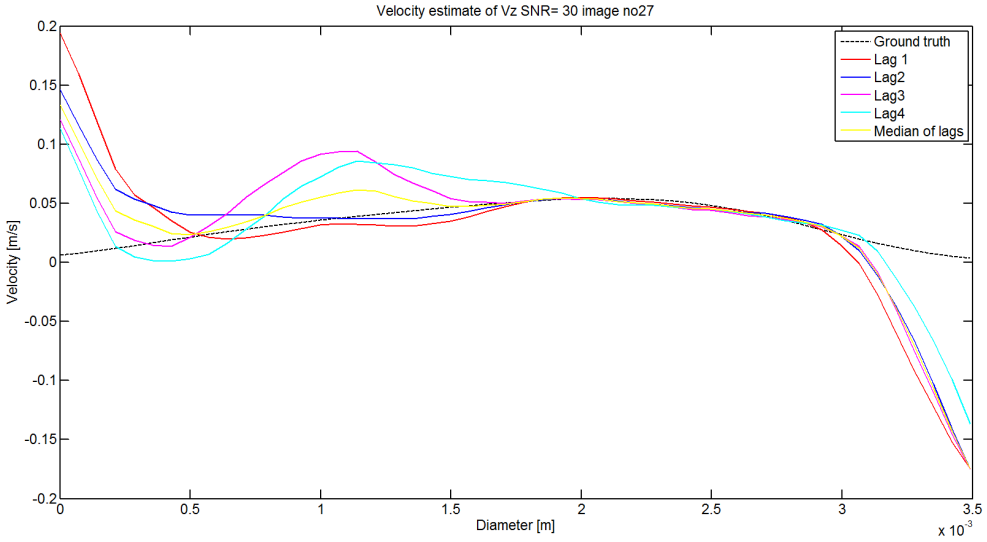

Figure 4.137: Velocity estimation in the z-direction for lag=1, lag=2, lag=3, lag=4 and the median of all the lags for flow frame 27 from area 2

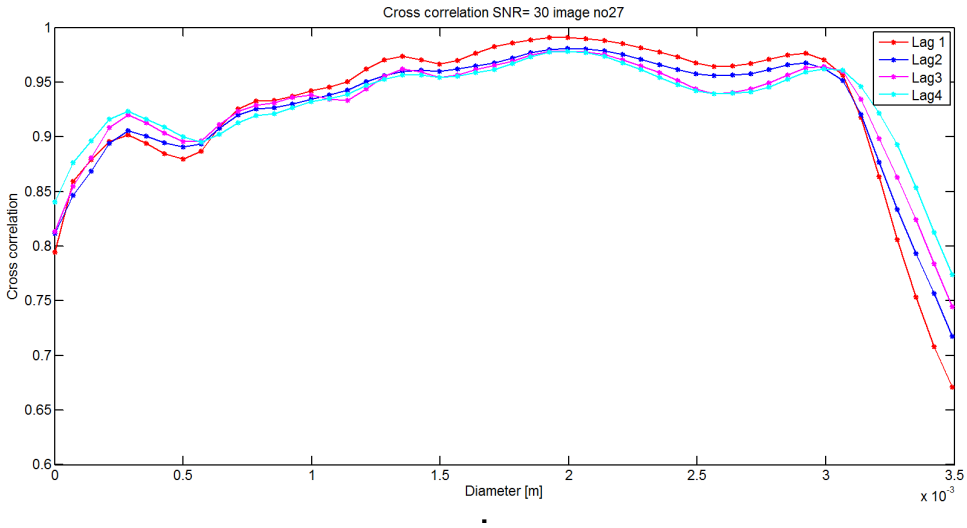

Figure 4.138: Cross correlation for lag=1, lag=2,lag=3 and lag=4 for flow frame 2 from area 27

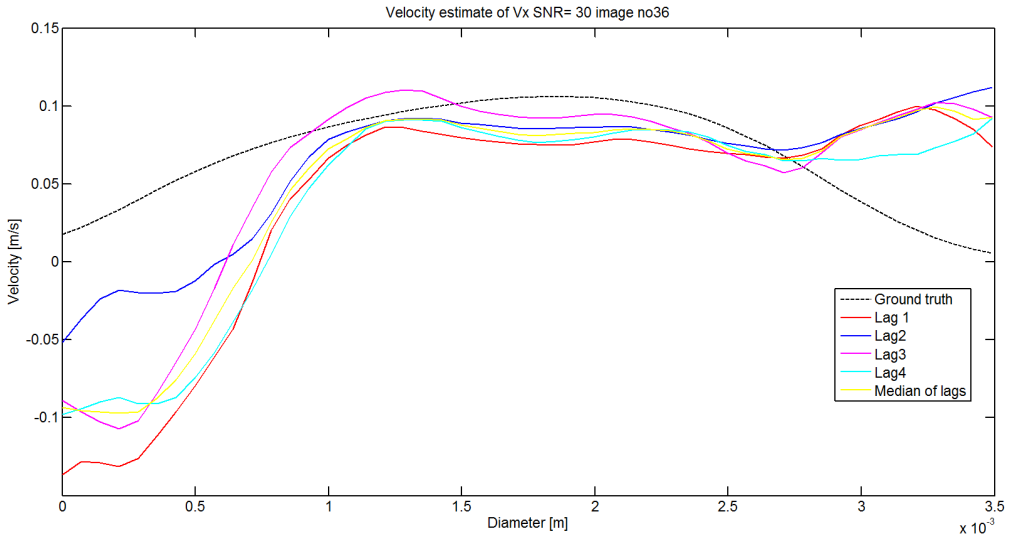

Figure 4.139: Velocity estimation in the x-direction for lag=1, lag=2, lag=3, lag=4 and the median of all the lags for flow frame 36 from area 2

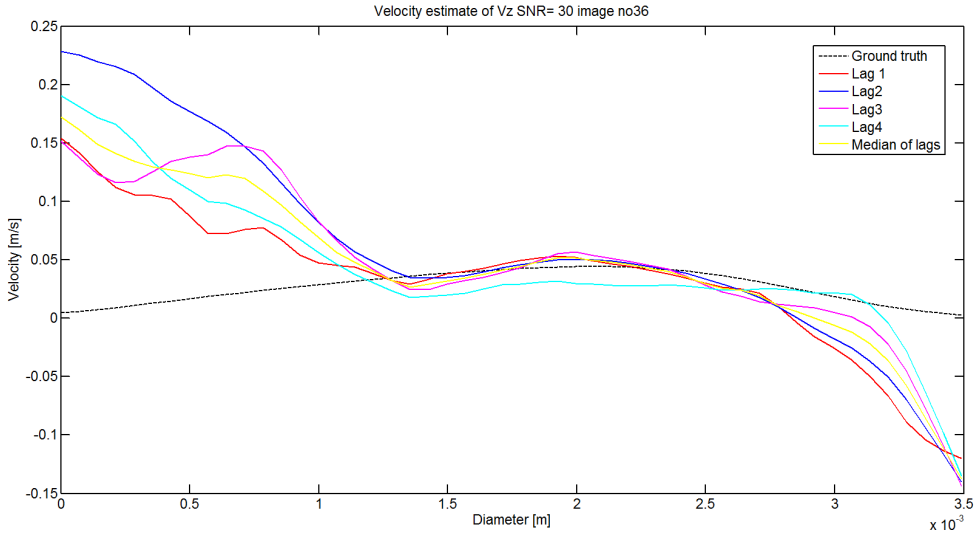

Figure 4.140: Velocity estimation in the z-direction for lag=1, lag=2, lag=3, lag=4 and the median of all the lags for flow frame 36 from area 2

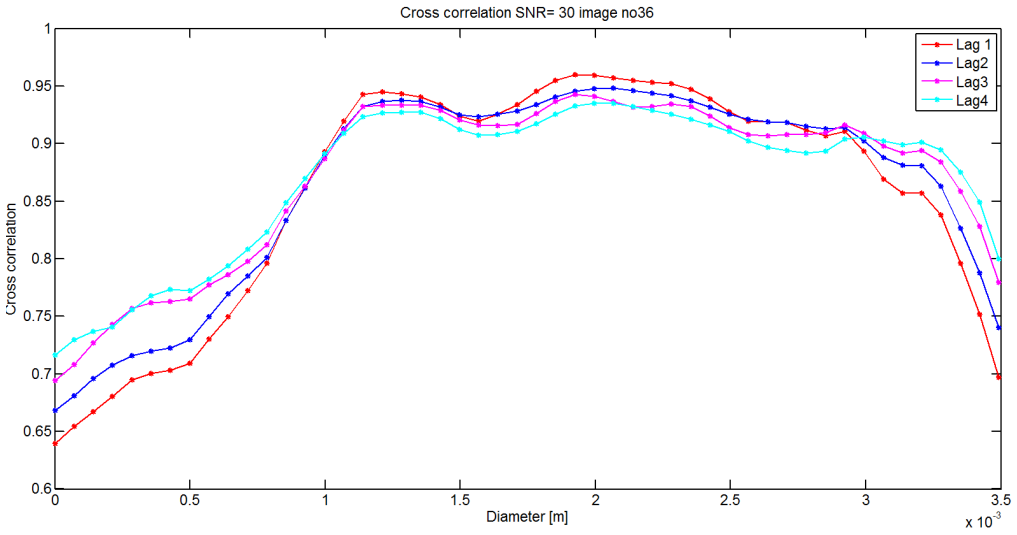

Figure 4.141: Cross correlation for lag=1, lag=2,lag=3 and lag=4 for flow frame 36 from area 2

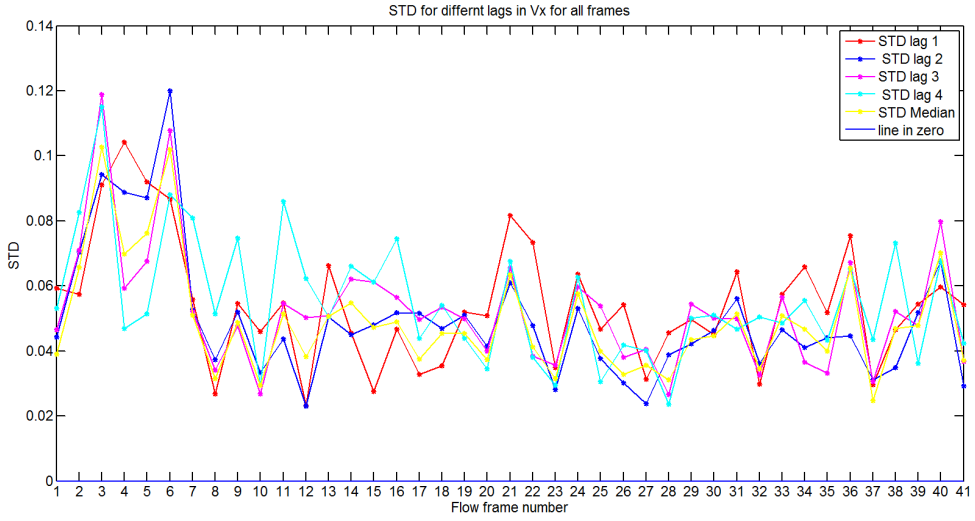

Figure 4.142: Standard deviation for the velocity estimates in the x-direction for lag= 1, lag=2, lag=3, lag=4 and median of all lags from area 2

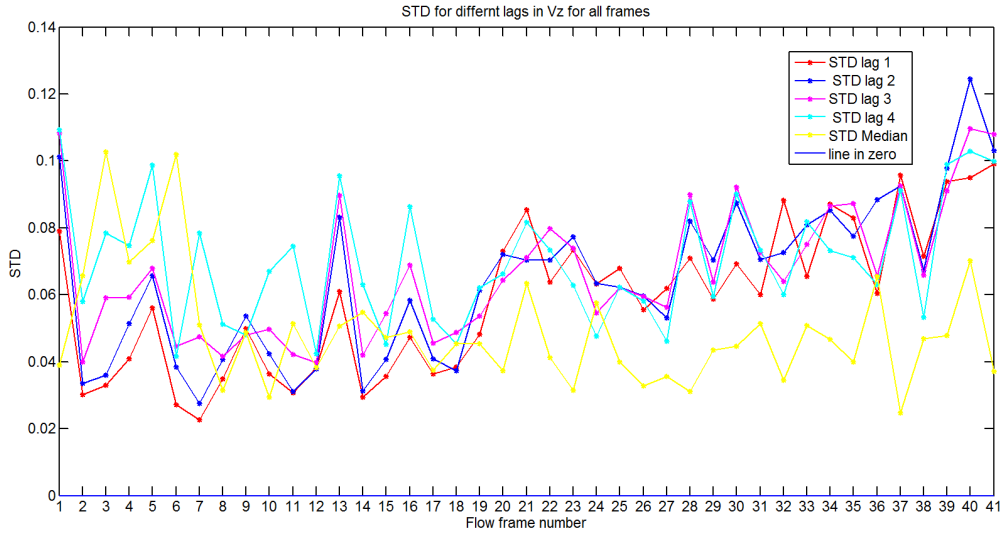

Figure 4.143: Standard deviation for the velocity estimates in the z-direction for lag= 1, lag=2, lag=3, lag=4 and median of all lags from area 2

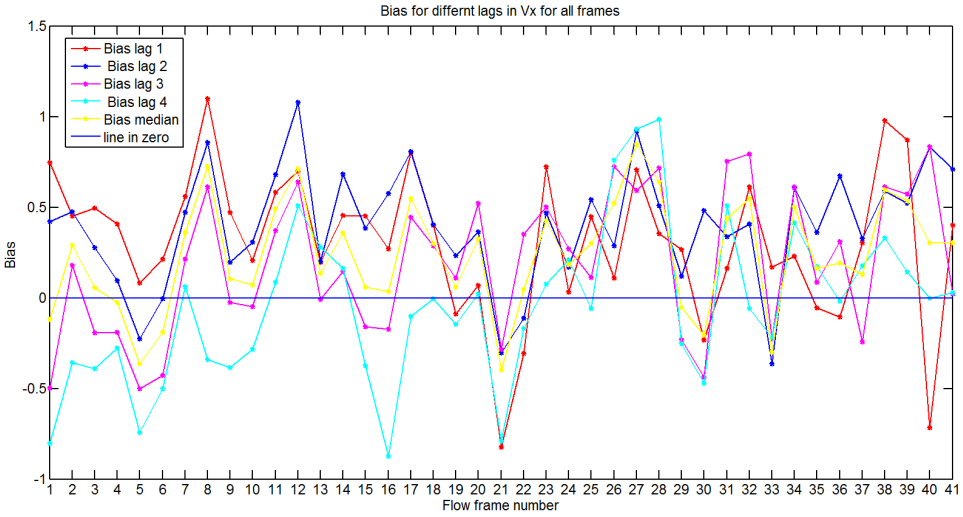

Figure 4.144: Bias between the velocity estimates in the x-direction for lag= 1, lag=2, lag=3 and lag=4 and ground truth from area 2

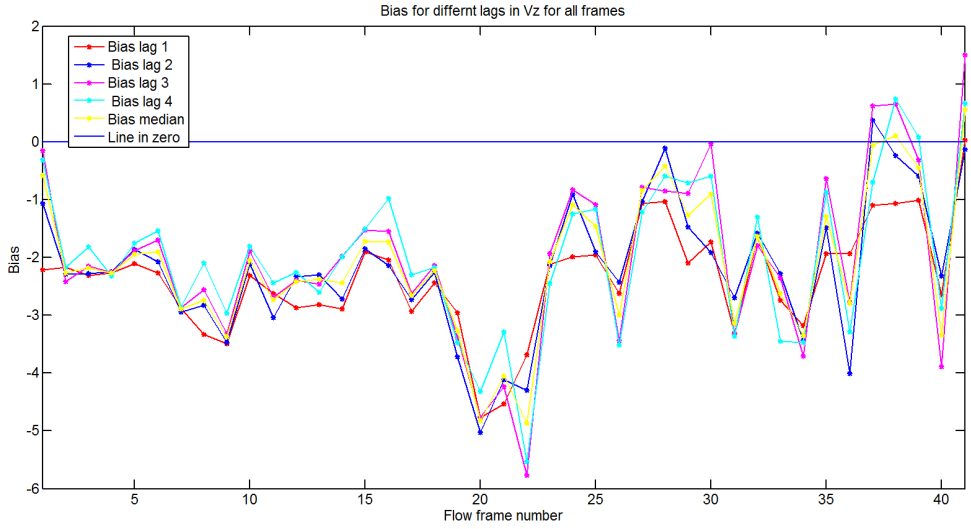

Figure 4.145: Bias between the velocity estimates in the z-direction for lag= 1, lag=2, lag=3 and lag=4 and ground truth from area 2

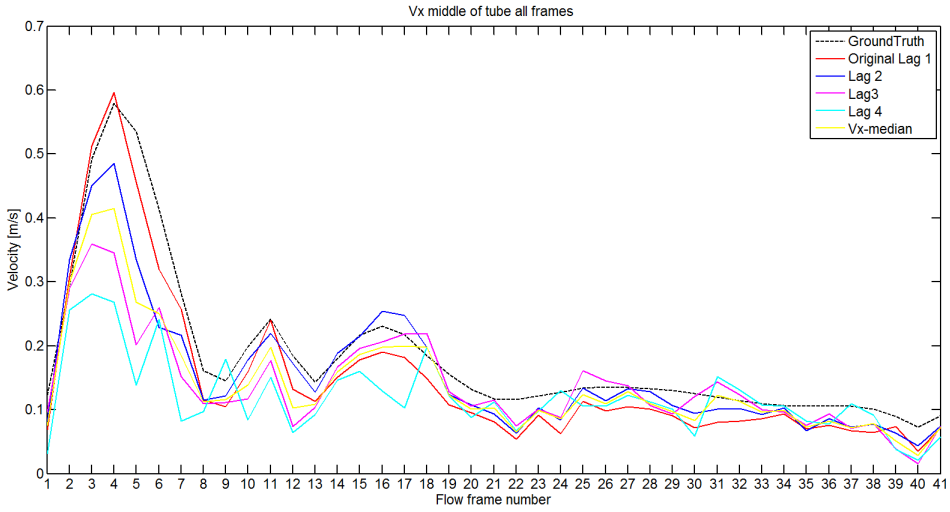

Figure 4.146: Velocity estimates in the x-direction for lag= 1, lag=2, lag=3, lag=4 and the median of all the lags in the middle of the tube for all flow frames from area 2

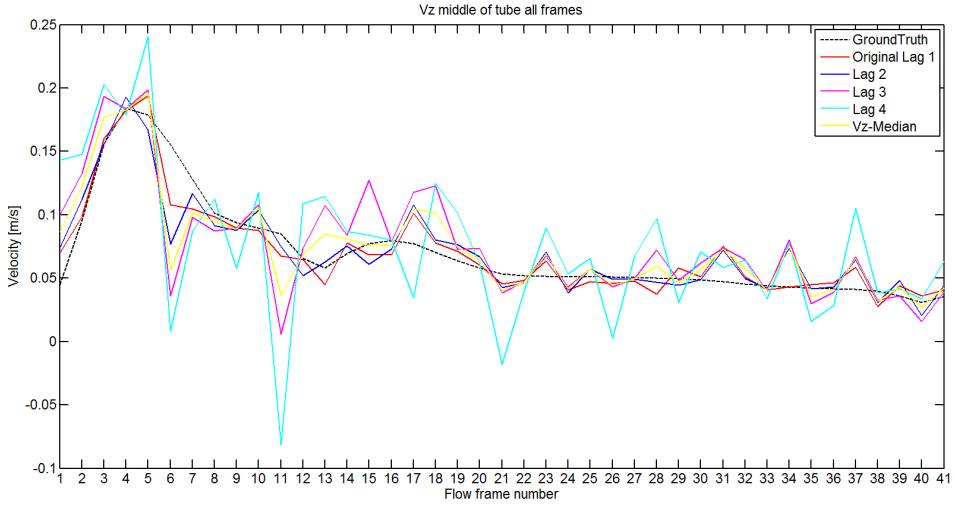

Figure 4.147: Velocity estimates in the z-direction for lag= 1, lag=2, lag=3, lag=4 and the median of all the lags in the middle of the tube for all flow frames from area 2

Results from area 3

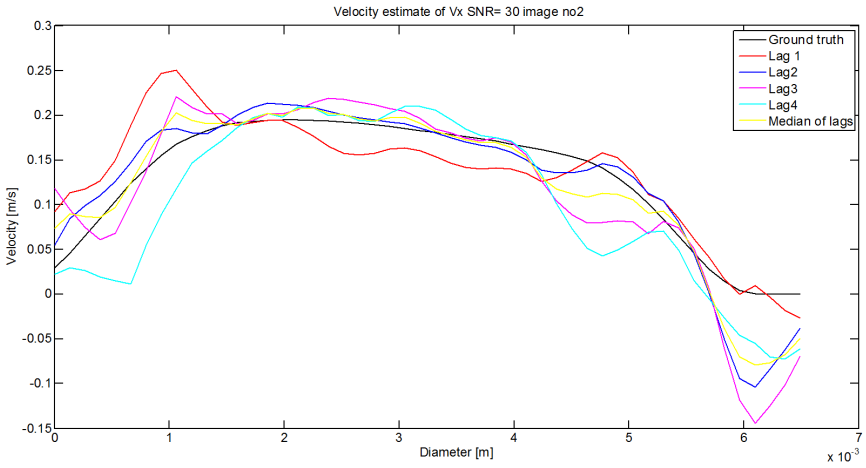

Figure 4.148: Velocity estimation in the x-direction for lag=1, lag=2, lag=3, lag=4 and the median of all the lags for flow frame 2 from area 3

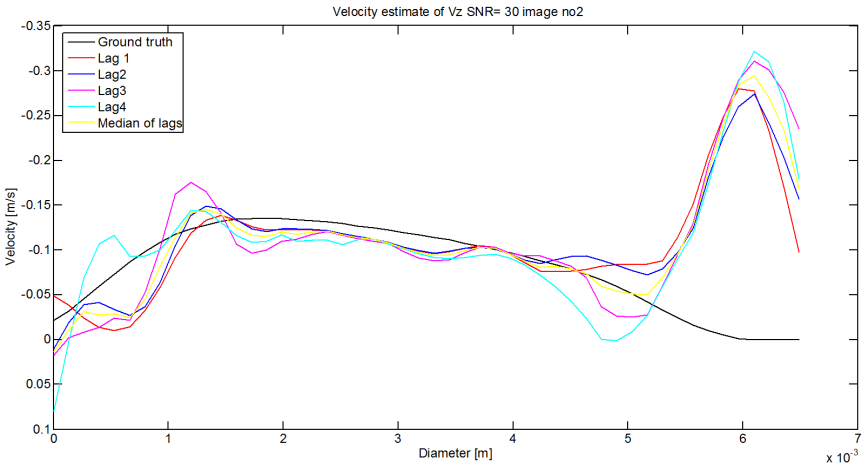

Figure 4.149: Velocity estimation in the z-direction for lag=1, lag=2, lag=3, lag=4 and the median of all the lags for flow frame 2 from area 3

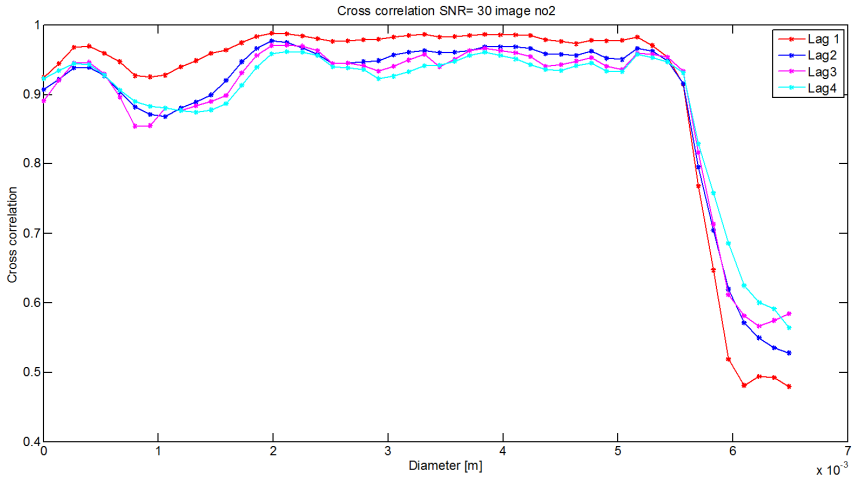

Figure 4.150: Cross correlation for lag=1, lag=2,lag=3 and lag=4 for flow frame 2 from area 3

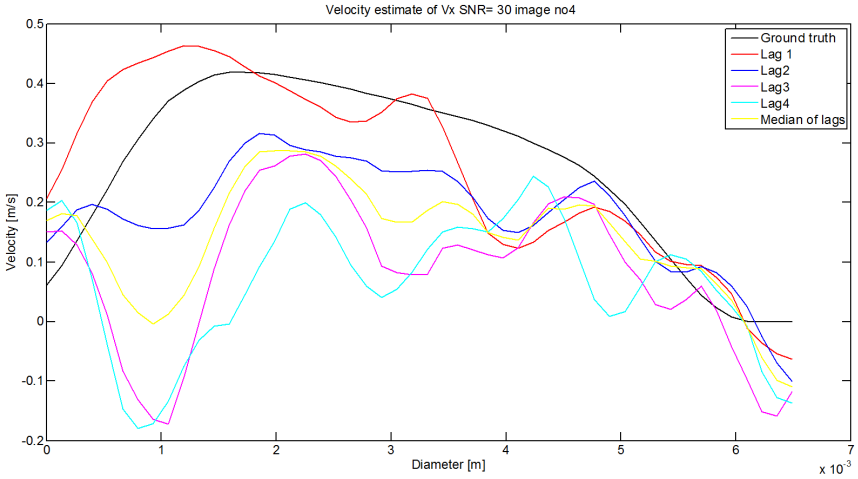

Figure 4.151: Velocity estimation in the x-direction for lag=1, lag=2, lag=3, lag=4 and the median of all the lags for flow frame 4 from area 3

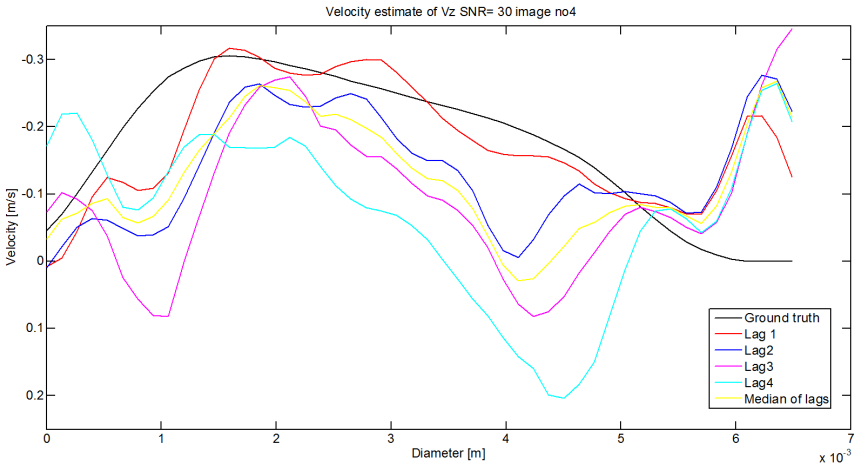

Figure 4.152: Velocity estimation in the z-direction for lag=1, lag=2, lag=3, lag=4 and the median of all the lags for flow frame 4 from area 3

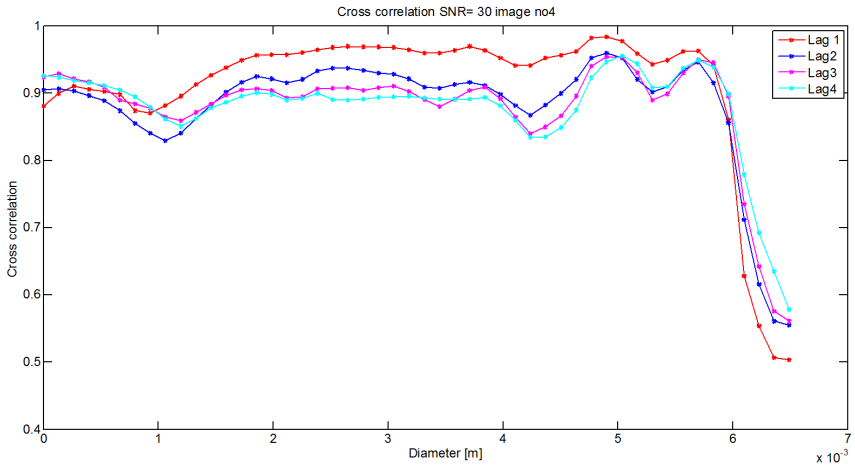

Figure 4.153: Cross correlation for lag=1, lag=2,lag=3 and lag=4 for flow frame 4 from area 3

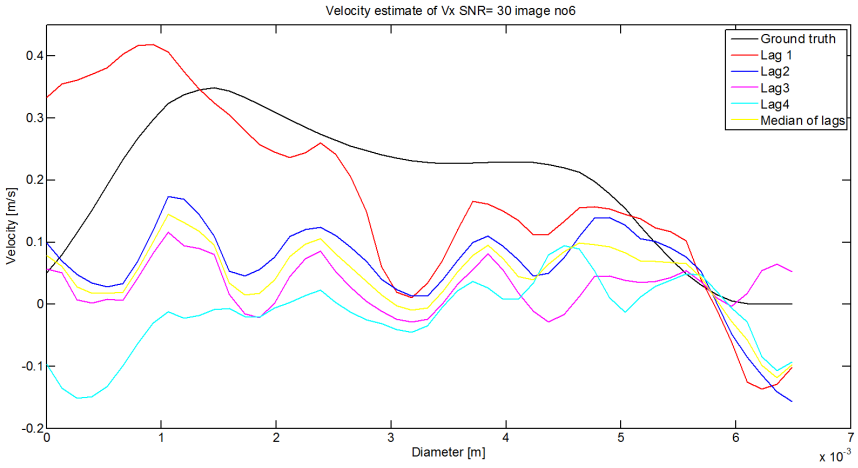

Figure 4.154: Velocity estimation in the x-direction for lag=1, lag=2, lag=3, lag=4 and the median of all the lags for flow frame 6 from area 3

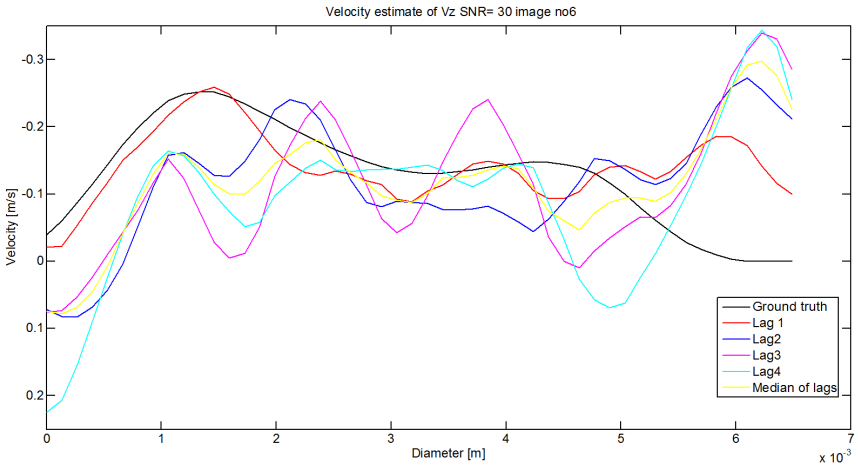

Figure 4.155: Velocity estimation in the z-direction for lag=1, lag=2, lag=3, lag=4 and the median of all the lags for flow frame 6 from area 3

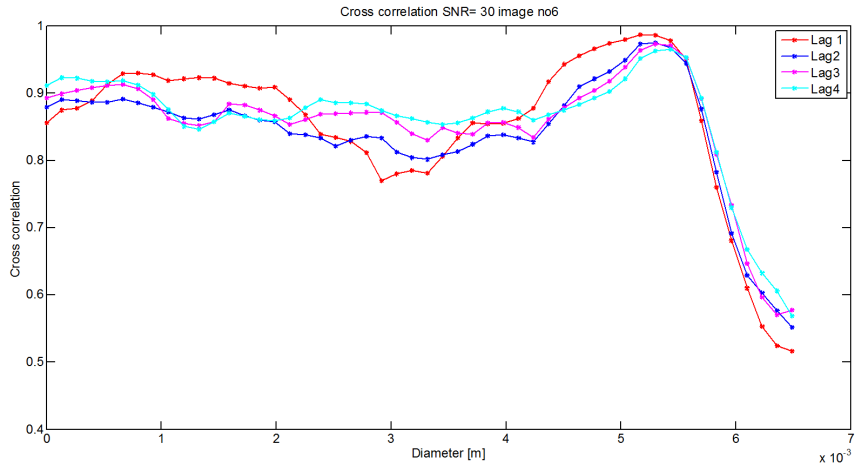

Figure 4.156: Cross correlation for lag=1, lag=2,lag=3 and lag=4 for flow frame 6 from area 3

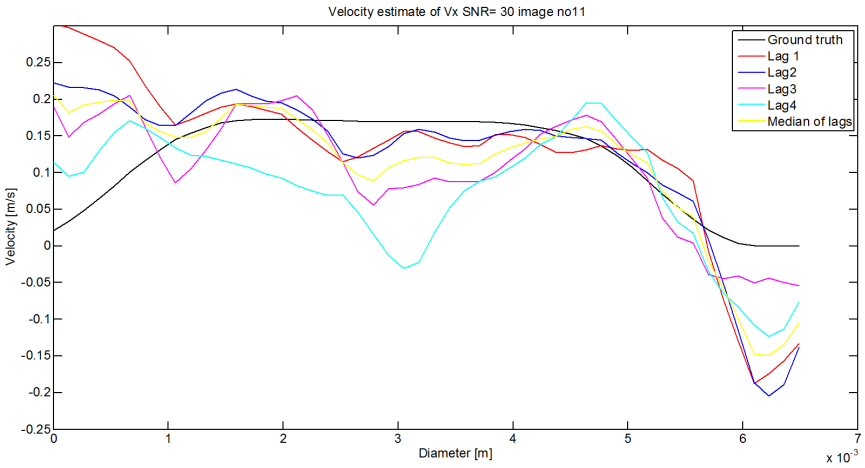

Figure 4.157: Velocity estimation in the x-direction for lag=1, lag=2, lag=3, lag=4 and the median of all the lags for flow frame 11 from area 3

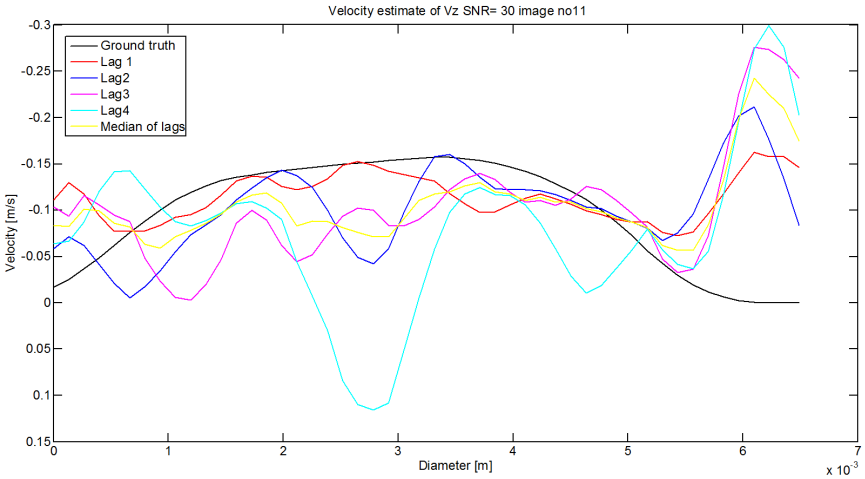

Figure 4.158: Velocity estimation in the z-direction for lag=1, lag=2, lag=3, lag=4 and the median of all the lags for flow frame 11 from area 3

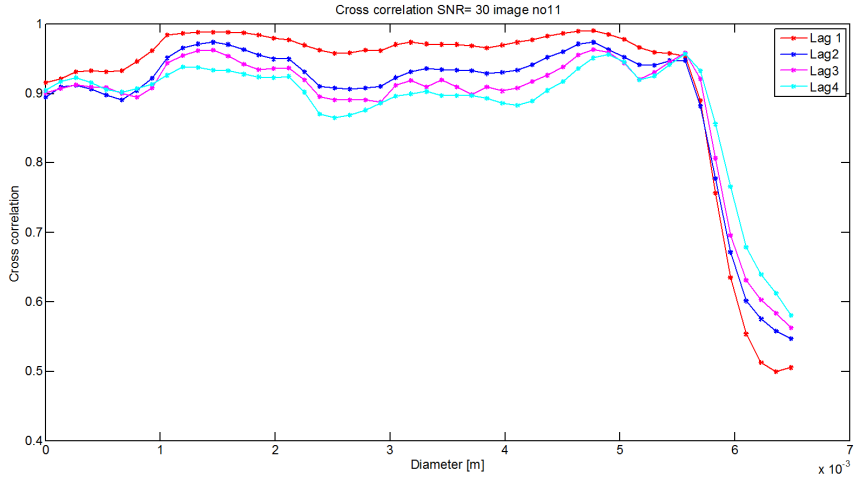

Figure 4.159: Cross correlation for lag=1, lag=2,lag=3 and lag=4 for flow frame 11 from area 3

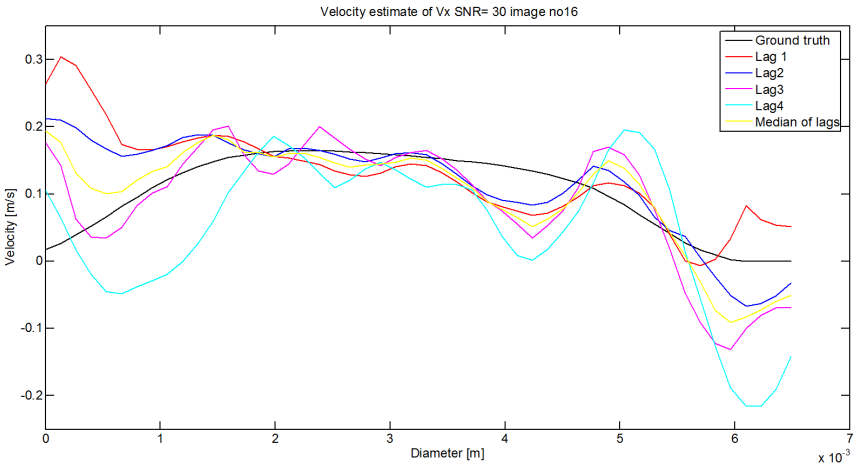

Figure 4.160: Velocity estimation in the x-direction for lag=1, lag=2, lag=3, lag=4 and the median of all the lags for flow frame 16 from area 3

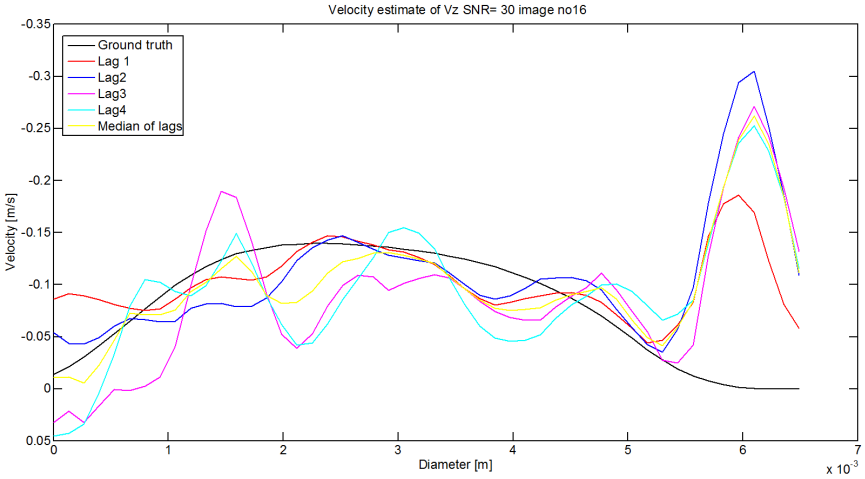

Figure 4.161: Velocity estimation in the z-direction for lag=1, lag=2, lag=3, lag=4 and the median of all the lags for flow frame 16 from area 3

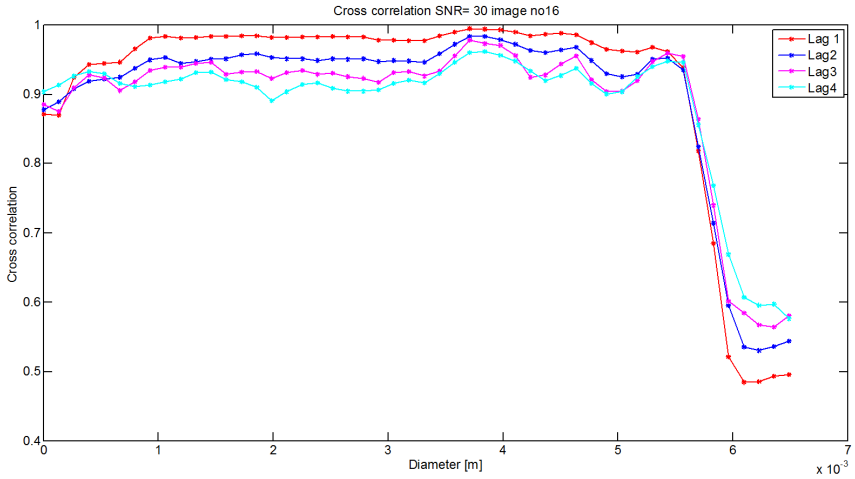

Figure 4.162: Cross correlation for lag=1, lag=2,lag=3 and lag=4 for flow frame 16 from area 3

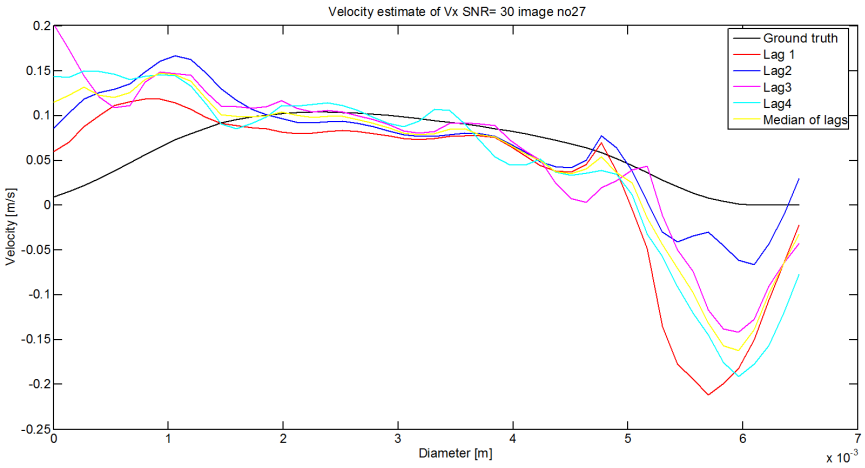

Figure 4.163: Velocity estimation in the x-direction for lag=1, lag=2, lag=3, lag=4 and the median of all the lags for flow frame 27 from area 3

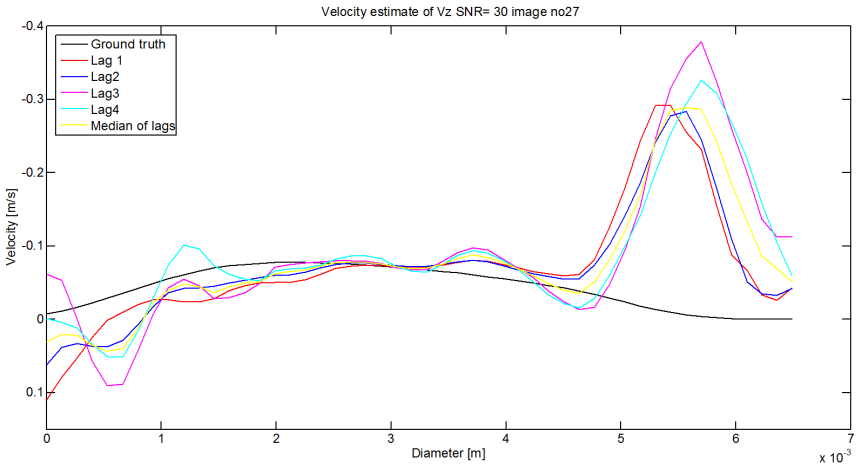

Figure 4.164: Velocity estimation in the z-direction for lag=1, lag=2, lag=3, lag=4 and the median of all the lags for flow frame 27 from area 3

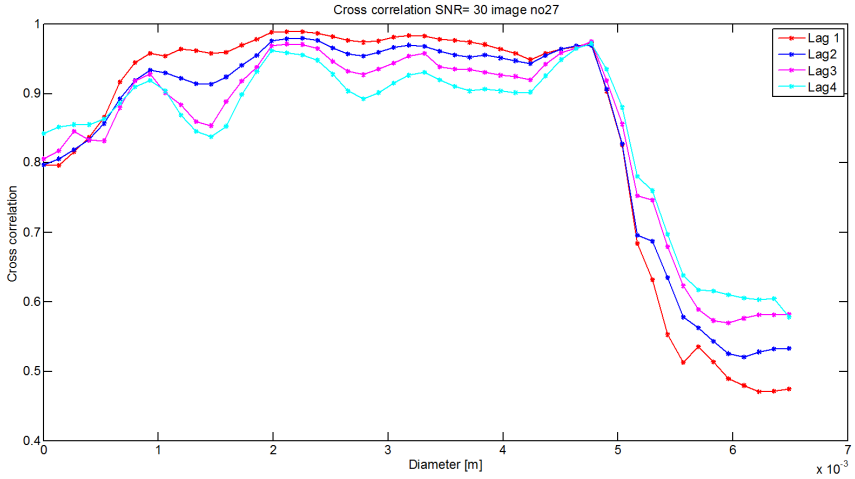

Figure 4.165: Cross correlation for lag=1, lag=2,lag=3 and lag=4 for flow frame 27 from area 3

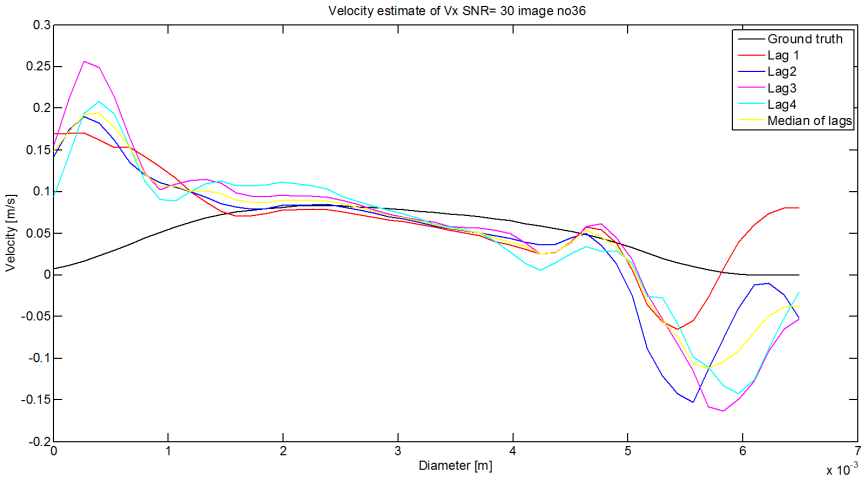

Figure 4.166: Velocity estimation in the x-direction for lag=1, lag=2, lag=3, lag=4 and the median of all the lags for flow frame 36 from area 3

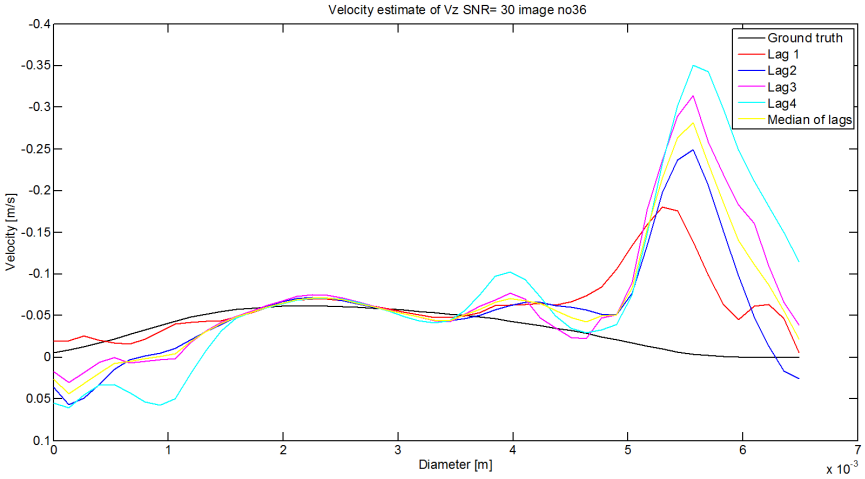

Figure 4.167: Velocity estimation in the z-direction for lag=1, lag=2, lag=3, lag=4 and the median of all the lags for flow frame 36 from area 3

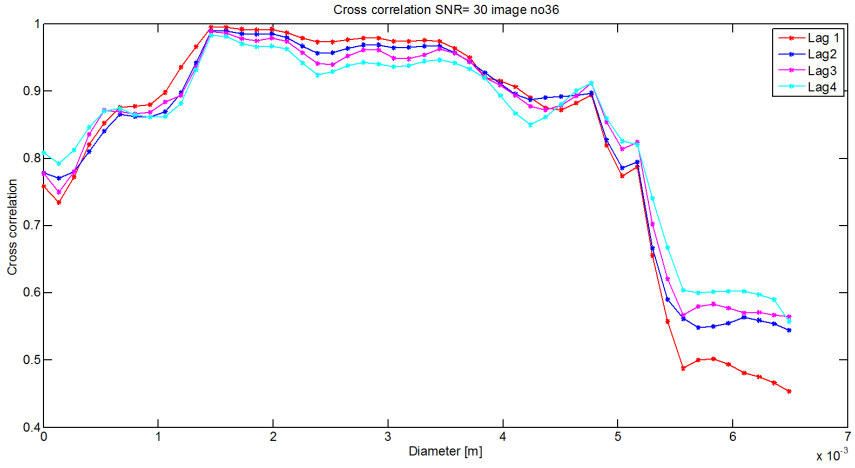

Figure 4.168: Cross correlation for lag=1, lag=2,lag=3 and lag=4 for flow frame 36 from area 3

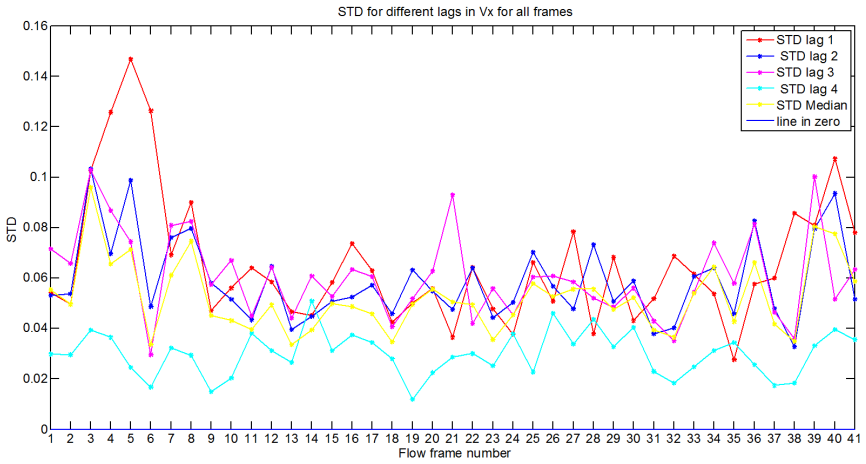

Figure 4.169: Standard deviation for the velocity estimates in the x-direction for lag= 1, lag=2, lag=3, lag=4 and median of all lags from area 3

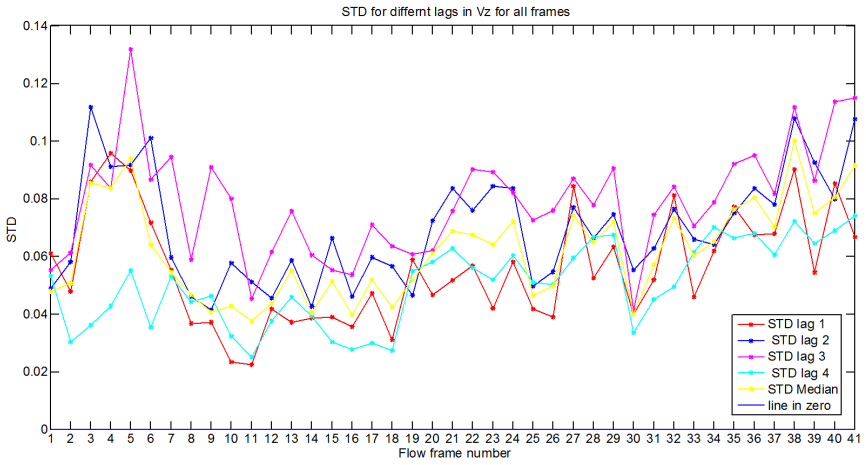

Figure 4.170: Standard deviation for the velocity estimates in the z-direction for lag= 1, lag=2, lag=3, lag=4 and median of all lags from area 3

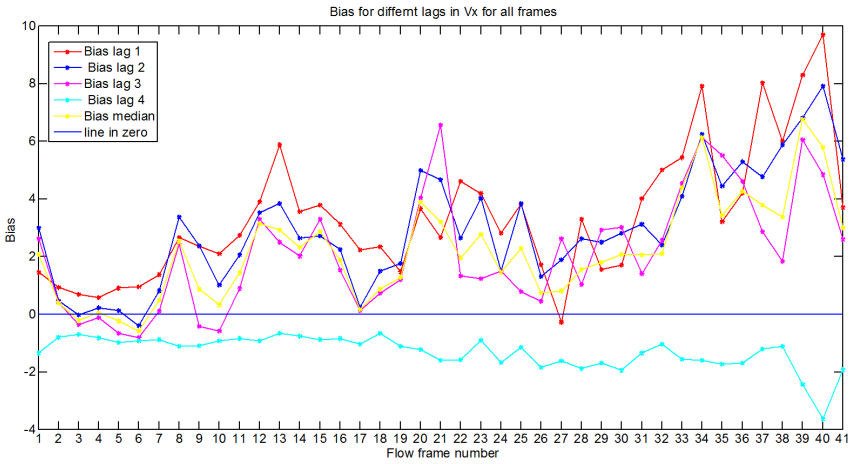

Figure 4.171: Bias between the velocity estimates in the x-direction for lag= 1, lag=2, lag=3 and lag=4 and ground truth from area 3

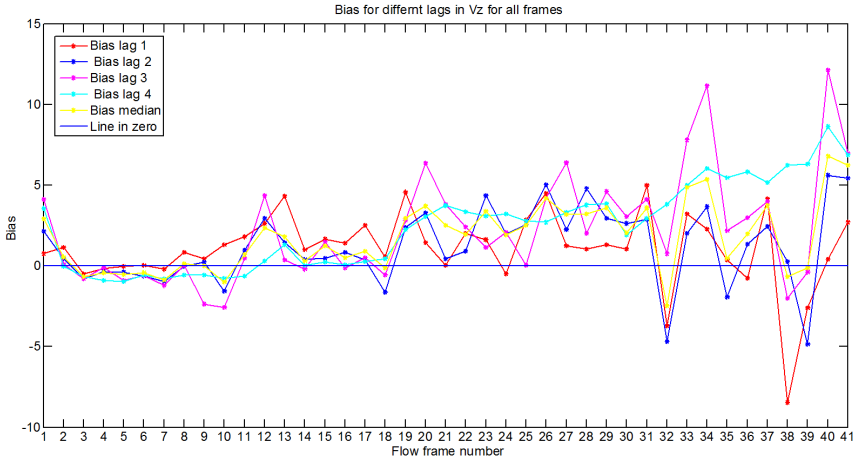

Figure 4.172: Bias between the velocity estimates in the z-direction for lag= 1, lag=2, lag=3 and lag=4 and ground truth from area 3

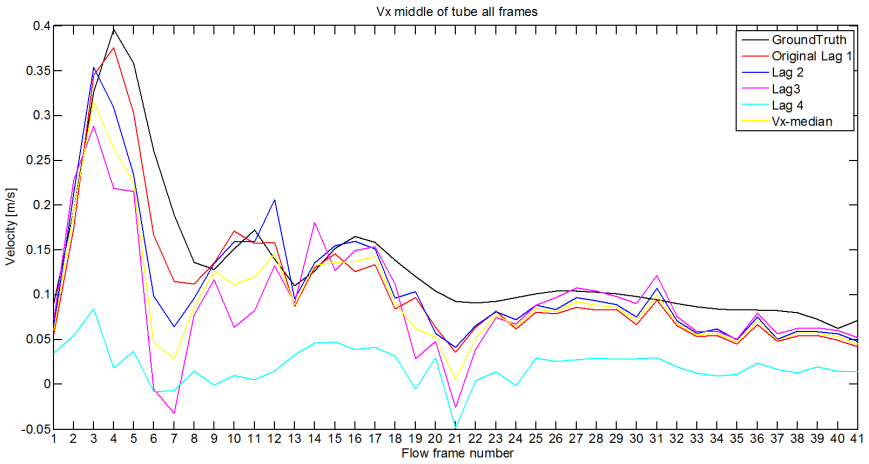

Figure 4.173: Velocity estimates in the x-direction for lag= 1, lag=2, lag=3, lag=4 and the median of all the lags in the middle of the tube for all flow frames from area 3

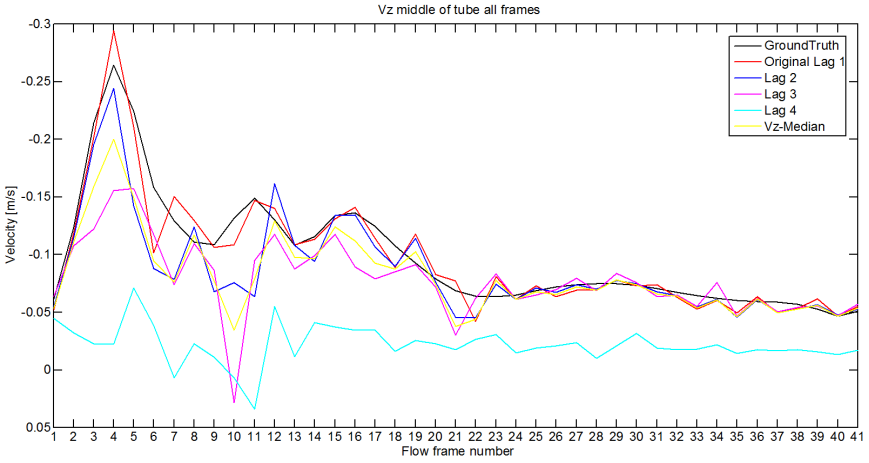

Figure 4.174: Velocity estimates in the z-direction for lag= 1, lag=2, lag=3, lag=4 and the median of all the lags in the middle of the tube for all flow frames from area 3

4.3 Adaptive speckle tracking algorithm -adjusted to the acceleration over flow frames/ Multi-lag tracking

The preceding figures represents the mean velocity estimates in the lateral and axial direction as a result of the speckle tracking with the original speckle tracking with lag=1, the adaptive speckle tracking algorithm with adjustment to the acceleration over flow frames and multi-lag tracking for the chosen areas. The bias between the ground truth and the velocity estimates from the different tracking algorithms was also found. Figure 4.192, 4.193 , 4.211 and 4.212, **??** and 4.231 represent the velocity in the lateral and axial direction in the middle of the tube for all the flow frames, respectively. The cross correlation over the frames between the best match and the kernel was calculated by using the normalized cross-correlation function in the equation 2.7, for the velocity estimates from the different tracking algorithms, as depicted in figure 4.187, 4.206 and 4.225 for the different areas. The standard deviation of the velocity estimates over a packet, all frames, was also found and is depicted in figure 4.188, 4.207, 4.226, 4.189, 4.208 and 4.227 for all frames, in area 1, 2 and 3 respectively.

Results from area 1

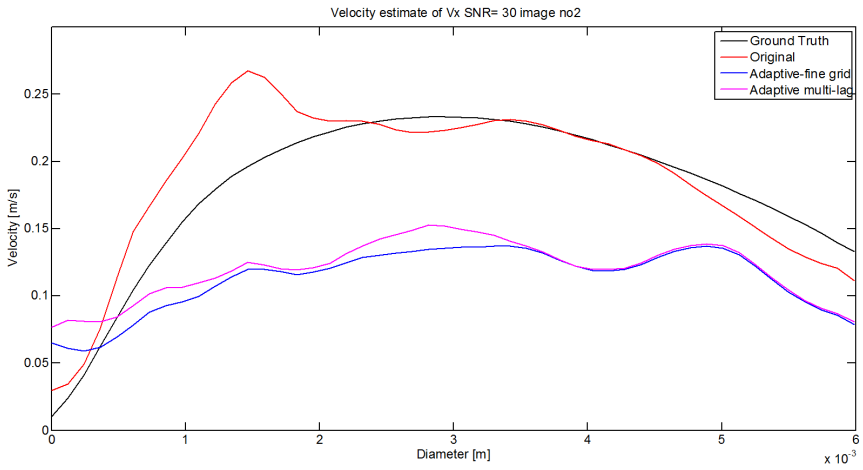

Figure 4.175: Velocity estimations in the x-direction with the original speckle tracking algorithm, the adaptive speckle tracking algorithm with finer grid and multi-lag tracking for flow frame 2 from area 1

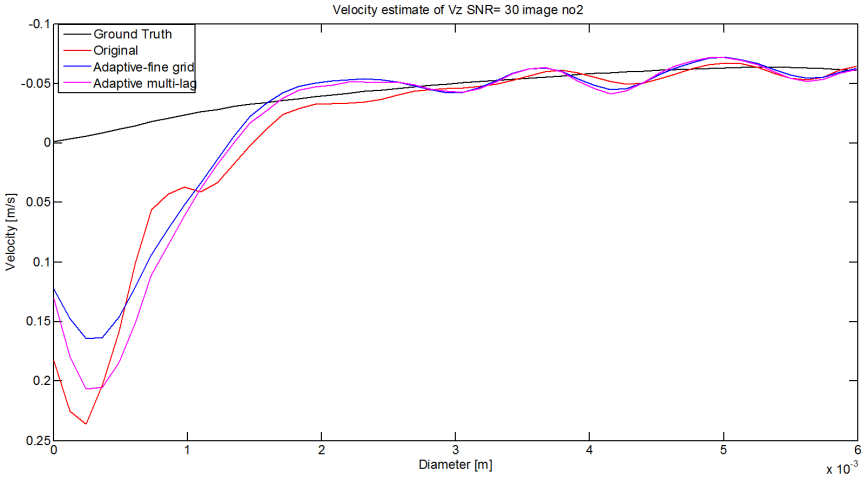

Figure 4.176: Velocity estimations in the z-direction with the original speckle tracking algorithm, the adaptive speckle tracking algorithm with finer grid and multi-lag tracking for flow frame 2 from area 1

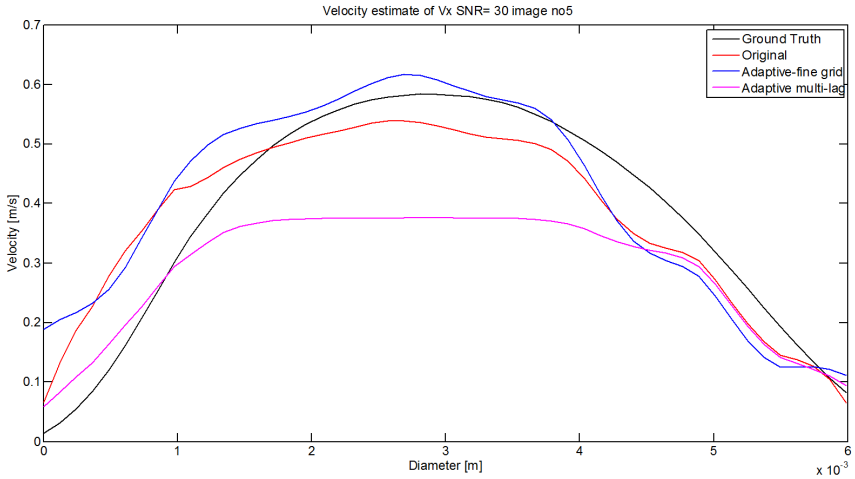

Figure 4.177: Velocity estimations in the x-direction with the original speckle tracking algorithm, the adaptive speckle tracking algorithm with finer grid and multi-lag tracking for flow frame 5 from area 1

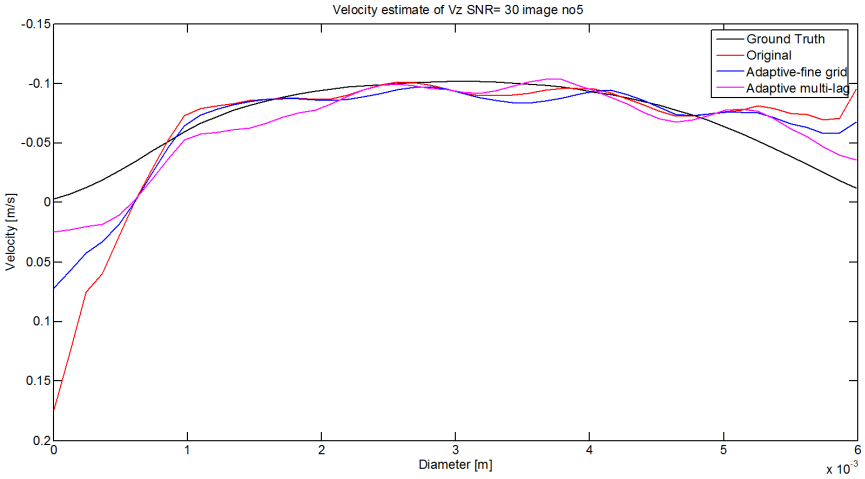

Figure 4.178: Velocity estimations in the z-direction with the original speckle tracking algorithm, the adaptive speckle tracking algorithm with finer grid and multi-lag tracking for flow frame 5 from area 1

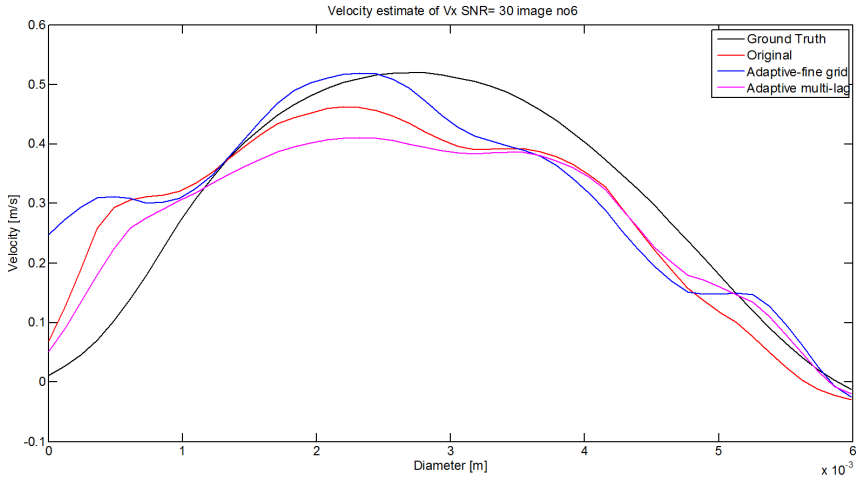

Figure 4.179: Velocity estimations in the x-direction with the original speckle tracking algorithm, the adaptive speckle tracking algorithm with finer grid and multi-lag tracking for flow frame 6 from area 1

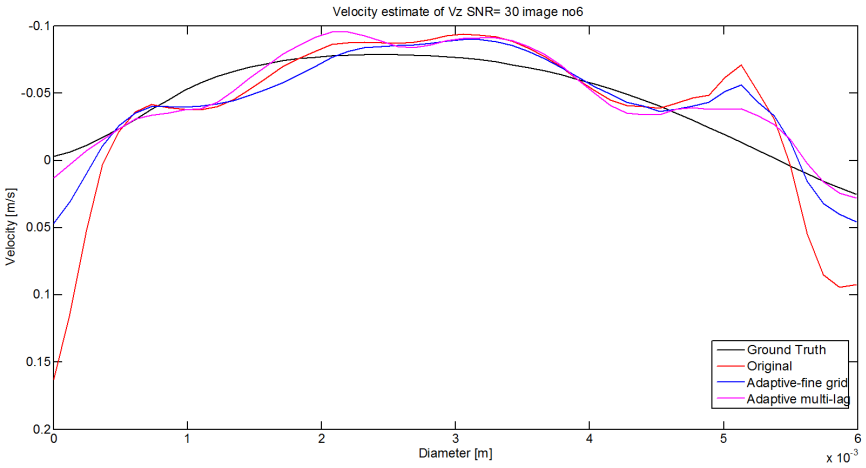

Figure 4.180: Velocity estimations in the z-direction with the original speckle tracking algorithm, the adaptive speckle tracking algorithm with finer grid and multi-lag tracking for flow frame 6 from area 1

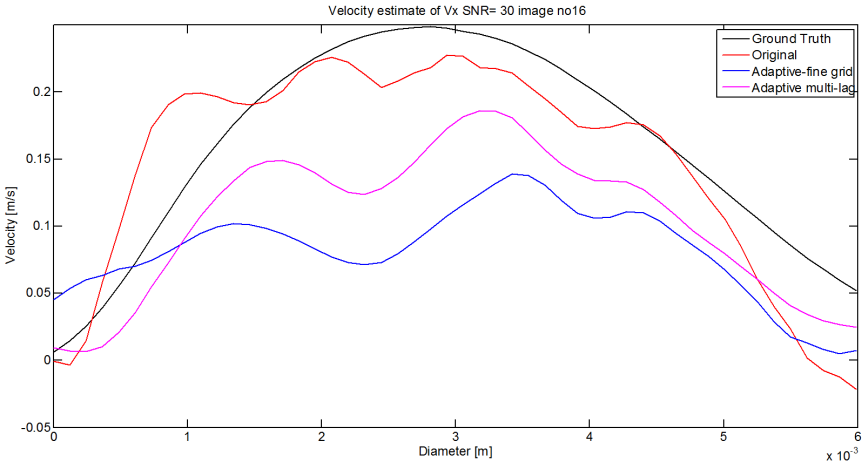

Figure 4.181: Velocity estimations in the x-direction with the original speckle tracking algorithm, the adaptive speckle tracking algorithm with finer grid and multi-lag tracking for flow frame 16 from area 1

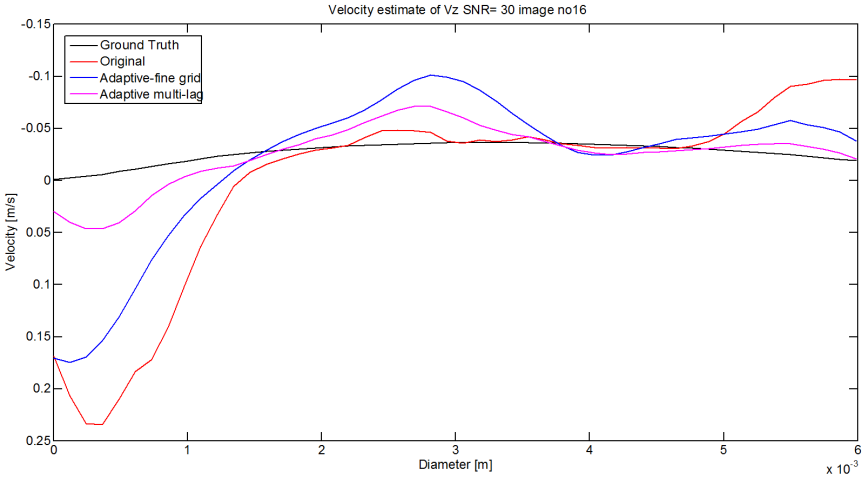

Figure 4.182: Velocity estimations in the z-direction with the original speckle tracking algorithm, the adaptive speckle tracking algorithm with finer grid and multi-lag tracking for flow frame 16 from area 1

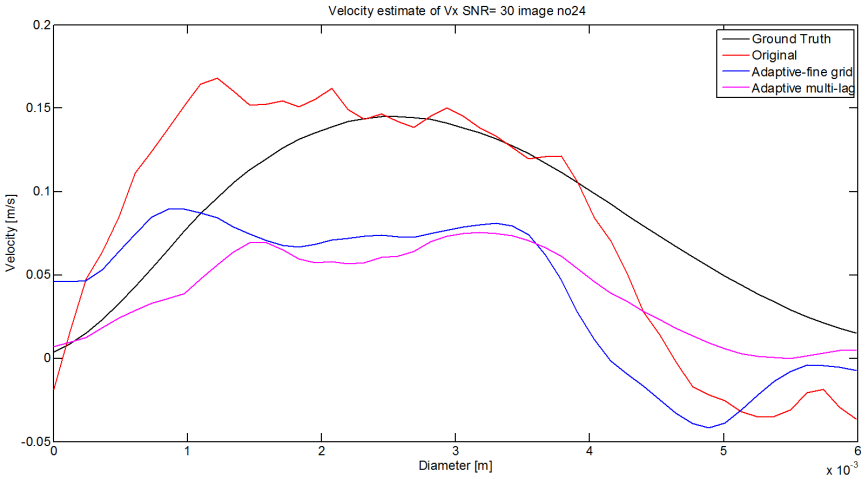

Figure 4.183: Velocity estimations in the x-direction with the original speckle tracking algorithm, the adaptive speckle tracking algorithm with finer grid and multi-lag tracking for flow frame 24 from area 1

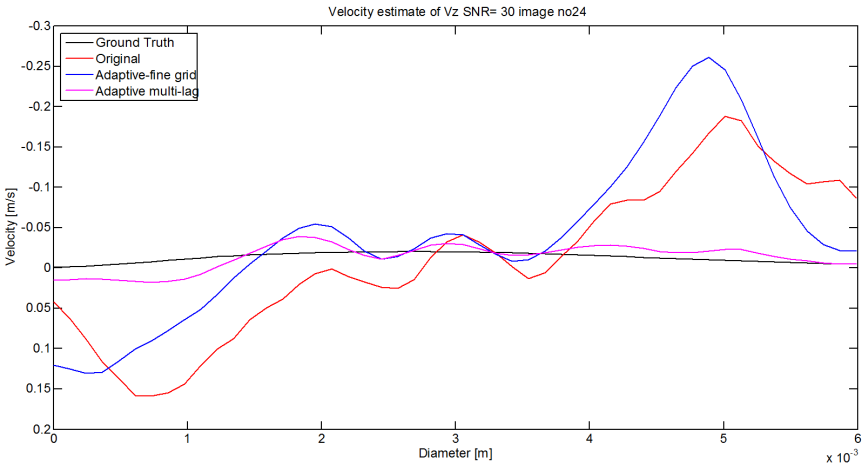

Figure 4.184: Velocity estimations in the z-direction with the original speckle tracking algorithm, the adaptive speckle tracking algorithm with finer grid and multi-lag tracking for flow frame 24 from area 1

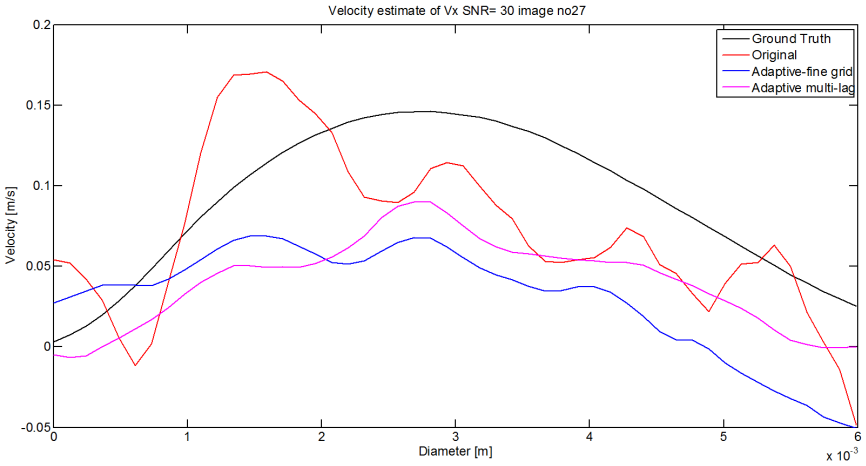

Figure 4.185: Velocity estimations in the x-direction with the original speckle tracking algorithm, the adaptive speckle tracking algorithm with finer grid and multi-lag tracking for flow frame 27 from area 1

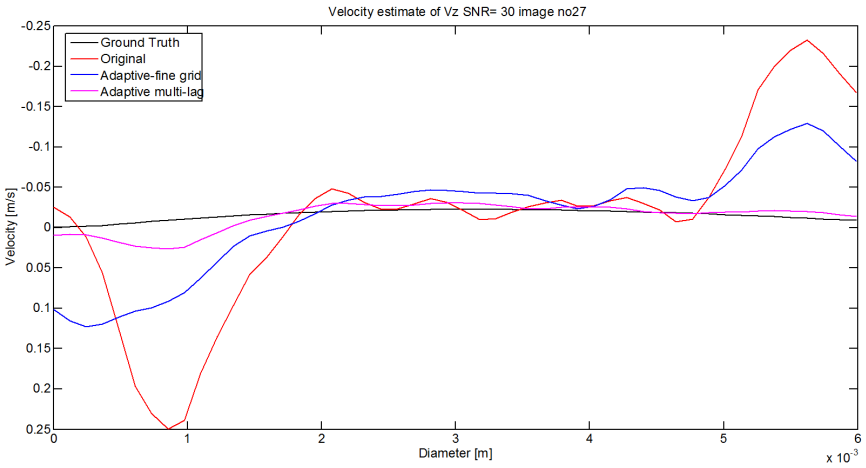

Figure 4.186: Velocity estimations in the z-direction with the original speckle tracking algorithm, the adaptive speckle tracking algorithm with finer grid and multi-lag tracking for flow frame 27 from area 1

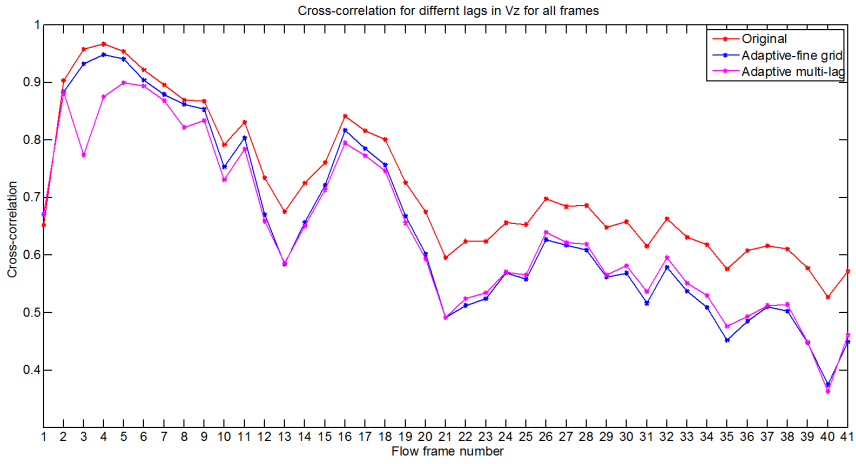

Figure 4.187: Mean cross correlation between the kernel and best match for the original speckle tracking algorithm, the adaptive speckle tracking algorithm with finer grid and multi-lag tracking for all frames from area 1

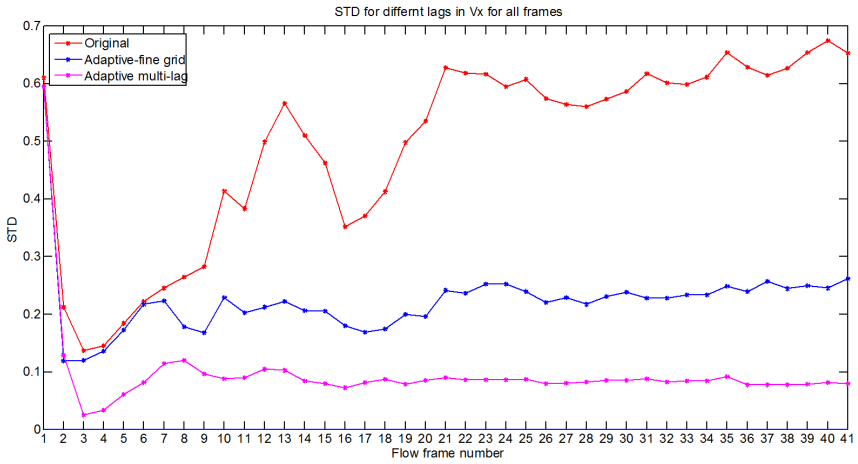

Figure 4.188: Standard deviation in velocity estimations in the x-direction with the original speckle tracking algorithm, the adaptive speckle tracking algorithm with finer grid and multi-lag tracking from area 2

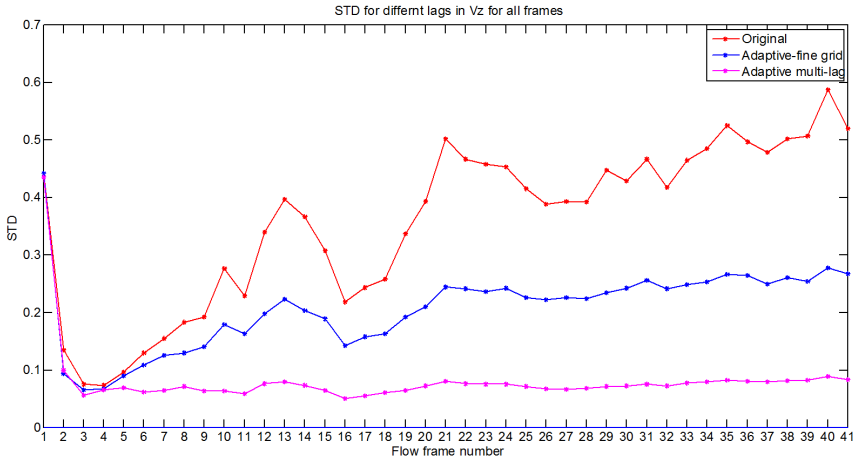

Figure 4.189: Standard deviation in velocity estimations in the z-direction with the original speckle tracking algorithm, the adaptive speckle tracking algorithm with finer grid and multi-lag tracking from area 1

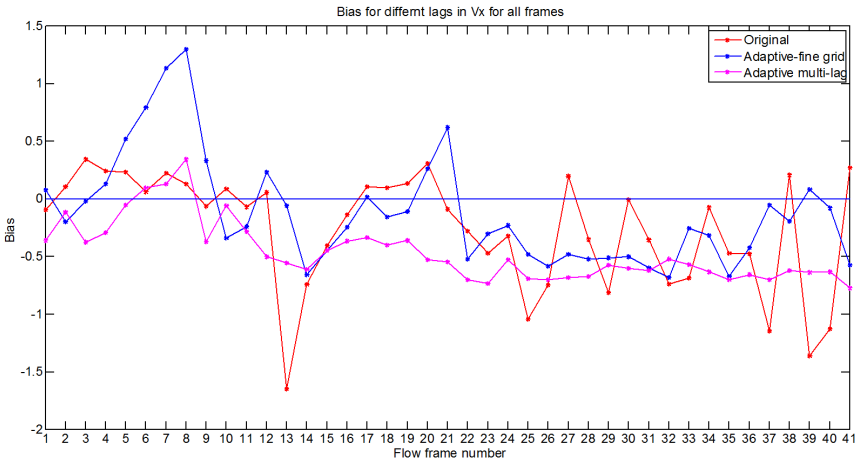

Figure 4.190: Bias between the velocity estimates in the x-direction with the original speckle tracking algorithm, the adaptive speckle tracking algorithm with finer grid and multi-lag tracking from area 1

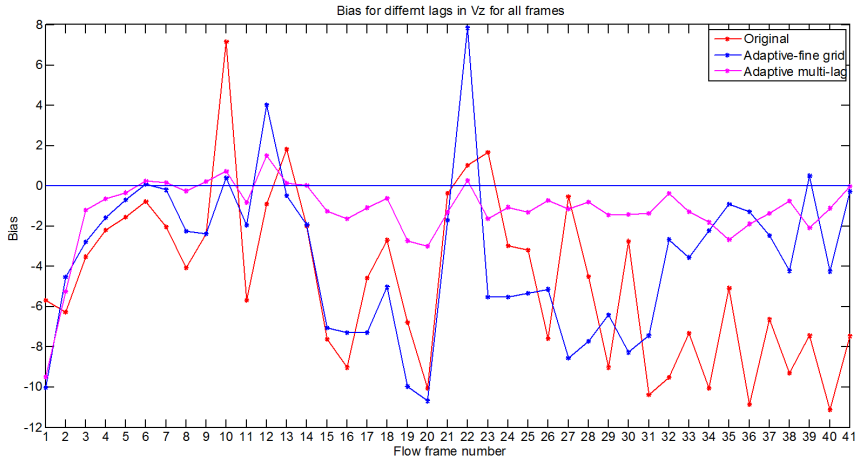

Figure 4.191: Bias between the velocity estimates in the z-direction with the original speckle tracking algorithm, the adaptive speckle tracking algorithm with finer grid and multi-lag tracking from area 2

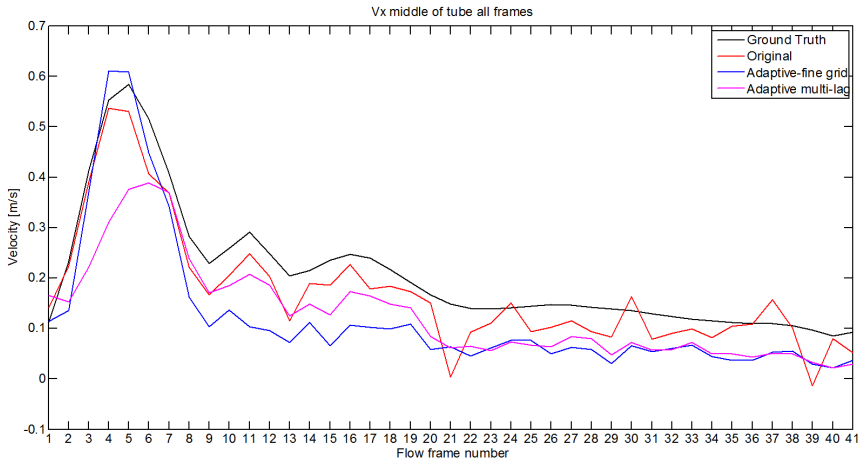

Figure 4.192: Velocity estimates in the middle of the artery in the x-direction with the original speckle tracking algorithm, the adaptive speckle tracking algorithm with finer grid and multi-lag tracking from area 1

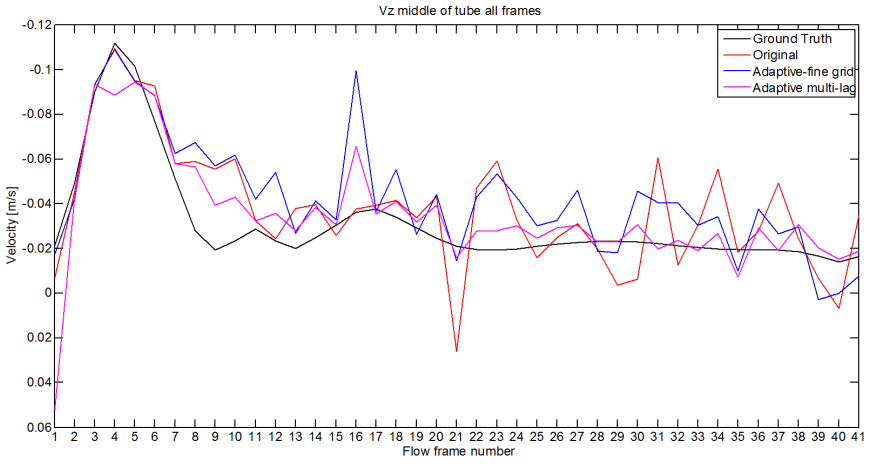

Figure 4.193: Velocity estimates in the middle in the z-direction with the original speckle tracking algorithm, the adaptive speckle tracking algorithm with finer grid and multi-lag tracking from area 1

Results from area 2

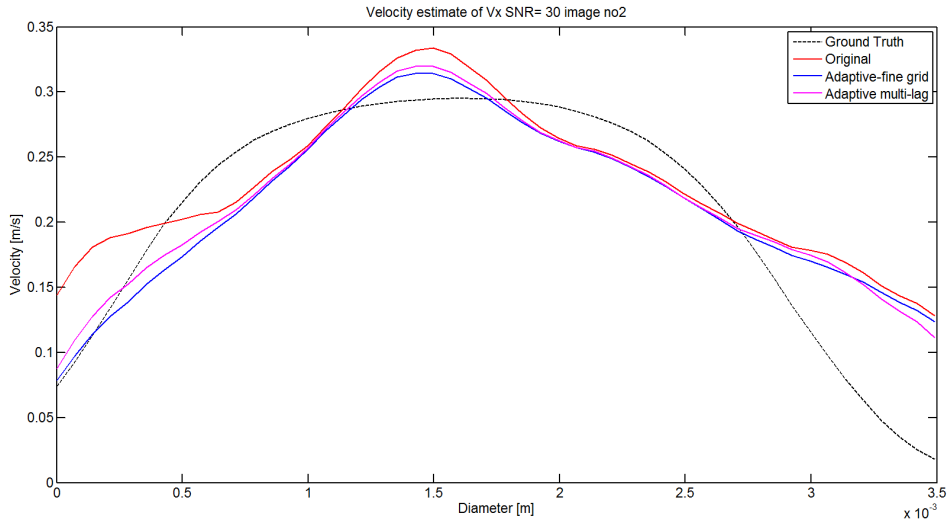

Figure 4.194: Velocity estimations in the x-direction with the original speckle tracking algorithm, the adaptive speckle tracking algorithm with finer grid and multi-lag tracking for flow frame 2 from area 2

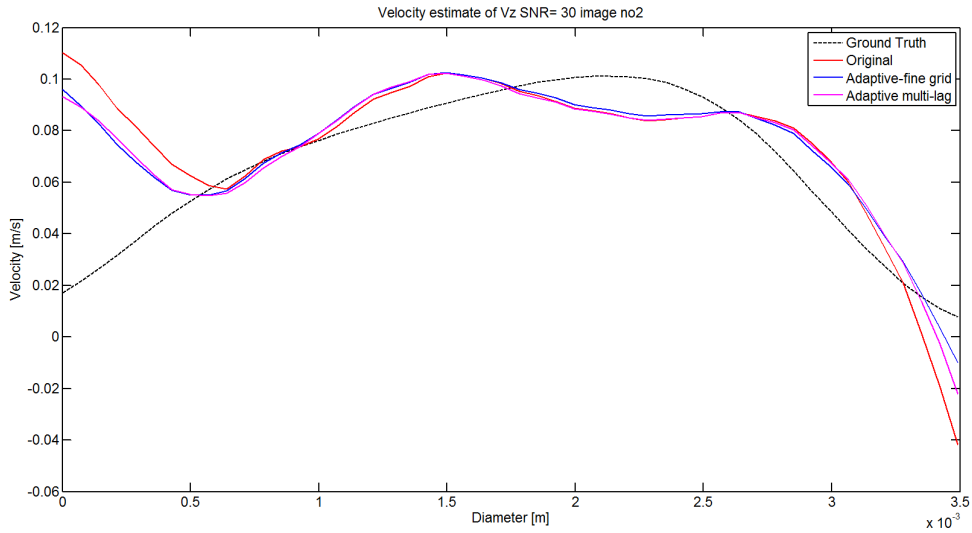

Figure 4.195: Velocity estimations in the z-direction with the original speckle tracking algorithm, the adaptive speckle tracking algorithm with finer grid and multi-lag tracking for flow frame 2 from area 2

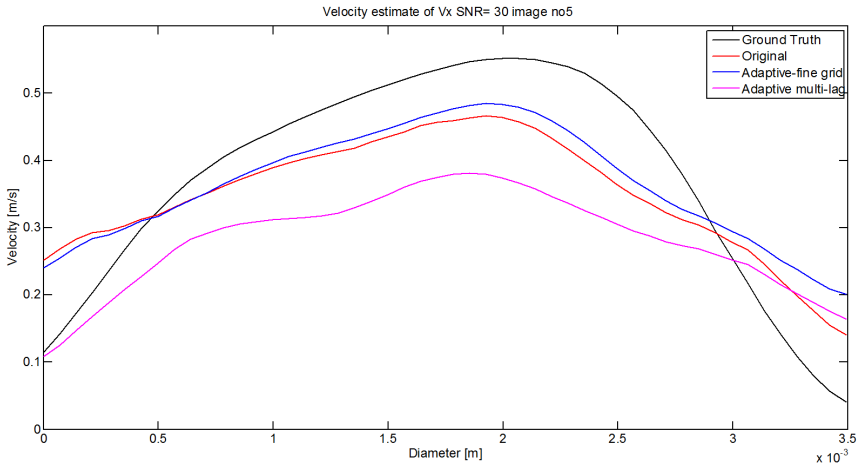

Figure 4.196: Velocity estimations in the x-direction with the original speckle tracking algorithm, the adaptive speckle tracking algorithm with finer grid and multi-lag tracking for flow frame 5 from area 2

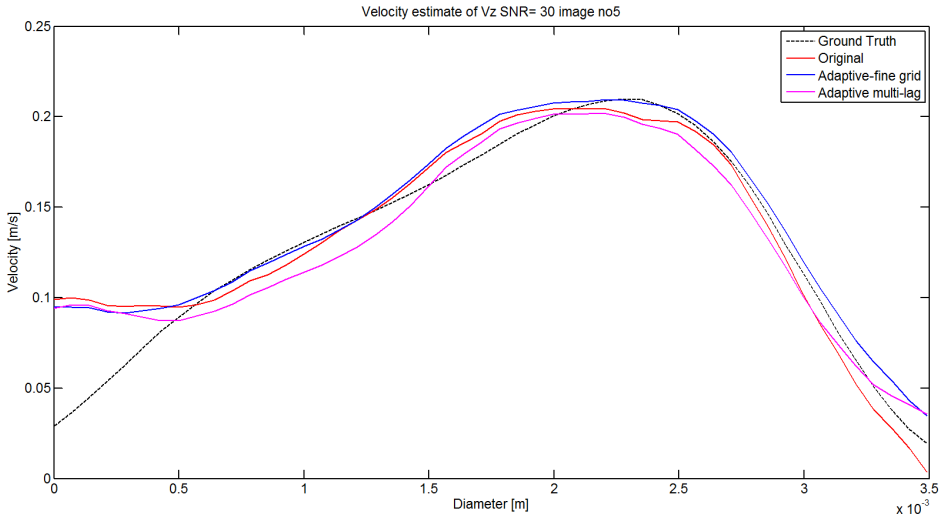

Figure 4.197: Velocity estimations in the z-direction with the original speckle tracking algorithm, the adaptive speckle tracking algorithm with finer grid and multi-lag tracking for flow frame 5 from area 2

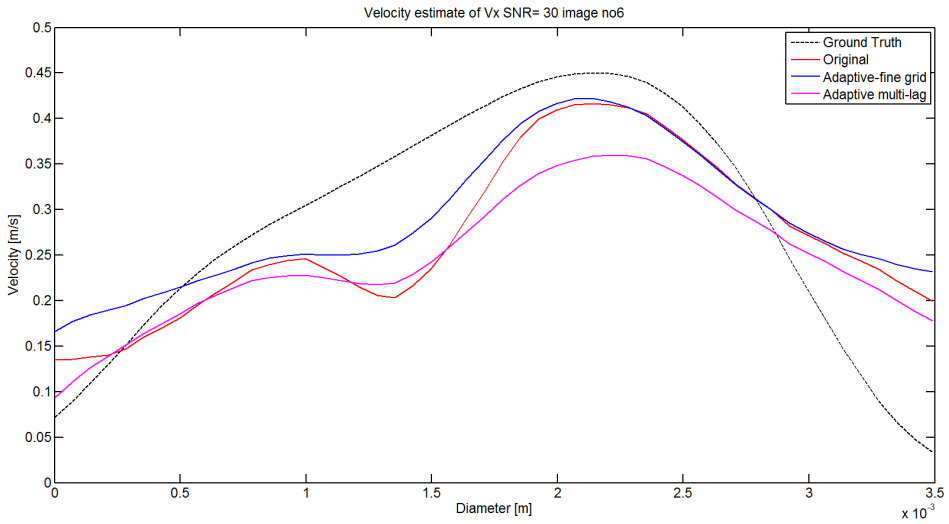

Figure 4.198: Velocity estimations in the x-direction with the original speckle tracking algorithm, the adaptive speckle tracking algorithm with finer grid and multi-lag tracking for flow frame 6 from area 2

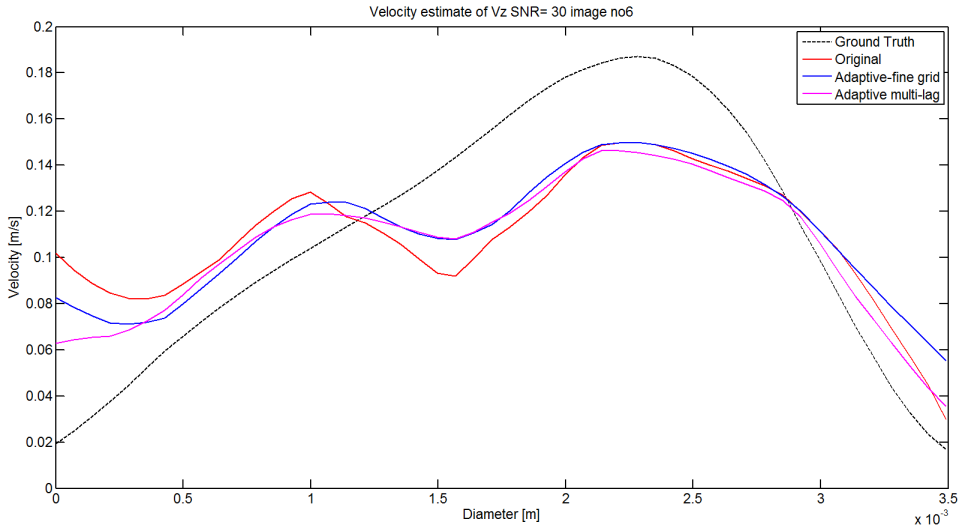

Figure 4.199: Velocity estimations in the z-direction with the original speckle tracking algorithm, the adaptive speckle tracking algorithm with finer grid and multi-lag tracking for flow frame 6 from area 2

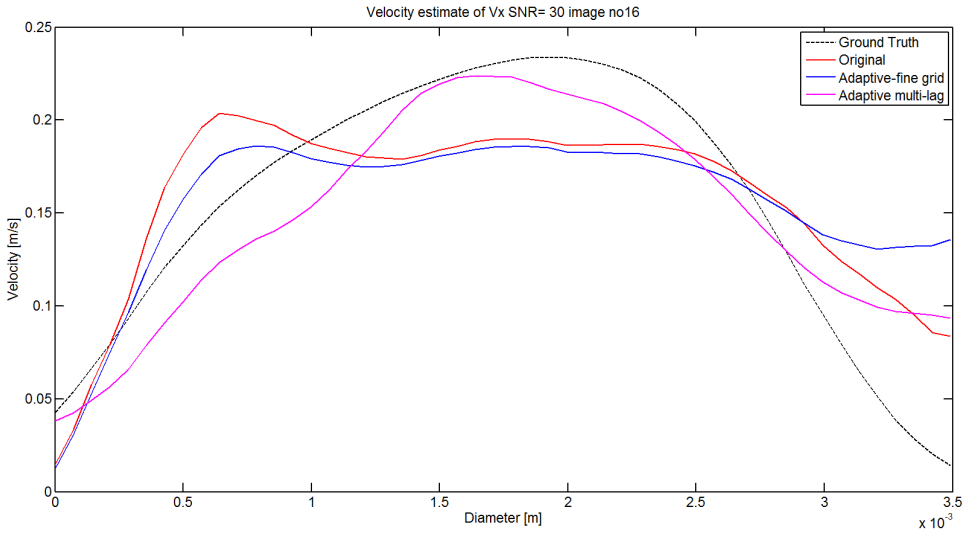

Figure 4.200: Velocity estimations in the x-direction with the original speckle tracking algorithm, the adaptive speckle tracking algorithm with finer grid and multi-lag tracking for flow frame 16 from area 2

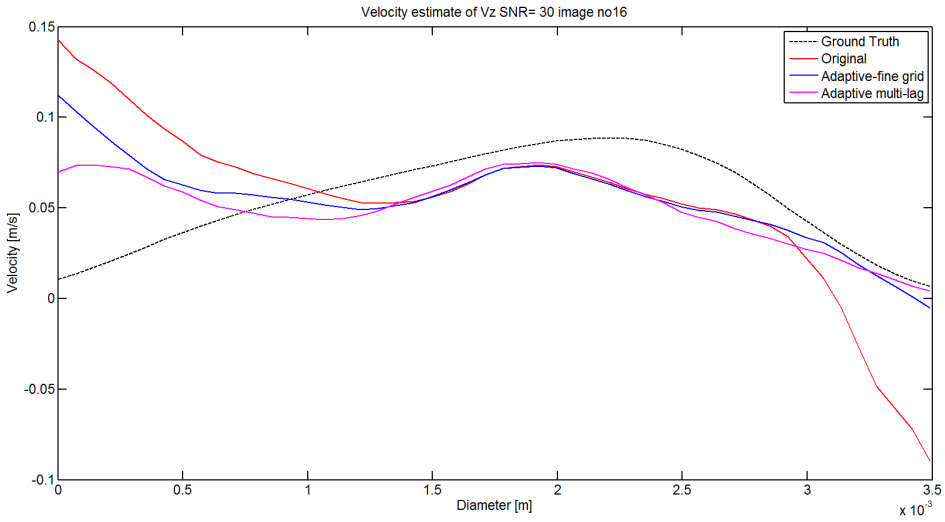

Figure 4.201: Velocity estimations in the z-direction with the original speckle tracking algorithm, the adaptive speckle tracking algorithm with finer grid and multi-lag tracking for flow frame 16 from area 2

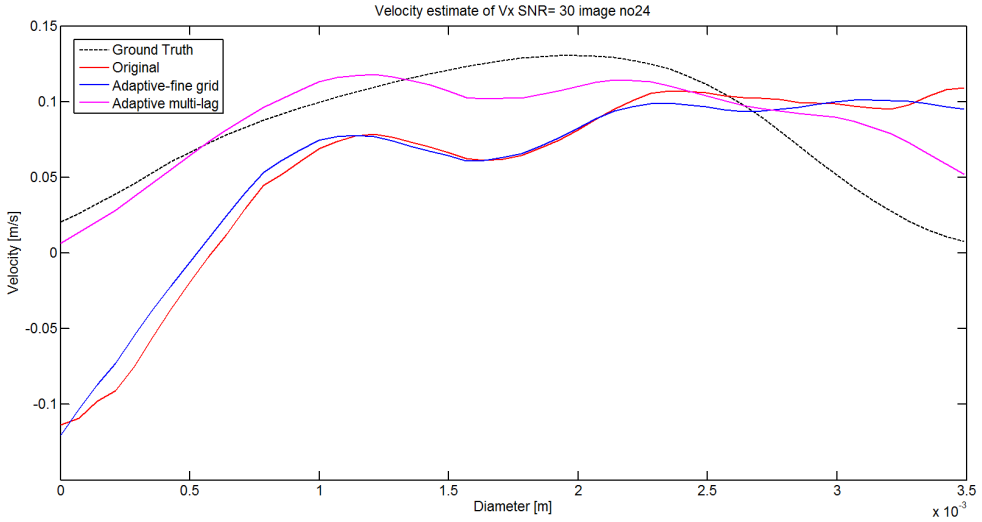

Figure 4.202: Velocity estimations in the x-direction with the original speckle tracking algorithm, the adaptive speckle tracking algorithm with finer grid and multi-lag tracking for flow frame 24 from area 2

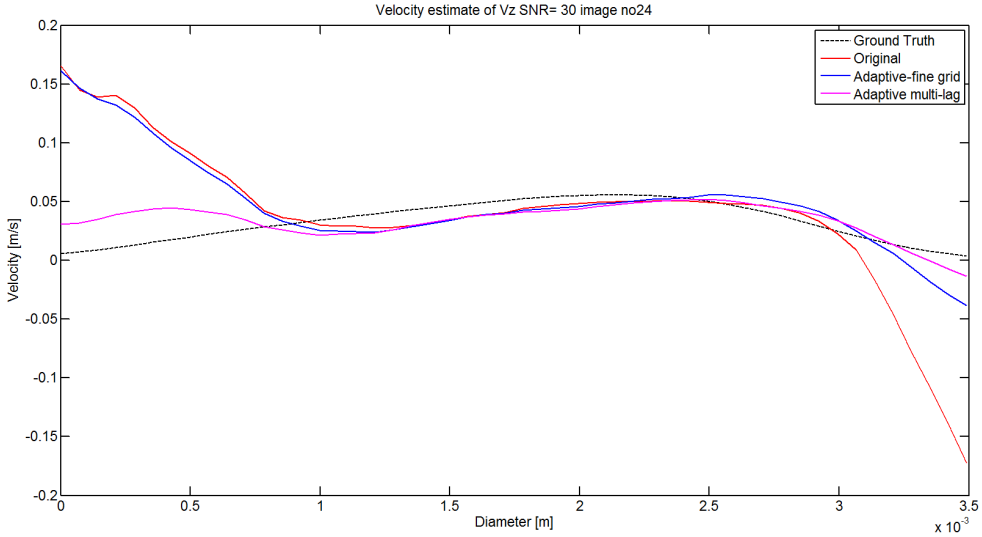

Figure 4.203: Velocity estimations in the z-direction with the original speckle tracking algorithm, the adaptive speckle tracking algorithm with finer grid and multi-lag tracking for flow frame 24 from area 2

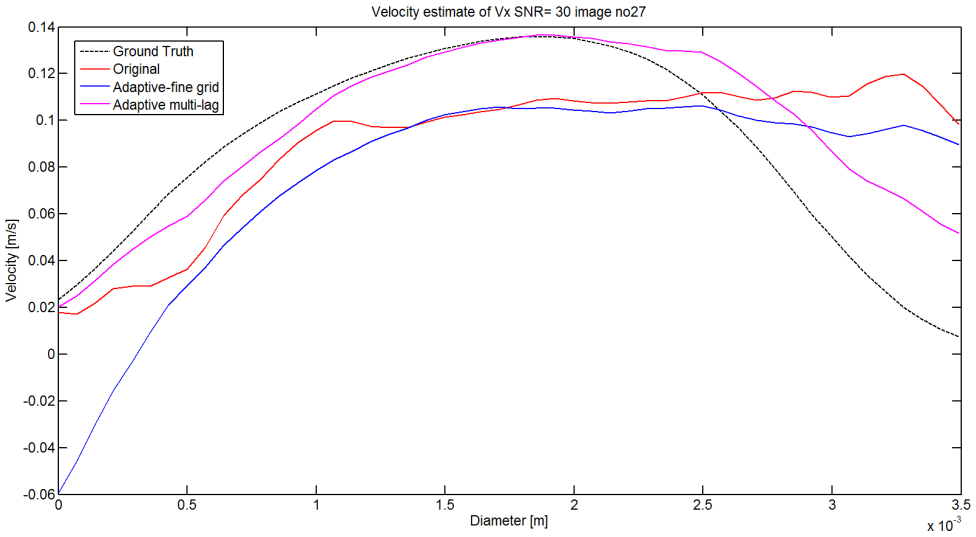

Figure 4.204: Velocity estimations in the x-direction with the original speckle tracking algorithm, the adaptive speckle tracking algorithm with finer grid and multi-lag tracking for flow frame 27 from area 2

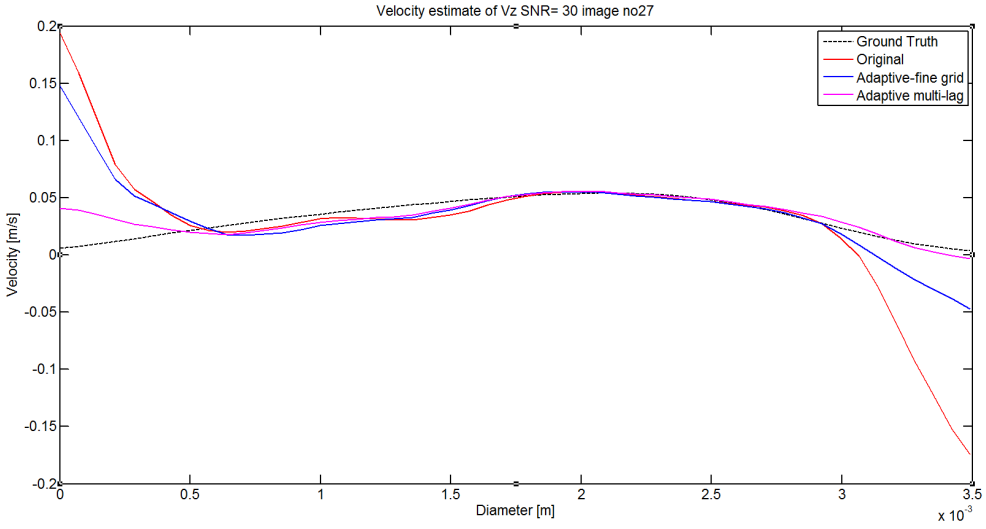

Figure 4.205: Velocity estimations in the z-direction with the original speckle tracking algorithm, the adaptive speckle tracking algorithm with finer grid and multi-lag tracking for flow frame 27 from area 2

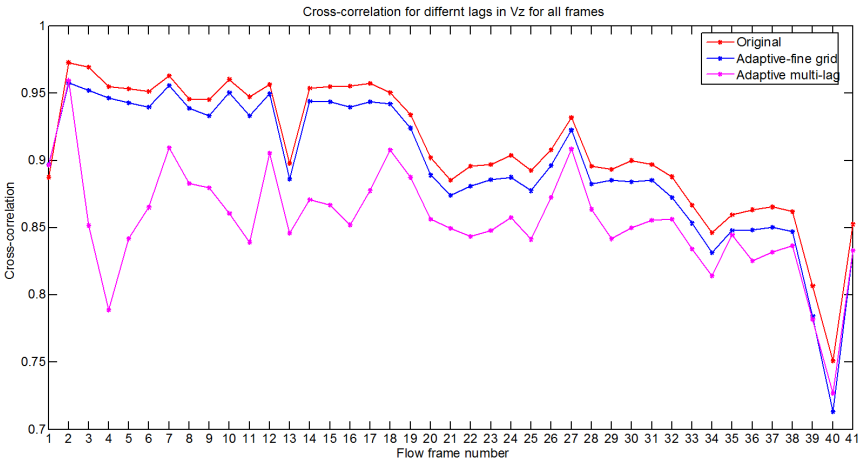

Figure 4.206: Mean cross correlation between the kernel and best match for the original speckle tracking algorithm, the adaptive speckle tracking algorithm with finer grid and multi-lag tracking for all frames from area 2

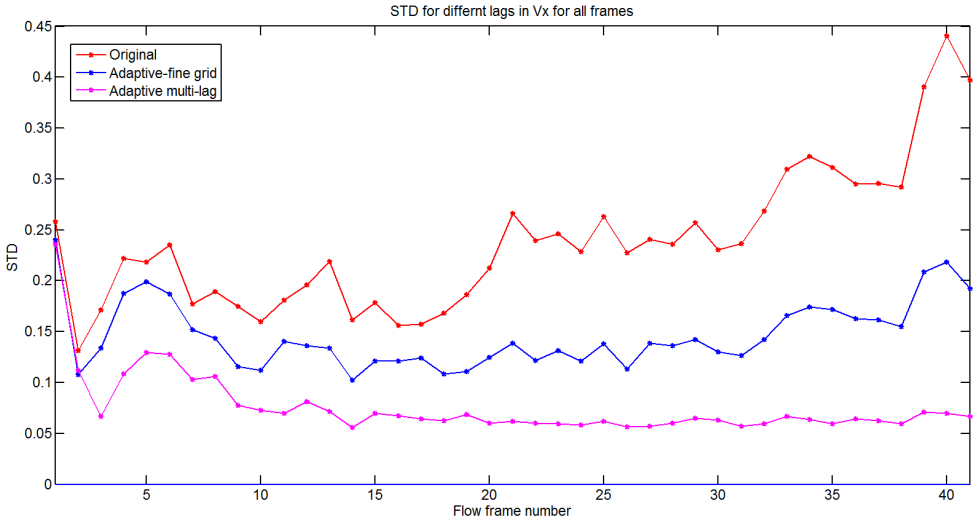

Figure 4.207: Standard deviation in velocity estimations in the x-direction with the original speckle tracking algorithm, the adaptive speckle tracking algorithm with finer grid and multi-lag tracking from area 2

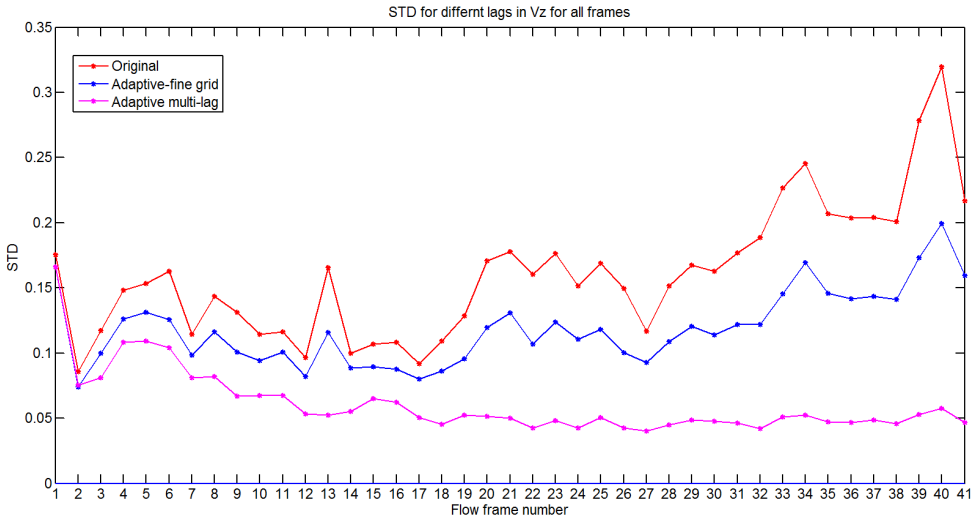

Figure 4.208: Standard deviation in velocity estimations in the z-direction with the original speckle tracking algorithm, the adaptive speckle tracking algorithm with finer grid and multi-lag tracking from area 2

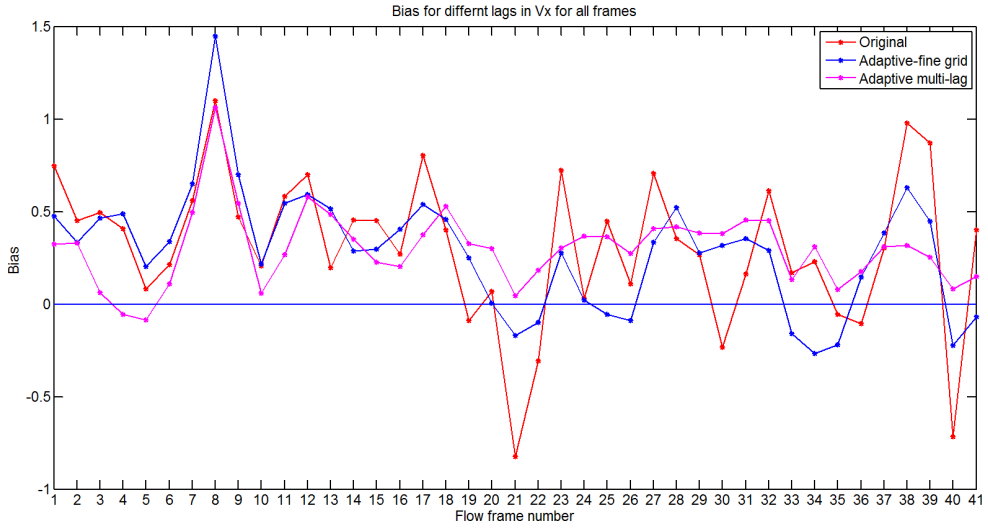

Figure 4.209: Bias between the velocity estimates in the x-direction with the original speckle tracking algorithm, the adaptive speckle tracking algorithm with finer grid and multi-lag tracking from area 2

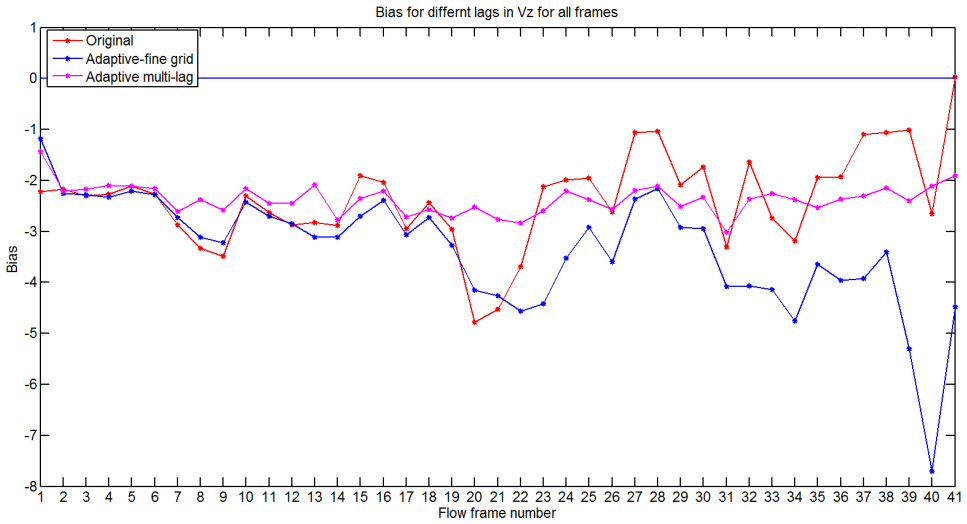

Figure 4.210: Bias between the velocity estimates in the z-direction with the original speckle tracking algorithm, the adaptive speckle tracking algorithm with finer grid and multi-lag tracking from area 2

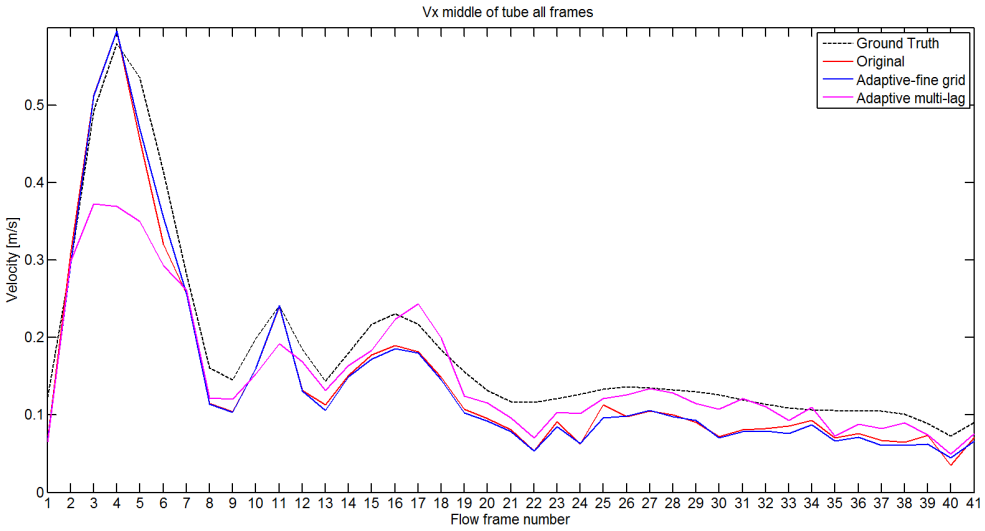

Figure 4.211: Velocity estimates in the middle of the artery in the x-direction with the original speckle tracking algorithm, the adaptive speckle tracking algorithm with finer grid and multi-lag tracking from area 2

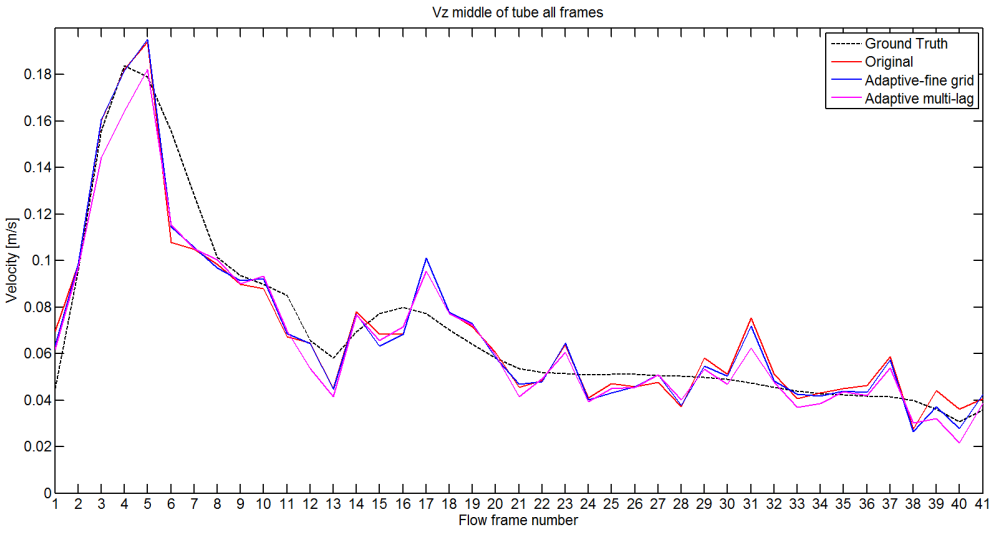

Figure 4.212: Velocity estimates in the middle in the z-direction with the original speckle tracking algorithm, the adaptive speckle tracking algorithm with finer grid and multi-lag tracking from area 2

Results from area 3

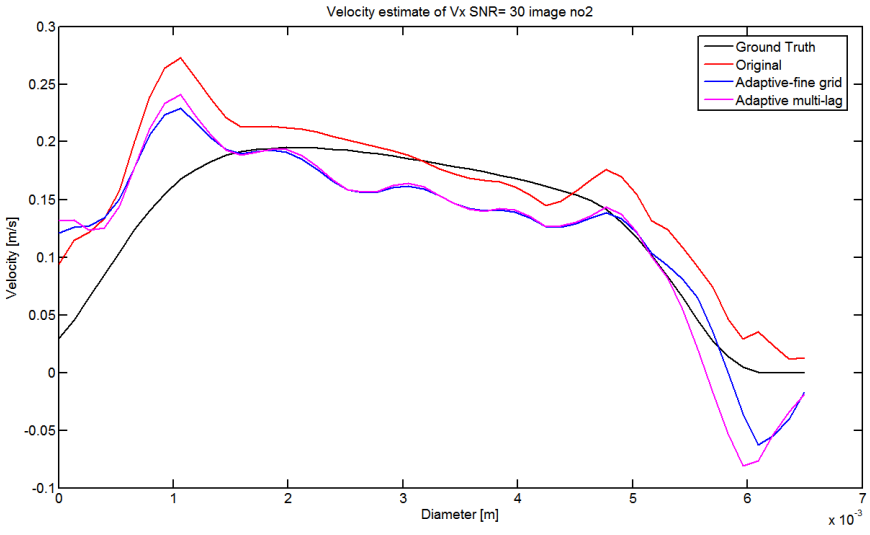

Figure 4.213: Velocity estimations in the x-direction with the original speckle tracking algorithm, the adaptive speckle tracking algorithm with finer grid and multi-lag tracking for flow frame 2 from area 3

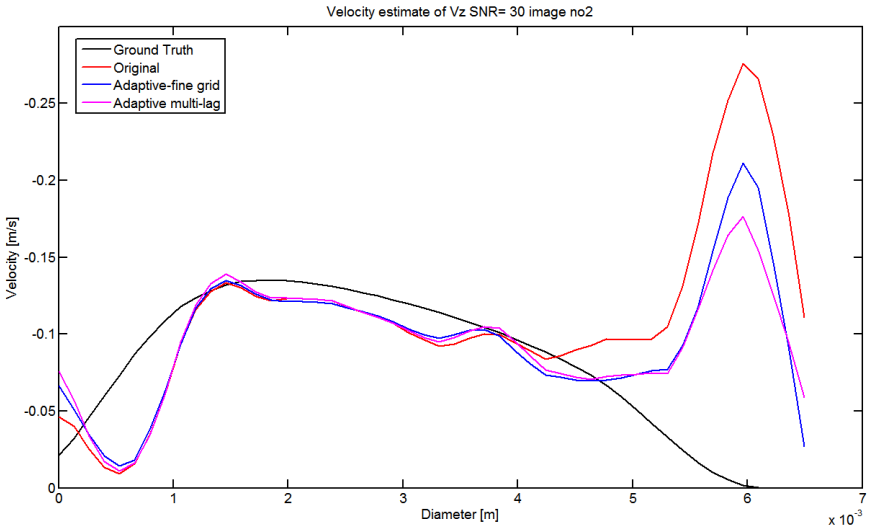

Figure 4.214: Velocity estimations in the z-direction with the original speckle tracking algorithm, the adaptive speckle tracking algorithm with finer grid and multi-lag tracking for flow frame 2 from area 3

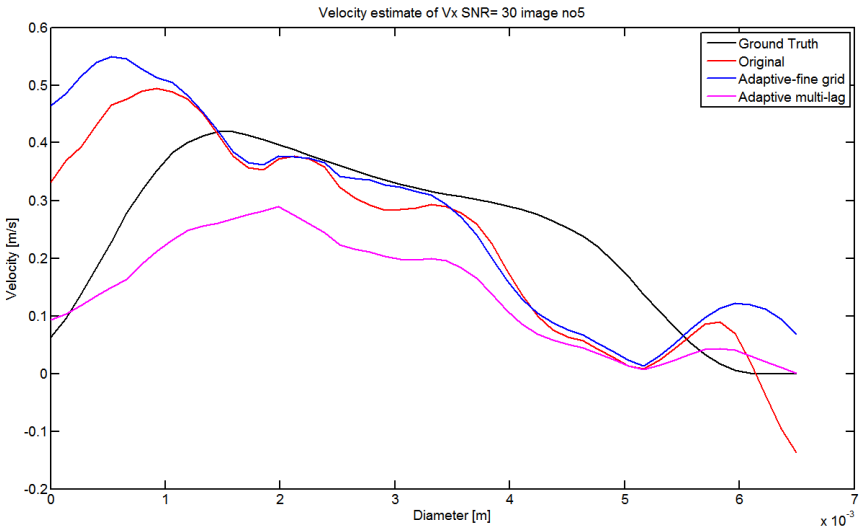

Figure 4.215: Velocity estimations in the x-direction with the original speckle tracking algorithm, the adaptive speckle tracking algorithm with finer grid and multi-lag tracking for flow frame 5 from area 3

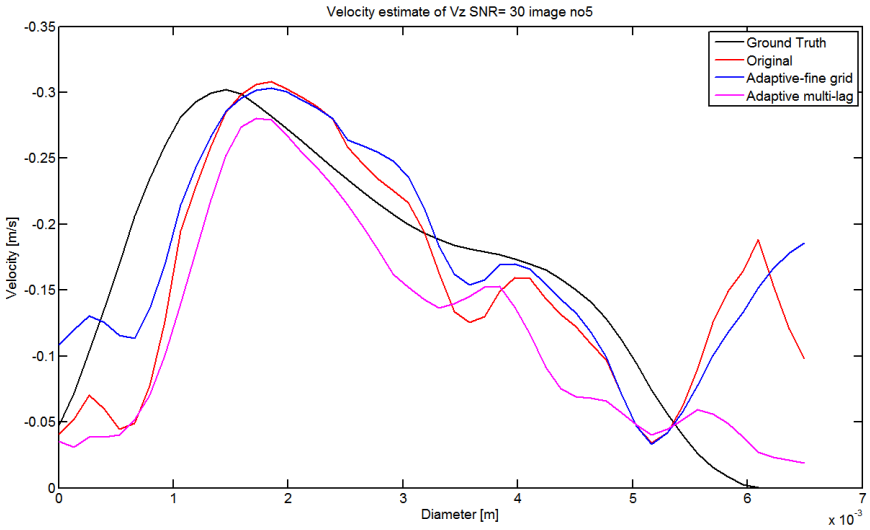

Figure 4.216: Velocity estimations in the z-direction with the original speckle tracking algorithm, the adaptive speckle tracking algorithm with finer grid and multi-lag tracking for flow frame 5 from area 3

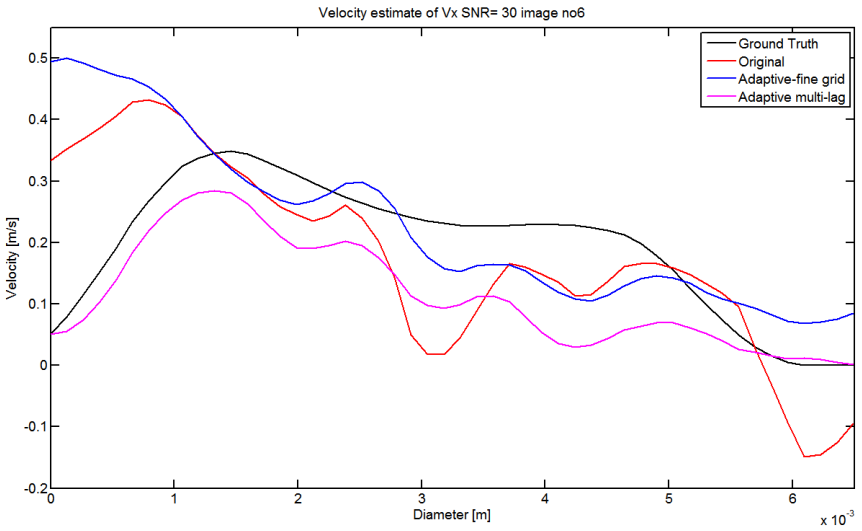

Figure 4.217: Velocity estimations in the x-direction with the original speckle tracking algorithm, the adaptive speckle tracking algorithm with finer grid and multi-lag tracking for flow frame 6 from area 3

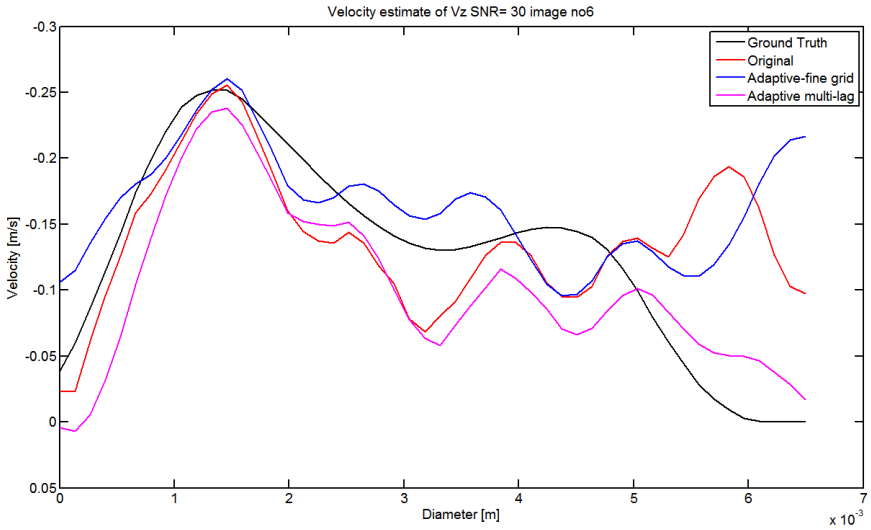

Figure 4.218: Velocity estimations in the z-direction with the original speckle tracking algorithm, the adaptive speckle tracking algorithm with finer grid and multi-lag tracking for flow frame 6 from area 3

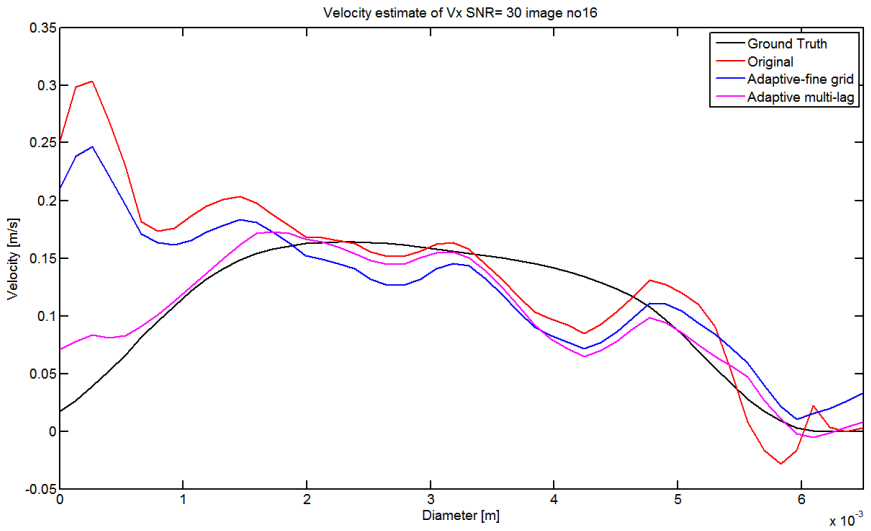

Figure 4.219: Velocity estimations in the x-direction with the original speckle tracking algorithm, the adaptive speckle tracking algorithm with finer grid and multi-lag tracking for flow frame 16 from area 3

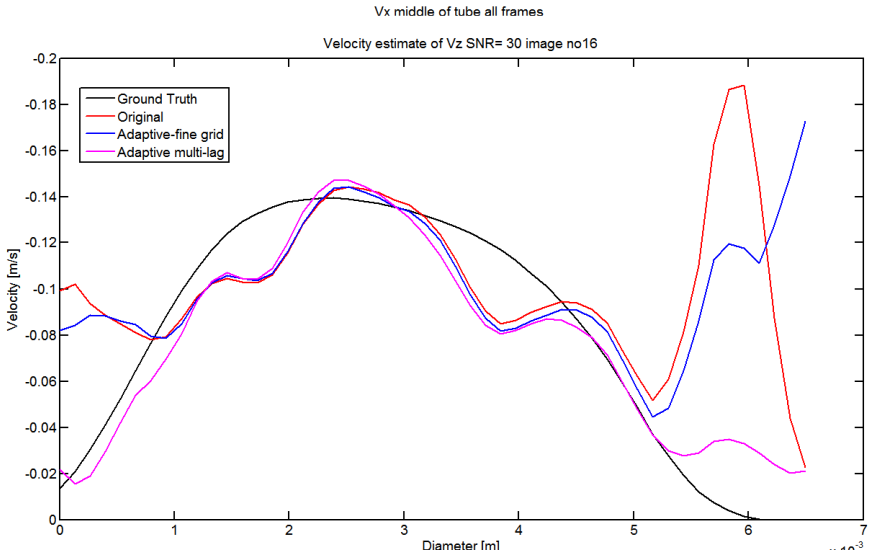

Figure 4.220: Velocity estimations in the z-direction with the original speckle tracking algorithm, the adaptive speckle tracking algorithm with finer grid and multi-lag tracking for flow frame 16 from area 3

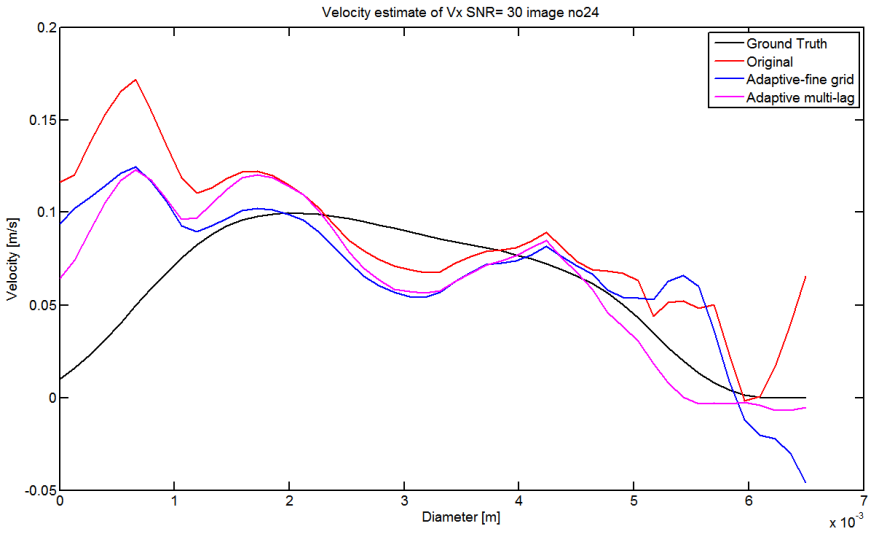

Figure 4.221: Velocity estimations in the x-direction with the original speckle tracking algorithm, the adaptive speckle tracking algorithm with finer grid and multi-lag tracking for flow frame 24 from area 3

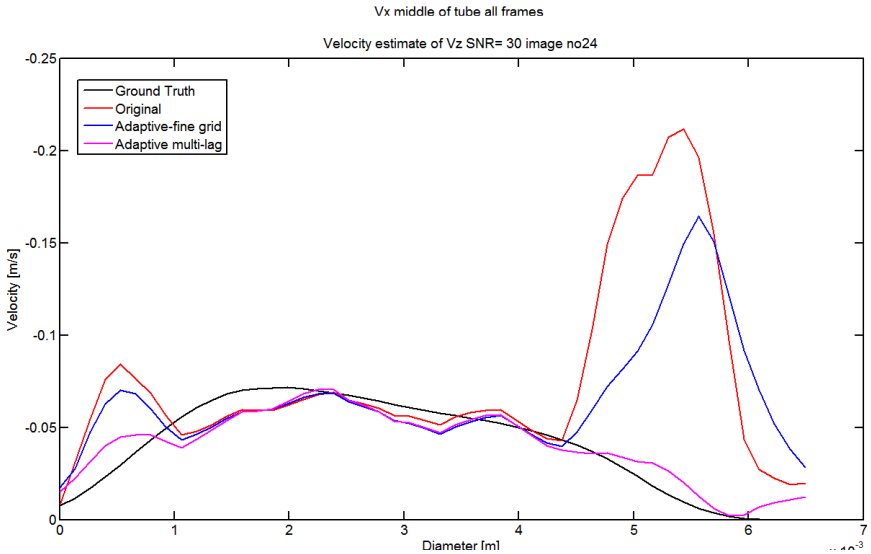

Figure 4.222: Velocity estimations in the z-direction with the original speckle tracking algorithm, the adaptive speckle tracking algorithm with finer grid and multi-lag tracking for flow frame 24 from area 3

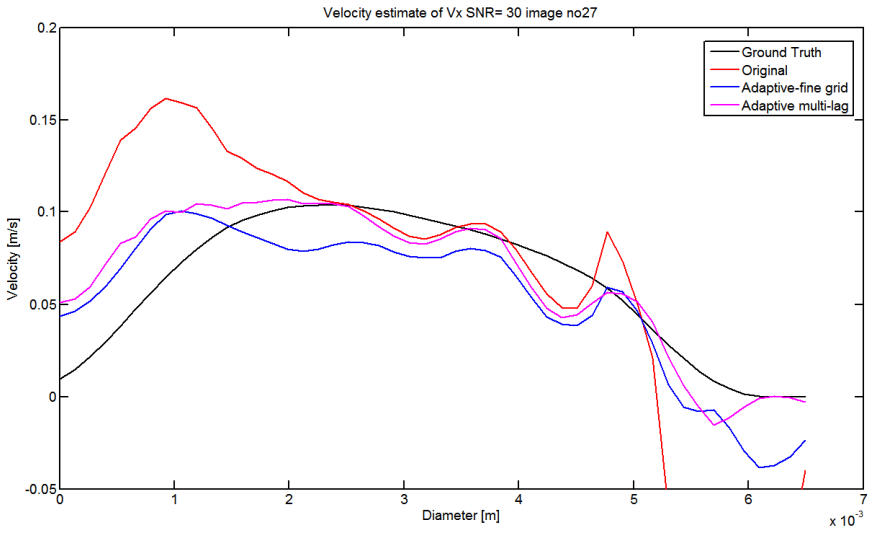

Figure 4.223: Velocity estimations in the x-direction with the original speckle tracking algorithm, the adaptive speckle tracking algorithm with finer grid and multi-lag tracking for flow frame 27 from area 3

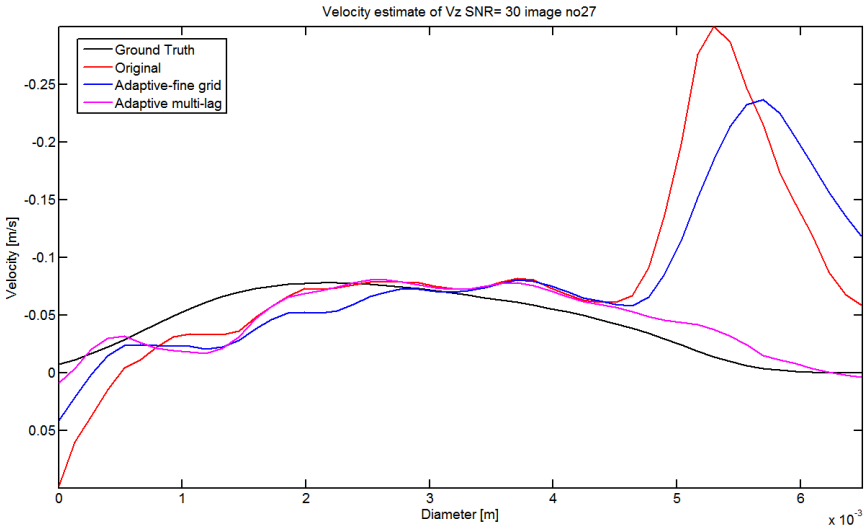

Figure 4.224: Velocity estimations in the z-direction with the original speckle tracking algorithm, the adaptive speckle tracking algorithm with finer grid and multi-lag tracking for flow frame 27 from area 3

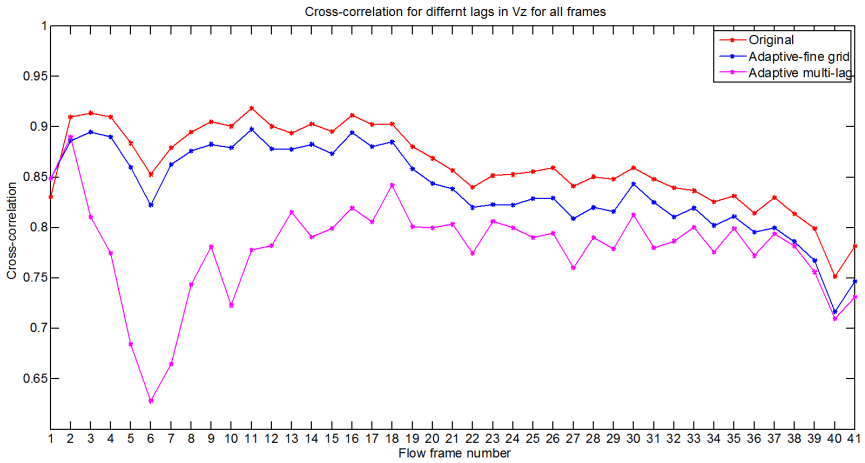

Figure 4.225: Mean cross correlation between the kernel and best match for the original speckle tracking algorithm, the adaptive speckle tracking algorithm with finer grid and multi-lag tracking for all frames from area 3

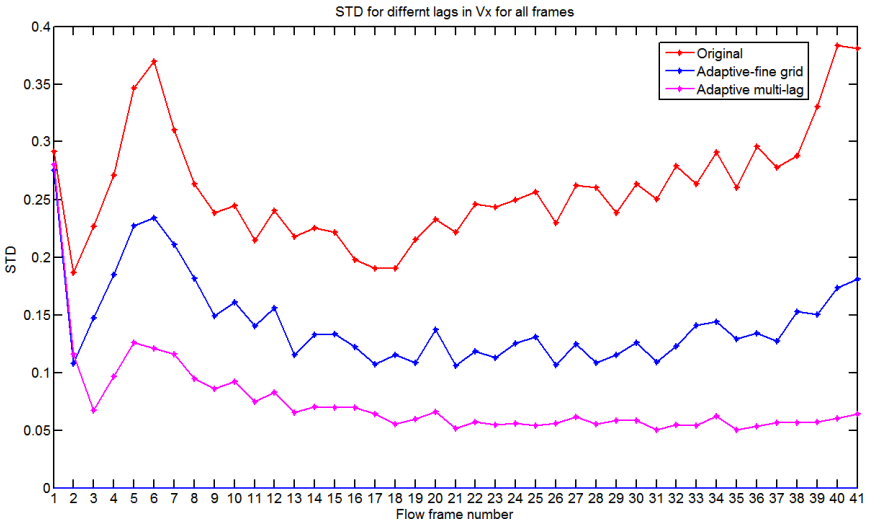

Figure 4.226: Standard deviation in velocity estimations in the x-direction with the original speckle tracking algorithm, the adaptive speckle tracking algorithm with finer grid and multi-lag tracking from area 3

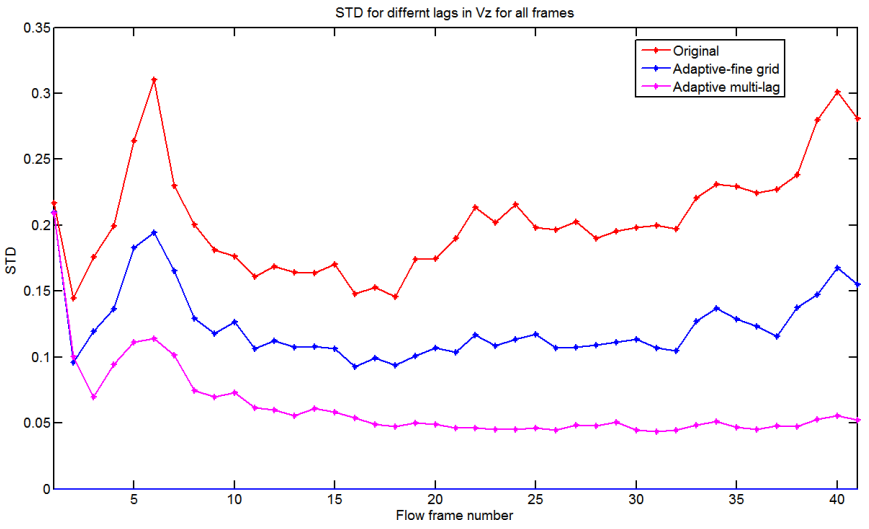

Figure 4.227: Standard deviation in velocity estimations in the z-direction with the original speckle tracking algorithm, the adaptive speckle tracking algorithm with finer grid and multi-lag tracking from area 3

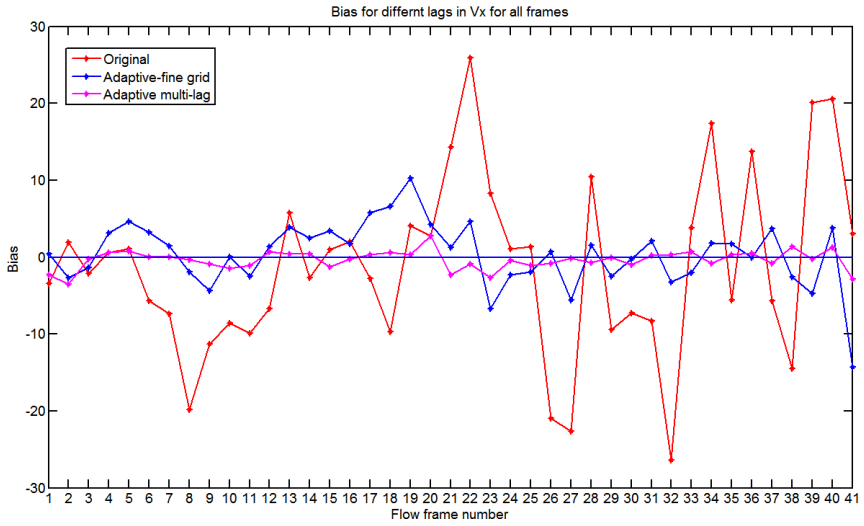

Figure 4.228: Bias between the velocity estimates in the x-direction with the original speckle tracking algorithm, the adaptive speckle tracking algorithm with finer grid and multi-lag tracking from area 3

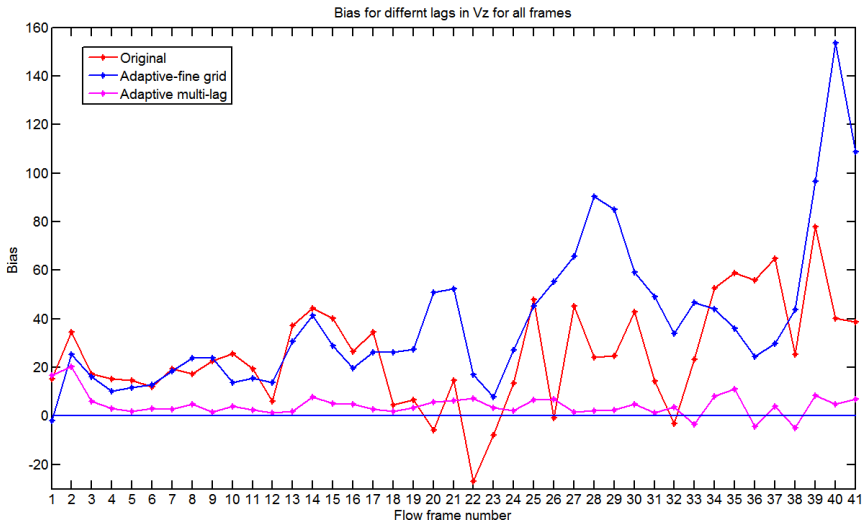

Figure 4.229: Bias between the velocity estimates in the z-direction with the original speckle tracking algorithm, the adaptive speckle tracking algorithm with finer grid and multi-lag tracking from area 3

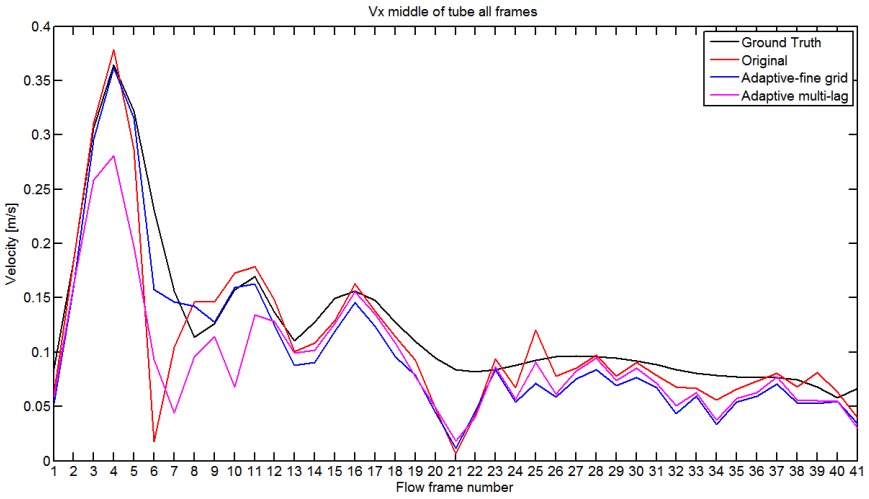

Figure 4.230: Velocity estimates in the middle of the artery in the x-direction with the original speckle tracking algorithm, the adaptive speckle tracking algorithm with finer grid and multi-lag tracking from area 3

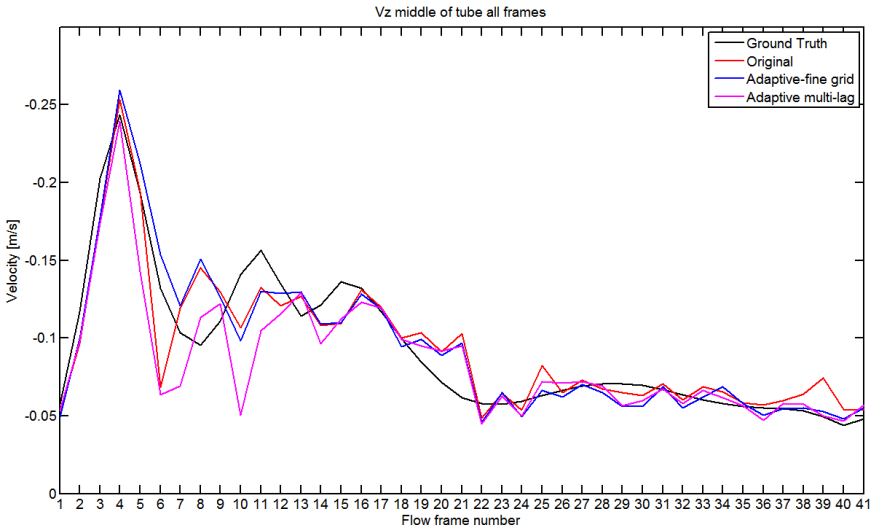

Figure 4.231: Velocity estimates in the middle of the artery in the z-direction with the original speckle tracking algorithm, the adaptive speckle tracking algorithm with finer grid and multi-lag tracking from area 3

Chapter 5

Discussion

5.1 Adaptive speckle tracking over one flow frame

The purpose of using the adaptive speckle tracking algorithm over one frame is too see if the outliers in the velocity estimates, the large errors in velocity estimates the speckle tracking algorithm finds at certain points could be moderated. The figures representing the velocity profiles of the velocity estimates in the lateral and radial direction, shows that there is a difference between the velocity profiles of the velocity estimates found in the different rounds of the adaptive speckle tracking algorithm. As the figures show the velocity estimates found by the adaptive speckle tracking algorithm in round 4 are closer to the Ground truth than the velocity estimates in the other rounds of the adaptive speckle tracking algorithm. One can especially see a difference in the velocity estimates in the lateral direction, where on the edges of the artery the velocity estimated for the different rounds is higher then the value of the ground truth. These outliers become smaller for round 4 than for the other rounds. The velocity profile of the estimated velocity in round 4 follows the velocity profile of the ground truth closer at the edge than the velocity estimated from the original speckle tracking algorithm. In the velocity estimates in the radial direction one can see that the velocity estimated is up to 0.2 m/s higher then the ground truth for the velocity estimated with the original algorithm. This variation become lower for each round of the adaptive speckle tracking algorithm, and the velocity profiles follows the ground truth closer and closer for each round.

The standard deviation in table 4.1 show the standard deviation in the velocity estimates of the adaptive speckle tracking algorithm for the velocity estimated in frame 4 with a signal-to-noise ratio equal to 30. The standard deviation becomes increasingly smaller for the different rounds of the speckle tracking algorithm.

The standard deviation of the velocity estimates is a measure of the spreading in the estimates. The tables for the standard deviation show that for round four the standard deviation becomes larger than the standard deviation in the previous round, this may be because the search region may be misplaced by the adaptive speckle tracking algorithm based on the velocity estimates in the previous round. The adaptive speckle tracking algorithm utilizes previous velocity estimates for placement of the search region. Since the search region is placed at the expected displacement the placement of the search region will be wrong if the velocity estimates is wrong. It is especially important that the direction of the velocity estimates is right, if the direction of the velocity estimated is wrong the search region will be placed in the wrong location. The pattern matching algorithm searches for the best match to the kernel within the each region, that is why the location of the search region is crucial for the performance of the adaptive speckle tracking algorithm.

The results from area 3 shows that the mean velocity in the x-direction for for the original speckle tracking algorithm and the adaptive speckle tracking algorithm is shifted to the left. As figure 5.1 and 5.2 that image the mean velocity found by the adaptive speckle tracking algorithm in round 4 and the ground truth in the x-direction. The mean velocity in the x-direction seem shifted upwards in the lateral direction compared to the ground truth. The blue dots in figure 5.1 indicates area 3 where the velocity profiles is found from, the image clearly show that this is placed wrong compared to the same area in the ground truth, giving the shifted velocity profile in the x-direction in figures 4.9 and 4.11. The figure 2.9 with the b-mode image of the carotid artery where area 3 is indicated with the white lines show that the coordinates where area 3 is found is correct. The reason for this shift was not practicable to find.

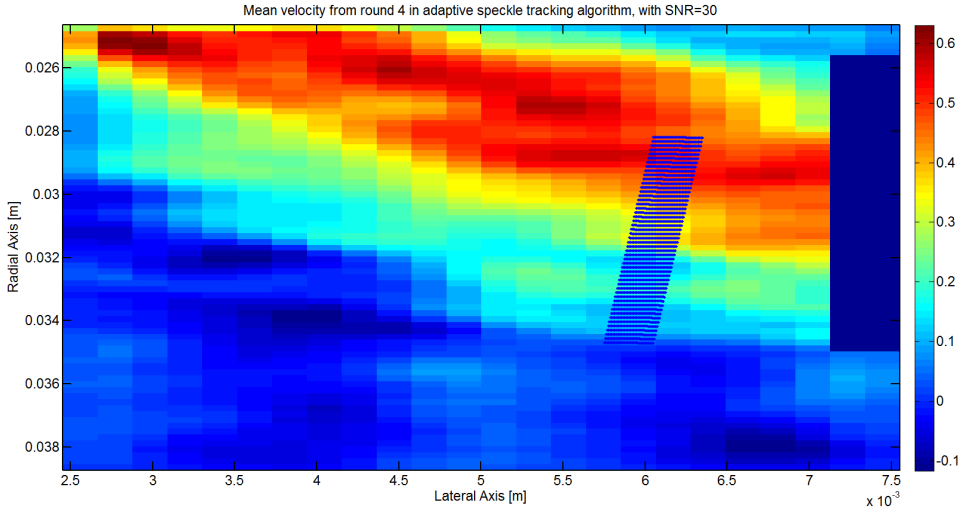

Figure 5.1: Mean velocity in the x-direction from round 4 in the adaptive speckle tracking algorithm with the region of interest indicated by the blue dots area 3 Flow frame 4

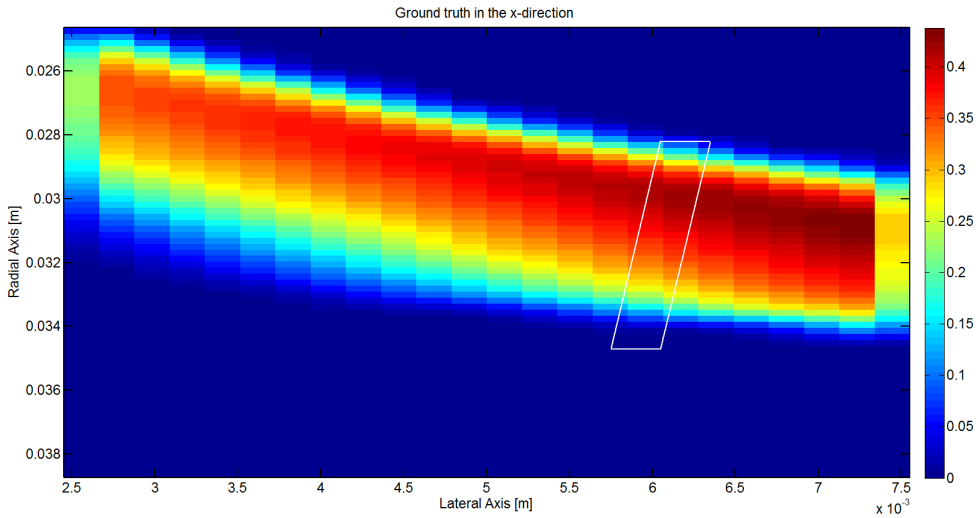

Figure 5.2: Velocity from Ground Truth in the x-direction with the region of interest indicated by the white lines area 3 Flow frame 4

5.2 Multi-lag

5.2.1 Multi-lag -same interpolation-factor for different lags

When the velocity in blood is small, the displacement of a particular speckle in blood from frame to frame is small, often only a fraction of the distance between the range and beam tracking points. As one can see from figure 4.13, 4.23, 4.15, 4.16, 4.17,4.18, 4.19, 4.20 and 4.21 which represents the velocity estimates in the lateral direction for lag 1, 2 and 3 compared to the ground truth for the various flow frames at area 1, that as the velocity changes the different lags gives a better estimate of the velocity than the others. From the figures one can see that the velocity estimated with lag =2 or lag=3 is better than the velocity estimated for lag=1 when the velocity is small. When the velocity in the middle of the tube is high as in figure 4.23 and 4.15 the estimated velocity for lag=1 is the best compared to the ground truth. The velocity estimates given by the speckle tracking algorithm for lag = 2 and lag=3 is underestimated for these high velocities.

The figures representing the bias between the velocity estimates and the ground truth for each flow frame show that for most flow frames the bias is higher for the velocity estimated with lag=3. The reason for that may be that for higher tracking lags the decorrelation between the best match and the kernel at a specific point increases.

In figure 4.13 where the velocity in the middle of the tube is approximately 0.23 m/s, the estimated velocity with lag=1 is underestimated and the velocity estimated with lag = 2 and lag= 3 is overestimated. The figures representing the mean velocity estimated in the lateral direction for different lags over the subsample of flow frames, show that as the velocity in the Carotid artery changes with time over the heart cycle, the speckle tracking algorithm gives a better estimation of the velocity compared to the ground truth for different lags. For times in the heart cycle where the velocity i high, upto 0.6 m/s at the maximum, speckle tracking with lag=1 give the best estimated velocity compared to the velocity estimated with the other lags. As for the velocity estimated with lag=2 and lag=3 is underestimated. This underestimation may be because for high velocities the the blood flows fast, and the displacement of the speckles between each frame is very large. Since the speckle tracking algorithm only searches for the best match within the search region, a high lag might give a displacement of the speckles that is outside of the search region. Thereby the speckle tracking algorithm will find

a best match that is not the true value and a will estimate a lower velocity than the actual best match.

As one can see from figure 4.33, 4.58 and 4.77 the cross correlation between the kernel and the best match for lag=2 and lag=3 is higher than the cross-correlation for lag=1. This does not concede with that a coarse grid where the displacement of the speckle pattern between each sample point should give less decorrelation.

5.2.2 Multi-lag variance

The velocity estimates was found for different lags because, for small velocities, the displacement of the speckles from frame to frame is very small, often only a fraction of the interpolation factor as explained earlier in section 3.5.1. By using a higher lag, the displacement becomes larger and the dependency on the subsample-interpolator become smaller, and possibly the velocity estimate for small velocities become more accurate. The correlation between the best match and the kernel will vary with the lag that are being used, where the highest correlation between the two is wanted. So there is a trade-of between using a higher lag and becoming more independent of the subsample-interpolator and achieving the best correlation possible.

The velocity in the carotid artery varies with the contraction and relaxation of the heart, so the velocity in the middle of the artery will vary over the flow frames, as they are images of the carotid artery at different times of the heart cycle.

.

From the figures one can see that when the velocity is high in the middle of the artery, speckle tracking with lag=1 give the best estimates of the velocity. When the velocity is high the velocity estimates is severely underestimated for lag=2, lag= 3 and lag=4.

The figures representing the standard deviation of the velocity estimated in the flow frames for all flow frames in the lateral and axial direction, respectively, show that the standard deviation, ergo the variance in the estimated velocities becomes lower when the median of lag=1, lag=2, lag=3 and lag=4 is calculated. Especially in the axial direction the variance in the velocity estimated becomes lower for flow frames where the velocity in the middle of the tube is low, from flow frame 19 to 41. This corresponds with the theory

that for a higher lag the velocity estimates of the small velocities will become more accurate.

As one can see from the figure of the bias of the velocity estimates over one flow frame compared to the true value of the ground truth, the bias of the median of all the lags is in general smaller than the bias for the velocity estimates with lag equal to one. The bias of the median is higher in certain places where one can see that the velocity for lag two, three or four is very underestimated or over estimated. So for the flow frames where the velocity estimates for one of the lags is far from the true value, the bias of the median becomes large. The standard deviation of the velocity estimates was calculated too see if the variance of the velocity estimates could be lowered by finding the median of the velocity estimates from speckle tracking with the different lags. The standard deviation of the velocity estimates is calculated of the mean velocity of all the velocity estimates found from the speckle tracking algorithm either in the lateral or the axial direction. The standard deviation of the velocity estimates is a measure of the spreading in the velocity estimates over the artery. Since the velocity changes much from the middle of the artery to the edges, the spreading in the estimates can be pretty large even if the the velocity estimated by the speckle tracking algorithm is pretty close to the true value at a specific point in the artery. So it is important to compare it to the bias found between then velocity estimated at a specific point and the true value at that point. As one can see from for example figure 4.97 the median velocity of all the lags follows the velocity profile of the ground truth closer than the velocity estimated with the use of lag equal to 1. But the standard deviation is higher than the standard deviation of the velocity estimated with lag equal to 1. As one can see from the figure the velocity estimated is very underestimated compared to the median value, since the velocity is under estimated, the spreading in the velocity estimates is smaller and thereby the standard deviation. But the velocity estimation is far from the true value of the velocity.

One can see from the figures that by tracking the velocity with different lags and taking the median of the velocity estimated with all the lags, the variance of the velocity becomes lower. The large outliers become smaller and when one lag might over or underestimate the velocity, the median of all the lags does that the under- or overestimation become smaller. Since the different lags estimates certain velocities better than others.

5.3 Adaptive speckle tracking algorithm -adjusted to the acceleration over flow frames/ Multi-lag tracking

The results show that in general the velocity estimates found by the adaptive speckle tracking algorithm where it is adjusted for the velocity changes over the flow frames, is better compared to then velocity estimates found by the original speckle tracking algorithm. The outliers at the edges is smaller for the the adaptive speckle tracking algorithm then for the original speckle tracking algorithm. For the velocity estimates from multi-lag tracking the result clearly show an improvement compared to the original speckle tracking algorithm. The velocity estimates found when adaptively adjusting the parameter lag to the velocity at the specific point over time follow the velocity profile of the ground truth closer than the velocity estimate found by the original speckle tracking algorithm. For flow frames where the velocity changes much from one flow frame to the next, the velocity estimates seem to be underestimated compared to the velocity estimates found by the original speckle tracking algorithm and the ground truth. As one can see from especially for flow frames where the velocity changes from very low to high from flow frame to flow frame, in flow frames 3, 4, 5 and 6 this phenomenon presents it's self. The reason for this underestimation may be that since the velocity estimates from the previous flow frame is being used to decide which lag to track with at the specific point in the current flow frame, and the velocity in the previous frame is much smaller than the velocity in the current frame, a higher lag will be chosen. As seen from the figures in the previous sections 3.5.1 and 3.5.2 lag=2 and lag=3 underestimates high velocities, so when the velocity changes very much from time to time (flow frame to flow frame) at a specific point in the artery the velocity will be under estimated. Because the velocity estimates from previous flow frames is used, this will be a recurrent problem, where the underestimation from one flow frame will lead to under estimation in the next, if the velocity increases in the next flow frame or is as high as in the previous low frame. The figures illustrating the normalized cross-correlation over the area, show that for the correlation for the adaptive multi-lag tracking algorithm the is smaller than the correlation between the best match and the kernel for the adaptive and original speckle tracking algorithm, this is coherent with the expected decorrelation when increasing lag since the blood speckles travels further. On can see from the figures representing the velocity profiles of the velocity estimates in the axial direction that for the adaptive multi-lag

tracking algorithm the estimates follow the ground truth much better than the two other speckle tracking algorithms, especially at the edges. This is coherent with the hypotheses that increasing lag will increase the accuracy of the velocity estimates for the small velocities. From figure 4.188, 4.207 and 4.226, representing the standard deviation in the velocity estimates in the x-direction, one can clearly see that the standard deviation is lower in the velocities when multi-lag tracking. This indicates that when adaptively finding the best lag over time give better velocity estimates that the original speckle tracking algorithm and the adaptive speckle tracking algorithm with a finer grid.

Chapter 6

Conclusion

In this thesis several ways to improve the robustness of the speckle tracking method have been investigated and tested with a simulated data set of a carotid artery.

An adaptive speckle tracking scheme, where the size and placement of the search region was updated according to the velocity estimates from previous flow frames was developed. The results show that by adaptively updating the search region in this way and using a finer grid for small velocities better velocity estimates is achieved.

A multi-lag tracking method where velocity estimates from the previous flow frame was utilized to adjusts the size and placement of the search region to the acceleration as in the adaptive speckle tracking scheme. In addition to updating the search region, the velocity estimates from the previous flow frames was utilized to adaptively find the best lag over time at a specific location in the image. The results show that velocity estimates from the multi-lag tracking scheme is better than the velocity estimates from tracking in the the original speckle tracking algorithm. Although, for preceding flow frames where the velocity changes very much from flow frame to flow frame, as in systole, the velocity estimates for the flow frames with high velocities become underestimated. This happens because the velocity from the previous flow frame (where the velocity is much lower than for the next flow frame) is utilized to decide which lag to do the speckle tracking with at the specific point. In general the multi-lag tracking scheme is the best of the speckle tracking schemes tested in this work.

In conclusion, the adaptive speckle tracking methods tested in this work, where previous velocity estimates are utilized give improved velocity esti-

mates compared to the speckle tracking method where no a priori knowledge of the blood flow map is taken into account.

Bibliography

[1] R. W. Gill, *Measurement of blood flow by ultrasound: Accuracy and source of error* (Ultrasound in Med. Bio Vol 11 (1985)pp.625-641)

[2] L.N. Bohs, B.J. Geiman, M.E. Anderson, S.C. Gebhart, G.E. Trahey, *Speckle tracking for multi-dimensional flow estimation* (Ultrasonics 38 (2000) pp.369-375)

[3] Prof.Bjørn A.J Angelsen, dr techn. Prof. Hans G. Torp, dr.techn., *Ultrasound Imaging - Waves, Signals, and Signal Processing". 2 volumes, 1416 pages, Emantec, Trondheim. 2000 p.1.52-1.54*

[4] Thomas L. Szabo, *Diagnostic ultrasound imaging: inside out* (ELSEVIER ACADEMIC PRES 2004 p. 346-371)

[5] Murtaza Ali, Dave Magee and Udayan Dasgupta, *Signal Processing Overview of Ultrasound Systems for Medical Imaging* (TEXAS INSTRUMENTS November 2008)

[6] B. Dunmire, K. W. Beach, K. Labs, M. Plett, and D. E. Strandness,*Cross-beam vector Doppler ultrasound for angle independent velocity measurements.* (Ultrasound in medicine and biology, vol. 26, no. 8, pp. 1213–35, Oct. 2000.)

[7] Prof.Bjørn A.J Angelsen, dr techn. Prof. Hans G. Torp, dr.techn., *Ultrasound Imaging - Waves, Signals, and Signal Processing". 2 volumes, 1416 pages, Emantec, Trondheim. 2000 p.1.28-1.31*

[8] Konstantinos G. Derpanis York University, *Relationship Between the Sum of Squared Difference (SSD) and Cross Correlation for Template Matching* (Version 1.0 December 23, 2005)

[9] Torbjør Hergum, student member IEEE, Tore Bjåstad, Student Member,IEEE, Kjell Kristoffersen, and Hans Torp, Member IEEE *"Parallel Beamforming Using Synthetic Transmit Beams"* (IEEE TRANS-

ACTIONS ON ULTRASONIC, FERROELECTRICS, AND FREQUENCY CONTROL, VOL.54 NO.2, FEBRUARY 2007)

[10] James C.Y. Guo, Professor and P.E Civil Engineering,U. of Colorado at Denver, *Theoretical Fluid Mechanics Laminar Flow Velocity Profile*

[11] Jørgen Arendt Jensen, Department of Information Technology, Technical University of Denmark, *Field: A Program for Simulating Ultrasound Systems*

[12] Ashrafian H. Anatomically specific clinical examination of the carotid arterial tree. Anat Sci Int. 2007 Mar;82(1):16–23

[13] Systolic and Diastolic Blood Pressure, Pulse Pressure, and Mean Arterial Pressure as Predictors of Cardiovascular Disease Risk in Men Howard D. Sesso, Meir J. Stampfer,Bernard Rosner,Charles H. Hennekens, J. Michael Gaziano, JoAnn E. Manson, Robert J. Glynn

[14] http://www.interactive-biology.com/75/

[15] http://www.uic.edu/classes/bios/bios100/f05pm/lect17.htm